ResearchOnline@JCU

This file is part of the following reference:

Yu, Hongyou (2015) *The role of angiopoietin-2 in experimental abdominal aortic aneurysm development.* **PhD thesis, James Cook University.**

Access to this file is available from:

http://researchonline.jcu.edu.au/46025/

JAMES COOK
UNIVERSITY
AUSTRALIA

The Role of Angiopoietin-2 in Experimental Abdominal Aortic Aneurysm Development

Thesis submitted by

Hongyou YU

B.D.S. and M.Sc. (*Orth*)

Sichuan University, Chengdu, P. R. China

in August 2015

for the Degree of Doctor of Philosophy

in the College of Medicine and Dentistry

James Cook University

Supervision

PRINCIPAL SUPERVISOR

Professor Jonathan Golledge, BA, MA BChir, Mchir, FRACS, FRACS

CO-SUPERVISOR

Dr Catherine M. Rush, BSc (Hons), PhD

ASSOCIATE SUPERVISOR

Dr Corey S. Moran, BSc, MSc, PhD

Dr Lynn Woodward, BSc, MSc, MA, PhD

Dr Robert T. Kinobe, BSc, MSc, PhD

FINANCIAL SUPPORT

Declaration

I, the undersigned declare that this research investigation is carried out on my own and it has not been previously submitted anywhere for another degree or diploma at any university or institution of tertiary education in or out of Australia. Information derived from the published or unpublished works of others has been acknowledged in the text and a list of reference is given.

August 2015

_____

Signature   Date

Hongyou YU

_____

Name

Statement of Access

I, the undersigned, author of this thesis, understand that James Cook University will make this work available for use within the university library and, by microfilm or other photographic means, allow access to users in other approved libraries. All users consulting this thesis will have to sign the following statement.

"In consulting this thesis, I agree not to copy or closely paraphrase it in whole or in part without written consent of the author, and to make proper written acknowledgement for any assistance which I have obtained from it."

August 2015

_____

Signature   Date

Hongyou YU

_____

Name

Declaration on Ethics

The research presented and reported in this thesis was conducted within the guidelines for research ethics outlined in the *James Cook University.* Animal studies were approved by ethics committee and experimental work performed in accordance with the institutional and ethical guidelines of James Cook University. All of the protocols were approved by the Animal Ethics Committee of James Cook University (Approval number: A1671).

August 2015

_____

Signature   Date

Hongyou YU

_____

Name

Acknowledgements

This thesis would not exist without the support and encouragement from my supervisors, for whom I would like to extend my sincerest appreciation. To Professor Jonathan Golledge, thank you for providing this extraordinary opportunity to finish a PhD degree under your supervision. Your academic achievements, acumen, and diligence impress and influence me deeply. I hope to model your attitude and achievements in my academic career. To Dr Catherine Rush, Dr Corey Moran, Dr Robert Kinobe, and Dr Lynn Woodward, I wish to express my sincere gratitude for your timely input in preparing this thesis, and your encouragements and understanding when I felt down. Your supervision has made a huge difference to the quality of my PhD thesis.

I would like to thank all of the previous and current students and staff in the Vascular Biology Unit. Thank you very much for helping me during my PhD study and for being so patient in listening to me. Tammy, Iyke, and Mal, thank you for sharing your PhD experience and encouraging me. David, Sai, and Yutang, thank you for enduring my visits and talking in your office and for your steady support. For all of the other members of Vascular Biology Unit, thank you for everything, from interesting talks in the coffee room to your constant support and encouragement.

I cannot express enough appreciation to my wife Jielin. We have spent our lives together in China, the Netherlands, and tropical Queensland. You inspire me to find my true interests and what are really meaningful in life. You are so patient in enduring such a long journey to my PhD study, and you have always been helpful in resolving all sorts of problems. We know where our strength and love come from and, in HIM, we have gone through an incredible journey with the members of NQCCC in Townsville.

Last but not least, I would dedicate this thesis to my parents and my elder brothers Honghai and Hongliang. You always stretch out your arms to me with unconditional love. I love your all!

感谢神，赐路旁玫瑰；感谢神，玫瑰有刺

Statement on the Contribution of Others

Nature of Assistance	Contribution	Names, Titles and Affiliations of Co-Contributors
Thesis presentation	Thesis formatting, ESL editing	Katharine J Fowler
Chapter 1: Nature of Assistance	**Contribution**	**Names, Titles and Affiliations of Co-Contributors**
Intellectual support	Editorial assistance	Golledge J, Prof, JCU
		Rush C, Dr, JCU
		Moran C, Dr, JCU
		Woodward L, Dr. JCU
		Kinobe R, Dr, JCU
Financial support		Golledge J, Prof, JCU
Chapter 2: Nature of Assistance	**Contribution**	**Names, Titles and Affiliations of Co-Contributors**
Intellectual support	Editorial assistance	Golledge J, Prof, JCU
		Rush C, Dr, JCU
		Moran C, Dr, JCU
		Woodward L, Dr. JCU
		Kinobe R, Dr, JCU
Financial support		Golledge J, Prof, JCU
Chapter 3: Nature of Assistance	**Contribution**	**Names, Titles and Affiliations of Co-Contributors**
Intellectual support	Editorial assistance	Golledge J, Prof, JCU
		Rush C, Dr, JCU
		Moran C, Dr, JCU
		Woodward L, Dr. JCU
		Kinobe R, Dr, JCU
Financial support		Golledge J, Prof, JCU
Chapter 4: Nature of Assistance	**Contribution**	**Names, Titles and Affiliations of Co-Contributors**
Intellectual support	Editorial assistance	Golledge J, Prof, JCU
		Rush C, Dr, JCU
		Moran C, Dr, JCU
		Woodward L, Dr. JCU
		Kinobe R, Dr, JCU
Financial support		Golledge J, Prof, JCU

Chapter 5: Nature of Assistance	Contribution	Names, Titles and Affiliations of Co-Contributors
Intellectual support	Editorial assistance	Golledge J, Prof, JCU
		Rush C, Dr, JCU
		Moran C, Dr, JCU
		Woodward L, Dr. JCU
		Kinobe R, Dr, JCU
Data collection	Part of aortic diameters and atherosclerosis data	Trollope A, Dr, JCU
Financial support		Golledge J, Prof, JCU

Chapter 6: Nature of Assistance	Contribution	Names, Titles and Affiliations of Co-Contributors
Intellectual support	Editorial assistance	Golledge J, Prof, JCU
		Rush C, Dr, JCU
		Moran C, Dr, JCU
		Woodward L, Dr. JCU
		Kinobe R, Dr, JCU
Financial support		Golledge J, Prof, JCU
		Graduate Research Scheme Grant, JCU

Chapter 7: Nature of Assistance	Contribution	Names, Titles and Affiliations of Co-Contributors
Intellectual support	Editorial assistance	Golledge J, Prof, JCU
		Rush C, Dr, JCU
		Moran C, Dr, JCU
		Woodward L, Dr. JCU
		Kinobe R, Dr, JCU
Financial support		Golledge J, Prof, JCU

Chapter 8: Nature of Assistance	Contribution	Names, Titles and Affiliations of Co-Contributors
Intellectual support	Editorial assistance	Golledge J, Prof, JCU
		Rush C, Dr, JCU
		Moran C, Dr, JCU
		Woodward L, Dr. JCU
		Kinobe R, Dr, JCU
Financial support		Golledge J, Prof, JCU

Abstract

Abdominal aortic aneurysm (AAA) is an abnormal dilatation of the aorta that is permanent and progressive. The most severe consequence of AAA is rupture, and as the aorta is the main vessel leading away from heart, it can be fatal. AAA affects around 2-5% of men over the age of 65. Only surgery can currently repair AAA. No other efficient clinical interventions currently exist to prevent AAA from progression to rupture, due to the lack of understanding the pathogenesis of AAA. Therefore, understanding the molecular and cellular mechanisms that lead to the development of AAA is critical for identifying strategies to interrupt disease progression before it leads to clinical consequences. Recently, Golledge and colleagues reported that serum angiopoietin-2 (Angpt2) was elevated in men with AAA, and associated with an increased risk of cardiovascular mortality in older men. This suggests that Angpt2 could play a role in AAA development and be a potential target for clinical treatment to limit AAA progression and rupture.

Angpt2 is a member of angiopoietin family that regulates angiogenesis and inflammation via its receptor Tie2. Angpt2 is originally identified as an antagonist of Tie2, and it subsequently induces endothelial cell activation, thereby facilitating angiogenesis and inflammation. However, Angpt2 has also been demonstrated to be an agonist of Tie2 in a context dependent manner both *in vitro* and *in vivo*. Exogenous Angpt2 has been reported to reduce atherosclerosis development, angiogenesis within the tumour, and cellular infiltration in the ongoing inflammation. Angiogenesis and inflammation have been implicated in aortic aneurysm and in the development of atherosclerosis. In this thesis, I examine the role of Angpt2 in aortic aneurysm and atherosclerosis development, using the angiotensin II (AngII) infused mouse model in apolipoprotein E-deficient (ApoE$^{-/-}$) mice.

Six-month-old male ApoE$^{-/-}$ mice were infused with AngII, in order to induce aortic aneurysm and the progression of atherosclerosis. Human Fc-protein (control), recombinant Angpt2 (rAngpt2), or Angpt2-Tie2 interacting inhibitor (L1-7) was subcutaneously administered to mice for 14 days. rAngpt2 administration significantly inhibited AngII induced suprarenal aortic

expansion ($p=0.002$) and atherosclerosis within the aortic arch ($p=0.017$). rAngpt2 administration also protected AAA from rupture ($p=0.034$). These effects were blood pressure and plasma lipoprotein independent. However, L1-7 administration did not alter AngII-induced AAA development and rupture and atherosclerosis.

By assessing inflammation, it was found that mice receiving rAngpt2 had significant Tie2 activation ($p=0.026$) and less MOMA-2 ($p=0.004$) positive immunostaining area within the aortic tissue, compared with mice receiving control protein, suggesting reduced inflammation. Consistently, in the mice receiving rAngpt2, it was found that there was less monocyte chemoattractant protein-1 (MCP-1) expression ($p=0.004$), within the aortic tissue. The plasma concentration of MCP-1 and interleukin-6 (IL-6) were significantly lower ($p=0.011$ and $p=0.013$ respectively). In mice receiving rAngpt2 for 14 days, Ly6C^{hi} inflammatory monocytes were lower within the peripheral blood ($p=0.003$), but increased within the bone marrow ($p=0.019$). At early stage of AngII infusion (5 days), rAngpt2 administration resulted in the retention of Ly6C^{hi} inflammatory monocytes and the elevation of neutrophils recycling in the spleen. These results suggest that exogenous Angpt2 administration reduced AngII-induced inflammation within the aortic tissue in ApoE$^{-/-}$ mice.

By assessing the angiogenesis, it was found that there was a smaller CD31 ($p=0.002$) positive immunostaining area and no difference in vascular endothelial growth factor expression within the aortic tissue from mice receiving rAngpt2 compared with mice receiving control protein. There was no difference in Akt/eNOS and Erk signalling pathway activation within the aortic tissue between the two groups of mice. These results suggest that mice receiving exogenous Angpt2 had limited angiogenesis within the aortic tissue in the AngII-infused ApoE$^{-/-}$ mice.

It was therefore concluded that exogenous Angpt2 administration attenuated AngII-induced aortic aneurysm and atherosclerosis in ApoE$^{-/-}$ mice associated with reduced aortic inflammation and angiogenesis. Endogenous Angpt2-Tie2 interacting induced Tie2 deactivation was not required for AAA and atherosclerosis development in this AngII infusion mouse model.

Communications, Awards, and Grants

Publications and Conferences

Angiopoietin-2 administration attenuates angiotensin II induced aortic aneurysm and atherosclerosis in the apolipoprotein E deficient mice. **Hongyou YU**, Trollope AF, Woodward L, Kinobe R, Moran CS, Rush CM, Golledge J. *Arteriosclerosis, Thrombosis, and Vascular Biology.* (Submitted and undergoing revision)

Influence of apolipoprotein E, age and aortic site on calcium phosphate induced abdominal aortic aneurysm in mice. Wang Y, Krishna SM, Moxon J, Dinh TN, Jose RJ, **Hongyou YU**, Golledge J. *Atherosclerosis.* 2014; 235:204–212.

Impaired Acetylcholine-Induced Endothelium-Dependent Aortic Relaxation by Caveolin-1 in Angiotensin II-Infused Apolipoprotein-E (ApoE−/−) Knockout Mice. Seto SW. Krishna SM, **Hongyou YU**, Liu D, Khosla S, Golledge J. *PLOS One.* 2013:8(3):e58481.

Angiopoietin-2 reduces angiotensin II-induced abdominal aortic aneurysm formation by attenuating angiogenesis and inflammation in ApoE$^{-/-}$ mice. **Hongyou YU**, Woodward L, Kinobe R, Moran CS, Rush CM, Golledge J. *Australasian Tropical Health Conference;* Abstract, Poster, and Oral Presentation; Cairns, 2014.

Angiopoietin-2 reduces angiotensin II-induced abdominal aortic aneurysm formation by attenuating angiogenesis and inflammation in ApoE$^{-/-}$ mice. **Hongyou YU**, Woodward L, Kinobe R, Moran CS, Rush CM, Golledge J. *North Queensland Festival of Life Sciences*; Townsville, 2014.

Angiopoietin-2 attenuates angiotensin-II induced abdominal aortic aneurysm by limiting MCP-1 expression. **Hongyou YU**, Woodward L, Kinobe R, Moran CS, Rush CM, Golledge J. *A Joint Meeting of the Australian Vascular Biology Society and the Australia and New Zealand Microcirculation Society*; Abstract and Poster; Adelaide, 2013.

Angiopoietin-2 attenuates angiotensin-II induced abdominal aortic aneurysm by limiting MCP-1 expression. **Hongyou YU**, Woodward L, Kinobe R, Moran CS, Rush CM, Golledge J. *North Queensland Festival of Life Sciences*; Abstract and Poster; Townsville, 2013.

The role of angiopoietin-2 in experimental abdominal aortic aneurysm development. **Hongyou YU**, Woodward L, Kinobe R, Moran CS, Rush CM, Golledge J. *North Queensland Festival of Life Sciences*; Oral Presentation; Townsville, 2013.

Angiopoietin-2: a role in abdominal aortic aneurysm development. *3 minutes thesis presentation*, Townsville, 2013.

Angiotensin II reduces Ly6C^{hi} inflammatory monocytes in bone marrow and spleen of ApoE$^{-/-}$ mice. **Hongyou YU**, Woodward L, Kinobe R, Moran CS, Rush CM, Golledge J. *North Queensland Festival of Life Sciences*; Abstract and Poster; Townsville, 2012.

Grants and Awards

Establishment of a microsurgery station. *Research Infrastructure Block Grant,* James Cook University as a student investigator*;* $13,213; 2014.

QTHA travel award for Australasian Tropical Health Conference, $1378, Cairns, Australia, 2014.

The role of angiopoietin-2 in aortic endothelial cells activation in vitro; *Graduate Research Scheme Grant*; $2860; May 2013.

Provision of care for research animal. *Research Infrastructure Block Grant*, James Cook University as a student investigator*;* $16,625; 2013.

Effects of angiopoietin-2 on abdominal aortic aneurysm development; *Graduate Research Scheme Grant;* $1197 ; November 2011.

James Cook University Postgraduate Research Scholarship; James Cook University, May 2011-November 2015.

School of Medicine HDR student support scheme; James Cook University, May 2011-May 2015.

Winner of best poster in PhD student category; *North Queensland Festival of Life Sciences*; Townsville, October 2014.

Winner of best poster in PhD student category; *North Queensland Festival of Life Sciences;* Townsville, October 2013.

Winner of immunology speed dating for student; *Australasian Society for Immunology*; May 2013.

Winner of 3 minutes thesis; *School of medicine and dentistry, James Cook University;* August 2013.

List of Abbreviations

A.U.	Arbitrial Unit
AAA	Abdominal Aortic Aneurysm
ABIN-2	A20 Binding Inhibitor of NF-κB
AngII	Angiotensin II
Angpt	Angiopoietin
ApoE$^{-/-}$	Apolipoprotein E-deficient
ARCH	Aortic Arch
BL	Baseline
BM	Bone Marrow
BMC	Bone Marrow Cell
BP	Blood Pressure
BSA	Bovine Serum Albumin
BSN	Bjurrum Schater-Nielsen
CaCl$_2$	Calcium Chloride
CBA	Cytometric Bead Array
CCR2	C-C Chemokine Receptor Type 2
CI	Confidence Interval
CVD	Cardiovascular Disease
DAPI	4',6-Diamidino-2-phenylindole Dihydrochloride
DBP	Diastolic Blood Pressure
DPBS	Dulbecco's Phosphate Buffered Saline
EC	Endothelial Cell
ECM	Extracellular Matrix
ELISA	Enzyme-linked Immunosorbent Assay
eNOS	Endothelial Nitric Oxide Synthase
FMO	Fluorescence-Minus-One
FSC	Forward Scatter
GAPDH	Glyceraldehyde-3-phosphate Dehydrogenase

HDL	High-density Lipoprotein
HR	Heart Rate
ICC	Intraclass Correlation
IFN	Interferon
IHC	Immunohistochemistry
IL	Interleukin
IQR	Interquartile Range
IRA	Infrarenal Aorta
LDL	Low-density Lipoprotein
LoA	Limits of Agreement
LSD	Least Significant Difference
MBP	Mean Blood Pressure
MCP	Monocyte Chemoattractant Protein
MFI	Median Fluorescence Intensity
MMP	Matrix Metalloproteinase
MVD	Micro-vessel Density
NF-κB	Nuclear Factor Kappa B
NO	Nitric Oxide
OCT	Optimal Cutting Temperature
OD	Optical Density
PBS	Phosphate Buffered Saline
PCNA	Proliferating Cell Nuclear Antigen
PI3K	Phosphatidylinositol 3'-Kinase
rAngpt2	Recombinant Angiopoietin-2
RBC	Red Blood Cell
SBP	Systolic Blood Pressure
SDS	Sodium Dodecyl Sulfate
SEM	Standard Error Of Mean
SI	Staining Index
SMC	Smooth Muscle Cell

SRA	Suprarenal Aorta
SSC	Side Scatter
TBS	Tris Buffer Saline
TBST	Tris Buffer Saline Tweent
Th	T Helper
THX	Thoracic Aorta
Tie2	Receptor Tyrosine Kinase Tie2
TNF	Tumour Necrosis Factor
Treg	T Regulatory
VE-PTP	Vascular Endothelial Phosphotyrosine Phosphatase
VEGF	Vascular Endothelial Growth Factor
VLDL	Very Low-density Lipoprotein

Table of Contents

List of Tables

List of Figures

CHAPTER 1

Introduction

An abdominal aortic aneurysm (AAA) is an abnormal dilatation of the abdominal aorta that extends the normal diameter by 50% or has a maximum aortic diameter ≥ 30 mm (Sakalihasan *et al.*, 2005). This dilatation is permanent and gradually increases, causing a life-threatening aortic rupture (Golledge *et al.*, 2006). As the aorta is a major vessel leading away from the heart, patients with a ruptured aneurysm have high mortality rates (Greenhalgh & Powell, 2008). Aneurysm rupture-related mortality is approximately 1,000 in Australia, 15, 000 in the United States, and 8,000 in the United Kingdom annually (Baxter *et al.*, 2008; Sakalihasan *et al.*, 2005; Golledge *et al.*, 2006).

The management of AAA includes reducing patients' exposure to risk factors, and patient participation in screening programmes. Several risk factors are associated with AAA development, expansion, and rupture, including smoking, atherosclerosis, and family history etc. (Golledge *et al.*, 2006; Reed *et al.*, 1992; Golledge & Norman, 2010). AAA is a gender- and age-specific disease. It affects approximately 2-5% of men aged over 65 years, but only 1.7% of women (Von Allmen & Powell, 2012). Screening programmes, targeting the population group (aged over 65), are essential for AAA diagnosis, as most AAAs are asymptotic until the rupture occurs. Small AAAs constitute 90% of the results of AAA diagnosis in the screening programmes. Ultrasonography is cost-effective for AAA screening, as it can accurately measure the size of the aorta in longitudinal, ante-posterior, and transverse directions (Quill *et al.*, 1989). The main goal of AAA management is to prevent a fatal rupture. Two randomised control trials, the United Kingdom Small Aneurysm Trial and the Aneurysm Detection and Management Study, found that it is safe to keep small aneurysms under surveillance (Participants, 1998; Merali & Anand, 2002). Currently, measurement of the aortic diameter is the only predictor of the risk of rupture, as the incidence of rupture has been found to be high in patients who have an

aneurysm larger than 50 mm. In clinical management, AAA patients with an aortic diameter of ≥ 50 mm are suggested to undergo elective surgical repair, which can significantly reduce the mortality rates compared to those who have surgical repairs of ruptured aortas (Nordon *et al.*, 2011). It has been found that patients who undergo elective sugary retain a better quality of life than patients who undergo emergency repairs for rupture (Hennessy *et al.*, 1998; Clifton, 1977). However, much debate continues over whether aortic diameter is an appropriate rupture predictor, as it is not rare for small aneurysms to rupture. Also arguably, a larger aneurysm may not rupture within the patient's lifespan. Therefore, it is pivotal to develop new non-invasive techniques that may be useful in predicting aneurysm expansion and rupture (Fillinger *et al.*, 2003).

The pathogenesis of AAA is a complex process involving inflammation, extracellular matrix (ECM) remodelling, and angiogenesis (Golledge *et al.*, 2006). Extensive inflammatory cell infiltration is a hallmark of AAA (Shimizu *et al.*, 2006). Activated macrophages are a primary source of matrix metalloproteinases (MMPs) and other proteases that are believed to contribute to aortic wall degeneration (Hellenthal *et al.*, 2009). Inflammation and ECM degradation provide a pro-angiogenic environment, which is conducive to neo-vessel formation (Imhof & Aurrand-Lions, 2006). Angiogenesis is believed to promote the development and progression of AAA by encouraging ECM remodelling and facilitating inflammatory cell infiltration (Golledge *et al.*, 2006; Daugherty *et al.*, 2000; Armstrong *et al.*, 2011). Human AAA rupture is associated with neovascularization (Choke *et al.*, 2006). Indeed, a higher density of micro‑vessels has been reported in biopsies from ruptured AAAs, compared to intact ones (Thompson *et al.*, 1996).

Efficient clinical intervention procedures to limit AAA progression are still lacking (Baxter *et al.*, 2008; Golledge & Norman, 2011). A randomised control trial showed that more than 60% of patients with small aneurysms required surgery within six years, predominantly because their aneurysms reached the intervention size (Participants, 1998). The mechanisms of AAA development and progression have been extensively investigated over the past two decades. Using experimental AAA rodent models, several mechanisms relevant to human AAA have

been identified (Daugherty, 2004). In pre-clinical studies, several approaches targeting these mechanisms have been proven effective in limiting AAA progression (Trollope *et al.*, 2011). However, there are still many challenges in applying these therapeutic interventions to patients (Golledge & Norman, 2011; Baxter *et al.*, 2008). Therefore, the biological factors that initiate aneurysmal degeneration and drive AAA progression must be better understood, to identify potential targets for clinical AAA treatment.

Factors that are related to the pathological features of AAA are potential targets for clinical treatment. Angiopoietins (Angpts) are a family of vascular growth factors, and are mainly expressed in endothelial cells (ECs). Angpts regulate endothelium integrity and inflammation of the aorta (Augustin *et al.*, 2009). Angiopoietin-1 (Angpt1) and Angiopoietin-2 (Angpt2) are two well-characterised ligands for the vascular endothelial receptor tyrosine kinase Tie2 (Tie2) (Koh *et al.*, 2002). The Angpt-Tie signalling axis is an important regulator of vascular homeostasis, angiogenesis, and inflammation (Augustin *et al.*, 2009; Peters *et al.*, 2004). Tie2 activation is essential for maintaining endothelium integrity, anti-permeability, and anti-inflammation effects. It is also required to maintain the quiescent state of the vasculature (Fiedler & Augustin, 2006). Nonetheless, Tie2 is deactivated in the processes that lead to angiogenesis and inflammation (Fiedler *et al.*, 2006; Murakami, 2012; Scharpfenecker *et al.*, 2005).

Angpt2 is an important regulator of angiogenesis and inflammation through regulating its receptor Tie2 (Ahmed *et al.*, 2009). Angpt2 is stored in Weibel-Palade Bodies, where it can be released rapidly to deactivate Tie2 in an autocrine manner in an angiogenic and inflammatory response (Thurston & Daly, 2012; Fiedler *et al.*, 2004; Imhof & Aurrand-Lions, 2006). As an antagonist of Tie2, Angpt2 induces Tie2 de-activation in the ECs (Maisonpierre *et al.*, 1997), which will induce destabilisation of the existing blood vessels. This facilitates vascular endothelial growth factor (VEGF)-mediated angiogenesis and blocks the anti-inflammatory function of Tie2 activation, to sensitise endothelium inflammation mediated by inflammatory cytokines (Holash *et al.*, 1999; Imhof & Aurrand-Lions, 2006). Nevertheless, Angpt2, unlike Angpt1, has a complex role, and dynamically regulates Tie2 in a context-dependent manner

(Thurston & Daly, 2012; Yuan *et al.*, 2009). As a challenge to the antagonistic function of Angpt2, exogenously administered Angpt2 has been demonstrated to activate Tie2 and limit angiogenesis both *in vivo* and *in vitro* (Cao *et al.*, 2007; Chen *et al.*, 2009; Chen *et al.*, 2011; Daly *et al.*, 2006; Yuan *et al.*, 2009).

Circulating levels of Angpt2 in patients with cardiovascular diseases (CVDs) is a topic of debate between researchers. Jaumdally *et al.* reported a significantly decreased Angpt2 level in patients with CVDs compared with healthy ones (Jaumdally *et al.*, 2007), whereas Lorbeer *et al.* reported that circulating Angpt2 level is positively associated with CVDs (Lorbeer *et al.*, 2015). Golledge *et al.* reported that serum Angpt2 is elevated in men with AAA, and associated with an increased risk of cardiovascular mortality in older men (Golledge *et al.*, 2012). Moreover, the up regulation in Angpt2 has been found to have a downstream effect on the factors that are associated with human AAA. For instance, osteopontin, abundantly present in patients with small AAAs, up-regulates Angpt2 expression, subjecting the human ECs to tumour necrosis factor (TNF)-α stimuli (Genre *et al.*, 2014).

Given the important roles of Angpt2 in inflammation and angiogenesis, it is hypothesised that:

1. Angpt2 plays an essential role in the AAA development through the Angpt2-Tie2 signalling pathway; and

2. Increased Angpt2 is associated with AAA progression and rupture.

To test these hypotheses, the Angiotensin II (AngII) infused experimental AAA mouse model in Apolipoprotein E-deficiency (ApoE$^{-/-}$) mouse was employed. This is a well-established mouse model for AAA, which is comparable to human aortic aneurysms including the gender propensity, lumen expansion, ECM fragmentation, and inflammatory cells accumulation (Bruemmer *et al.*, 2011). Six-month-old mice were used as older age is recognized as an important risk factor for human AAA. AngII plays an essential role in CVD development and progression (Daugherty & Cassis, 2004). Indeed, interventions targeting the renin angiotensin system reduced AAA expansion, although its mechanisms in AAA remain to be clarified

(Thatcher *et al.*, 2014). Atherosclerosis is commonly found in the biopsy of human AAA (Golledge & Norman, 2010). In this mouse model, AngII induces atherosclerosis development that is likely independent of the AAA formation, as ApoE$^{-/-}$ mice fed with a western diet develop atherosclerosis without AAA formation (Nakashima *et al.*, 1994) and chronic infusion of AngII into wild-type C57BL/6J mice induced AAA formation in 39% of mice (Deng *et al.*, 2003).

The specific aims of this thesis are to:

1. Assess the role of Angpt2-Tie2 signalling pathway in AAA development and atherosclerosis progression in the AngII infused experimental AAA mouse model;

2. Assess the effects of systemic rAngpt2 administration on AAA development and atherosclerosis progression in the AngII infused experimental AAA mouse model;

3. Define the possible mechanisms by which exogenous Angpt2 may contribute to AAA development and atherosclerosis progression.

CHAPTER 2

Literature Review

2.1 The normal aorta

2.1.1 Anatomy and structure

The aorta is the largest artery in the body, which directly leads away from heart. It originates from the left ventricle of the heart and runs down to the abdomen, where it divides into two smaller arteries. The elasticity of the aorta converts the heart's pulsatile flow to steady flow in peripheral vessels. Based on its anatomical compartment, the aorta is classified as the aortic arch (ARCH), the thoracic aorta (THX), the suprarenal aorta (SRA), and the infrarenal aorta (IRA). Structurally, the aorta consists of three layers separated by elastic laminae, which are known as the tunica intima, the tunica media, and the tunica external or adventitia (**Figure 2.1**). The intima, comprised of a single layer of ECs, forms an interface between the blood and the rest of the artery wall, and is important for maintaining vascular tone and homeostasis. The tunica media is the middle and thickest layer of the artery, characterised by concentric alternating layers of elastin and smooth muscle cells (SMCs). The organisation of the media affords the aorta circumferential resilience, a physical characteristic necessary to facilitate vasodilatation and constriction, and to accommodate haemodynamic changes. The outer layer of the aorta, the Adventitia, is comprised primarily of collagen, which maintains the structural integrity of the vessel, fibroblasts, nerves, and nutrient capillaries (vasa vasorum).
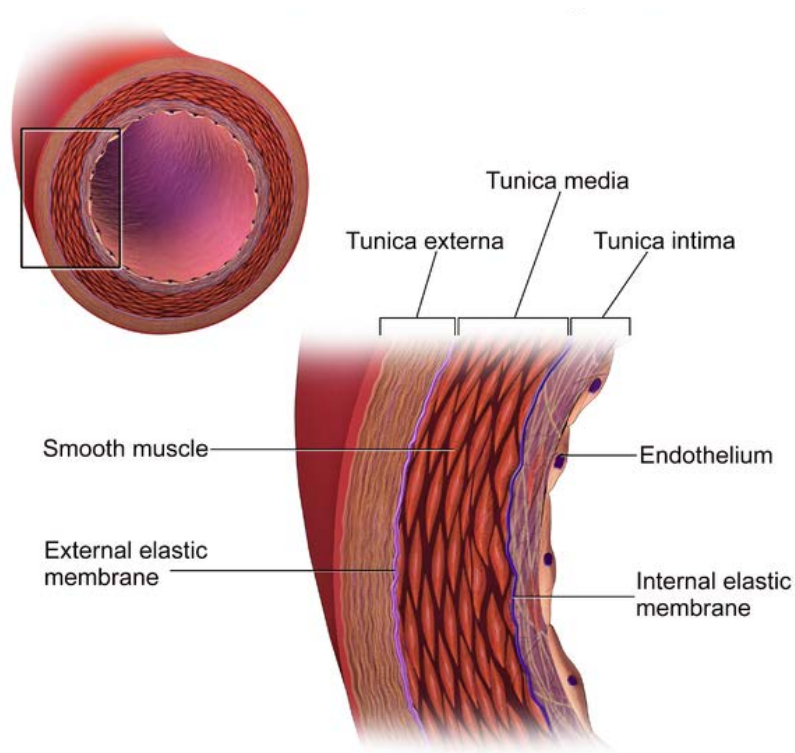
Figure 2.1 The aortic wall
Source: https://upload.wikimedia.org/wikipedia/commons/c/c8/Blausen_0055_ArteryWallStructure.png.

2.1.2   Physiology and response to pathological stimuli

The *endothelium* is a monolayer of tight junction ECs that plays a critical role in vascular

homeostasis (Tousoulis *et al.*, 2006). ECs produce a balance of vasodilator and vasoconstrictor

factors to modulate vasomotor tone. The endothelium maintains an anti-thrombotic and anti-

inflammatory state to strictly control the exchange of lipoproteins and leukocytes between the

bloodstream and aortic wall (Tousoulis *et al.*, 2006). Under pathological conditions, impaired

endothelium-derived vasodilatation is implicated in the progression of CVD (Cai & Harrison,

2000). In the presence of cardiovascular risk factors, EC activation is the initial step of most

CVDs (Nakashima *et al.*, 1998; Dai *et al.*, 2004), whereby activated ECs express adhesion

molecules and increase permeability to capture and extravasate immune-inflammatory cells

(Saito *et al.*, 2012). The accumulation of these cells within the aortic wall propagates an

immune-inflammatory response involving ECM degradation via the action of MMPs (Freestone *et al.*, 1995).

The *aortic media* contains ECM and SMCs that are essential for vessel homeostasis and the maintenance of the mechanical proprieties of the aorta (Wolinsky & Wolinsky, 1964). Imbalance of ECM degradation and synthesis contributes to the pathogenesis of the CVDs (Libby & Lee, 2000). For instance, accumulation of stiffer collagen and loss of elastin result in aortic stiffness in a hypertensive and ageing aorta (McEniery *et al.*, 2007). Loss of elastin and degradation of collagen cause aortic wall weakening and ultimately cause rupture (Knox *et al.*, 1997). ECM also supports lipoprotein binding and accumulation within the aortic wall to initiate atherosclerosis development (Olin *et al.*, 1999). In response to atherogenic and cytokine stimulus, medial SMCs migrate to the intima and switch to a "synthetic" phenotype with high capacity for collagen synthesis and lipid up-take, to form a fibrous cap and foam cells respectively (Doran *et al.*, 2008; Raines & Ferri, 2005). Medial SMCs support infiltrated inflammatory cell survival by direct contact with adhesion molecules (Isner *et al.*, 1995; Stary *et al.*, 1995). In return, the inflammatory cells generate mediators to provoke SMC death, that consequently reduces collagen synthesis and release of proteases. This results in progressive aortic wall weakening and aneurysm formation (Libby, 2009).

The *adventitia* is a collagen-rich connective tissue containing fibroblasts, resident immune cells, and vasa vasorum (Majesky *et al.*, 2011). Evidence is emerging showing that the adventitia plays a critical role in vascular "outside-in" inflammation, that is, inflammation initiating in the adventitia and progressing toward the intima (Michel *et al.*, 2007; Recinos *et al.*, 2007; Ramshaw *et al.*, 1994). Adventitial inflammation has been implicated in aortic aneurysms and atherosclerotic vascular disease (Coen *et al.*, 2011). Indeed, adventitia contains major immune cells that have been observed in human aneurysmal tissue (Kuivaniemi *et al.*, 2008; Nangaku *et al.*, 2007). Experimental studies have revealed the involvement of adventitial mast cells, for example, in aortic aneurysm formation in ApoE^{-/-} mice (Tsuruda *et al.*, 2008). The vasa vasorum, a network of small blood vessels supplying the aortic adventitia, serves as a conduit

for inflammatory cell transportation to the inner layers of the aortic wall (Gavrila *et al.*, 2005; Gossl *et al.*, 2007; Herrmann *et al.*, 2001; Moulton *et al.*, 2003).   Animal studies have demonstrated that development of vasa vasorum is positively correlated with the severity of vascular disease (Gossl *et al.*, 2007). Moreover, phenotype-switch and proliferation in adventitial fibroblast is believed to be important in aortic aneurysm and atherosclerosis. Using a mouse model, Tieu and colleagues described the interaction between adventitial fibroblasts and infiltrating leukocytes to promote vascular inflammation, ECM remodelling, and aortic destabilisation (Tieu *et al.*, 2009). Arora and colleagues reported that adventitial fibroblasts switched into myofibroblasts that subsequently migrated to intimal lesions in response to injury (Arora & McCulloch, 1994).

2.2   Abdominal aortic aneurysms (AAA)

2.2.1   AAA and its prevalence

AAA is defined as a dilatation of the abdominal aorta that exceeds the normal aortic diameter by 50% or maximum aortic diameter ≥ 30 mm (Sakalihasan *et al.*, 2005). The dilatation is permanent and progressive, resulting in weakening of the aortic wall and eventually aortic rupture (Golledge *et al.*, 2006). The ruptured cases have a high mortality rate because the aorta is the major vessel leading away from the heart (Greenhalgh & Powell, 2008). Most AAAs are asymptotic and often detected incidentally by other abdominal physical examination.

AAA is a sex and age specific disease. It affects approximately 2-5% of men aged over 65 years, but only 1.7% of women (Von Allmen & Powell, 2012). Nowadays, AAA screening programmes have been successfully implemented, and the risk factors for AAA have been well managed. The prevalence of AAA has declined to the lowest reported 1.7% in men over 65 (Von Allmen & Powell, 2012). However there is not much changed in older women (Greenhalgh & Powell, 2008). There are approximately 1,000 deaths related to aneurysm rupture in Australia annually, while there are 15, 000 in the United States, and 8,000 in the United Kingdom (Baxter *et al.*, 2008; Sakalihasan *et al.*, 2005; Golledge *et al.*, 2006).

2.2.2   AAA Diagnosis and screening

The AAA diagnosis is accurate and efficient with imaging techniques such as ultrasonography. Ultrasonography is a simple and cost-effective to accurately measure the size of the aorta in longitudinal, anteroposterior, and transverse directions (Quill *et al.*, 1989). Therefore, it has been used in the initial assessment, follow-up surveillance, and screening for high-risk populations. The screening programmes are essential for AAA diagnosis, as most of the AAAs are asymptotic until rupture. Small AAA constitutes 90% of the AAA diagnosis in the screening programmes (Alcorn *et al.*, 1996). The limitation of ultrasonography is that it cannot distinguish the features of AAA such as the thickness of the aortic wall and mural thrombus. It is also impossible to be diagnostic of aneurysm rupture. The other image techniques such as

Computerised Tomography scan and Magnetic Resonance Imaging can provide details of the individual AAA to facilitate the surgical procedures (Sakalihasan *et al.*, 2005). The Computerised Tomography scan can also be used to evaluate the risk of rupture by visualising the blood within thrombus (an imminent rupture marker) and the extravasation by introducing contrast materials to the blood stream (Klink *et al.*, 2011). Magnetic Resonance Imaging can evaluate the aneurysm wall stress and tension that are thought to be more accurate in rupture prediction than size of the aneurysm (Fillinger *et al.*, 2003; Vorp & Vande Geest, 2005; Klink *et al.*, 2011).

2.2.3　　　Risk factors for AAA

Large-scale and cross-sectional studies have been performed to describe the risk factors for AAA. Through epidemiological screening studies, AAA is known to be closely associated with advanced age, male sex, atherosclerosis, hypertension, cigarette smoking, and genetic predisposition (Golledge *et al.*, 2006; Alcorn *et al.*, 1996). Female gender and diabetes are negative associated with AAA (Lederle *et al.*, 2000; Shantikumar *et al.*, 2010). Risk factors currently believed to be associated with AAA are summarised in **Table 2.1**.

Smoking is a most important risk factor for AAA development, expansion, and rupture (Brady *et al.*, 2004). There is overwhelming evidence of a significant clinical association between smoking and aortic aneurysm (Murphy *et al.*, 1998; Vardulaki *et al.*, 2000). The risk of AAA development in chronic smokers is four times greater than in non-smokers, and the aneurysm growth rate is higher in current smokers compared with non-smokers (Brady *et al.*, 2004; Sakalihasan *et al.*, 2005). The mechanisms of tobacco smoking on AAA remain unknown. Murphy *et al.* suggested that the function of Nicotine on α1-anti-trypsin oxidisation and its metabolite cotinine could contribute to the development of AAA (Murphy *et al.*, 1998). In addition, Nordskog *et al.* reported that tobacco smoking may stimulate human ECs and macrophages/monocytes to release proteolytic enzymes and neutrophils to release elastase and MMPs (Nordskog *et al.*, 2005).

The relationship between atherosclerosis and AAA remains uncertain (Golledge & Norman, 2010). Atherosclerosis is commonly associated with AAA and is a universal finding in the degenerated aortic wall; therefore, atherosclerosis is considered a potential cause of AAA (Dobrin, 1989). This theory, however, has been challenged by evidence arising from more recent epidemiological, genetic, biochemical, and aetiological studies (Nordon *et al.*, 2011). For example, the prevalence of atherosclerosis largely exceeds that of AAA. There are approximately 48% of men developing atherosclerosis, while AAA only occurs in approximately 5% men older than 60 (Jaffer *et al.*, 2002). Moreover, atherosclerosis disease was more common in black Americans compared with white Americans, whereas AAA was the reverse (LaMorte *et al.*, 1995). These facts suggest that atherosclerosis is unlikely to be the cause of AAA, but shares similar pathological processes and some traditional risk factors.

Table 2.1 Risk factors for AAA

Risk factors	Evidence	Reference
Male gender	Five times prevalence than female	(Lederle, 2011)
Ethnicity	More common in Caucasians than Asians or Africans	(Salem *et al.*, 2009)
Age	High prevalence ≥ 60 years old Increases by 40% every 5 years after 65 years old	(Vardulaki *et al.*, 2000)
Smoking	Four times prevalence of AAA compared with non-smoker	(Sakalihasan *et al.*, 2005)
	Higher aneurysm expansion rate	(Brady *et al.*, 2004)
Hypertension	A high diastolic blood pressure (DBP) with rupture A weak association with AAA	(Wilmink *et al.*, 2002)
Genetic component	~19.2% AAA patients with a positive family history	(Helgadottir *et al.*, 2008)
	~70% heritability in twins	(Wahlgren *et al.*, 2010)
	Genetic component contributing 75% susceptibility	(Sandford *et al.*, 2007)
Atherosclerosis	Common finding in AAA biopsy	(Golledge & Norman, 2010)
Hyperlipidaemia	High plasma cholesterol positively associated with risk of an AAA High-density lipoprotein reduced the risk of AAA	(Forsdahl *et al.*, 2009)
Diabetes mellitus	Negative associated with AAAs Slow AAA expansion	(Shantikumar *et al.*, 2010)
Female gender	Less prevalence than Male	(Cho *et al.*, 2009)

2.2.4 Management of AAA patients

The main goal of AAA management is to prevent a fatal rupture. Two randomised control trials, the United Kingdom Small Aneurysm Trial and the Aneurysm Detection and Management Study, suggested that it is safe to keep patients with small aneurysm under surveillance, with education to reduce exposure to the risk factors for AAA (Participants, 1998; Merali & Anand, 2002). There is still a lack of effective pharmacological therapies to completely inhibit aortic aneurysm growth and prevent rupture. The efficiency of the currently available drugs targetting the mechanisms implicated in AAA pathology still need further investigation with a large clinical trial (Golledge & Norman, 2011).

Surgical intervention is the only treatment for ruptured AAA, or AAA with high risk of rupture (Nordon *et al.*, 2011). The two primary methods of aneurysm repair are surgical open repair and Endo-Vascular Aneurysm Repair (participants, 2005a). The conventional open surgical repair is suitable for fit patients who can tolerate the major surgery. Endo-Vascular Aneurysm Repair is a less invasive approach that is suitable for most of the patients with an aneurysm $\geq$ 55 mm (participants, 2005b). Three randomised control trials showed that Endo-Vascular Aneurysm Repair could significantly reduce the 30-day mortality compared with open surgical repair, whereas there was no difference in mortality and health-related quality of life between the two groups after the first postoperative year (participants, 2005a; participants, 2005b; Blankensteijn *et al.*, 2005). The incident of rupture is high in patients who have an aneurysm $\geq$ 50 mm (Choke *et al.*, 2005). AAA patients with an aortic diameter $\geq$ 50 mm need to undergo elective surgical repair, which can significantly reduce mortality rate compared with surgical repair of the ruptured cases (Nordon *et al.*, 2011). It is found that the patients with elective sugary retain a better quality of life compared to patients undergoing emergency repair after rupture (Hennessy *et al.*, 1998; Clifton, 1977). However, both surgical open repair and Endo-Vascular Aneurysm Repair have their limitations (participants, 2005b). It is still a high priority to identify effective medical therapies that could reduce the growth rate of the small AAAs and ultimately prevent them from rupture.

2.2.5   Predicting AAA progression and rupture

Rupture is a severe consequence of AAA, with a high mortality rate (Thompson *et al.*, 2002). The benefits of selective surgical repair AAA before its rupture have been discussed above. Therefore, it is pivotal to find reliable parameters for aneurysm expansion and rupture prediction (Fillinger *et al.*, 2003). Nowadays, the aortic diameter is the accepted standard to predict the risk of rupture, as the incidence of rupture is doubled when an aneurysm reaches a diameter ≥ 55 mm (Sakalihasan *et al.*, 2005). However, there is still much debate as to whether aortic diameter is appropriate for rupture prediction, as it is not rare for small aneurysms to rupture (Limet *et al.*, 1991). It is also arguable that a larger aneurysm may not necessarily rupture within the patient's lifespan (Baxter *et al.*, 2008). Some researchers proposed that biomechanics-based approach was superior to the maximum diameter assessment (Vorp & Vande Geest, 2005). The understanding of the pathophysiology of AAA provides the possibility of choosing specific circulating biomarkers to predict AAA growth and risk of rupture, and to determine the efficiency of therapies (Hellenthal *et al.*, 2009c; Hellenthal *et al.*, 2009b; Treska *et al.*, 2000). The biomarkers associated with AAA progress have been intensively studied in clinical trials and summarised risk factors and biomarkers are listed in **Table 2.2** (Hellenthal *et al.*, 2009c; Hellenthal *et al.*, 2009b; Fillinger *et al.*, 2003; Choke *et al.*, 2005; Golledge *et al.*, 2012; Golledge *et al.*, 2004). However, there is still lack of a reliable biomarker for predicting AAA expansion and rupture. State-of-the-art applications, such as proteomics and mass spectrometry imaging, might help to identify biomarkers that will lead to new diagnostic and therapeutic strategies, solving the challenge of AAA progress and rupture prediction.

Table 2.2 Biological factors associated with AAA progress and rupture

Risk factors	Association	References
Factors associate with risk of rupture		
Diameter	9.4% ruptured for AAA of 55 to 59 mm; 10.2% ruptured for AAA of 60-69 mm; and 32.5% ruptured for AAA ≥ 70mm	(Lederle *et al.*, 2002)
Expansion rate	High expansion rate is associated with increased rupture risk	(Brown *et al.*, 2003)
Female sex	Risk of rupture aortic diameter is smaller compared with male gender	(Brown *et al.*, 2003)
Blood pressure	A high DBP is associated rupture risk	(Lindblad *et al.*, 2005)
Smoking	~ Four times incidence of rupture in current smoking patients compared with Non-smoking ones	(Forsdahl *et al.*, 2009)
Wall stress	Peak AAA wall stress associated with increased rupture risk	(Fillinger *et al.*, 2003)
Biomarker associate with AAA progression		
Inflammation	Inflammatory Cytokines; MIF; Osteoprotegrin; tPA	(Hellenthal *et al.*, 2009a) (Golledge *et al.,* 2004)
ECM degeneration	MMPs; Tissue Inhibitor of MMPs; serum elastin-peptide; PIIINP	(Hellenthal *et al.*, 2009b) (Golledge *et al.,* 2004)
Angiogenesis	VEGF	(Kaneko *et al.*, 2011)

MIF: macrophage migration inhibitory factor; tPA: tissue-type plasminogen activator; PIIINP: procollagen-IIIN-terminal pro-peptide

2.2.6 Pathogenesis of AAA

AAA development and progression are the consequences of multiple ongoing factorial processes; however, little is known about the initiation of AAA. The histological features of human late stage AAA include disruption and degradation of elastin, high collagen content, diminutive SMCs, high number of medial micro-vessels, and inflammatory cell infiltration (Hellenthal *et al.*, 2009a). Experimental AAA studies have suggested that AAA development is a dynamic process that involves ECM degradation, followed by inflammation and angiogenesis within the aortic wall (Manning *et al.*, 2002). These studies of human and experimental AAAs highlight the important roles of proteolytic ECM degradation, inflammation, and angiogenesis in AAA development and progression (Michel *et al.*, 2011; Choke, 2006; Wassef *et al.*, 2001).

Aneurysm dilatation is the consequence of connective tissue destruction within the aortic wall (Davies, 1998) and alternation of connective tissue is a key feature of AAA (Thompson *et al.*, 2002; Lindholt *et al.*, 2001b). The initiation and progression of AAA is partially due to improper remodelling of ECM arising from an imbalance in the synthesis and degradation of structural proteins, such as collagen (Dobrin & Mrkvicka, 1994). Elastin sustains the mechanical stress of pulsation, and collagen is responsible for resistance of the aorta (Antoniou *et al.*, 2011). An increase in elastin-degrading enzymes and loss of elastic fibres were observed in human AAA (Baxter *et al.*, 1994). This, together with collagen degradation, is the ultimate cause of aneurysm rupture (Antoniou et al., 2011, #140; (Vorp & Vande Geest, 2005). Dobrin *et al.* demonstrated that elastin degradation alone was associated with aortic dilatation, while collagen degradation was essential for aneurysm rupture (Dobrin & Mrkvicka, 1994). SMCs are an important source of elastin and collagen; therefore, SMC apoptosis and subsequent attrition in the population of these cells within the artery wall is likely associated with the inadequate ECM remodelling that underlies AAA development (Henderson *et al.*, 1999; Rowe *et al.*, 2000). ECM remodelling in the aortic wall is dependent on the production of protease by resident cells and infiltrated inflammatory cells (Shimizu *et al.*, 2006). Proteases activation within the AAA wall includes members of MMPs, cysteine, and serine protease families (Hellenthal *et al.*, 2009c). Study of human aortic aneurysm suggests an acceleration of connective tissue breakdown, up-regulation of different MMPs, and reduction of tissue inhibitor of metalloproteinases (TIMPs) within the aortic wall (Brophy *et al.*, 1991; Davies, 1998). An increased concentration of MMPs, such as MMP8 and MMP9, has been demonstrated at the rupture site of AAA tissue (Choke *et al.*, 2006). Expression of α1-antitrypsin, an inhibitor of proteolytic enzymes, was found to be abnormal in human AAAs (Pulinx *et al.*, 2011). The active form of MMP2 and MMP9 has been shown at higher levels in both AAA tissue and serum of AAA patients compared with healthy controls (Lindholt *et al.*, 2001a; Sakalihasan *et al.*, 1996), while the incidence of elastase-induced AAAs was significantly reduced in a MMP9

deficiency mouse model (Pyo *et al.*, 2000). These are supporting evidence for the role of protein-degrading enzymes in AAA.

Chronic inflammation is considered to be an important feature of AAA, as inflammatory cell infiltration is observed in the media and adventitia of the aorta, and pro-inflammatory cytokines were abundantly presented in human aortic aneurysms (Hellenthal *et al.*, 2009a). It is still largely unknown whether inflammation cell accumulation in the medial and adventitia is the cause of AAA, or a secondary outcome of the ECM remodelling, as elastin degradation peptides could attract mononuclear phagocytes to the aortic wall through ECM breakdown (Hance *et al.*, 2002; Lacraz *et al.*, 1995). Accumulated inflammatory cells are activated by pro-inflammatory cytokines to produce MMPs, leading to ECM degradation and aortic aneurysm formation (Eagleton, 2012). Indeed, Samadzadeh and colleagues found that circulating monocytes in AAA patients had enhanced MMP9 production (Samadzadeh *et al.*, 2014). A Deficiency of inflammatory monocytes in the circulating blood inhibited AAA development in the animal model (MacTaggart *et al.*, 2007; Ishibashi *et al.*, 2004). Pro-inflammatory cytokines also regulate the SMC apoptosis that is implicated in the AAA progression (Jordan *et al.*, 1997). Inflammatory cells release a number of angiogenic factors to promote neovascularisation (Albini *et al.*, 2005). The newly formed micro-vessels are leaky, and that induces further inflammatory cell infiltration (Ribatti *et al.*, 2008). The inflammatory cells observed within the human aortic wall are mainly macrophages, lymphocytes, inflammatory monocytes, neutrophils and mast cells (Koch *et al.*, 1990).

Macrophages are a key source of MMPs and pro-inflammatory cytokines leading to ECM degradation and inflammatory cell activation and recruitment, respectively (Krettek *et al.*, 2004; Lepidi *et al.*, 2001; Eagleton, 2012). Assessment of the late-stage surgical AAA samples showed that macrophages only constituted 2% of the isolated inflammatory cells (Forester *et al.*, 2005). However, this could not represent the early stage of the aneurysm formation. The

paucity of macrophages at the late-stage human AAAs are supported by elastase infusion experimental AAA that macrophages regressed to control level at late stable aneurysm stage (Anidjar *et al.*, 1992). In this study, macrophage infiltration was observed at the early stage of aneurysm formation, and was correlated with the progressive enlargement of the aneurysm. There are two distinct phenotype macrophages: classically activated (M1) and alternatively activated (M2) macrophages. M1 macrophages are predominantly present in the chronic inflammation sites, and promote tissue degradation via production of proteolytic enzymes and pro-inflammatory mediators (Hasan *et al.*, 2012). M1 macrophage associated pro-inflammatory cytokines, such as TNF-α, interleukin (IL)-6, and IL-β, were elevated in AAA patients and interferon-γ (IFN-γ), a stimulator for M1 macrophage polarisation, had a positive correlation with AAA progression (Juvonen *et al.*, 1997). Experimental AAA modes indicated that deletion of M1 polarisation related receptor and stimulus reduced macrophage infiltration and attenuated AAA formation (Blomkalns *et al.*, 2013; Johnston *et al.*, 2014; Xiong *et al.*, 2009b). M2 macrophages are associated with anti-inflammation and wound repair; therefore an imbalance of M1 and M2 macrophages is proposed in AAA development and progression (Hasan *et al.*, 2012). In assessing M2 macrophage marker CD206, the presence of M2 macrophage in human AAA and experimental AAA were contradictory (Dutertre *et al.*, 2014; Rateri *et al.*, 2011; Boytard *et al.*, 2013). These contradictory data may be related to the difference between human and experimental AAA, or poor M2 macrophage identification by CD206 marker only.

T lymphocytes are abundantly accumulated in human AAA, and the majority of CD4+ T cells are T helper (Th) cells (Schonbeck *et al.*, 2002). Th cells are divided into three subsets: Th1, Th2, and Th17 (Shimizu *et al.*, 2006). Th1 cells are activated by IL-12 to produce IFN-γ that activates macrophages (Xiong *et al.*, 2004). In human aneurysm, IFN-γ is over expressed, suggesting a role of Th1 polarisation in the late stage of human AAA (Galle *et al.*, 2005). However, experimental AAA showed contradictory data. For example, CD4 deficient mice have no aneurysm formation in the $CaCl_2$ mouse model (Xiong *et al.*, 2004), whereas loss of mature T cells still produced aneurysm in AngII-infused ApoE$^{-/-}$ rag-1$^{-/-}$ mice (Uchida *et al.*, 2010). Th2

type lymphocytes modulate the immune response by attracting other inflammatory cells and stimulating the macrophages/monocytes to produce MMPs (Lindholt & Shi, 2006; Duftner *et al.*, 2006). Although there is an increased level of Th2-associated cytokines in human aneurysm tissue, the experimental AAA data is contradictory in the role of Th2 cells in AAA formation (Dale *et al.*, 2015). Th7 cells produce IL-17 to promote macrophages recruited to the aortic wall. There is also emerging evidence showing that Th7 cells promote inflammation that was implicated in the experimental aneurysm formation (Dale *et al.*, 2015). T regulatory (Treg) cells remove auto reactive T cells and block IFN-γ and TNF-α expression, thereby preventing macrophage activation induced ECM degradation (Shimizu *et al.*, 2006). Indeed, the proportion of Treg cells was reduced in the AAA patients (Yin *et al.*, 2010) and translating splenic Treg cells attenuated AngII-induced AAA formation in ApoE$^{-/-}$ mice (Zhou *et al.*, 2015).

Inflammatory monocytes, expressing C-C chemokine receptor type 2 (CCR2) antigen, were increased in human AAAs (Ghigliotti *et al.*, 2013). Inflammatory monocytes egress from bone marrow (BM) to peripheral blood and enter peripheral tissue in dependence of monocyte chemoattractant protein (MCP-1)-CCR2 axis (Crane *et al.*, 2009; Jia *et al.*, 2008). Inflammatory monocytes preferentially migrate into the aortic wall and predominantly differentiate into macrophages (Jia *et al.*, 2008; Swirski *et al.*, 2007). In pre-clinical studies, circulating inflammatory monocytes are diminished in CCR2 deficient mice (Jia *et al.*, 2008; Crane *et al.*, 2009). Consistently, AAA development was suppressed in the CCR2-/- mice (Ishibashi *et al.*, 2004a; Daugherty *et al.*, 2010; Boring *et al.*, 1998).

Neutrophils and mast cells have been observed in human and experimental AAA tissue (Anidjar *et al.*, 1992; Ramos-Mozo *et al.*, 2011). Neutrophils are a source of MMP2 and MMP9 and Neutrophil depletion inhibited experimental AAA formation (Eliason *et al.*, 2005). Polymorphonuclear neutrophils from AAA patients have diminished catalase levels (Ramos-Mozo *et al.*, 2011). Mast cell-dependent activation MMPs show strong correlation with SMCs apoptosis, augmentation of inflammation, and neovascularization that are associated with AAA pathogenesis (Swedenborg *et al.*, 2011). In human AAA tissue, mast cells were abundantly

presented in the media compared with the control aorta, and the density of mast cells was correlated with the neovascularisation area (Mayranpaa *et al.*, 2009). Mast cell deficient mice failed to develop AAA in response to elastase perfusion or peri-aortic chemical injury, which was resolved by reconstitution with BM derived mast cells from TNF- α $^{-/-}$ mice instead of IL-6 $^{-/-}$ or IFN- γ $^{-/-}$ mice. This suggests that the mast cell participates in AAA development by releasing IL-6 and IFN-γ (Sun *et al.*, 2007).

2.2.6.3   Angiogenesis in AAA

Medial neovascularisation is a feature of established AAA in humans (Choke *et al.*, 2006; Thompson *et al.*, 1996). The evidence of angiogenesis presenting in human AAAs is shown in **Table 2.3**. Histopathological studies of late stage human AAA samples demonstrated that angiogenesis is an ongoing process associated with the increased inflammation and the risk of rupture (Paik *et al.*, 2004; Choke *et al.*, 2006; Thompson *et al.*, 1996). Indeed, recombinant human VEGF treated mice exhibited higher incidence of AAA in response to AngII infusion with larger maximum aortic diameters compared with vehicle control mice (Choke *et al.*, 2010). Studying human AAA tissues, Choke and colleagues reported an up-regulated gene expression of key angiogenic factors and increased medial neovascularisation in the edge of ruptured AAA compared with paired aneurysm anterior sac (Choke *et al.*, 2006). Homes *et al.* found that there was 15 times higher micro-vessel density (MVD) in human AAAs compared with control healthy aorta (Holmes *et al.*, 1995). Spin *et al*. assessed the SRA from AngII-infused mice using whole genome expression profiling, and found that the angiogenesis signalling pathway was up-regulated among other signalling pathways (Spin *et al.*, 2011). Kaneko *et al.* reported that VEGF-A was over-expressed in both experimental and human AAAs, and inhibited VEGF-A receptor attenuated experimental AAA development associated with angiogenesis *in vivo* (Kaneko *et al.*, 2011). Furthermore, inhibition of angiogenesis in the mouse model is associated with reduced inflammatory cell infiltration, MMP activity, and ECM degradation, resulting in the protection against induced AAA (Kaneko *et al.*, 2011). Overall, these results support the role of angiogenesis in aneurysm progression and rupture. This mechanism is potentially linked

Table 2.3 Evidence of neovascularisation in human AAAs

Reference	Sample	Method	Result
(Thompson *et al.*, 1996)	Surgical AAA samples compared with atherosclerotic samples	IHC	Nevascularisation in all layers of aneurysm; Neovascularisation positively correlated with inflammatory infiltration;
(Choke *et al.*, 2006)	Aneurysmal ruptured edge samples compared with paired anterior sac	IHC & RT-PCR	Up-regulation of pro-angiogenic cytokines; Increased medial neovascularization at the aneurysm rupture edge;
(Scott *et al.*, 2013)	Elective surgical AAA samples compared with age-matched aortic tissue	IHC	Increased micro-vascular density; Maximal vascularity in the inflammatory area; Increased VEGFR-3 and VEGF-A expression;
(Paik *et al.*, 2004)	Elective surgical AAA samples compared with normal aortic tissues	IHC	Increased wall vascularisation; Neovascularisation in the medial, adventitia, and intima;
(Kaneko *et al.*, 2011)	Elective surgical AAA samples compared with autopsy aortic tissues unrelated to AAA	IHC	Marked inflammatory cells; Increased VEGF-A expression and MVD;
(Holmes *et al.*, 1995)	AAA tissues compared with non-AAA related aortic tissue	IHC	Increased neovascularisation in AAA tissues;

with ECM remodelling, facilitating tube formation, EC migration, and inflammatory cell recruitment (Jeltsch *et al.*, 2013; Fukuhara *et al.*, 2010; Jackson, 2002; Pepper, 2001). Micro-vessels in AAA are poorly organised and highly permeable. ECs of these vessels are activated and express adhesion molecules crucial for leukocytes adhesion and transmigration into aortic wall, thereby promoting inflammation (Vijaynagar *et al.*, 2013). The infiltrated inflammatory cells produce angiogenic factors inducing further angiogenesis (Carmeliet, 2003). This cycle potentiates inflammation and ECM degeneration within the aneurysm wall. Indeed, the degree of neovascularisation is positively associated with the extent of the inflammatory cell

infiltration and accumulation within the aortic wall of human AAA (Thompson *et al.*, 1996; Holmes *et al.*, 1995).

2.2.7   **Experimental AAA murine models**

Knowledge regarding AAA aetiology and pathogenesis is still lacking. Histological analyses of the aneurysm wall from surgery could characterise the pathological changes; however, it gives less information on the process of the AAA development. Therefore, *in vivo* animal models are critical in order for researchers to understand AAA pathogenesis and develop new interventions for AAA treatment. There are several experimental AAA murine models established for studying the mechanisms of AAA, and examples of experimental AAA murine model are given in **Table 2.4** (Daugherty, 2004; Tsui, 2010). The three commonly used experimental AAA models are the calcium chloride ($CaCl_2$) model, the elastase infusion model, and the systemic AngII infused into hyperlipidaemia ApoE$^{-/-}$ mice model.

2.2.7.1   *Calcium chloride induced experimental AAA mouse model*

The $CaCl_2$ experimental AAA model was first developed in rabbits by applying $CaCl_2$ (0.25-1.0 M) to the adventitia surface of the aorta between the rental branches and iliac bifurcation (Wang *et al.*, 2013). This approach would not immediately have induced aortic expansion and there was significant luminal expansion in three weeks (Gertz *et al.*, 1988). In the C57BL/6 mice, an AAA was formed in three weeks after the $CaCl_2$ was applied. The histological features of the AAA include vascular SMC depletion, elastin degeneration, inflammatory cell infiltration, and high expression of pro-inflammatory cytokines and MMPs (Yoshimura *et al.*, 2005; Chiou *et al.*, 2001). These pathological features have been observed in the biopsy of human AAAs, which suggests this is a clinically relevant model.

The $CaCl_2$ mouse model has been used to investigate the roles of different factors in AAA formation and expansion. Proteas-driven ECM degeneration within the aortic media and adventitia has been considered to be critical in AAA formation and progression, as MMPs were

Table 2.4 Examples of experimental AAA murine model

Model of AAA	Characteristics	Relevant to human AAA
Genetically predisposed model		
Blotchy (Andrews *et al.*, 1975)	Medial Degeneration; Predominantly in THX;	Irrelevant copper levels in AAA patients;
LDL receptor -/- (Tangirala *et al.*, 1995)	Medial degeneration; Atherosclerosis;	High serum triglycerides; Similar position as human AAA; Medial elastolysis;
ApoE$^{-/-}$ mice (Ishibashi *et al.*, 1994)	Medial Degeneration; Thickening of the adventitia; "Pseudo-micro aneurysms";	High serum triglycerides; AAA generated in male elder mice without saturated fat diet;
Chemical model		
Calcium Chloride (Wang *et al.*, 2013)	Inflammation; Medial degeneration;	Similar to human AAAs with medial elastic disruption and inflammatory response;
Elastase infusion (Halpern *et al.*, 1994)	Inflammation; Medial degeneration;	Support the role of elastolytic activity in medial disruption;
AngII infusion model		
ApoE$^{-/-}$ mice (Daugherty *et al.*, 2000)	Inflammation; Medial degeneration; Atherosclerosis and dissection;	Gender propensity; Atherosclerosis; Inflammatory cells infiltration; Angiogenesis; Hyperlipidemia;
C57BL/6 (older) mice (Tieu *et al.*, 2009)	Dissection; Inflammation; Medial degeneration;	Match to clinical elder population without genetically modification;

abundantly expressed in human AAA tissue (Knox *et al.*, 1997). Mice with MMP2 and/or MMP9 gene knockout showed attenuated AAA formation in this mouse model (Xiong *et al.*, 2009a; Longo *et al.*, 2002). Anti-inflammatory agents, such as doxycycline and pentagalloyl glucose, have been demonstrated to reduce AAA formation using this mouse model (Isenburg *et al.*, 2007; Prall *et al.*, 2002). Chemokine plays an important role in inflammatory cells egressing from BM and infiltrating in the aortic wall. CCR2 gene knockout mice showed attenuated AAA formation with reduced inflammatory cell infiltration, whereas CCR5 and Chemokine receptor

CXCR3 gene deletion has no effects on AAA formation in this mouse model (MacTaggart *et al.*, 2007).

2.2.7.2   Elastase infusion induced experimental AAA mouse model

The Elastase infusion induced experimental AAA model is another important model used to investigate the pathogenesis of AAA. The procedure involves the insertion of a catheter *via* the femoral aorta into the iliac bifurcation, and isolation of a segment of the abdominal aorta that is perfused with hog pancreatic elastase for 5 min (Halpern *et al.*, 1994). The infused pancreatic elastase results in the disruption of media elastin network, to induce an immediate aortic dilatation with AAA formation in 2-5 days in rats (Anidjar *et al.*, 1990). This approach can induce 100% greater aortic dilatation compared with the aortic diameter before perfusion. The histological features of the AAA include inflammatory cell infiltration, high concentrations of MMPs, and pronounced medial elastic lamellae destruction (Thompson *et al.*, 2006).

The elastase infusion model has been used to investigate the role of chronic inflammation, MMPs, and risk factors on AAA formation. Gadowski *et al.* demonstrated that systolic blood pressure (SBP) was positively correlated with AAA expansion, by using hypertensive Wistar-Kyoto rats infused with elastase (Gadowski *et al.*, 1993). A study of the role of gender in AAA formation showed that gonadal hormones regulated AAA growth by altering inflammatory cell infiltration (Cho *et al.*, 2009). Exposing mice to cigarette smoke resulted in accelerated AAA growth independent of aortic MMPs levels (Bergoeing *et al.*, 2007). Mice with IL-6 gene knockout displayed inhibited AAA formation with reduced inflammatory response in this model (Thompson *et al.*, 2006).

2.2.7.3   The Angiotensin II infusion induced experimental AAA mouse model

AngII is delivered via subcutaneously implanted osmotic mini-pumps to generated AAA in the suprarenal region in the $ApE^{-/-}$ or LDL receptor knock-out mice (Daugherty et al., 2000). The histological features of AAA include inflammatory cell accumulation, high concentrations of MMPs, elastin degradation, prominent vascular haematomas, ECM deposition, and

neovascularisation (Saraff, 2003; Thompson et al., 2006). Atherosclerosis is also apparent in this mouse model (Daugherty et al., 2010).

The AngII infusion mouse model has been used to investigate the various factors in AAA formation. The hypertension in this model was independent of AAA formation and AT1 antagonist induced AAA attenuation, suggesting a role of renin-angiotensin system in AAA formation (Manning *et al.*, 2002). Doxycyline, a MMP inhibitor, significantly reduced the incidence and severity of AAA in this mouse model (Manning *et al.*, 2003). Combined with genetically modified mice, it has been demonstrated that nuclear factor kappa B (NF-κB) and urokinase plasminogen activator played a role in the AAA formation in this mouse model (Deng *et al.*, 2003; Tham *et al.*, 2002). Simvastatin reduced the AAA formation by inhibition of the inflammatory response in the aortic wall (Jones *et al.*, 2009).

AAA in this mouse model has some key features similar to human AAA, including inflammation, angiogenesis, and accelerated atherosclerosis (Manning *et al.*, 2002; Daugherty, 2004); therefore, this mouse model is favourable for AAA studies. Another merit of this model is its minimal required physical manipulation of the aorta (Barisione *et al.*, 2006). It has to be acknowledged that there are differences between human AAA and this mouse model: infrarenal aortic region is the common dilatation site and dissection is uncommon in human AAAs, however AAA formation in the AngII model is typically suprarenal, and dissection is a contributing factor to aortic rupture (Manning *et al.*, 2002). Despite these differences, AngII-infusion induced experimental AAA in the ApoE$^{-/-}$ mouse model is still one of the most useful models for studying pathogenesis of AAA.

2.3   Current understanding of atherosclerosis

Atherosclerosis affects the aorta and medium sized elastic and muscular arteries at the sites of decreased shear stress and increased turbulence (Nakashima *et al.*, 1998). Animal experiments and observations of human specimens reveal that atheromatous plaque formation is a complex multistep process. The change of intima, a monolayer of ECs, is the initial step. A changed shear stress and/or injury induce intracellular adhesion molecule expression in ECs, resulting in leukocytes capture. Increased permeability of the ECs allows leukocytes and LDL to enter and accumulate within the aortic wall. Once resident under the intima, monocytes differentiate to macrophage that engulfs lipoprotein particles to become foam cells. These inflammatory cells and foam cells secrete chemokines and cytokines, contributing to the inflammation response. The foam cells undergo apoptosis and release extracellular lipids and cellular debris, contributing to the formation of a lipid-rich pool called the necrotic core of the plaque. Atheromatous plaque formation also involves SMC migration from media to intima, where they proliferate in response to mediators. SMCs produce ECM molecules to form a fibrous cap. The inflammatory cells produce MMPs to degrade collagen and generate mediators to provoke SMC death, which results in plaque disruption; therefore, the rupture fibrous cap is characterised with a thin collagen-poor fibrous cap containing few SMCs but abundant macrophages (Amento *et al.*, 1991; Libby, 2002; Libby, 2009). In general, the mechanisms of atherosclerosis pathogenesis are divided into ECs activation and dysfunction, inflammation, and angiogenesis.

2.3.1   Endothelial cell activation/dysfunction in atherosclerosis

ECs play a critical role in controlling leukocytes rolling and adhesion on the surface of the intima. In the presnece of injury or inflammatory stimuli, e.g. shear stress, ECs are activated and adhesion molecule expression is up-regulated, subsequently leading to leukocyte attachment and transmigration to the sub-endothelial space. Studies in gene knockout mice have identified several adhesion molecules, such as E-selectin, P-selectin, and ICAM-1, as being important in atherosclerosis development (Nakashima *et al.*, 1998; Amento *et al.*, 1991; Dong *et al.*, 1998).

Endothelial dysfunction, a loss of nitric oxide (NO) bioactivity in the vessel wall, contributes to atherosclerosis. ECs are a source of NO via endothelial NO synthase (eNOS), and endothelial-derived NO has been shown to play a protective role in limiting atherosclerosis. In ApoE$^{-/-}$ mice, eNOS deletion results in increased atherosclerosis (Knowles *et al.*, 2000). In human studies, transitional risk factors for atherosclerosis predispose to EC dysfunction, which suggests the role of endothelial dysfunction in the pathogenesis of atherosclerosis (Giannotti & Landmesser, 2007; Kinlay & Ganz, 1997).

2.3.2   Inflammation in atherosclerosis

Inflammatory cell accumulation is a feature of atherosclerotic lesion and important in the atherosclerosis development and progression. Macrophages, foam cells, and T lymphocytes are major inflammatory cell types in the shoulder of the atherosclerotic lesions; however, neutrophils are notable lacking (Glass & Witztum, 2001). Oxidised LDL and inflammatory mediators, such as MCP-1 and IL-8, mediate migration of monocytes to the intima (Libby, 2002). Once accumulated in the intima, monocytes are activated by macrophage colony-stimulating factor to express scavenger receptor A, by means of which monocytes uptake modified forms of LDL, leading to foam cell formation (Smith *et al.*, 1995). CD4+ T cells are predominantly present in the atherosclerotic lesion. The cytokines present in the atherosclerotic lesion promote Th1 response and Th1 effector cells produce IFN-γ (Shimizu *et al.*, 2006). IFN-γ could exert anti-inflammatory effect via regulation of scavenger receptor expression on macrophages, thereby anti-atherosclerotic formation. Conversely, IFN-γ could stimulate macrophages to produce pro-inflammatory cytokines and up regulate MHC class 2 molecule expression, thereby promoting atherosclerosis formation (Glass & Witztum, 2001). In the animal study, IFN-γ gene deletion in ApoE$^{-/-}$ mice showed attenuated atherosclerosis development (Whitman *et al.*, 2002; Gupta *et al.*, 1997), which suggests a pro-atherosclerostic role of IFN-γ. Inflammatory cells contribute to plaque rupture via production of pro-inflammatory cytokines and proteolytic enzymes. For instance, IFN-γ can inhibit collagen production by SMCs leading to a thin fibrous cap. IL-β and TNF-α enhances mononuclear

phagocyte expression of MMPs leading to ECM degradation. A thin fibrous cap with ECM degradation eventually leads to rupture.

2.3.3   Angiogenesis in atherosclerosis

The observation of VEGF and Angpts in the early and advanced atherosclerotic lesions provides evidence for the role of angiogenesis in the development of atherosclerosis (Chen *et al.*, 2005). Increased density of micro-vessels has been observed in unstable and ruptured plaques (Kolodgie *et al.*, 2003; Jeziorska & Woolley, 1999; Kockx *et al.*, 2003). Barger and colleagues suggested that capillaries within the plaque are fragile and prone to rupture, and are thus a potential cause of intraplaque haemorrhage (Barger & Beeuwkes, 1990). The number of vasa vasorum in experimental atherosclerotic plaques produced in animal studies has been demonstrated to be 2- to 4-times higher in unstable and ruptured lesions compared with stablised lesions (Herrmann *et al.*, 2001). This finding supports an earlier report that a loss of vasa vasorum was associated with plaque regression (Williams *et al.*, 1988). Moreover, administration of inhibitors of angiogenesis has been shown to reduce plaque area, whereas VEGF administration promoted atherosclerosis, providing strong evidence that the angiogenesis promots atherosclerosis (Moulton *et al.*, 1999; Celletti *et al.*, 2001). Importantly, neovascularistaion is positively associated with extravasation of inflammatory cells into the plaque, as the new vessels are immature and 'leaky', with the infiltrated cells further contributing to angiogenesis via production of pro-angiogenic factors (Virmani *et al.*, 2005).

2.4   Angiopoietins and their receptors

2.4.1   Angiopoietin family

Angpts are a family of angiogenic factors that are critical for vascular development. The Angpt family has four members, namely Angpt1, Angpt2, and Angpt3 (mice) or Angpt4 (human) (Davis *et al.*, 1996; Maisonpierre *et al.*, 1997; Valenzuela *et al.*, 1999). Angpts are secreted glycoproteins with approximately 75 kDa molecular weight and have analogous structure with a coiled-coil and a fibrinogen-like domain (Koh *et al.*, 2002; **Figure 2.2**). Angpt1 and Angpt2 have been well characterised and intensively studied, whereas the Angpt3 and Angpt4 are still largely unknown. Angpt1 and Angpt2 have approximately 60% identical sequence (Maisonpierre *et al.*, 1997; Koh *et al.*, 2002). Angpt1 is predominated with high order multi-dimers while Angpt2 is predominated with homo-dimers (Koh *et al.*, 2002).
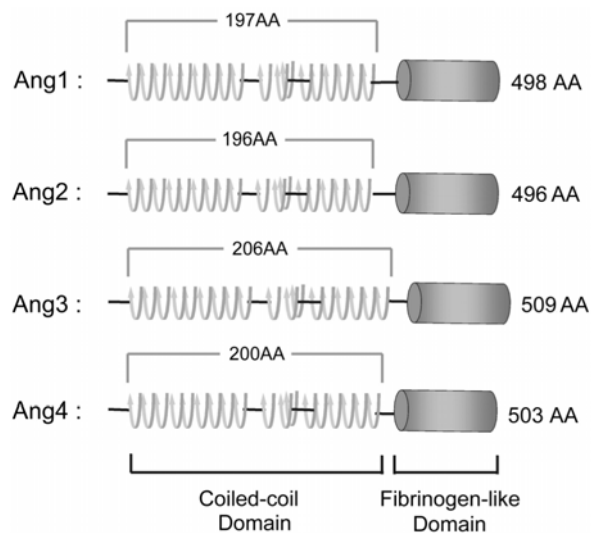
Figure 2.2 Angiopoietins have similar structure with a coiled-coil domain and a fibrinogen-like domain.
AA = amino acid; Ang = angiopoietin (From Koh *et al.*, 2002).

2.4.2   Angiopoietin-1 and Angiopoietin-2 expression

Angpt1 is expressed by various cell types but mainly by pericytes covering micro- and macro-vascular ECs (Chen *et al.*, 2009; De Spiegelaere *et al.*, 2011; Ichihara *et al.*, 2011). In the adult vasculature, Angpt1 expression is constitutive to maintain vascular quiescence and support EC

cell survival through phosphatidylinositol 3'-Kinase (PI3K)/Akt pathway (Koh, 2013). The factors regulating Angpt1 mRNA expression are still largely unknown. Angpt2 is almost exclusively expressed by ECs, and stored in the Weibel-Palade Bodies (Fiedler *et al.*, 2006; Gale *et al.*, 2002). Angpt2 mRNA is under-detectable in quiescence ECs but abundantly expressed in the adult tissue undergoing remodelling (Maisonpierre *et al.*, 1997). Angpt2 is released quickly by cytokines or micro-environmental factors stimulation in an autocrine manner (Stratmann *et al.*, 1998; Ziegler *et al.*, 1993). Hypoxia stimuli up-regulates Angpt2 expression in ECs, suggesting a role of Angpt2 in hypoxia-induced neovascularisation (Mandriota & Pepper, 1998; Mandriota *et al.*, 2000; Oh *et al.*, 1999). TNF-α is a pro-inflammatory cytokine that induces Angpt2 expression through NF-κB activation *in vitro* to regulate EC inflammatory response (Fiedler *et al.*, 2006). In adipose tissue, adipocytes secreted leptin increases Angpt2 expression without altering VEGF expression, thereby leading to vascular regression within the adipose tissue (Cohen *et al.*, 2001). AngII is an angiogenic factor regulating Angpt2 expression both *in vivo* and *in vitro* (Otani *et al.*, 2001; Fujiyama *et al.*, 2001). Mechanical lower shear stress has been observed to up-regulate Angpt2 expression *in vitro* (Chlench *et al.*, 2007).

2.4.3 Angiopoietin receptors

Angiopts are ligands for two receptor tyrosine kinases: Tie1 and Tie2 (Yancopoulos *et al.*, 2000). Tie1 and Tie2 share an identical structure, with an extracellular ligand-binding domain, a single transmembrane domain, and an intracellular kinase domain (Peters *et al.*, 2004). The extracellular ligand-binding domain consists of three EGF-like repeats flanked by two Ig-like domains, and the second Ig-like domain is followed by a fibronectin 3-like domain adjacent to the transmembrane domain (Fiedler *et al.*, 2003; Davis *et al.*, 2003; **Figure 2.3**). Both Tie1 and Tie2 are expressed in ECs and hemaetopoietic stem cells throughout embryogenesis (Sato *et al.*, 1995; Sato *et al.*, 1998). Recently, it has been found that Tie2 is also expressed in various cell types (Martin *et al.*, 2008). However, the roles Tie1 and Tie2 in embryonic vasculature

development are different, which can be observed by studying the mice with Tie1 or Tie2 gene deletion (Sato *et al.*, 1995; Dumont *et al.*, 1994).

All the Angpts bind Tie2 on the Ig-like domain and EGF-like repeat (Fiedler *et al.*, 2003). Angpt1 is a strong agonist of Tie2, whereas Angpt2 acts as an antagonist of Tie2, inhibiting Angpt1-induced auto-phosphorylation of the Tie2 intercellular kinase domain (Koh *et al.*, 2002). Nevertheless, Angpt2 can stimulate Tie2 activation, weaker than Angpt1, in a context-dependent manner (Gale *et al.*, 2002; Kim *et al.*, 2000b; Teichert-Kuliszewska *et al.*, 2001; Daly *et al.*, 2006). Angpt3 is an agonist of Tie2 and Angpt4 is an antagonist of Tie2 (Valenzuela *et al.*, 1999). Angpts bind Tie1 with a low affinity. It is still unclear whether Angpts are independent ligands for Tie1 (Yancopoulos *et al.*, 2000) and whether there is any interaction of Tie1 and Tie2 in regulating the signal transduction when Angpt1/2 binding Tie2 receptor. The schematic representation of Angpt and their receptor interaction is shown (**Figure 2.3**).
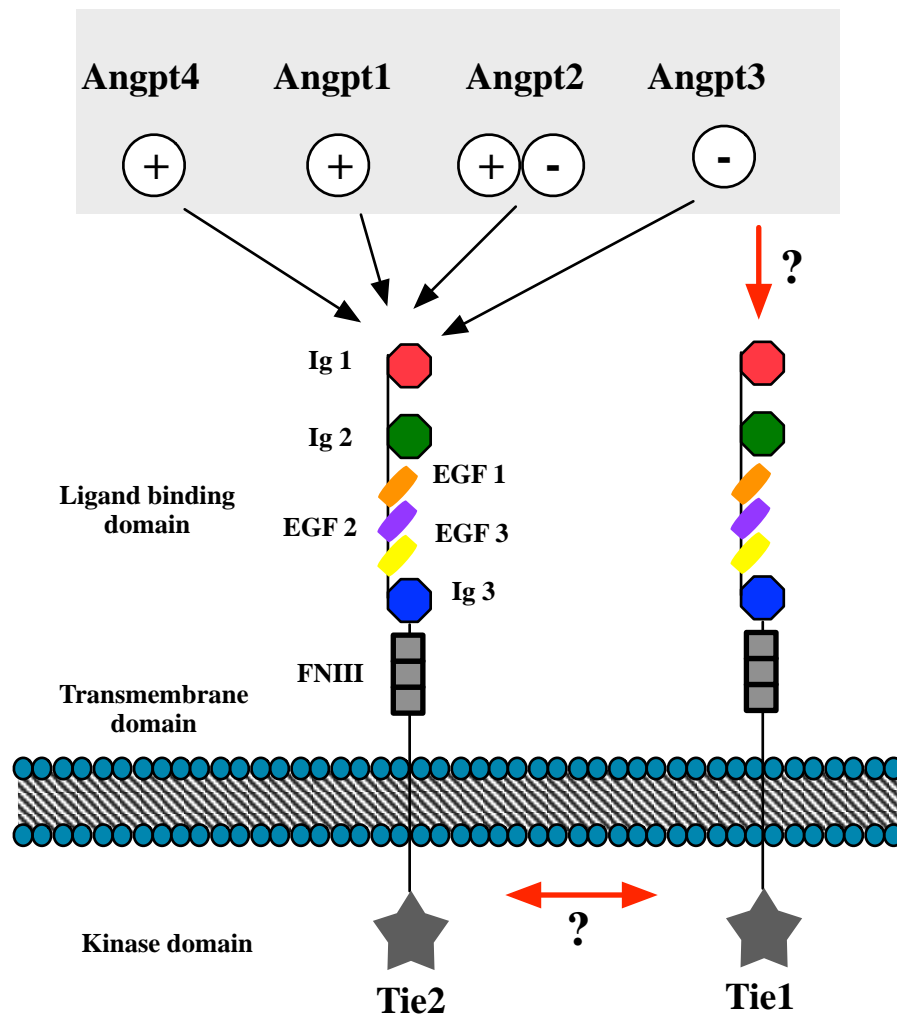
Figure 2.3 The schematic overview of the structure of Tie receptor and their interaction with angiopoietins

Tie1 and Tie2 have similar structure with a ligand-binding domain, transmembrane domain, and intercellular kinase domain. The ligand-binding domain contains two Ig domain, a EGF repeats and FNIII repeats. Angpt1 and Angpt4 are agonists of Tie2, Angpt3 is an antagonist of Tie2, and Angpt2 can be an agonist or antagonist in a context dependent manner. The interaction of Tie1 and Tie2, and Angpts binding Tie1 are still unclear, which needs to be confirmed in the future. EGF=epithelial growth factor; Ig=immunoglobulin; FNIII=fibronectin 3 (Adapted from Peters *et al.*, 2004; Yancopoulos *et al.*, 2000; and Barton *et al.* 2006).

2.4.4   Tie2 activation and signal transduction

Tie2 activation is initiated by ligand-mediated dimerisation or multi-merisation and auto-phosphorylation on specific tyrosine residues, thereby recruiting different adaptor proteins to activate signalling pathways for cell survival, migration, inflammation, and permeability (Peters *et al.*, 2004). Tie2 has three phosphotyrosine residues (pTyr) at the site of 1101 (pTyr1101), 1107 (pTyr1107), and 1112 (pTyr1112). The p85 subunit of PI3K interacts with activated Tie2

at pTyr1101 through Src homology 2 domain or phosphotyrosine domain, which actives Akt (Kim *et al.*, 2000a; Jones *et al.*, 1999; Kontos *et al.*, 1998). PI3K/Akt signalling pathway activation results in phosphorylation and inhibition of forkhead transcription factor FOXO-1 expression, to up-regulate survivin and caspase-9 expressin in ECs, thereby supporting EC survival. PI3K/Akt activation increases cell mobility via modulating Rac1 and RhoA (Cascone *et al.*, 2003). PI3k activates mDia through Rho, resulting in an association of Src and mDia. This prevents Src induced VE-cadherin activation and internalisation, thereby maintaining the integrity of the cell-cell contacts (Gavard *et al.*, 2008). Dok-R interacts with activated Tie2 at pTyr1102 and is phosphorylated, which creates interaction sites for Nck and p21 activating kinase. Dok-R and Nck interaction is essential for maximum p21 activating kinase activation to mediate EC migration (Jones *et al.*, 2003). Grb2 interacts with activated Tie2 at Tyr1101 to regulate mitogen activated protein kinase (MAPK) by modulating Erk1/2 phosphorylation (Huang *et al.*, 1995). Shp-2 interacts with activated Tie2 at Tyr1112 and also stimulates Erk1/2 phosphorylation through its ability to recruit Grb2 (Huang *et al.*, 1995). Tie2 activation, interacting with A20 binding inhibitor of NF-κB activation -2 (ABIN-2), inhibits NF-κB activation and induces anti-inflammatory and anti-apoptotic effects in ECs (Tadros *et al.*, 2003; Hughes *et al.*, 2003). Tie2 activation has also been found to interact with Bmx to regulate EC adhesion and migration (Rajantie *et al.*, 2001), with signal transducers and activators of transcription (STATs) to regulate EC proliferation, differentiation, migration, and survival (Korpelainen *et al.*, 1999), and with vascular endothelial phosphotyrosine phosphatase (VE-PTP) to inhibit para-cellular permeability. Tie2 activation and signal transduction is summarised in **Figure 2.4.**
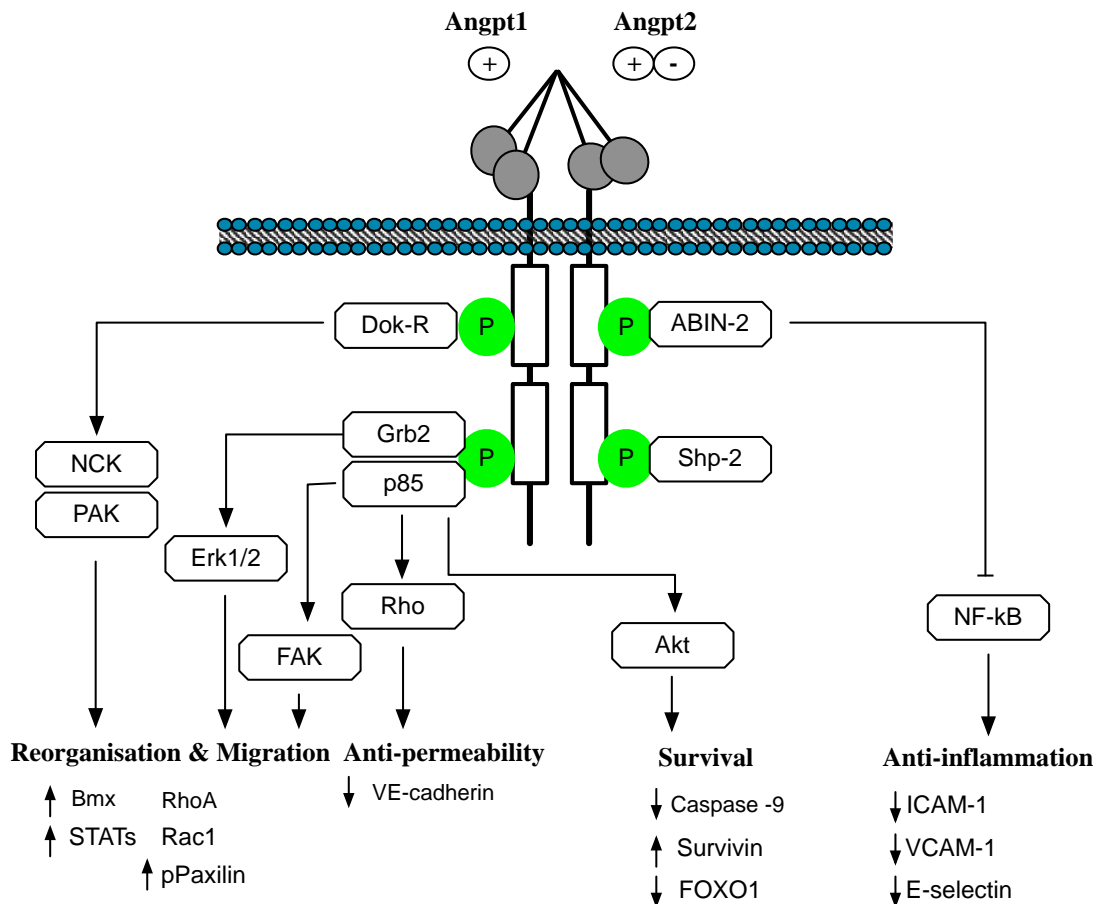
Figure 2.4 Schematic representation of Tie2 activation and its signal transduction.
Angpt1 binding to Tie2 leads to dimerisation or multimerisation and subsequently auto-phosphorylation (P). The adaptor proteins are recruited to the phosphotryrosine residues and subsequently activated, which leads to the downstream signalling pathway activation. Dok-R: downstream-of-kinase-related protein; Grb2: Growth factor receptor-bound protein 2; Shp-2: Src homology 2 (SH2)-containing protein tyrosine phosphatase; ABIN-2: A20-binding inhibitor of NF-κB-2; STATs: signal transducer and activator of transcriptions; ICAM-1: intracellular adhesion molecule-1; VCAM-1: vascular cell adhesion molecule 1; FOXO-1: forkhead box protein O 1; and FAK: focal adhesion kinase.

2.4.5   Integrin-dependent binding of Angpt1 and Angpt2

The direct evidence of both Angpt1 and Angpt2 binding to integrins was observed in Tie2 receptor negative fibroblasts (Carlson *et al.*, 2001). The highly conserved fibronectin-like domain in Angpts could be functionally associated with integrin binding (Yokoyama, 2000); however, it remains to be elucidated. Angpts binding specific integrin subunits have been found to regulate different functions in various cell types (i.e. ECs, myocyte, and tumour cells) (Carlson *et al.*, 2001; Scholz *et al.*, 2011; Hu *et al.*, 2006). Felcht *et al.* found that Angpt2 binding integrins, in a Tie2-independent manner, will induce focal adhesion kinase phosphorylation, resulting in EC migration and sprout angiogenesis (Felcht *et al.*, 2012).

Carlson *et al.* also demonstrated that both Angpt1 and Angpt2 can bind to hamster ovary-B2 cells. However, Angpt1 binding integrin was α5 subunit dependent, whereas Angpt2 was α5 independent (Carlson *et al.*, 2001). It still needs to be elucidated how Angpt1 and Angpt2 bind integrin.

2.4.6 Angiopoietin-1: an agonist of Tie2

Angpt1 is a strong agonist of Tie2. Angpt1 forms multimeric form binding with the ligand-binding domain of Tie2 that induces phosphorylation of Tie2 (Hansen *et al.*, 2010). The first Ig-like domain and EGF-like repeats of Tie2 are required for Angpt1 binding (Fiedler *et al.*, 2003). Seegar *et al.* proposed that Angpt1 could stimulate Tie2 clustering in both the presence and absence of a Tie1 receptor (Seegar *et al.*, 2010). By activating Tie2, Angpt1 increases vessel size, instead of vessel numbers (Yancopoulos *et al.*, 2000). In addition to its effects on vascular morphology, Angpt1 maintains vessel integrity by activating Tie2, which inhibits VEGF or inflammatory agents induced vessel permeability by the inhibition of NF-κB signalling pathway (Hughes *et al.*, 2003; Saharinen *et al.*, 2008; Tadros *et al.*, 2003).

2.4.7 Angiopoietin-2: an agonist or antagonist of Tie2?

Angpt2 was originally identified as an antagonist of Tie2 blocking Angpt1 induced Tie2 phosphorylation in ECs (Maisonpierre *et al.*, 1997). Angpt2 is required for angiogenesis to destabilise the existing vessels by blocking Angpt1-Tie2 interaction to facilitate VEGF-induced angiogenesis (Thomas & Augustin, 2009). Both Angpt1 and Angpt2 bind with Tie2 in a similar affinity (Fiedler *et al.*, 2003; Stratmann *et al.*, 1998; Ziegler *et al.*, 1993); However, Angpt2 acts as an antagonist of Tie2, inhibiting Angpt1-induced auto-phosphorylation of Tie2 intercellular kinase domain (Koh *et al.*, 2002). The opposing actions of Angpt2 and Angpt1 on Tie2 may be attributed to Tie1 (Seegar *et al.*, 2010). It is proposed that Angpt2 can activate Tie2 in the absence of Tie1, whereas Angpt2 deactivates Tie2 in the presence of Tie1 (Seegar *et al.*, 2010). Angpt2 can be an agonist of Tie2 in a context-dependent manner (Gale *et al.*, 2002; Kim *et al.*, 2000b; Teichert-Kuliszewska *et al.*, 2001; Daly *et al.*, 2006). Angpt2 is also required in

embryonic lymphatic vasculature development (Gale *et al.*, 2002). In mice lacking Angpt2, lymphatic vessel defects can be rescued by Angpt1, which suggests Angpt2 acts as a Tie2 agonist in lymphatic ECs (Gale *et al.*, 2002). There is emerging evidence showing that Angpt2 is an agonist of Tie2 in ECs. Kim *et al.* observed that Angpt2 at a high concentration could enhance EC survival through PI3K/Akt signalling pathway *in vitro* (Kim *et al.*, 2000b). Daly and colleagues demonstrated that Angpt2 could activate Tie2 both *in vivo* and *in vitro* (Daly *et al.*, 2006). Yuan *et al.* also observed Angpt2 is an agonist of Tie2 in ECs, but suggested that Angpt2 was a weaker agonist than Angpt1 (Yuan *et al.*, 2009).

2.4.8   Angiopoietin-Tie2 signalling pathway in embryonic and adult vasculature

Angpt-Tie2 signalling pathway has a critical role in embryonic vasculature development, which has been studied in mice with gene deletion. Tie2-deficient mice showed poorly organised vessels, fewer branches, reduced pericyte coverage, and died at E10.5 (Dumont *et al.*, 1994; Sato *et al.*, 1995; Suri *et al.*, 1996). Mice with Angpt1-deficiency had similar phenotype of Tie2-deficient mice, which indicates that the Angpt1-Tie2 axis plays a critical role in embryonic vasculature development. However, Angpt2-deficient mice did not have vascular defects but developed a chylous ascites, indicating defects in the lymphatic system (Gale *et al.*, 2002). Overexpression of Angpt2 results in embryonic lethality because of vascular defects similar to the phenotype of Angpt1-deficient mice, which indicates the antagonistic role of Angpt2 on Tie2 during embryonic angiogenesis (Maisonpierre *et al.*, 1997).

The Angpt-Tie2 axis is critical for both maintaining vessel homeostasis and maturation, and vascular destabilisation and remodelling in adult vasculature (Holash *et al.*, 1999). Angpt1 is constitutively expressed by pericytes covering ECs of the vasculature, which induces Tie2 activation in order to maintain the vessel quiescence and homeostasis (Koh, 2013). Angpt2 is only expressed in the active remodelling sites, such as ovary, placenta, and uterus (Maisonpierre *et al.*, 1997). Angpt2 is also expressed in pathological conditions such as cancer,

atherosclerosis, and AAA, as angiogenesis is also a common feature in these conditions (Martin *et al.*, 2008).

2.4.9   Angiopoietins in angiogenesis

The Angpt-Tie2 signalling system plays a critical role in the process of angiogenesis. Angpt1 and Angpt2 play different roles in regulating the vessel destabilisation, ECM base membrane degradation, EC proliferation and migration, and tube formation (Carmeliet & Jain, 2000). It has been found that Angpt2 was expressed at the leading edge of angiogenesis whereas Angpt1 was expressed behind the leading edge of angiogenesis, which suggests that Angpt2 destabilises the existing vasculature to facilitate angiogenic factor induced angiogenesis, and Angpt1 mediates Tie2 activation triggering stabilising of the neo-vasculature (Maisonpierre et al., 1997; Peters et al., 2004).

Angpt2 destabilises the pre-existing vessels by antagonising Angpt1 induced low phosphorylation of Tie2 to disassociate ECs with pericytes, which will facilitate VEGF induced EC survive, proliferation, and migration (Maisonpierre *et al.*, 1997). Prolonged exposure of Angpt2 to ECs could induce EC apotosis and vessel regression in the absence of VEGF (Veikkola & Alitalo, 2001; Oshima *et al.*, 2004). In the animal study, Angpt2-deficient mice lacked vascular remodelling in the retinal eyes, which supports the notion that Angpt2 is required for vascular remodelling (Yancopoulos *et al.*, 2000). Angpt2 also up-regulates MMP-9 and MMP-2 expression to facilitate ECM digestion facilitating EC migration (Das, 2003; Hu *et al.*, 2003; Zhang *et al.*, 2012).

Angpt1 is important for the later steps of neovessel stabilisation via the Angpt1-Tie2 axis (Chavakis, 2002). Angpt1 induces EC survival and migration (Fiedler *et al.*, 2003). Pericytes secrete Angpt1 inducing Tie2 phosphorylation to stabilise ECs, and Angpt1 further enlarges the lumen of the new-formed capillary tube (Jain & Munn, 2000; Hattori *et al.*, 2001). Indeed, over-expressing Angpt2 induces impaired pericytes recruitment and abnormal retinal angiogenesis (Crowley *et al.*, 2006).

2.4.10   Angiopoietins in inflammation

Angpt1 exerts anti-inflammatory effects through activation of Tie2 (Jeon *et al.*, 2003). NF-κB signalling pathway activation is essential for VEGF and TNF-α induced adhesion molecule expression in ECs (Kim *et al.*, 2001a; Imhof & Aurrand-Lions, 2006). Kim *et al.* reported that Angpt1 suppressed VEGF-induced adhesion molecule expression in human umbilical vascular ECs, thereby reducing leukocyte adhesion (Kim *et al.*, 2001b). Angpt1 counteracts the inflammatory effects of TNF-α through inhibition of NF-κB signalling pathway (Imhof & Aurrand-Lions, 2006; Gamble *et al.*, 2000). Using intracellular domain of Tie2 bait, Hughes *et al.* firstly isolated a cDNA clone code for a well-known inhibitor of NF-κB activation ABIN-2 (Hughes *et al.*, 2003). ABIN-2 is a negative modulator of NF-κB activation (Krikos *et al.*, 1992). Angpt1 stimulates Tie2 phosphorylation resulting in ABIN-2 recruitment and subsequently inhibits NF-κB signalling pathway, thereby inhibiting adhesion molecule expression in ECs (Hughes *et al.*, 2003; Tadros *et al.*, 2003).

Angpt1 counteracts vascular permeability by modulating cell-cell conjunctions, intracellular calcium, and Tie2 localisation (Koh, 2013). Vascular permeability is maintained by the integrity of the EC contacts. Transgenic overexpression of Angpt1 induces leakage-resistant vessels and prevents VEGF stimulated vessel permeability (Thurston *et al.*, 2000; Gamble *et al.*, 2000; Lee *et al.*, 2014; Thurston *et al.*, 1999). VEGF induces vascular permeability by regulating VE-cadherin phosphorylation, redistribution, and internalisation via Src (Gavard & Gutkind, 2006). Angpt1 induced activation of Tie2 promotes Src sequestration, thereby counteracting VEGF-induced permeability (Gavard *et al.*, 2008). VE-PTP is another important factor for vascular permeability. It forms a complex with VE-cadherin and Tie2 to maintain the integrity of the EC monolayer. The VEGF disassociates the VE-PTP complex to compromise vascular integrity (Gavard & Gutkind, 2006), whereas Angpt1 promotes VE-PTP and Tie2 interaction to enhance the vascular integrity (Saharinen *et al.*, 2008). Several studies suggested that Angpt1 exerts anti-permeability through inhibiting calcium influx and small GTPase Rho activation (Li *et al.*, 2004).

Conversely, Angpt2 induces vascular leakage in acute inflammation (Roviezzo *et al.*, 2005). Transgenic overexpression of Angpt2 results in time-dependent myeloid cell accumulation in numerous organs, in the absence of inflammatory stimuli and increased cell adhesion in models of acute inflammation (Scholz *et al.*, 2011). As an antagonist of Tie2, Angpt2 may block the anti-inflammatory effect of Angpt1 by competitive binding of Tie2, thus sensitising EC stimulation (Fiedler *et al.*, 2006). Angpt2 deficient mice have impaired TNF-α-induced leukocyte adhesion and extravasation (Fiedler *et al.*, 2006). In a tumour, Angpt2 actives Tie2 expressing macrophages (TEMs) in the tumour, to enhance their pro-angiogenic activity (Fiedler *et al.*, 2006). Increased TEMs infiltration was found in a tumour grown in transgenic overexpression Angpt2, which is consistent with the *in vitro* study, which showed that human Tie2 monocytes, not Tie2 negative monocytes, responded to Angpt2 stimulation (Coffelt *et al.*, 2010; De Palma & Naldini, 2011). Angpt2 can enhance TEM immunosuppressive activity by promoting IL-10 expression that resulted in T cell proliferation suppression and Treg cell expansion (Coffelt *et al.*, 2011). Despite the evidence of Angpt2 promoting vascular leak and enhancing TNF-α-mediated inflammation, Daly *et al.* demonstrated that Angpt2, similar as Angpt1, significantly inhibited mustard oil-induced extravasation of Evans blue dye from the ear vasculature (Daly *et al.*, 2006) and Nakanen *et al.* observed similar anti-inflammatory effect of Angpt2 in cardiac allografts (Nykänen *et al.*, 2006). Interestingly, Roviezzo *et al.* found that Angpt2 reduced cellular infiltration in tissues in the presence of ongoing inflammation (Roviezzo *et al.*, 2005). Further investigation is required to elucidate the mechanisms of Angpt2 responsiveness to inflammation.

2.4.11   Antiopoietins-Tie2: a potential target for therapies

The Angpt-Tie2 signalling pathway has vital roles in regulating inflammation and angiogenesis that are common in pathological conditions. Therefore, targeting the Angpt-Tie2 signalling pathway may have potential as a therapeutic strategy for the treatment of diseases. Angpt1-induced Tie2 activation has anti-inflammatory, anti-permeable, and anti-apoptotic effects; therefore, Angpt1 delivery could be a potential therapy for diseases caused by inflammation,

vascular leakage, and micro-vessel regression. Diabetic retinopathy in mice is featured with EC apotheosis, high permeability, and vascular inflammation. Intraocular injection of Angpt1 results in inhibitory of oedema in diabetic mice (Joussen *et al.*, 2002). Vascular leakage after ischaemic stroke increases the volume of infarct, and administration of recombinant Angpt1 had been proved to reduce the infarct size by inhibiting of VEGF-induced vascular permeability in a mouse model (Zhang *et al.*, 2002). The ability of Angpt1 to suppress adhesion molecule expression in ECs has been observed in a mouse model of allograft arteriosclerosis (Nykanen *et al.*, 2003). Despite the significant therapeutic potentials, Angpt1 may have some severe side effects, including pulmonary hypertension, promoting angiogenesis, and negative vessel remodelling (Moss, 2013).

Angpt2, unlike constitutively expressed Angpt1, is dynamically regulated and mostly upregulated in pathological conditions. Therefore, modification of Angpt2 is more favoured in therapies (Gerald *et al.*, 2013). Angpt2 is induced at early stage to destabilise the vessel facilitating VEGF-induced angiogenesis that has been observed in tumours (Thurston & Daly, 2012). Therefore, to block Angpt2 activity may have a potential anti-angiogenic effect. In pre-clinical studies, the methods used to block Angpt2 activity include monoclonal antibodies, high-affinity nuclease resistant RNA ligands, peptide-Fc fusion proteins, and a bivalent Angpt2-binding peptide-antibody fusion protein (Moss, 2013). Administration of L1-10, a peptide-Fc fusion inhibiting the interactions between Angpt2 and its receptor Tie2, reduced prostate tumour volume *in vivo* (Morrissey *et al.*, 2010). Tumour-bearing mice receiving MEDI3617, an Angpt2 specific blocking monoclonal antibody, resulted in a reduction of angiogenesis and an increased hypoxia (Leow *et al.*, 2012). Recently, a combined blocking of Angpt2 and VEGF produced a greater reduction of angiogenesis and tumour size compared with any agent alone (Daly *et al.*, 2012). Anti-angiogenic therapy combining paclitaxel and AMG 386, a peptide-Fc protein neutralising the interaction of Angpt1/2 with Tie2, has been shown to be safe and effective in phase II randomised trials (Karlan *et al.*, 2012). However, clinical anti-angiogenic therapy is currently limited to advanced cancer patients with short life expectancy and limited options. The

application of anti-angiogenic therapy for management of other clinical conditions requires further investigation.

2.4.12   Angiopoietins in AAA and atherosclerosis

Both AAA and atherosclerosis are associated with pathological angiogenesis and inflammation, as discussed above. However, the role of Angpts in AAA and atherosclerosis remains unclear. Induction of Angpt2 is important in facilitating TNF-α-induced adhesion molecule expression in ECs (Fiedler *et al.*, 2006), which may have implications for atherosclerosis and AAA development. Osteopontin (OPN) is abundantly present in human atherosclerosis tissue, and plays an important role in AAA pathogenesis (Bruemmer *et al.*, 2003). Mangan *et al.* demonstrated that OPN up-regulated adhesion molecule expression in ECs in response to TNF-α, which was associated with induction of Angpt2 (Mangan *et al.*, 2007). However, despite evidence for Angpt2 in promoting angiogenesis and inflammation, exogenous administration of Angpt2 in hyperlipidaemic ApoE$^{-/-}$ mice led to reduced atherosclerosis severity (Ahmed *et al.*, 2009). The reduction in plaque development was associated with decreased presence of inflammatory cells and content of oxidized LDL, and attributed to an Angpt2-mediated increase in nitric oxidase release within the vessel wall (Ahmed *et al.*, 2009). Earlier work by Nykanen *et al.,* using a rat model, demonstrated that intra-coronary perfusion of cardiac allografts with an adenoviral vector encoding human Angpt1 limited leukocyte infiltration and arteriosclerosis development associated with reduced microcirculation expression of Angpt2 (Nykanen *et al.*, 2003). Analysis of human atherosclerotic specimens showed that VEGF and Angpt1 were expressed in early lesions whereas VEGF and Angpt2 were expressed in advanced lesions (Calvi, 2004). This suggests that Angpt1 and Angpt2 play different roles in atherosclerosis development. Unstable atherosclerotic lesions with high MVD exhibit an Angpt1: Angpt2 ratio favouring Angpt2 (Post *et al.*, 2008). On the other hand, circulating levels of Angpt2 in CVDs are controversial. Cross-sectional studies investigating circulating and tissue level of Angpts in patients with or without CVD are summarised in **Table 2.5**. Most of the patients with CVDs had a higher circulating Angpt2 (Lorbeer *et al.*, 2015; David *et al.*, 2009; Post *et al.*, 2008).

Nevertheless, Jaumdally and colleagues reported that Angpt2 was lower in patients with CVD (Jaumdally *et al.*, 2011). In plaques with high MVD, the local balance between Angpt1 and Angpt2 favours Angpt2 (Post *et al.*, 2008). The development of unstable plaque is associated with Angpt2 level with MMP-2 activity (Post *et al.*, 2008). However, Chen *et al.* showed that there is no difference of Angpt2 between stable and unstable plaques (Chen *et al.*, 2005).

Table 2.5 Angiopoietin expression in human and experimental atherosclerosis and AAA

Reference	Sample	Method	Result
(Chen *et al.*, 2005)	Human stable and unstable angina;	IHC staining sections	No difference of Angpt1 and Angpt2;
(Lim *et al.*, 2005)	Diabetes patients with and without CVD;	Serum ELISA	No difference of Angpt1; Angpt2 raised regardless of CVD;
(Le Dall *et al.*, 2010)	Conditioned media from hemorrhagic (Hem) and non-hemorrhagic (NHem) carotid plaques;	ELISA	Low Angpt1 in Hem conditioned media; No difference of Angpt1 release; Angpt2 raised regardless of CVD;
(Lopez-Mejias *et al.*, 2013)	Rheumatoid arthritis (RA) patients with and without CVD;	Serum ELISA	Higher level of Angpt2 in RA patients with CVD;
(Lorbeer *et al.*, 2015)	Cross-sectional data of participants;	Serum ELISA	Angpt2 positively correlated with number of carotid plaques;
(David *et al.*, 2009)	Hypertensive patients with or without atherosclerosis;	Serum ELISA	Higher level of Angpt2 in hypertensive patients with CVD;
(Post *et al.*, 2008)	Plaques with high MVD and low MVD;	Western blotting	Higher Angpt2 in high MVD plaques;
(Jaumdally et al., 2011).	CVD with and without Diabetes compared with healthy controls;	Plasma ELISA	Lower Angpt2 in both CVD with and without diabetes;
(Golledge *et al.*, 2012)	Men with AAA and without AAA;	Serum ELISA	Higher level of Angpt2 in men with AAA;

2.5   Conclusion leading to research in this thesis

The relationship between Angpts and AAA development is still unknown. There are still few studies investigating the role of Angpts in AAA development and progression, although pre-clinical studies and end-edge ruptured human AAA assessment have implicated angiogenesis and inflammation in the pathogenesis of AAA. It has been demonstrated that exogenous Angpt2 reduced atherosclerosis development *in vivo*; however, it does not fit with the role of Angpt2 as an antagonist of Tie2. In addition, Golledge *et al.* reported that serum Angpt2 is elevated in men with AAA, and is associated with an increased risk of cardiovascular mortality in older men (Golledge *et al.*, 2012). However, the finding of elevated Angpt2 in AAA patients is still unknown due to the cause or consequence of AAA. Importantly, Angpt2 can activate or de-activate Tie2 in a context-dependent manner, thereby inducing different signalling pathways facilitating angiogenesis and inflammation. This indicates that Angpt2 may have a role in atherosclerosis and AAA development. Although considered to elicit pro-inflammatory effects as an antagonist of Tie2, administration of Angpt2 in experimental models suggests a protective role. This thesis will further examine the role of Angpt2 in AAA and atherosclerosis, and assess the efficacy of exogenous Angpt2 to limit these in the AngII-infusion mouse model. The outcomes of the study will provide new information upon which the value of a therapeutic strategy involving Angpt2 can be measured.

CHAPTER 3

General Materials and Methods

3.1 Angiotensin II infused experimental AAA model in ApoE$^{-/-}$ mice

3.1.1 Ethics approval

Animal studies and all experimental protocols were approved by the Animal Ethics Committee of James Cook University (Approval number: A1671). All experimental work was performed in accordance with the institutional and ethics guidelines of James Cook University.

3.1.2 ApoE$^{-/-}$ mice

Male B6.129P2-Apoe^{tm1Unc}/J (ApoE$^{-/-}$) mice on a C57BL/6 background (eight weeks old) were obtained from commercial colonies (Animal Resource Centre, Western Australia). Mouse homozygous for Apoe^{tm1Unc} mutation shows a marked increase in total plasma cholesterol level (> 500 mg/dL) on a standard chow diet, which is not affected by age and sex (Zhang *et al.*, 1992). Fatty streaks in the proximal aorta are found from 3 months of age (Meir & Leitersdorf, 2004). This pro-atherosclerosis mouse shows increased lesions with age and progresses to typical advanced stage of pre-atherosclerotic lesions. Mice were housed in the Small Animal Facility at James Cook University, in a pathogen-free environment, maintaining a 12:12 hours of light and dark cycle in an individually ventilated, temperature/humidity-controlled cage system (Canning Vale, Australia). Mice were given standard chow diet and water *ad libitum*. All male mice were acclimated in the Small Animal Facility and aged to six-month-old for use in all experiments. Experimental mice were checked daily to monitor changes in behaviour, physiology, and incidence of mortality.

3.1.3 Preparation of Angiotensin II

Human AngII was purchased from Sigma-Aldrich (A9525-50MG, USA). This product is a synthetic peptide ($C_{50}H_{71}N_{13}O_{12}$, 1046.18 Da). AngII was dissolved in sterilised Milli-Q water to make a final stock concentration equivalent to 25 µg/µl. In order to achieve the desired AngII subcutaneous dispensing rate (1000 ng/kg/min), the following equation was used to calculate the concentration of AngII required for each mouse:

$$C_d = K_0 \cdot W/Q$$

Where C_d is the concentration of AngII (ng/µl), K_0 is the mass delivery rate (1000 ng/min/kg), W is the weight of the mouse (kg), and Q is the volume delivery rate.

3.1.4 Preparation of micro-osmotic pump filled with Angiotensin II

Micro-osmotic pumps (Model# 1004, Alzet, USA) were purchased from Bio Scientific (Gymea, Australia) and were used to deliver AngII continuously during the experimental period. These miniature implantable pumps have 100 µl volume reservoirs and are designed to continuously deliver for up to 28 days at a flow rate of 0.11 µl per hour (equal to 0.00183 µl/min).

An empty Micro-osmotic pump and its flow moderator were weighed prior to filling. The filling was accomplished with a 1 ml syringe and provided 27 gauge blunt-tipped filling tube at room temperature. The micro-osmotic pump was held upright and the filling tube was inserted through the opening at the top of the pump until it could go no further. Then the AngII solution was slowly pushed into the pump until the solution appeared at the top of the outlet, which reduced the chance of air bubbles being trapped in the pump. The filling tube was carefully removed and the flow moderator was inserted. The filled pump was weighed again to assure a loading of over 90% of reservoir volume. This was confirmed by subtracting the pump weight before filling from the weight after the filling. Prior to implantation, the filled umps were placed in 0.9% isotonic saline for at least 48 hours at 37°C. This will activate the pumps to reach a stable dispense rate at 0.11 µl per hour on implantation.

3.1.5   Micro-osmotic pump subcutaneous implantation

Micro-osmotic pumps were surgically implanted while the mice were under anaesthesia. Six-month-old ApoE$^{-/-}$ mice were anaesthetised by intraperitoneal injection of ketamine (150 mg/kg) and xylazine (10 mg/kg). A small incision was made in the skin between the scapulae and the connective tissue was carefully spread apart using a haemostat to create a small pocket along the dorsal midline. The AngII filled pump was subcutaneously implanted in the space along the dorsal midline with the flow mediator pointing away from the incision. The incision was closed with sutures. Mice were allowed to recover in a warm, dark, and quiet environment, and the mice typically recovered from anaesthesia within 30 min. Mice were intensively checked for health and behaviour during the next 3 days and mice were assessed for signs of poor health such as paraplegia, sudden death or other complications of aortic aneurysm formation, or surgery.

3.2   Human Fc protein, recombinant angiopoietin-2, and angiopoietin-2-Tie2 interacting inhibitor

Regeneron (Tarrytown, USA) generously provided recombinant angiopoietin-2 (rAngpt2), Angpt2-Tie2 interacting inhibitor (L1-7), and control human Fc protein for all of the experiments. These recombinant proteins were generated by the Preclinical Manufacturing and Process Development Group in Regeneron.

3.2.1   Sequence of human Fc protein, rAngpt2, and L1-7

Human Fc portion was used to generate peptide-Fc fusion L1-7 and Angpt2-Fc fusion protein described previously (Kim *et al.*, 2000; Oliner *et al.*, 2004; Davis *et al.*, 2003). The amino acid sequence of human Fc protein is shown in **Table 3.1**. This human Fc protein has been proven to have no effect on Angpt-Tie2 neutralisation and VEGF-VEGF-R neutralisation (Oliner *et al.*, 2004).

L1-7 is an Angpt2 specific binding peptide-Fc fusion protein inhibiting Angpt2 from interacting with Tie2 (Oliner *et al.*, 2004). L1-7 was derived from phage clones and the consensus sequences expressed in *E.Coli* was fused to human IgG1 Fc, named RS753 L1-7 (N).Fc (L1-7). This peptide Fc-fusion protein was selected based on its ability to neutralise human Angpt2 and Tie2 interaction ($IC_{50}=54$), which is the same in *musculus,* whereas it lacks VEGF-VEGF-R neutralisation activity. The amino acid sequence of L1-7 is shown in **Table 3.1**.

rAngpt2 construction has been described by Davis and colleagues (Davis *et al.*, 2003). Briefly, the amino acid sequence of Angpt2 was divided into three regions. The sequence begins with a stretch of ~50 residues known as N-terminal region (denoted as "N"), followed by a domain known as coiled-coil domain (denoted as "C") and a C-terminal domain of fibrinogen (denoted as "F"). The F domain has been proven to be the functional domain that distinguishes the different functions of Angpt1 and Angpt2. AngF2-Fc-F2 has precisely four Angpt2 F domains, and this Angpt2 chimera is a context-dependent agonist or antagonist analogous to native Angpt2. The amino acid sequence of rAngpt2 is shown in **Table 3.1**.

Table 3.1 Sequence of the human Fc protein, rAngpt2, and L1-7

Name	Structure
Human Fc protein	DKTHTCPPCPAPELLGGPSVFLFPPKPKDTLMISRTPEVTCV VVDVSHEDPEVKFNWYVDGVEVHNAKTKPREEQYNSTYR VVSVLTVLHQDWLNGKEYKCKVSNKALPAPIEKTISKAKG QPREPQVYTLPPSRDELTKNQVSLTCLVKGFYPSDIAVEWES NGQPENNYKTTPPVLDSDGSFFLYSKLTVDKSRWQQGNVFS CSVMHEALHNHYTQKSLSLSPGK
rAngpt2	Ang-DSVQRLQV(**F2**)-**Fc** -GGGSGAP-FRDCAEVF (**F2**)
L1-7	MGAQTNFMPMDDLEQRLYEQFILQQGLEGGGGG**Fc**

3.2.2   Administration of human Fc protein, rAngpt2, and L1-7

Human Fc protein, rAngpt2, or L1-7 was dissolved in phosphate buffered saline (PBS, Life Technologies, Australia), to a final stock concentration of 1 mg/ml. A dose of 4 mg/kg dosage in a total volume 200 µl PBS was prepared according to the weight of the mice. This dosage was suggested by the provider and has been published previously (Tressel *et al.*, 2008; Yan *et al.*, 2012). Human Fc protein, rAngpt2, or L1-7 was subcutaneously injected into the loose skin over the neck, using a 1 ml syringe with a 27 gauge needle. Caution was taken to ensure a negative pressure prior to injection. Mice were returned to their cages and observed for complications, such as bleeding, inflammation, abscesses, or ulcers after the injection. Mice were administrated with human Fc protein, rAngpt2, or L1-7 a day prior to AngII infusion commencing, and then every other day for the duration of the experiment.

3.3   Sample collection:

3.3.1   Peripheral blood collection

During the experiment, peripheral blood was collected via the lateral tail vein. A white lamp was used to heat up the environment. Mice were then accustomed in the restrainer and the lateral tail vain was nicked with a surgical scalpel blade half way down the tail. Blood was collected into a lithium heparin coated tube (BD Biosciences, USA), capped, inverted several times, and then placed on ice. After blood collection, the tail incision was compressed with a dry sterile gauze pad until homeostasis occurred. A total volume of 150 µl blood was collected for each mouse.

At the end of the experiment, Mice were euthanased with carbon dioxide and the abdomen were opened to expose the heart. Blood was drawn from the right ventricle using a 3 ml syringe with a 25 gauge needle. The syringe was uncapped and the blood was transferred into a lithium heparin coated tube, inverted several times, and then placed on ice.

3.3.2   Plasma collection

Peripheral blood was centrifuged at 2000 x g for 30 min at 4°C to pellet cells and platelets. This separated the sample into two layers: the plasma layer and the cell and platelet layer. The plasma was carefully collected with a pipette without disturbing the cell and platelet layer and immediately transferred into a pre-chilled 1.5 ml polypropylene tube. Plasma samples were stored at -80°C for future assessment.

3.3.3   Whole aorta dissection and photography

On completion of the experiments, mice were euthanased with carbon dioxide. The abdomen was opened to expose the aorta. The aorta was slowly flushed with 10 ml Dulbecco's phosphate buffered saline (DPBS, Life Technologies, Australia), through the left ventricle using a 5 ml syringe. The extraneous adipose and connective tissue was carefully removed under a Zoom Stereomicroscope (Olympus SZX7, Olympus, Japan). The whole aorta, from aortic valve to

iliac bifurcation, including three large vessels sprouting from the ARCH, was isolated intact from the dorsal wall. During the isolation procedure, aortic tissue was prevented from drying out by applying DPBS on the surface. The dissected whole aorta was immediately placed on a graduated template to be photographed using a digital camera (CoolPix 4500, Nikon, Japan). The aorta was then cut into four parts, according to its anatomical positions: ARCH, THX, SRA, and IRA. All of the aortic tissues were immersed in Tissue-Tek® Optimal Cutting Temperature (OCT, ProSciTech, Australia) compound and snap frozen in liquid nitrogen. Samples were stored at -80°C for future analysis.

3.3.4 Collection of bone marrow cell

Bone marrow cells (BMCs) were collected from left femur of the mouse. Left femurs of the mice were dissected immediately following mouse euthanasia. Muscle tissue was removed from the femur bones by rubbing with tissue. Dissected femurs were immersed in 75% ethanol for 30 sec and immediately transferred to a 1.5 ml polypropylene tube with 1 ml DPBS, containing 0.5% Bovine Serum Albumin (BSA, Sigma-Aldrich, USA) on ice. The femur was cut open at both ends. A 1 ml syringe with a 27 gauge needle was used to flush out the BMCs with a total of 2 ml DPBS containing 0.5% BSA. The medium containing BMCs was centrifuged at 350 x g for 10 min at 4°C. The supernatant was carefully discarded and the cell pellet was resuspended in 2 ml DPBS containing 0.5% BSA, followed by filtering through 60 micron nylon mesh. Samples were placed on ice and ready for red blood cell (RBC) lysis and cell surface staining for flow cytometry.

3.3.5 Collection of splenic cells

Spleens were harvested and stored on ice prior to splenic cell harvest in a 1.5 ml polypropylene tube with 1 ml DPBS containing 0.5% BSA. The spleen was transferred to an 80 micron cell strainer (BD Biosciences, USA) placed on the top of 50 ml tube. The spleen was homogeneously macerated through the filter using the back of a 1 ml syringe plunger at room temperature. The filter was regularly rinsed with DPBS containing 0.5% BSA. The tube was

filled with cold DPBS containing 0.5% BSA and centrifuged at 300 x g at 4°C for 10 min. The supernatant was discarded carefully, without disturbing the cell pellet. The cell pellet was resuspended in 20 ml cold DPBS containing 0.5% BSA and the centrifugation and the resuspending procedure was repeated once. The final cell pellet was resuspended in 20 ml cold DPBS containing 0.5% BSA and filtered through a 60 micron nylon mesh. Samples were placed on ice for RBC lysis and cell surface staining for flow cytometry.

3.4   Morphometry of aorta and AAA categorisation

3.4.1   Morphometry of aorta

Adobe Photoshop CS5 extended software (v12, Adobe, USA) was used to measure the maximum aortic diameter in each region. Prior to measurement, a 5 mm length line was drawn based on the ruler in the image and the pixel of this 5 mm length was calculated by the software. This pixel length was set to 5 mm logical length in the custom scale setting dialogue. This procedure was repeated for each aorta measurement. The maximum outer diameter in different aortic regions was visually identified and a line was then drawn between the outer walls of the aorta. By clicking the measurement menu, the logical length of the drawn line was calculated based on the customized measurement scale. Each region of the aorta was measured 5 times and recorded. The maximum length among the measurements was recorded as the maximum aortic diameter of this region.

3.4.2   Categorisation of different form AAA

AAAs were categorised using the scale described by Daugherty and colleagues (Daugherty *et al.*, 2001). The scale is: Type 0: no aneurysm, Type I: dilated lumen in the SRA region with no thrombus, Type II: remodelled tissue in the SRA region that frequently contains thrombus, Type III: a pronounced bulbous form of type II that contains thrombus, and Type IV: a form in which there are multiple aneurysms containing thrombus, some overlapping in the suprarenal area of the aorta.

3.5 Atherosclerosis assessment

3.5.1 *En face* analysis of Sudan IV stained atherosclerotic lesion in the aortic arch

The ARCH was washed with cold DPBS twice and used for *en face* staining with Sudan IV. The extraneous adventitia tissue was thoroughly trimmed, and the ARCH was cut open longitudinally and pinned down on a sheet of wax, in order to obtain flat aortic tissue with the endothelium facing up. The samples were fixed with 70% ethanol for 5 min followed by immersing in the filtered Sudan IV staining solution (5 grams of Sudan IV dissolved in 500 ml acetone and 500 ml 70% ethanol) for 10 min with rocking periodically. Eighty percent ethanol was then added for 5 min to differentiate the stained tissue and to eliminate background staining (Chen & Nadziejko, 2005; Chen *et al.*, 2010). Stained samples were then washed once with DPBS and immediately placed on a graduated template to be photographed using a digital camera (CoolPix 4500, Nikon, Japan).

3.5.2 Atherosclerotic lesion measurement

ImageJ software (v1.4d, NIH, USA) was used to quantify the Sudan IV stained ARCH. A custom scale was set using the ruler in the image, and this procedure was repeated for each image before commencing the measurements. The outline of the intima was then manually traced and measured as the total tissue area. Sudan IV stained lesions were contrasted with intact white pink intima so that the lesion areas could be manually traced and measured as the total stained lesion area.

3.6 Preparation of single suspension cells and cell surface staining for flow cytometry

3.6.1 Red blood cell lysis bufer:

Erythrocytes were depleted from peripheral blood, BMCs, and splenic cells using commercial RBC lysis buffer (10 X, stock) containing ammonium chloride, potassium carbonate, and EDTA (eBioscience, USA). The stock RBC lysis buffer was diluted to working solution (1 X) in deionized water. The pH of the working solution fell within the range of pH 7.1-7.4. The solution was warmed to room temperature prior to use.

3.6.2 Preparation of single-cell suspension from peripheral blood cells, bone marrow cells, and splenic cells

A total volume of 35 µl whole blood (Section 3.3.1), 500 µl BMCs (Section 3.3.4), or 500 µl splenic cells (Section 3.3.5), was used to prepare a single-cell suspension for flow cytometry assessment. RBCs were lysed by adding 2 ml RBC lysis buffer for 10 min at room temperature protected from light, followed by adding 2 ml DPBS to stop the reaction. Samples were immediately centrifuged at 250 x g for 5 min at 4^oC and the supernatant was carefully discarded. The cell pellet was then resuspended in 1 ml FACS staining buffer (DPBS containing 1% BSA and 0.1% sodium azide), at 4^oC. For peripheral blood, samples were centrifuged again and resuspended in the staining buffer with a final volume of 100 µl in a 12 x 75 mm round bottom test tube (BD Biosciences, USA). For BMCs and Splenic cells, cells concentration was determined using a Scepter Handheld Automated Cell Counter (Millipore, USA) as described in the following Section 3.6.3. One million BMCs or splenic cells per sample were transferred to a new 12 x 75 mm round bottom test tube and centrifuged at 250 x g for 5 min at 4 ^{o}C. The cell pellet was resuspended in 100 µl of FACS staining buffer ready for staining for flow cytometry.

3.6.3 Cell counting using Scepter Handheld Automated Cell Counter

The Scepter Handheld Automated Cell Counter (Millipore, USA) was use to count cells. A volume of 200 µl of prepared BMC or splenic cell, described in Section 3.6.2, was used to

perform cell counting. Samples were centrifuged at 250 x g for 5 min. Cell pellets were

resuspended in 200 µl DPBS ready for cell counting. A 60 µm Sensor was attached to the

Scepter and submersed in the sample for sample loading. When the cell counting was

completed, a histogram would be displayed. In the histogram screen, the lower gate and higher

gate of the histogram was adjusted to 12 µm and 36 µm respectively. Cell concentration was

automatically calculated.

3.6.4   Cell surface staining for flow cytometry

Rat anti-mouse CD16/CD32 (BD Biosciences, USA) was added to the cells in FACS staining

buffer to block nonspecific binding of the Fc receptor. Samples were incubated on ice for 20

min and then centrifuged at 250 x g for 5 min at $4^{\circ}C$. The supernatant was carefully aspirated

and the cell pellet was resuspended in 100 µl FACS staining buffer. A cocktail of different

fluorochrome conjugated antibodies was added and samples were incubated at room

temperature for 30 min in the dark. The samples were then washed 3 times with FACS staining

buffer. The cell pellets were resuspended in 300 µl FACS staining buffer ready for analysis

using flow cytometry.

3.7 Flow cytometer instrument setting and sample acquisition for cell phenotype analysis

3.7.1 Flow cytometers

Two flow cytometers, BD FACSCalibur (BD Biosciences, USA) and CyAn ADP 9-colour analyser (CyAn ADP, Beckman Coulter, USA), were used to analyse leukocyte populations in peripheral blood, BMCs, and splenic cells in AngII-infused ApoE$^{-/-}$ mice receiving human Fc protein or rAngpt2. BD FACSCalibur was used in the experiment lasting for 14 days and CyAn ADP was used in the experiment lasting for 5 days.

The standard BD FACSCalibur system includes a 15-mW, 488-nm, argon-ion laser and detectors for three fluorescent parameters. It also includes a second 635-nm, red-diode laser, and an additional detector. BD CellQuest Pro software (v9, BD Biosciences, USA) was used to set-up the instrument and for sample acquisition. The standard CyAn ADP system includes a 20-mW, 488-nm, a 27.5-mW, 635-nm, and a 27.5-mW, 405-nm laser. Summit software (v4.3, Beckman Coulter, USA) was used to set-up the instrument and for sample acquisition.

3.7.2 Optimisation of flow cytometer instrument setting

BD FACSCalibur setting was optimised as following: the forward scatter (FSC) Amp Gain and side scatter (SSC) Voltage were adjusted using an unstained peripheral blood sample to display the population of interest in the FSC *versus* SSC plot. Debris was excluded by adjusting the threshold of FSC. Both FSC and SSC were in linear (Lin) mode. Fluorescence detector settings were adjusted using an isotype stained peripheral blood sample to display cells in the negative quadrant, intersection to 10^1 on the x-and y-axes respectively. The mode for FL1 (FITC), FL2 (PE) and FL4 (APC) were set to Log in the Detector/Amps window. FL1, FL2 and FL4 Voltages were adjusted to place the cells in the lower-left quadrant of the FL1 *versus* FL2, FL1 *versus* FL4 and FL2 *versus* FL4 plot. Compensation settings were adjusted to correct for spectral overlap using single a fluorescence conjugated antibody for the experiments. FL2-%FL1 was adjusted to place FITC positive events in the lower-right quadrant of the FL1 *versus*

FL2 plot. FL1-%Fl2 was adjusted to place PE positive events in the upper-left quadrant of the FL1 *versus* FL2 plot. FL3-%Fl4 was adjusted to place APC positive events in the upper-left quadrant of the FL3 *versus* FL4 plot. The optimised instrument settings were saved and used for all sample acquisitions. The parameters of the instruments setting are listed in **Table 3.2**.

Table 3.2 FACSCalibur instrument setting for cell phonotypes

Detector	Voltage	Amp Gain	Mode	Compensation
FSC	E00	2.09	Lin	
SSC	471	1.32	Lin	
FL1 (FITC)	480		Log	FL1 - 1.4% FL2
FL2 (PE)	409		Log	FL2 - 37.1% FL1
FL4 (APC)	742		Log	FL4 - 14.5% FL3

Establishing instrument settings for CyAn ADP were similar to FACSCalibur; however, the Summit software performs full inter-laser compensation of fluorescence parameters, and data saved as a sample file was saved with both compensated and uncompensated parameters. The optimised parameters of the instruments setting are listed in **Table 3.3.**

Table 3.3 CyAn ADP instrument setting for cell phenotypes

Detector	Voltage	Amp Gain	Mode	Compensation
FSC	N/A	1.2	Lin	
SSC	550	1.0	Lin	
FITC	620	1.0	Log	PE - 16.67% FITC
PE	720	1.0	Log	
PE-Cy5.5	850	1.0	Log	
APC	920	1.0	Log	

3.7.3 Sample acquisition

Prior to loading for acquisition on a flow cytometer, samples were gently mixed for 10 sec. To run the sample through the flow cytometer, software was used to control the sample running based on the software instructions. Prior to acquire data for saving, a pre-run was used to ensure the interested cells appeared on the scale. In between samples, a sterilised Milli-Q water sample was run through the machine to flush out the cells from the previous run.

Viable cells were gated according to FSC and SSC (G1) in both the BD FACSCalibur and the CyAn ADP flow cytometers. For the BD FACSCalibur, the collection criteria was set to stop acquisition when 10,000 events in G1 were collected and the results were auto saved to file in the Global Acquisition and Storage menu of the CellQuest Pro software. For CyAn ADP, the total events were set in the Acquisition Sample Panel of the Summit software to stop and auto save data when 10,000 in G1 was collected. This setting would equally collect and record 10,000 viable cells for each sample. The saved files were then analysed.

3.8 Cytometric Bead Array (CBA) Mouse Inflammation Kit

3.8.1 Preparation of plasma for CBA

The CBA Mouse Inflammation Kit (Cat# 552364, BD Biosciences, Australia) was used to quantitatively measure inflammatory protein levels (IL-6, IL-10, MCP-1, IFN-γ, TNF and IL-12p70) in the mouse plasma samples. Six vials of Capture Bead suspension with known size, different median fluorescence intensities (MFIs), and capture specific antibodies were provided. Each Capture Bead suspension was vigorous vortexted and a 10 µl aliquot of each Capture Bead was added to a single tube as mixed Capture Beads. A 2-fold dilution series of provided recombinant standard were used in parallel to samples for preparation of the standard curve (20-5000 pg/ml). The samples and standards were stained with 50 µl mixed Capture Beads and 50 µl PE-conjugated detection antibodies for 2 hour at room temperature. The samples were then washed with 1 ml provided washing buffer. The samples were centrifuged with 200 x g for 5 min at room temperature and the supernatant was carefully aspirated and discarded. The bead pellet was resuspended by adding 300 µl provided washing buffer and ready to analysis on a CyAn ADP flow cytometer.

3.8.2 CyAn ADP instrument setting for CBA Mouse Inflammation Kit

CyAn ADP was used to perform measurement of the cytokines in plasma. Instrument setting for CBA Mouse Inflammation kit was performed using the Cytometer Setup Beads provided in the kit. A volume of 50 µl Cytometer Setup Beads was added to 450 µl washing buffer followed by vortexing ready for flow cytomety. SSC Voltage was adjusted to show the beads population in the upper-right quadrant and the singlet bead population was gated as R1 in the FSC log *versus* SSC log plot. Then APC Voltage and FITC voltage were adjusted to put the dim and bright beads to 10^1 to 10^2 and 10^3 to 10^4 on the y-axes respectively in the FITC log *versus* APC log plot. Then PE voltage was adjusted to put the dim and bright beads to 0 to 10^1 on x-axes in the PE log *versus* APC log plot. The optimised parameters of the instrument setting are listed in **Table 3.4**.

Table 3.4 CyAn ADP instrument setting for CBA Mouse Inflammation kit

Detector	Voltage	Amp Gain	Mode
FSC	N/A	1.0	log
SSC	380	1.0	log
FITC	540	1.0	log
PE	660	1.0	log
APC	530	1.0	log

3.8.3   Sample acquisition for CBA Mouse Inflammation Kit

Prior to sample acquisition, samples were vigorous vortexted for 10 sec to ensure a single-bead suspension. The sample acquisition procedure is same as previously described (Section 3.7.3). The singlet bead population was gated as R1 in FSC log *versus* SSC log plot. The total events were set in the Acquisition Sample Panel of the Summit software to stop and auto save data when 2,000 events in R1 was collected. The saved files were then analysed.

3.8.4   FCAP Array software for analysis of CBA data

Data analysis was performed using FCAP Array Software (v3, Soft Flow, USA), according to the manufacturer's instructions. In the software, a new empty experiment was created. The standard and test samples associated flow cytometry files were added and assigned with Standard and Test respectively. CBA Mouse Inflammation Kit was then chosen in the Beads and Model list, which would automatically load the parameters required for quantitative analysis of each analyte included in the kit. Bead clusters were assigned to their corresponding analytes based on the MFI in the FL8 APC channel. The standards were defined by clicking the Standards and QC in the navigation panel and standard curves for each analyte could be viewed by clicking Standard Curve in the navigation panel. In this thesis, a five parameter logistic fit with 98% Fitting Accuracy and without weighting were chosen to plot the standard curves. The concentration of each analyte in the test samples was determined from its standard curve.

3.9   Protein extraction and quantification

3.9.1   Preparation of whole protein extracts from aortic tissue

Aortic tissues stored at −80°C in OCT compound were thawed on ice and washed in cold PBS twice, followed by weighing. The samples were then snap frozen in liquid nitrogen and thawed on ice for 3 cycles and then cut into small pieces with a pair of scissors. A modified radio-immunoprecipitation assay (RIPA) buffer (50mM Tris-HCl pH7.4, 150 nM NaCl; 2 mM EDTA, 1% TritonX-100, 0.1% sodium dodecyl sulfate (SDS), and 0.1% sodium deoxycholate) was added to the tissues in a ratio of 80 µl per 100 µg tissue, in the presence of a protease inhibitor cocktail (Roche, USA). The samples were incubated on ice with vortexing every 20 min over 1 hour period. After the incubation, 5 µg 0.005 mm Bullet Blender beads (Next Advance, USA), were added per 100 µg tissue to blend at speed 8 for 30 sec, using a Bullet Blender (Next Advance, USA). The homogenised samples were immediately cooled down in an ice and water bath for 2 min. This was repeated for a total 5 cycles. The samples were placed on ice for another 30 min followed by centrifugation at 13,000 x g for 30 min at 4°C. The supernatants were collected in 1.5 ml polypropylene tubes, and the samples were ready for protein concentration determination. The protein extracts were stored at −80°C for future analysis.

3.9.2   Preparation of nuclear protein extracts from aortic tissue

Nuclear proteins were extracted using the Thermo Scientific NE-PER Nuclear and Cytoplasmic Extraction Kit (Cat# 78833, Thermo Scientific, USA), according to the manufacturer's instructions. Tissues were weighed to determine the volume of reagent to be used for extraction. The tissues were cut into pieces, washed with cold DPBS, and centrifuged at 500 x g for 5 min. The supernatant was removed, leaving the tissue pieces dry as possible. A volume of 200 µl CER I reagent per 20 mg tissue was added and tissues were homogenised using a tissue grinder. This was followed by vigorous vortexing on the highest setting for 15 sec, in order to resuspend the tissue pellet. Then the sample was incubated on ice for 10 min, after which a volume of 11

µl ice-cold CER II per 20 mg tissue was added to the sample. This was followed by vortexing for 5 sec on the highest setting and 1 min incubation on ice thereafter. The samples were vortexed again and centrifuged at 18,000 x g for 5 min at 4°C. The supernatants, cytoplasmic extract, were immediately transferred to a pre-chilled 1.5 ml polypropylene tube. The insoluble pellets containing nuclei were suspended in a volume of 100 µl ice-cold NER per 20 mg tissue, followed by vortexing on the highest setting for 15 sec. They were then incubated on ice for 40 min, with continued vortexing for 15 sec every 10 min. The samples were then centrifuged at 18,000 x g for 5 min at 4°C. The supernatants, the nuclear extract, were transferred to clean pre-chilled 1.5 ml polypropylene tubes. Samples were stored at −80°C for further analysis.

3.9.3   Determination of protein concentration using Bradford Protein Assay

The Bradford Protein Assay is a dye-binding assay in which a differential dye colour change occurs in response to various concentrations of protein. Lyophilised bovine gamma globulin (IgG) was reconstituted in Milli-Q water and used as protein standard. Six serial dilutions of the protein standard within the linear range of 0.02-1.5 mg/ml were used to create a standard curve. The standard proteins and sample proteins were diluted in Milli-Q water and mixed with Bio-Rad Protein Assay dye reagent concentrate (Bio-Rad, USA), at a ratio of 4:1 to a final volume of 200 µl in a flat bottom 96-well-plate. The mixture was well mixed followed by 30 min incubation in dark at room temperature. The 96-well-plate was then measured the optical density (OD) at 595 nm using a micro-plate reader (Tecan, USA). The standard curve was plotted by standard protein concentrations *versus* their ODs. Each sample's protein concentration was determined according to the standard curve.

3.10 Western blotting

3.10.1 SDS-PAGE gels and electrophoresis to separate protein mixture

4–20% Mini-PROTEAN TGX precast polyacrylamide gels with 15-well combs were purchased from Bio-Rad (Cat# 456-1096). Single concentration SDS-polyacrylamide gels were cast using the Bio-Rad gel kit. The concentration of polyacrylamide gel used was determined by the molecular weight of the targeted proteins. The SDS-PAGE gel includes a "stacking" gel and a "separation" gel.

Protein extracts (20-60 μg) were mixed with 1x SDS gel-loading buffer (2% SDS, 2 mM beta-mercapto-ethanol, 4% Glycerol, 50 mM Tris-HCl, pH 6.8, 0.01% Bromophenolblue, and 100mM dithiothreitol) and boiled at 95 ^{o}C for 5 min, followed by rapid cooling on ice. The denatured protein samples were then loaded into each well of the gel. Molecular weight standards (8 μl) were loaded into one well to facilitate the estimation of the sizes of the targeted after resolution by electrophoresis. The gel was run with 1x Tris/Glycine/SDS electrophoresis buffer (25 mM Tris, 192mM glycine, and 0.1% SDS, and pH 8.3) (Bio-Rad, USA) at 110 V for 70 min or until the blue loading dye approached at the bottom of the gel. The gel cassette was carefully disassembled to remove the gel, which was transferred to a container with Bjurrum Schater-Nielsen (BSN) buffer (48 mM Tris, 39 mM Glycine, 10% Methanol and 0.0375% SDS, pH 9.2). The gel was then washed on a shaker at a low speed for 20 min.

3.10.2 Transfer of proteins from gel to membrane and staining

A Semi-dry transfer method was used to transfer protein from the gel to an activated PVDF membrane (Bio-Rad, USA) (immersing PVDF membrane in 100% methanol). Cotton absorbent filter papers (Bio-Rad, USA) and PVDF membranes were soaked in BSN buffer and the gel and membrane were sandwiched between two stacks of the absorbent filter papers. They were then placed directly in contact with the plate electrodes of the Trans-Blot SD Semi-Dry transfer cell

(Bio-Rad, USA). The transfer condition was 0.09 amps constant current per 10 x 7.5 cm membrane for 60 min.

After transfer, PVDF membranes were washed with Milli-Q water for 5 min, followed by incubation in 5% BSA in Tris buffered saline (TBS) for 1 hour at room temperature at a low speed on a shaker, to block nonspecific antibody binding sites. Primary antibody in TBS containing 0.05% Tweent (TBST) was then added to the membrane to probe the targeted proteins on a rotator at 4^oC overnight. The membrane was washed 3 times for 15 min in TBST, and incubated with HRP-conjugated secondary antibody in TBST at room temperature for 1 hour. This was followed by washing 3 times for 15 min in TBST and a 10 min wash in TBS, in order to get rid of remaining tween on the membrane ready for protein visualisation.

3.10.3   Protein visualisation

Amersham ECL Plus Western blotting Detection Reagent (GE, USA) was equilibrated to room temperature for 20 min prior to use. A working solution was prepared by adding Luminol to Peroxide in equal volumes and mixing well. The detection reagent was added to the membrane at the volume of 0.1 ml per cm^2 membrane, followed by incubation for 5 min in dark. Excess detection reagent was drained off by holding the membrane edge gently against a piece of tissue. The membrane was then placed on the sample tray in the CCD camera compartment. The intensity of the targeted protein was visualised by ChemiDoc XPS (Bio-Rad, USA) and acquired using QuantityOne software (v1.0, Bio-Rad, USA).

3.10.4   Densitometry analysis of Western blots

Densitometry was performed using the software Image Lab (v5, Bio-Rad, USA). The saved digital Western blot image was imported to Image Lab. The lanes tool was used to create lanes. The bands of targeted protein was identified according to its molecular weight compared with the molecular weight standards. The background was subtracted with a rolling disc size (mm)

that determines how closely the background level follows the intensity profile. The volume (intensity, INT) of the band was then measured by the software automatically.

3.11 Immunofluorescence staining

3.11.1 Preparation of tissue sections for immunofluorescence staining

Cryopreserved aortic tissues were washed with PBS and embedded in an OCT compound. The embedded tissues were snap frozen by immersing them in isopentane in a liquid nitrogen bath. The snap frozen tissues were stored at -80°C for at least 48 hours before they were ready for cryostat sectioning. The aortic tissues were sectioned transversely into 6 μm thick, and mounted on Poly-L-Lysine coated slides (Braunschweig, Germany). The sections were air dried for 15 min. The slides were then fixed in ice cold acetone for 15 min, air dried and stored in -80°C for future immunofluorescence staining.

3.11.2 Immunofluorescence staining

Six micron cryostat sections were prepared as described above. Slides containing sections were air dried for 20 min followed by rehydration in PBS for 5 min. Sections were blocked with 5% normal serum of the species, producing the highly cross-absorbed secondary antibody in PBS containing 0.5% BSA and 0.1% Triton X-100 for 60 min at room temperature. This was followed by incubation with primary antibody in PBS containing 0.5% BSA overnight at 4°C. Sections were incubated with PBS, containing 0.5% BSA only as negative controls. After sections were gently washed in PBS 3 times for 15 min each, Alexa fluor 488-conjugated secondary antibody (Excitation 495 nm and mission 519 nm) in PBS containing 0.5% BSA was applied to the tissue sections for 1 hour at room temperature. This was followed by gentle wash in PBS 3 times for 15 min each in dark. 4',6-Diamidino-2-phenylindole dihydrochloride (DAPI) (Sigma-Aldrich, USA) was added to the tissue sections for 3 min in dark at room temperature to stain cell nuclei. This was followed by a wash in deionized water for 5 min. The sections were

then mounted with water based mounting medium and covered with a coverslip ready for

fluorescence microscopy (Zeiss, Germany).

3.11.3   Immunofluorescence microscope

The immunofluorescence stained sections were imaged using a Zeiss fluorescence microscope

(AXIO Imager Z1, Germany) equipped with a Zeiss AxioCam Mrm (monochrome CCD)

camera and a FluoArc mercury lamp (Zeiss, Germany), to generate excitation light. Images

were observed using DAPI filter (Excitation 365 nm and Emission 445/50 nm) for nuclear

DAPI staining, and Cy2/GFP filter (Excitation 450-490 nm and Emission 515-565 nm) for

surface antigen staining labelling with Alexa Fluro 488-conjugated secondary antibody. Slides

were loaded and observed using a 10X N PLAN objective lens with 0.3 Numerical Aperture to

identify the area of interest on the image. A 20X PL APO objective lens with 0.8 Numerical

Aperture was then switched into the light path, followed by the acquisition of the digital image.

The digital images of the microscopic fields of aortic tissue were acquired by Axiovision

software (v4.5, Zeiss, Germany) (20X PL APO objective Len). A multidimensional acquisition

including both DAPI and Cy2/GFP channels weas set up to acquire images. The brightest

channel (DAPI) was activated to adjust camera exposure by an automatic measure. Each

wavelength has a slightly focal plane because of the poor chromatic correction of objectives and

the filter block effect. Thus Focus Offset was set for focus-correction in each channel. The

specimen was then focused in the live window and was ready to acquire. After this, the image

was captured and the brightness and contrast were adjusted in each channel by clicking "Best

Fit" with 1%. A ZVI type image was saved for future analysis.

3.11.4   Quantification of immunofluorescence staining

ImageJ software (v1.4d, NIH, USA) with the Bio-Formats plugin (v5.0, LOCI, USA) was used

for computerised quantification of the positive immunostaining area. ZVI images were loaded

into ImageJ software and monochrome images acquired in each channel were separated prior to

analysis. A 5x5 convolution kernel matrix was applied to the monochrome images to smooth and sharpen the image. This was done with a filter in the process menu followed by contrast enhancement. Then the image was converted to a binary image, which converted positive staining area into grey scale. The image was then analysed using 'analysed particles' with setting parameters (0-infinity (pixel^2) for size and 0.01-1.00 for circularity) to outline the grey areas representing the positive staining area. The outline of the microscopic field of the tissue area was traced and measured as total measured area.

CHAPTER 4

Protocol Optimisation and Measurement Validation

4.1   Introduction

It is critical to choose suitable methods for the primary and secondary outcome assessments so that the role of Angpt2 in experimental AAA and atherosclerosis development may be elucidated. Every method has its limitations; therefore, the experimental procedures must be standardised. Also, the concentration of the reagents used in procedures must be optimised, in order to eliminate the interference of background noise, which may cause false reports. Moreover, it is also important to validate whether the method is suitable for detecting changes with sufficient specificity and sensitivity. Measurement error is another source of subject bias. Therefore, the precision of the data collection procedures must be validated, with a good repeatability and reproducibility, in order to avoid bias and error associated with the size of measurements or the effect of using different observers. The aims of this chapter are as follows:

1. To assess the repeatability and reproducibility of the measurements, including aortic morphometry, atherosclerotic lesion area quantification, characterisation of AAA forms, and positive immunofluorescence staining area measurement,

2. To validate the feasibility to use Western blotting for protein expression quantification within the aortic tissue and CBA Mouse Inflammation Kit for plasma cytokine expression quantification, and

3. To determine the optimised antibody concentration for cell surface staining and use Fluorescence-Minus-One (FMO) control for cell phenotype analysis in flow cytometry.

4.2   Statistical analysis

Intraclass correlation (ICC) was used to determine reliability between two measurements by intra-observer or inter-observers, using reliability analysis in SPSS (v22, IBM, USA). The ICC is estimated using a one-way random effect analysis of variance for intra-observer repeatability and a two-way random effect analysis of variance for inter-observer reproducibility. An ICC value over 0.950 was considered an excellent agreement between two measurements.

Limits of agreement (LoA) between variables is plotted using the Bland-Altman method, using Graphpad Prism (v6, USA) software. It can be used to visually inspect the difference between two measurements repeated by the thesis author or by the thesis author and the second observer. The variability of the difference between two measurements indicates how well the measurement agrees and whether the measurement bias is consistent and the error SD is different (Bartlett & Frost, 2008). The difference was calculated as the second measurement subtracts from the first measurement for repeatability and external observer's measurement subtracts from the thesis author's first measurement for reproducibility. The LoA gave a range between two measurements (95% of the difference in the future measurements) (Altman & Bland, 1983).

The categorical analysis was performed using *kappa* statistic in SPSS (v22, IBM, USA). The strength of agreement is based on the standard *kappa* coefficient proposed by Landis and Koch as follow: 0.41-0.60 as moderate, 0.61-0.80 as substantial, and 0.81-1.00 as almost perfect agreement (Landis & Koch, 1977).

4.3 Validation of aortic morphometry, atherosclerotic lesion measurement, and characterisation of different forms of AAAs

4.3.1 Study design

Whole dissected aortas were digitally photographed and Photoshop CS5 Extended was used to measure the maximum aortic diameter in the SRA region (Chapter 3, Section3.3.3 and 3.4.1). Ten aortas, a mixture of different form AAAs, were randomly chosen to perform the repeatability and reproducibility test. Atherosclerotic lesion staining and measurement were performed as described previously (Chapter 3 Section 3.5). Ten Sudan IV stained ARCH samples were randomly chosen to perform the repeatability and reproducibility test. For characterisation of different forms of AAAs, The criteria are adapted from a previous publication as described previously in Chapter 3 Section 3.4.2. Twenty-eight digitally photographed aortas, a mixture of SRA AAAs from no dilatation to multiple dilatations, were chosen to be analysed using the repeatability and reproducibility test. The repeatability was assessed by comparing the results measured by the thesis author within an interval of one week. The reproducibility was assessed by comparing the results measured by the thesis author (first measurement) and the second observer (YW).

4.3.2 Results and conclusion

4.3.2.1 *Repeatability and reproducibility of aortic morphometry*

The reliability tests showed that there was excellent agreement both within the intra-observer and between the inter-observers (ICC= 0.997 and ICC=0.994 respectively, **Figure 4.1** A and C) and the average difference within the intra-observer and between inter-observers was close to zero at 0.012 mm (95% LoA: -0.088 - 0.113) and 0.025 mm (95% LoA: -0.108 - 0.150) respectively (**Figure 4.1** B and D).
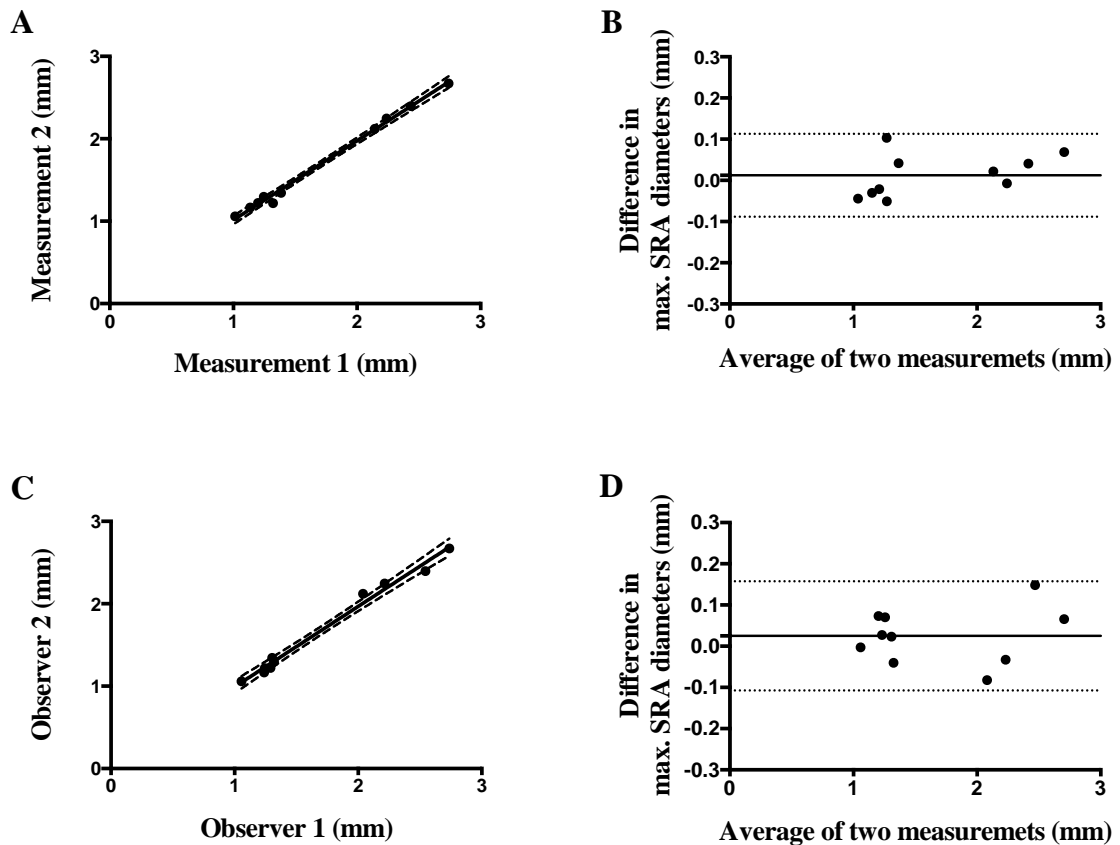
Figure 4.1 Repeatability and reproducibility of the SRA morphometry.
Data were plotted with the SRA maximum aortic diameter (mm) between two measurements with a line
of equality: **A**) within the intra-observer (ICC=0.997, 95% confidence interval (CI): 0.988-0.999); and **C**)
between the inter-observers (ICC=0.994, 95% CI: 0.976-0.998). The dotted line represents error bar and
the solid line represents 95% CI of the best-fit. **Bland-Altman analysis** was used to plot LoA: difference
in two SRA maximum diameter measurements against their average: **B**) within the intra-observer; and **D**)
between the inter-observers. The solid line represents the average difference between two measurements
and the dotted lines represent the upper and lower 95% CI of LoA. Each dot represents 1 of 10
measurements.

4.3.2.2   Repeatability and reproducibility of atherosclerotic lesion assessment

The reliability tests showed that there was an excellent agreement both within the intra-observer

and between the inter-observers (ICC= 0.973 and ICC=0.895 respectively, **Figure 4.2** A and C)

and the average difference within the intra-observer and between inter-observers was close to

zero at 0.132% (95% LoA: -2.90-2.63) and 0.056% (95% LoA: -6.02-6.13) respectively (**Figure**

4.2 B and D).
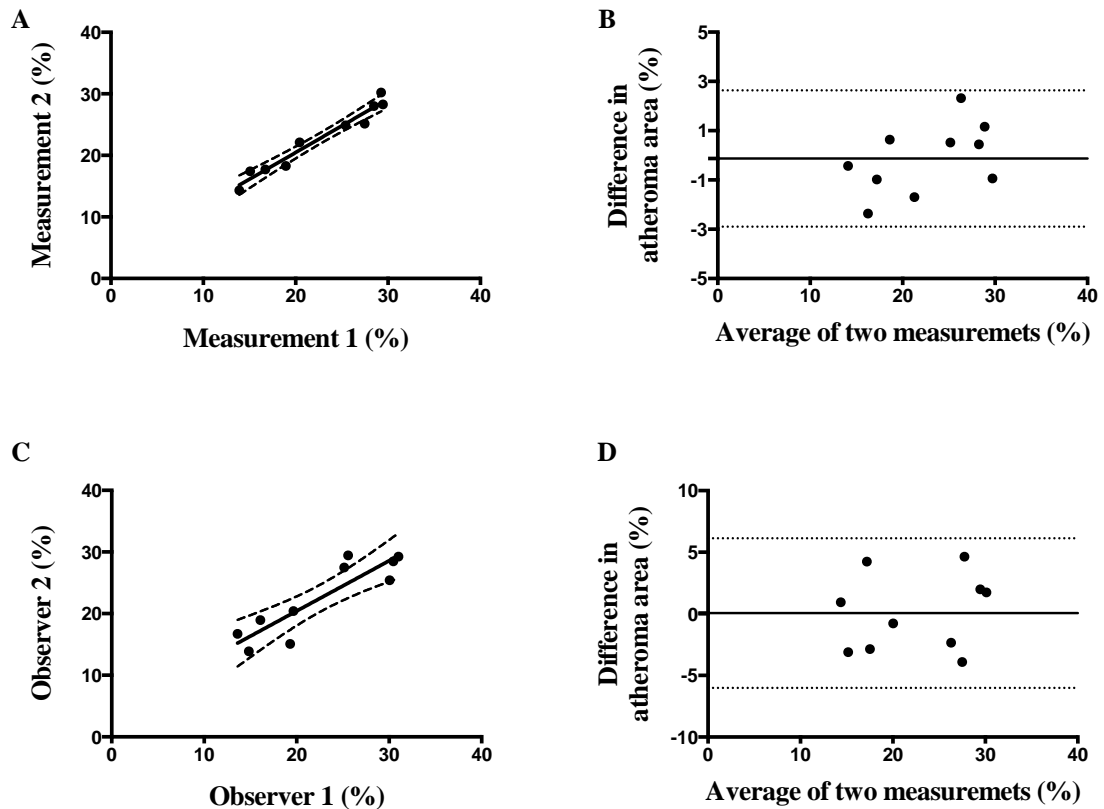
Figure 4.2 Repeatability and reproducibility of the atheroma area measurement.
Data were plotted with the percentage of atheroma area between two measurements with a line of equality: **A**) within the intra-observer (ICC=0.973, 95% CI: 0.897-0.993); and **C**) between the inter-observers (ICC=0.895, 95% CI: 0.630-0.973). The dotted line represents error bar and the solid line 95% CI of the best-fit. Bland-Altman analysis was used to plot LoA: difference in percentage of atheroma area measurements between two measurements against their average: **B**) within the intra-observer; and **D**) between the inter-observers. The solid line represents the average difference between two measurements and the dotted lines represent the upper and lower 95% CI of LoA. Each dot represents 1 of 10 measurements.

4.3.2.3   Repeatability and reproducibility of AAA characterisation

The reliability tests showed that there was an almost perfect strength of agreement within the intra-observer, with a *kappa* value of 0.946. The agreement between two observations by one observer was 27 of 28 aortas (96%), as depicted in **Table 4.1**. There was a substantial strength of agreement within the inter-observers with a *kappa* value of 0.727. The agreement between two observers was 23 of 28 aortas (82.1%) depicted in **Table 4.2**.

Table 4.1 Cross-tablulation of AAA forms grading between two independent gradings by the same observer within one-week interval in SRA

			HY 2nd grading					Total
			Type 0	Type I	Type II	Type III	Type IV	
HY 1st grading	Type 0	Count	14	0	0	0	0	14
		Expected Count	7.5	1	1	2	2.5	14
	Type I	Count	1	2	0	0	0	3
		Expected Count	1.6	0.2	0.2	0.4	0.5	3
	Type II	Count	0	0	2	0	0	2
		Expected Count	1.1	0.1	0.1	0.3	0.4	2
	Type III	Count	0	0	0	4	0	4
		Expected Count	2.1	0.3	0.3	0.6	0.7	4
	Type IV	Count	0	0	0	0	5	5
		Expected Count	2.7	0.4	0.4	0.7	0.9	5
Total		Count	15	2	2	4	5	28
		Expected Count	15	2	2	4	5	28

Table 4.2 Cross-tabulation of AAA forms grading between two observers in SRA

			YW grading					Total
			Type 0	Type I	Type II	Type III	Type IV	
HY grading	Type 0	Count	14	0	0	0	0	14
		Expected Count	8.0	0.5	0.5	3.5	1.5	14.0
	Type I	Count	1	1	0	1	0	3
		Expected Count	1.7	0.1	0.1	0.8	0.3	3.0
	Type II	Count	1	0	1	0	0	2
		Expected Count	1.1	0.1	0.1	0.5	0.2	2.0
	Type III	Count	0	0	0	4	0	4
		Expected Count	2.3	0.1	0.1	1.0	0.4	4.0
	Type IV	Count	0	0	0	2	3	5
		Expected Count	2.9	0.2	0.2	1.3	0.5	5.0
Total		Count	16	1	1	7	3	28
		Expected Count	16.0	1.0	1.0	7.0	3.0	28.0

4.4 Validation the immunofluorescence staining and the measurement of positive staining area

In this thesis, indirect immunofluorescence staining was used to detect and visualise monocytes/macrophages and ECs within the suprarenal aortic (SRA) wall, using fluorescence microscopy. The persistent difficulty in the indirect immunofluorescence labelling technique is that background noise staining can occur as a result of no-specific binding, or a combination of ionic and hydrophobic interactions. The background noise staining can be reduced by applying blocking solution and using an optimised dilution of antibody. The aim of this section is to determine whether the indirect immunofluorescence staining method established previously in our laboratory, is suitable for detecting monocytes/macrophages or ECs within the SRA wall using MOMA-2 or CD31 antibody respectively, and to validate the reliability of the measurement of immunofluorescence positive staining area.

4.4.1 Study design

For protocol validation, three 6-μm SRA cryostat transverse sections were prepared, as described previously in Chapter 3, Section 3.11.1. Two sections were stained with both primary and secondary antibody as full staining and one section was stained with secondary antibody only as a negative control. The staining procedure was described previously (Chapter 3, Section 3.11.2). Briefly, non-specific binding site was blocked by adding 5% goat serum in PBS containing 0.1% Triton X-100 for 60 min at room temperature for all sections. Primary antibody rat anti-MOMA-2 (Abcam, UK) or rat anti-CD31 (Santa Cruz, USA) was added to corresponding section at a dilution of 1:100 in PBS containing 0.5% BSA and held overnight at 4°C. The control section was incubated with PBS containing 0.5% BSA. Alex fluo 488-conjugated goat anti-rat (Life Technologies, USA) was added to all sections at a dilution of 1:200. Cell nuclei were labelled by DAPI at a concentration of 1 nM/μl (Sigma-Aldrich, USA). All sections were mounted in a water based mounting medium, covered with a coverslip, and immediately examined using a Zeiss fluorescence microscope, as described previously in Chapter 3, Section 3.11.3.

For the measurement reliability test, twelve captured images (six MOMA-2 and six CD31 immunofluorescence stains) (x200 total magnification), were randomly selected as subjects of the repeatability and reproducibility test. The percentage of positive staining area (MOMA-2 or CD31) was measured using ImageJ (v1.4d, NIH, USA), as described previously in Chapter 3, section 3.11.4. The repeatability was assessed by comparing the results of percentage positive staining area of total staining area measured by the thesis author within an interval of one week. The reproducibility was assessed by comparing the results measured by the thesis author (first measurement) and the second observer (YW).

4.4.2 Results and conclusion

The results showed that the staining was specific and the background noise staining had been eliminated by blocking the sections with 5% goat serum in PBS and labelling with primary antibody and secondary antibody at a dilution of 1:100 and 1:200 respectively (**Figure 4.3**). The quality of the images was also sharp and suitable for further analysis. In conclusion, this protocol was proven suitable for the subsequent MOMA-2 and CD31 immunofluorescence staining on frozen transverse SRA sections, in order to detect monocytes/macrophages and ECs within the SRA wall.

<div align="center">

MOMA-2 **CD31**

Negative control **Full staining**

</div>
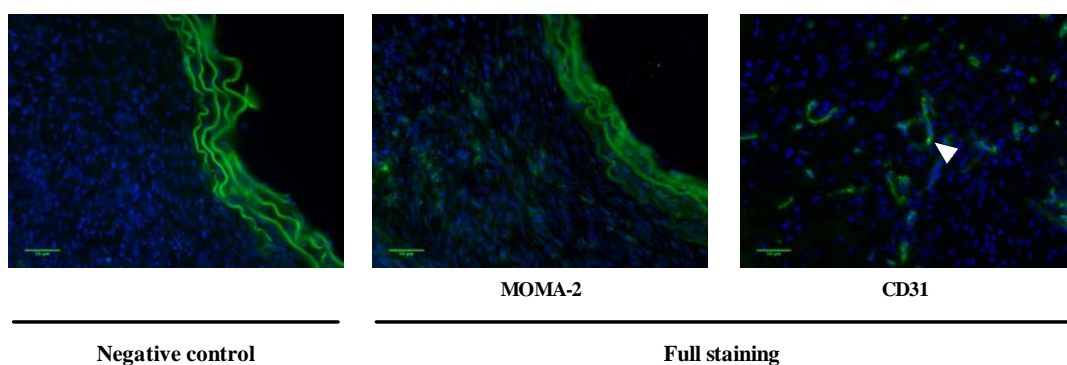
Figure 4.3 MOMA-2 and CD31 immunofluorescence staining.
The media elastin shows green auto fluorescence. Nucli were stained with DAPI (blue); monocytes/macrophages were staned with MOMA-2 (green); and ECs were stained with CD31 (green). The white arrow indicates a typical micro-vessel structure. The magnification is x 200 and the scale bar is 50 μm.

Reliability tests showed that there was excellent agreement both within the intra-observer and

between the inter-observers (ICC=0.993 and ICC=0.972 respectively **Figure 4.4** A and C).

Also, the average difference within the intra-observer and between inter-observers was close to

zero, at 0.063% (95% LoA: -0.471-0.346) and 0.075% (95% LoA: -0.926-1.080) respectively

(**Figure 4.4** B and D).
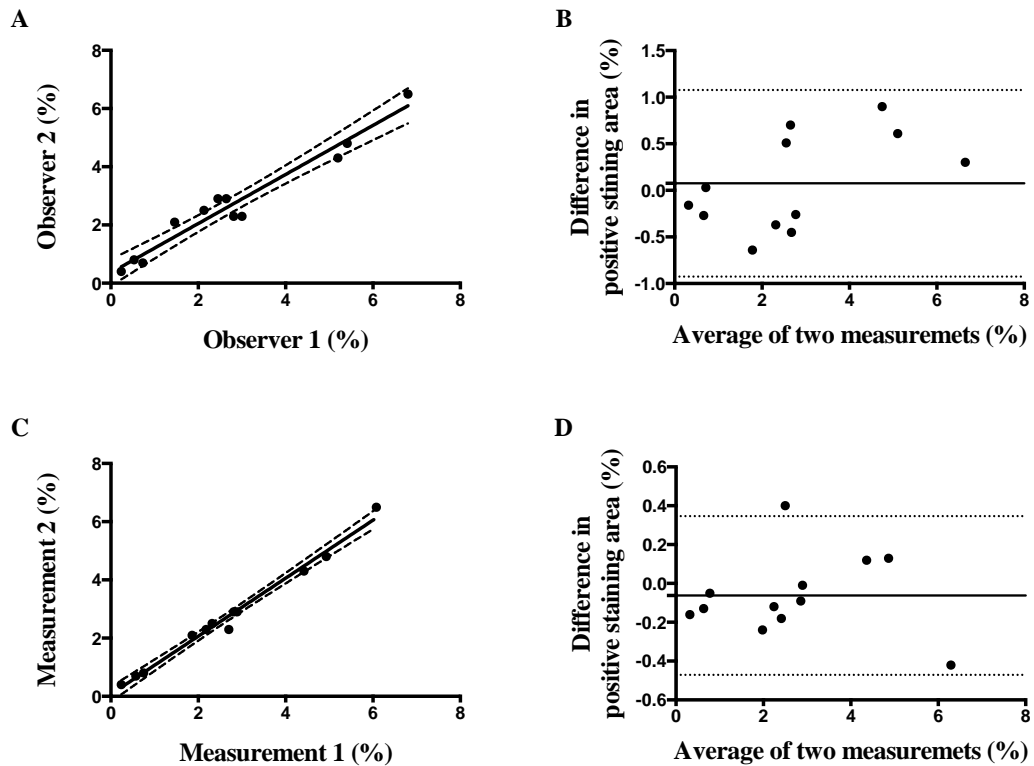
Figure 4.4 Repeatability and reproducibility of immunofluorescence positive staining area measurements.
Data were plotted with percentage of positive staining area between two measurements with a line of equality: **A**) within the intra-observer (ICC=0.993, 95% CI: 0.976-0.998); and **C**) between the inter-observers (ICC=0.972, 95% CI: 0.907-0.992). The dotted line represents error bar and the solid line 95% CI of the best-fit. **Bland-Altman analysis** was used to plot LoA: difference in percentage of positive staining area between two measurements against their average: **B**) within the intra-observer and **D**) between the inter-observers. The solid line represents the average difference between two measurements and the dotted lines represent the upper and lower 95% CI of LoA. Each dot represents 1 of 12 measurements.

4.5   Quantification of Western blots

Western blotting has been broadly used to detect the presence and absence of interested protein and to semi-quantification of interested proteins in a convenient format for rapid evaluation (Towbin *et al.*, 1979). Western blotting procedures have been standardised; however, the quantification of the protein expression level requires validation based on the Western blot density, as the major variation data of Western blots is derived from background subtraction (Gassmann *et al.*, 2009). Theoretically, the intensity of the band is correlated with the amount of the protein. The aim of this section is to validate the process of semi-quantification of Western blots, and to test the correlation of the protein concentrations and densities of the Western blots.

4.5.1   Study design

Glyceraldehyde-3-phosphate dehydrogenase (GAPDH) is a housekeeping protein expressed abundantly within cells. It has been universally used to ensure a similar amount of protein loading, and also to ensure the same transfer efficiency for each sample. In this section, GAPDH was detected by Western blotting, and its Western blots were used to validate the method of Western blot quantification in this section. Liver protein was extracted and quantified using Bio-Rad Bradford Assay, as described previously in Chapter 3, Section 3.9. A total of 20 µg, 25 µg, 30 µg, 40 µg, or 50 µg protein was loaded into each well of 10% SDS-PAGE gel. This was separated by electrophoresis, and transferred to PVDF membrane for probing as described previously in Chapter 3, Section 3.10. The membrane was probed as described previously (Chapter 3, Section 3.10.2). Briefly, the membrane was probed with primary monoclonal rabbit anti-GAPDH antibody (Cell Signaling, USA), at a dilution of 1:5000 in PBS containing 5% BSA. The membrane was then probed with secondary polyclonal HRP-conjugated goat anti-rabbit immunoglobullins (Dako, Germany) at a dilution of 1:2000 in PBS containing 5% BSA. ChemiDoc XPS (Bio-Rad, USA) was used to visualise the Western blots with a 30 sec exposure time. Then the image was saved for densitometry. Densitometry was performed using software Image Lab as described previously in Chapter 3, Section 3.10.4. A

Two-tailed Pearson Correlation analysis was performed to determine the correlation of Western

blot density and total loading protein using Graphpad Prism (v6, USA).

4.5.2 Results and conclusion

The images of Western blots showed that the density of the Western blot is positively correlated

with the amount of protein loaded for Western blotting (**Figure 4.5** A). Background subtraction

was set using a rolling disc for densitometry. The rolling disc values were set to subtract the

background at a consistent level, so that the line is contact with both the lowest points of the

slope (**Figure 4.5** B). The density of the Western blots had an excellent correlation (r=0.991,

p<0.001) to the amount of loaded protein (**Figure 4.5** C). This result suggests that it is

appropriate to use Western blotting for protein expression level detection.
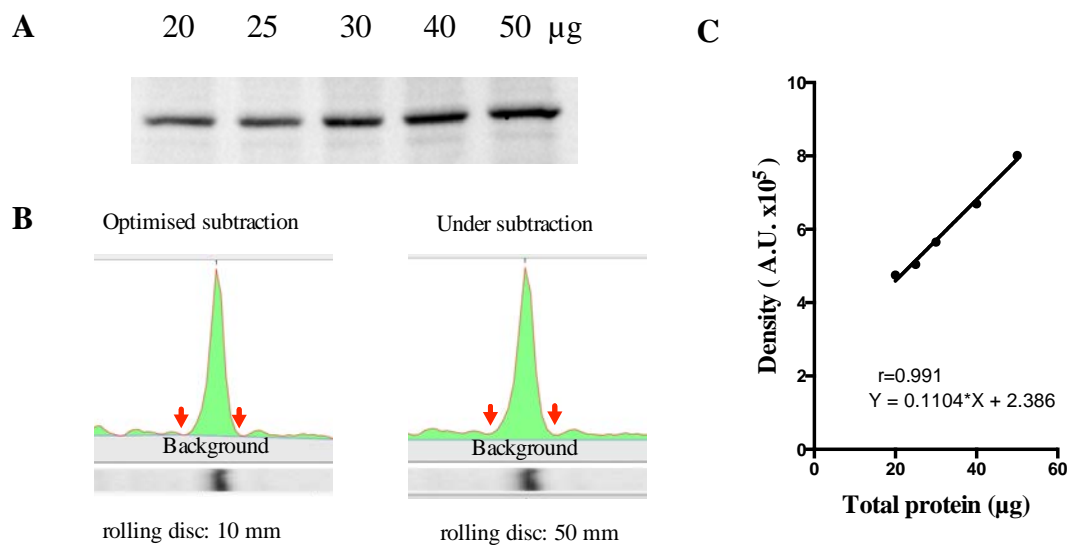
Figure 4.5 Quantification of Western blots using densitometry.
A) an image of the GAPDH Western blots from various amount of total protein loading; **B**) different
rolling disc size on background subtraction (the red arrows represent the lowest points of the slope); and
C) the correlation of total loading protein and the GAPDH Western blot density.

4.6 Flow cytometry: antibody titration and Fluorescence-Minus-One control for cell phenotype analysis

Flow cytometry is used to perform measurements on fluorochrome-conjugated antibody stained cells, in order to identify their phenotypes. It is critical to use an optimised concentration of antibody to label cell surface antigen. An inadequate concentration of the antibody would underestimate the proportion of positive cells, whereas an over saturated antibody would mask the true amount of antigen. Compensation setting of a flow cytometer is required to avoid a false signal caused by spectrum overlap. After the data are collected, a control is essential to accurately define the boundary between the positive and negative population. A FMO control is a mixture of lineage marker antibodies, excepting the one of interest, compared to a designated mixture of full lineage marker antibodies. A FMO control is also useful in determining whether there is any spread of the fluorochrome into the channel of interest. In this thesis, a three-colour panel staining by flow cytometry was used to identify monocytes and neutrophils in peripheral blood and BM. The aims of this section are 1) to optimise the concentration of antibody for cell surface staining for flow cytometry; and 2) to determine the feasibility of using FMO as a control in assisting to define the negative and positive boundary, and thus to facilitate the compensation setting.

4.6.1 Study design

Mouse peripheral blood and BMCs were collected as described previously in Chapter 3, Section 3.3.1 and Section 3.3.4, respectively. RBC depletion and single-cell suspensions were prepared as described previously (Chapter 3, Section 3.6.1 and Section 3.6.2 respectively). A volume of 100 µl peripheral blood samples (equivalent to 35 µl whole blood) or 100 µl BMCs (containing 10^6 cells), was used for cell surface staining.

For antibody titration, a serial volume (10 µl, 5 µl, 2.5 µl, 1.2 µl, 0.8 µl, and 0.4 µl) of APC-CD11b, FITC-Ly6C, PE-Ly6G, PerCP-Cy5.5-Ly6G, or PE-CCR2 was used to stain peripheral blood cells and BMCs.

A three-colour panel was used to identify cell phenotypes: FITC-Ly6C, APC-CD11b, and PE-Ly6G. A FMO control contains all the fluorochrome-conjugated antibodies in a panel except for the one that is measured; therefore, there were three separate FMO controls as shown in **Table 4.3**. A mixture of FITC-Ly6C, APC-CD11b, and PE-Ly6G antibodies was added to peripheral blood as full staining. A mixture of FITC-Ly6C and APC-CD11b, FITC-Ly6C and PE-Ly6G, or APC-CD11b and PE-Ly6G antibodies was added to peripheral blood as three different FMO controls.

The staining method was described previously (Chapter 3, section 3.6.4), and the stained samples were acquired using the CyAn ADP flow cytometer. Data were analysed using Summit software v4.3 (Chapter 3 Section 3.7).

Table 4.3 FMO controls

Antigen	APC	PE	FITC
CD11b FMO	---	Ly6G	Ly6C
Ly6G FMO	CD11b	---	Ly6C
Ly6C FMO	CD11b	Ly6G	---

4.6.2   Results and conclusion

An example of stained peripheral blood using the highest (10 µl) and the lowest (0.4 µl) amount of PerCP-Cy5.5-Ly6G antibody was shown in **Figure 4.6** A. Excess antibody not only increased the MFI of the positive population, but also the MFI of the negative population. Inadequate antibody will result in a vague boundary between the positive and the negative population. The optimised antibody concentration was determined according to the staining index (SI). The following equation was used to calculate SI (Telford *et al.*, 2009):

$$SI = (MED_{pos} - MED_{neg})/[(84^{th}\text{ percentile } MED_{neg} - MED_{neg})/0.995]$$

Here MED$_{pos}$ is the MFI of the positive signal and MED$_{neg}$ is the MFI of the negative signal. A

curve of antibody concentration *versus* SI was plotted and a typical curve was shown in **Figure**

4.6 B.
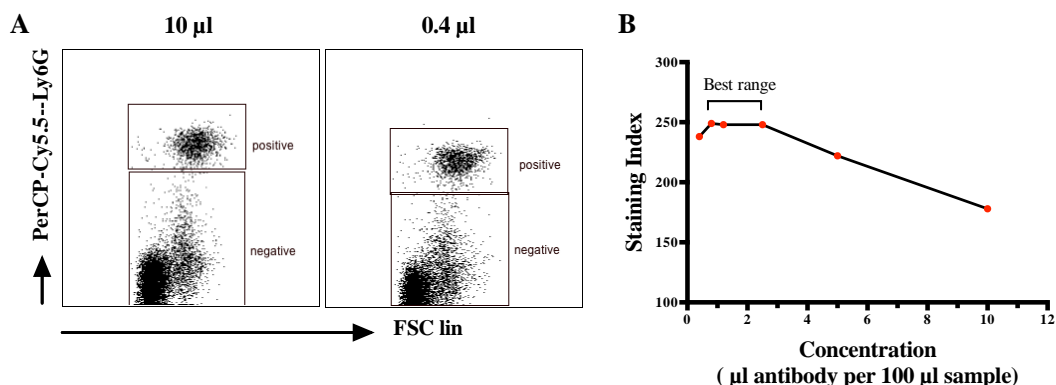
Figure 4.6 An example of antibody titration for flow cytometry.
A) an example of peripheral blood stained with 10 μl or 0.4 μl PerCP-Cy5.5-Ly6G antibody; **B**) a typical
curve of antibody concentration *versus* SI showing the best range of the antibody concentration.

The best range of antibody concentration is defined as a certain concentration of antibody is

used to stain cells resulting in a highest SI. Above the best range produces a decreased SI

because of the increased MFI in the negative population, whereas below the best range produces

a decreased SI because of the decreased MFI in the positive population. The optimised

concentrations of the antibodies determined in this thesis were shown in **Table 4.3.**

Table 4. 1 Antibody titration for cell surface staining for flow cytometry

	APC-CD11b	FITC-Ly6C	PerCP-Cy5.5-Ly6G	PE-CCR2	PE-Ly6G
Concentration	0.2 mg/ml	0.5 mg/ml	0.2 mg/ml	N/A	0.2 mg/ml
Whole blood (μl per 100 μl)	0.5	1	1	1	1
BMCs (μl per 10^6 cells/100 μl)	1	1	1	1	1

FMO control is an easy and accurate control to facilitate the determination of the boundary

between positive, especially dull-stained population, and negative population. FMO control

allows a simple decision to place the upper boundary for the non-stained population in the

channel opted out (**Figure 4.7**). FMO control is also useful to assess whether compensation is

set correctly to ensure no spread of the fluorochromes into the unlabelled channel (**Figure 4.8**)
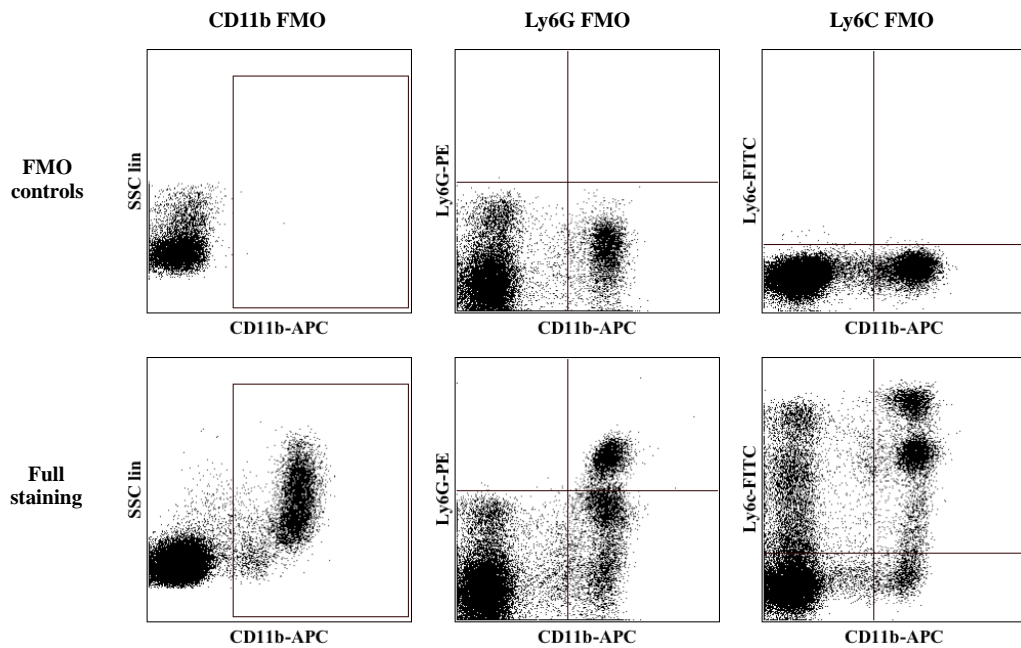
Figure 4.7 Different subset cells were gated in full stained sample according to FMO control.
FMO controls are important in determining the positive and the negative population boundary. For
example, the boundary of Ly6C positive and negative population is vague and a Ly6C FMO control can
accurately facilitate the decision where to put the boundary between the positive and the negative
population.
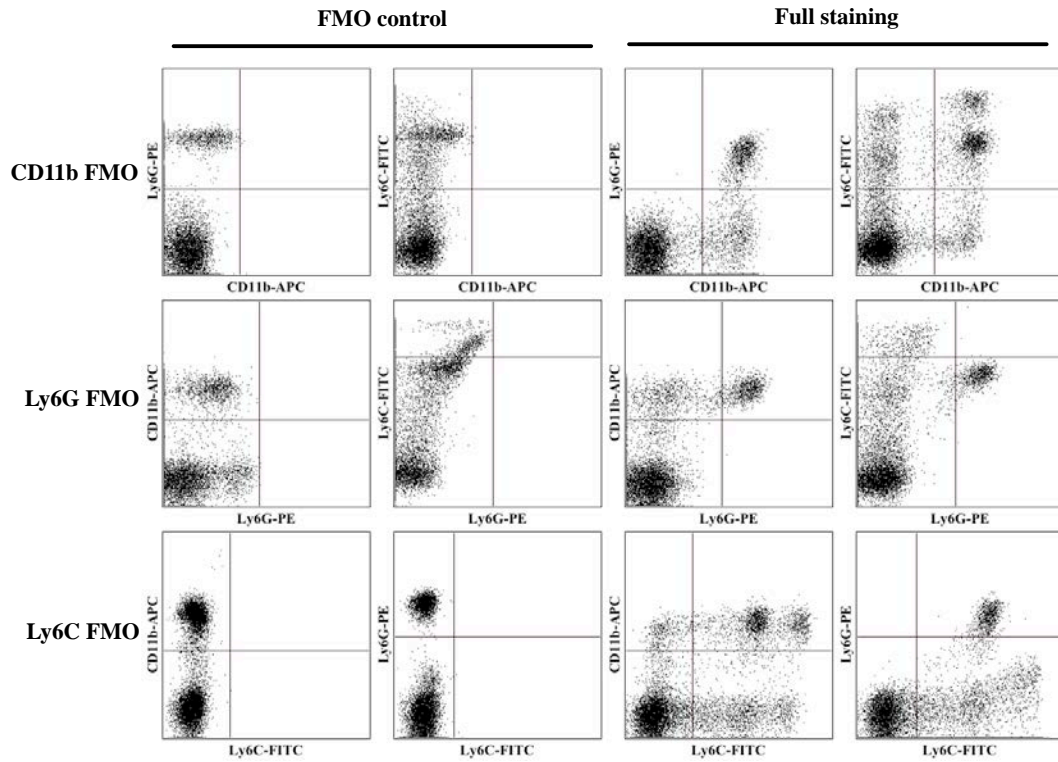
Figure 4.8 FMO controls are useful to determine whether the compensations were set properly.
By comparing the FMO control and its corresponding full staining samples, it showed that there was no signal spread to the channel in which staining was opted out in the FMO control. This indicates that the compensation was set properly without signal spreading.

4.7 Quantification of inflammatory cytokines in plasma using Cytometric Bead Array Mouse Inflammation Kit

The CBA contains known size capture beads that are coated with specific antibody. CBA Mouse Inflammation Kit (BD biosciences, USA) can simultaneously measure six cytokines (IL-6, IL-10, MCP-1, IFN-γ, TNF and IL-12p70), using flow cytometry. Six bead populations with distinct MFI, resolved in FL8 APC channel, were coated with capture antibodies specifically for IL-6, IL-10, MCP-1, IFN-γ, TNF, and IL-12p70 proteins. The capture beads were mixed with samples containing cytokines and detection reagent (PE-conjugated antibody), to form sandwich complexes that can be detected by a flow cytometer. The aim of this section is to validate the method using CBA Mouse Inflammation Kit to measure cytokine concentration using the standard provided in the kit.

4.7.1 Study design

The provided lyophilised mouse inflammation standard was reconstituted with 2.0 ml of Assay Diluent with a final concentration of 5000 pg/ml. Then the concentration of 20 pg/ml, 156 pg/ml, and 625 pg/ml standards were prepared by adding corresponding Assay Diluent. A volume of 50 µl per standard, 50 µl mixture of beads provided in the kit, and 50 µl detection reagent were mixed in a 3 ml round tube and incubated in dark for 2 hours (Chapter 3, section 3.8.1). Samples were then washed with 300 µl of the provided washing buffer and then centrifuged. The supernatant was carefully discarded and the bead pellet was resuspended in 300 µl washing buffer, ready for acquisition by the CyAn ADP flow cytometer, as described previously in Chapter 3, Section 3.8.3. Data were analysed using software Summit (v4.3, Germany).

4.7.2 Results and conclusion

BD CBA Mouse Inflammation Kit contains six types of capture beads, coated with different antibodies: IL-12p70, TNF, IFN-γ, MCp-1, IL-10 or IL-6. These can be resolved in the FL8 APC channel according to its MFI using flow cytometry (**Figure 4.9** A). The MFI (FL2 PE

channel) increased in response to increased standard concentrations (**Figure 4.9** B). For analysis, IL-6 beads cluster is gated in dot-plot graph (**Figure 4.9** C left) and Overlay of the histogram of different concentration of IL-6 showed that IL-6 concentration was positively correlated with the MFI (**Figure 4.9** C right). In conclusion, CBA Mouse Inflammation Kit is sensitive and efficient for cytokine concentration measurement.
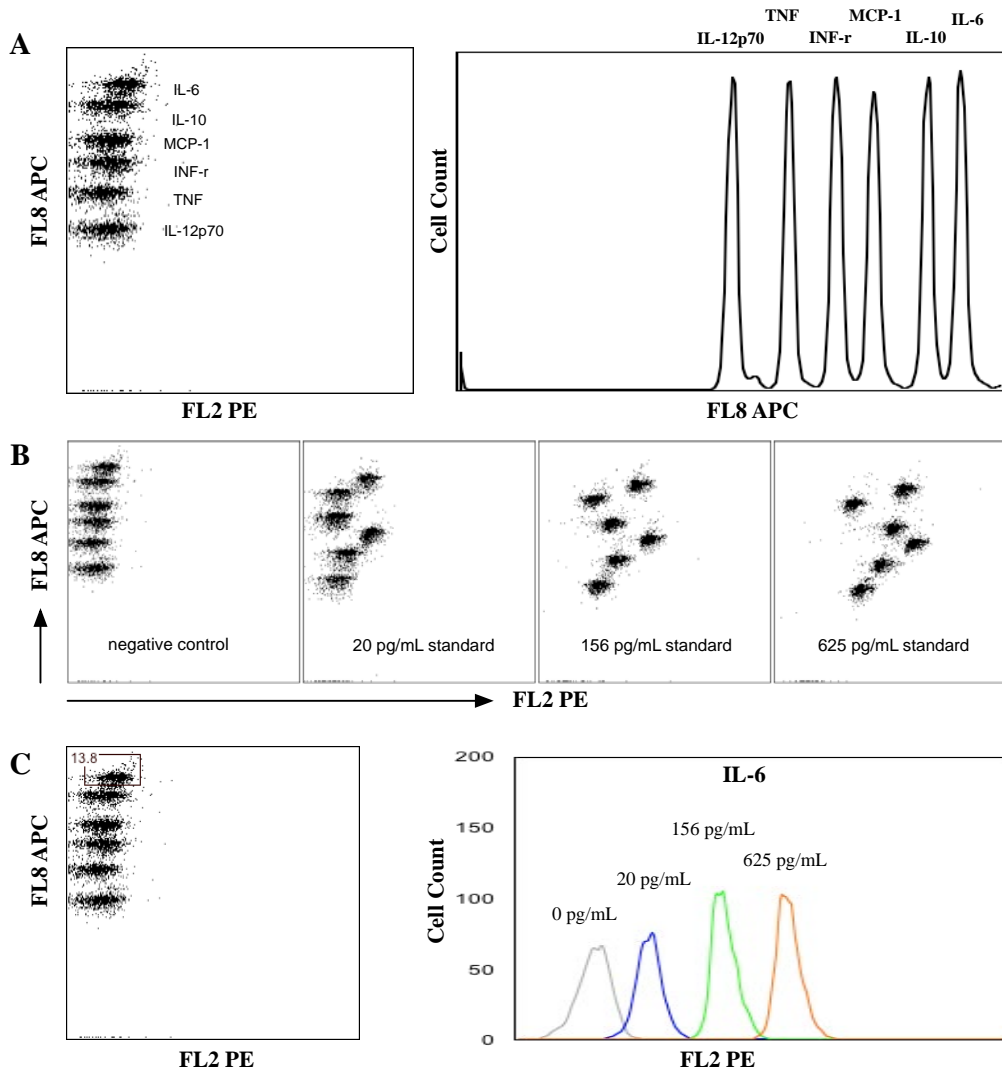
Figure 4.9 The feasibility of using CBA Mouse Inflammation Kit for cytokine concentration assessment.
A) beads coated with different cytokine antibodies have different MFIs that could be resolved in FL8 APC channel showed as dot plot (left) and histogram (right); **B**) the MFIs of the bead populations increased when they were incubated with different concentrations of the standard; **C**) gate of IL-6 antibody coated beads (left) and overlay of histogram of FL2 PE with different IL-6 concentrations (right).

CHAPTER 5

The Role of Angiopoietin-2 in the Angiotensin II-induced Abdominal Aortic Aneurysm and Atherosclerosis in the ApoE$^{-/-}$ Mice

5.1 Introduction

AAA is an abnormal dilatation of the abdominal aorta, and is generally defined as a maximal aortic diameter of $\geq$ 30 mm (Alcorn *et al.*, 1996; Golledge *et al.*, 2006). The dilatation is gradual and permanent (Alcorn *et al.*, 1996). When an aortic diameter reaches 55 mm, there is likely to result in life-threatening aortic rupture (Von Allmen & Powell, 2012; Golledge & Norman, 2011; Choke *et al.*, 2005). When an aneurysm ruptures, less than 10% of patients survive to the operating theatre, with a rate of post-surgery mortality greater than 40% (Greenhalgh & Powell, 2008). AAA affects 2-5% of men aged over 65 years, and there are approximately 1000 deaths per year caused by AAA rupture in Australia (Nicholls *et al.*, 1992). The pathogenesis of AAA has been intensively investigated over the past two decades. However, the transition to an effective drug-based therapy to halt or limit AAA progression remains incomplete (Golledge & Norman, 2011). Currently, surgical repair is the only treatment option for AAAs, although clinical trials suggest that elective surgical repair should be limited to large AAAs (Brady *et al.*, 2004).

The pathogenesis of AAA is a complex process involving inflammation, ECM remodelling and angiogenesis (Golledge *et al.*, 2006). Extensive inflammatory cell infiltration within the aortic wall is a hallmark of AAA (Shimizu *et al.*, 2006). Activated macrophages are a primary source of MMPs and other proteases contributing to degradation of the aortic ECM (Hellenthal *et al.*, 2009). Inflammation and ECM degradation provide a pro-angiogenic environment, initiating angiogenesis to form neo-vessels (Imhof & Aurrand-Lions, 2006). Angiogenesis promotes AAA and atherosclerosis development and progression through encouraging ECM remodelling

and facilitating inflammatory cell infiltration (Golledge *et al.*, 2006; Daugherty *et al.*, 2000; Armstrong *et al.*, 2011). Indeed, a higher density of micro-vessels has been reported in biopsies from ruptured AAAs than intact ones, which suggests a role of angiogenesis in AAA rupture (Thompson *et al.*, 1996; Choke *et al.*, 2006). Similar pathological features have also been observed in the atherosclerotic lesion, a recognised risk factor for AAA, which is usually found in biopsies of end-stage AAA (Golledge *et al.*, 2006). This supports the view that the association of atherosclerosis and AAA reflects common risk factors. Nevertheless, it needs further investigation to confirm whether atherosclerosis is causative for AAA (Reed *et al.*, 1992; Golledge & Norman, 2010).

Aortic dilatation induced by subcutaneous infusion of AngII in ApoE$^{-/-}$ mouse is a well-established rodent model for investigating the pathophysiology of AAA (Tsui, 2010). This experimental model has been used to examine the mechanisms of AAA development and progression (Meir & Leitersdorf, 2004; Tsui, 2010), as the AngII-induced AAA exhibits similar pathological features which are observed in human AAA samples, such as medial remodelling, inflammation, angiogenesis, and male gender susceptibility (Manning *et al.*, 2002; Daugherty, 2004). Moreover, AngII-infusion accelerates atherosclerosis, which is consistent with the common presence of atherosclerosis in human AAAs (Golledge & Norman, 2010).

Angpt2 is a member of Angpts, a vascular growth factor family known to regulate angiogenesis (Augustin *et al.*, 2009). Angpt2 was originally identified by its ability to interfere with the action of Angpt1, through competition for the receptor Tie2 (Fiedler & Augustin, 2006). Angpt1 activates Tie2 to maintain vascular endothelium quiescence, anti-inflammation effect, and integrity (Augustin *et al.*, 2009). Angpt2 acts as an antagonist to Tie2 to deactivate Tie2, facilitating the initiation of angiogenesis, increased permeability of the vascular, and inflammation (Augustin *et al.*, 2009). However, evidence is emerging that supports Angpt2 as an agonist in a context-dependent manner (Fiedler & Augustin, 2006). Transgenic mice over-expressing Angpt2 have disrupted vessel formation that is similar, but more severe than mice with a deficiency of Angpt1 or Tie2 (Maisonpierre *et al.*, 1997). In the rat pupillary membrane

model, Angpt2 inhibits angiogenesis through EC death and vessel regression in the absence of endogenous VEGF (Lobov *et al.*, 2002). In humans, increased serum Angpt2 is associated with AAA prevalence and cardiovascular mortality in older men (Golledge *et al.*, 2012). However, a direct role for Angpt2 in AAA remains to be discovered.

Given the importance of angiogenesis and inflammation in AAA and atherosclerosis, the hypothesis of this chapter is that Angpt2 plays a key role in AAA and atherosclerosis development. To test this hypothesis, studies were performed using the AngII-infused experimental AAA mouse model in the ApoE$^{-/-}$ mice. The aims of this chapter are as follows:

1. To examine the effects of endogenous Angpt2 and Tie2 interacting inhibitor administration on the AAA and atherosclerosis development in the AngII-infused experimental AAA mouse model in the ApoE$^{-/-}$ mice;

2. To examine the effects of recombinant Angpt2 administration on the AAA and atherosclerosis development in the AngII-infused experimental AAA mouse model in the ApoE$^{-/-}$ mice.

5.2   Materials and methods

5.2.1   Human Fc protein, recombinant angiopoietin-2, and peptide inhibiting Angpt2-Tie2 interaction

Control human Fc protein (control), recombinant Angpt2 (rAngpt2), and peptide inhibiting Angpt2-Tie2 interacting (L1-7) were kindly provided by Regeneron (Tarrytown, NY, USA). The rAngpt2 (equivalent to AngF2-Fc-F2) and L1-7 used in this study has been described in details by Davis *et al*. (Davis *et al.*, 2003) and Oliner *et al*. (Oliner *et al.*, 2004) respectively. The sequence of these recombinant proteins has been described previously, in Chapter 3, Section 3.2.1.

5.2.2   Mouse studies

Animal ethics approval was obtained prior to commencing the research (JCU Animal Ethics Approval Number A1671) and all procedures were performed in accordance with the institutional and ethical guidelines of James Cook University. ApoE$^{-/-}$ mice were housed as described previously (Chapter 3 Section 3.1.2). All male ApoE$^{-/-}$ mice were aged until six month old for the experiments. The primary outcome measure for the mouse study was the diameter of suprarenal aorta (SRA), as this is the main site of aneurysm formation in the mouse model used (Daugherty, 2004). Based on a previous study by Golledge (Golledge *et al.*, 2010), a sample size of 20 mice per group was estimated to have at least 80% ability to detect a 25% difference in SRA diameter (alpha 0.05). In order to allow for potential dropouts due to fatalities, 25 mice per group were included (**Table 5.1**). Two subset experiments were performed (n=15 and n=10 respectively in each group), by two researchers: Dr Alexandra Trollope (JCU) (Experiment 1, n=15 in each group) and the thesis author (Experiment 2, n=10 in each group).

Table 5.1 Experimental groups in this study

Group	n	AngII infusion	Administration
Control	25	Yes	Control Fc-fusion protein
rAngpt2	25	Yes	rAngpt2
L1-7	25	Yes	L1-7

5.2.3 Primary outcome and secondary outcomes

In the ApoE$^{-/-}$ mouse, the primary aortic region susceptible to dilatation in response to AngII infusion is the SRA (Daugherty, 2004). In humans, the risk of AAA rupture is positively associated with the maximum diameter of the aneurysm. Therefore, the primary outcome of this study was to determine the maximum aortic diameter in the SRA region. This was assessed by combining data from two subset experiments.

The secondary outcomes of this study were determining the percentage of aneurysm rupture free survivals, and the percentage of the atherosclerosis lesion area in the ARCH. Additional outcomes were assessed from the mice in one subset experiment (performed by the thesis author), including: the incidence of dissection in ARCH, blood pressure (BP) and heart rate (HR), and plasma lipid concentration. Mice that died prior to the study endpoint were excluded from the secondary outcomes analysis, with the exception of the survival proportion study.

5.2.4 AngII infusion, and control human Fc protein, rAngpt2, and L1-7 administration, and experimental design

All mice received 1000 ng/kg/min of AngII (Sigma-Aldrich, USA) for 14 days via subcutaneous osmotic micro-pumps (Model 1004, ALZET, USA) as described previously in Chapter 3, Section 3.1. In brief, mice were anaesthetised by intra-peritoneal injection of ketamine (150 mg/kg) and xylazine (10 mg/kg). Osmotic micro-pumps containing corresponding concentration of AngII dissolved in sterile water were inserted into the subcutaneous space along the left dorsal midline (Day 0). Control, rAngpt2, or L1-7 was

subcutaneously injected every other day at a dose of 4 mg/kg, starting the day before AngII infusion commenced (Chapter 3, Section 3.2.2) based on the manufacture's recommendation and previously published work (Morrissey *et al*., 2010). The experimental design is illustrated in **Figure 5.1**.Prior to recombinant protein or peptide administration, HR and BP were measured. Peripheral blood was collected by tail-bleeding technique as baseline. HR and BP were measured again at day 14.
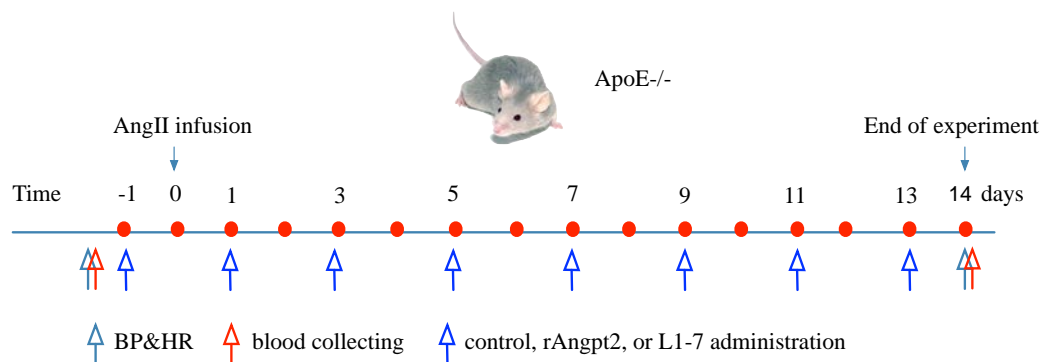
Figure 5.1 Illustration of the experimental design.
BP and HR were measured before the rAngpt2 or L1-7 administration (Baseline) and at the end of experiment (Day 14). Peripheral blood was collected via tail-bleeding before the experiment commenced. (Baseline) and cardiac puncture at day 14; human Fc control protein, rAngpt2, or L1-7 was subcutaneously injected every other day.

5.2.5   Tissue and plasma collection

Mice were euthanised by CO_2 asphyxiation at the completion of the experiment. Whole aortas were harvested and digitally photographed as described previously (Chapter 3, Section 3.3.3). Peripheral blood collection and plasma collection were described previously (Chapter 3, Section 3.3.1 and 3.3.2). The whole dissected aorta was digitally photographed (Coolpix 4500, Nikon, Japan) on a graduated template (Moran *et al.*, 2013). Then, aortic tissues were snap frozen in OCT compound and stored at -80°C for future analysis. Mice that died prior to completion of the experimental period were subject to post-mortems, and aortas were harvested for subsequent aortic diameter measurement. Rupture was confirmed by intra-thoracic, intra-abdominal or retroperitoneal blood.

5.2.6   Aortic dissection and Haematoxylin & Eosin staining of the aortic arch

The ARCH dissection is determined by the gross appearance, which has been previously published (Tieu *et al.,* 2009). The localised dissection showed red with an accumulation of hematoma, compared with the pink white unaffected tissue. When the dissection was cut open longitudinally, double layers were observed with blood trapped between.

Transverse sections of ARCH, prepared as described previously (Chapter 3, Section 3.11.1), were fixed in 4% frozen formaldehyde for 20 min. Slides were then brought to room temperature and air-dried for 20 min, followed by rehydration in PBS for 5 min. Nuclei were stained with a drop of haematoxylin, covering the whole section for 4 min, followed by rinsing in running tap water for 5 min. Then sections were differentiated with 10 dips in 0.25% acid alcohol (HCl in absolute ethanol v/v) and rinsed in tap water for 2 min. The staining was blued with 10 dips in 0.09% ammonia chloride (NH_4Cl in distilled water w/v), followed by rinsing in running tap water for 5 min. After 10 dips in 95% alcohol, sections were counterstained in eosin for 15 sec. Slides were then dehydrated through 95% alcohol and two changes of absolute alcohol for 5 min each. Slides were finally cleared in two changes of xylene for 5 min each and mounted with xylene based mounting medium (ProSciTECH, Australia). The stained sections were air-dried for 24 hr, and were then ready for viewing under a microscope (Nikon, Japan).

5.2.7   Aortic diameter measurement and categorisation of AAA

The harvested aortas were subjected to measurement of the maximum diameters of the following aortic regions using established techniques (Chapter 3, Section 3.4.1): ARCH (from aortic valve to 3 mm beyond left subclavian artery), THX (from the end of arch to the diaphragm), SRA (from the diaphragm to the renal arteries), and IRA (from the renal arteries to bifurcation of the iliac arteries). The maximum external diameter of each aortic region was determined using Adobe Photoshop CS5 software (v12, Adobe, USA). This method has been validated to have good intra-observer repeatability and inter-observer reproducibility (Chapter 4, Section 4.3.2.1). AAA in ApoE$^{-/-}$ mouse is defined as maximum SRA diameter $\geq$ 1.20 mm,

based on previous research results (Cao *et al.*, 2010; Deng *et al.*, 2003). A scale was used to grade different forms of aneurysms based on previous research (Daugherty *et al.*, 2001), and described previously (Chapter 3, Section 3.4.2). This AAA categorisation method has been validated to have good intra-observer repeatability and inter-observer reproducibility (Chapter 4 Section 4.3.2.3).

5.2.8 *En face* analysis of Sudan IV stained atherosclerotic lesion of aortic arch intima and measurement

All ARCHs from the mice surviving to the end of the experiments were used to evaluate the percentage of intimal atherosclerotic area using Sudan IV staining, as described previously (Chapter 3, Section 3.5.1). ARCHs, stored in OCT compound, were collected and prepared as described (Chapter 3 Section 3.3.3), were washed with PBS twice and used for *en face* staining with Sudan IV. The stained ARCHs were digitally photographed on a graduated template and the Sudan IV staining area was measured using ImageJ software, as described in Chapter 3, Section 3.5.2. The data were expressed as percentage of total area. This method has been validated to have a good intra-observer repeatability and inter-observer reproducibility (Chapter 4, Section 4.3.2.2).

5.2.9 Non-invasive tail-cuff blood pressure and heart rate measurement

BP and HR were measured using a computerised, non-invasive, tail-cuff system (Kent Scientific, USA), with a CODA monitor controller at day -2 (baseline) and day 14 (Day 14). CODA was configured to mouse mode with a 10 sec interval of repeat measurement and 15 sec length of deflation. A clear acrylic restrainer (Kent Scientific, USA), with built-in nose cone was used to hold the mouse. The measurements were made in a quiet environment, and the mouse was accustomed to a restrainer on a warming pad prior to measurement to avoid anxiety. The occlusion cuff was placed close to the base of the mouse tail and secured inside the groove on the top of the fastener. Then the volume pressure recorder cuff was placed on the tail. Each cycle measured SBP, DBP, and HR. The measurement was repeated for 5 cycles in order to

reach a relatively stable result. The parameters of the sixth cycle were then recorded. The Mean

BP (MBP) is calculate based on the equation MBP= [DBP + (SBP - DBP)/3]. This method has

been found to have accurate BP measurement over the physiological range of BP in mice (Feng

et al., 2008). Reproducibility of this technique has been established previously in our group

(mean of absolute difference for HR: 21.1 beats per minute, 95% CI: 14.8–27.5 and mean of

absolute difference for mean BP: 12.3 mmHg, 95% CI: 8.4–16.1) (Seto *et al.*, 2013). Mice that

died prior to the end of the experiment were excluded.

5.2.10 Measurement of plasma lipids

Circulating lipid concentration was measured using an Abcam high-density lipoprotein (HDL)

and low and very low-density lipoprotein (LDL/VLDL) Cholesterol Assay Kit (Abcam, UK),

following the manufacturer's instructions. Briefly, plasma samples stored at -80°C were thawed

and centrifuged at 2000 x g at 4°C for 5 min. A volume of 4 µl per sample was diluted 25 times

with PBS and mixed with 100 µl provided 2x precipitation buffer. This was followed by

incubation at room temperature for 10 min. Samples were then centrifuged at 2500 x g for 10

min. The supernatant, containing HDL fraction, was transferred to a new 1.5 ml polypropylene

tube. The precipitated pellet, containing LDL/VLDL fraction, was resuspended in 200 µl PBS.

A total of 25 µl per sample were used to measure the HDL or LDL/VLDL concentration. Free

cholesterol of each fraction was detected by adding 50 µl reaction mix (47.6 µl cholesterol

assay buffer, 0.4 µl cholesterol probe and 2 µl enzyme mix). The total cholesterol of each

fraction was detected by adding 50 µl reaction mix with cholesterol esterase that hydrolyses

cholesterol ester to free cholesterol (45.6 µl cholesterol assay buffer, 0.4 µl cholesterol probe, 2

µl enzyme mix and 2 µl cholesterol esterase). In parallel with the experimental samples, a

standard curve was created using provided 2 µg/µl cholesterol standard. The cholesterol

standard was diluted to 0.025 µg/µl by adding 2 µl of the cholesterol standard to 140 µl of

provided Cholesterol Assay Buffer. The appropriate volume of diluted cholesterol standard was

added to cholesterol assay buffer with a final volume of 50 µl per well in 96-well-plate, to

generate 0, 0.1, 0.2, 0.3, 0.4, and 0.5 µg/well of the cholesterol standard. Then 50 µl reaction

mix with cholesterol esterase was added. The samples and standards were incubated at 37°C for 60 min while being protected from light. This was followed by a reading of the OD value at 570 nm using OMEGA PolarStar (BMG Labtech, Germany). A linear expression of concentration *versus* OD was generated by GraphPad Prism (v6.0, USA). The concentration of total HDL or LDL/VLDL, and free HDL or LDL/VLDL was determined by fitting to the standard curve. The combined HDL or LDL/VLDL was calculated by subtracting the free HDL or LDL/VLDL from total HDL or LDL/VLDL respectively.

5.2.11   Statistical analysis

The D'Agostino test was used to test the distribution of all data. Normally distributed continuous data were expressed as mean ± Standard Error of Mean (SEM), and each group was compared with the control group by using a one-way ANOVA followed by Fisher's Least Significant Difference (LSD) test. Non-normally distributed data were expressed as median (interquartile range (IQR)). Statistical analyses were performed using the Kruskal-Willis nonparametric ANOVA test followed by Dunn's multiple comparison test. Survival, free from aneurysm rupture related mortality, was assessed using Kaplan Meier analysis and compared between groups using a log-rank test. The categorical data were tested using Two-tailed Fisher's exact test. Data was analysed using GraphPad Prism (v6.0, USA). A value of $p<0.05$ was considered statistically significant.

5.3 Results

5.3.1 Recombinant Angpt2 administration protected mice from AngII-induced aortic rupture

One mouse per group died from unknown causes, but aortic aneurysm rupture was excluded by a post-mortem. One mouse was euthanised because of paraplegia in the control group, and two mice died immediately after the surgery in the L1-7 group. These mice were excluded from the study because of mortality unrelated to aneurysm (**Table 5.2**). Aneurysm rupture related death occurred as early as 4 days in the L1-7 group and 5 days in the control group. The percentage of aneurysm rupture related mortality in the control group was 17.4% (4 out of 23), and 22.7% (5 out of 22) in the L1-7 group. There was no rupture in the rAngpt2 group (**Table 5.2**). The rAngpt2 administration significantly reduced the number of mice with aneurysm rupture related mortality (Chi-square 4.465, p=0.034), whereas L1-7 administration did not affect the aneurysm rupture related mortality (Chi-square 0.151, p=0.697). The aneurysm rupture related mortality also showed significant difference between rAngpt2 group and L1-7 group (Chi-square 5.994, p=0.014; **Figure 5.2**).

Table 5.2 The causes of mortality in the control, rAngpt2, and L1-7 group

Death reason	Group	Experiment 1[#] (n)	Experiment 2^ (n)
	Control	2	2
Aortic rupture	rAngpt2		
	L1-7	3	2
	Control		1
Unknown causes	rAngpt2	1	
	L1-7	1	
Paraplegia	Control	1	
Surgery	L1-7	2	

\# Experiment was performed by Dr. Alexander Trollope (n=15 per group)

^ Experiment was performed by thesis author (n=10 per group)
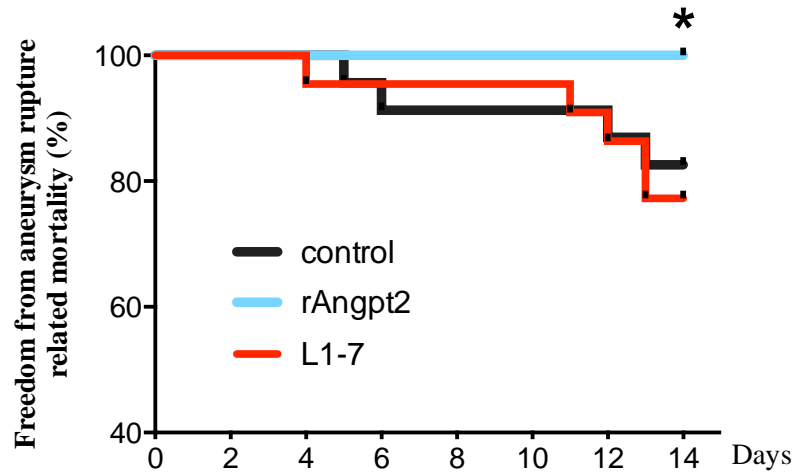
Figure 5.2 Kaplan-Meier survival curves of AngII infused mice receiving control, rAngpt2, or L1-7 were plotted versus the days of the experiment.
The log-rank (Mantel-Cox) test had a Chi-squared value of 4.465 ($p=0.034$, rAngpt2 *versus* control), a Chi-square value of 5.994 ($p=0.014$, rAngpt2 *versus* L1-7) and a Chi-square value of 0.151 ($p=0.697$, L1-7 *versus* control). The control group and L1-7 group had similar aneurysm rupture related mortality (~20%) while the rAngpt2 group was free from aneurysm rupture (n=23 in the control group, n=24 in the rAngpt2 group, and n=22 in the L1- group); * $p<0.05$ (rAngpt2 *versus* control and rAngpt2 *versus* L1-7 on day 14).

5.3.2   rAngpt2 administration reduced the incidence of aortic arch dissection

ARCH and SRA are the two regions that are prone to rupture in the AngII-infused ApoE^{-/-} mouse model (Babamusta *et al.*, 2006). A focal intramural haemorrhage (IMH) is a feature which is likely to precede rupture of the aortic wall and could be observed after intra-ventricular PBS perfusion to remove blood cells **Figure 5.3** A). Histological sections of the ARCH region clearly showed medial hypotrophy, adventitia thickening and blood filled false lumens located in the tunica adventitia (**Figure 5.3** B and C). ARCH IMH was observed in all three groups. The incidence of ARCH dissection was 70% and 50% in the control and L1-7 groups (n=10), respectively. However, the rAngpt2 group had significantly less incidence of ARCH dissection than the other two groups at 10% (*p*=0.020, **Figure 5.3** D).
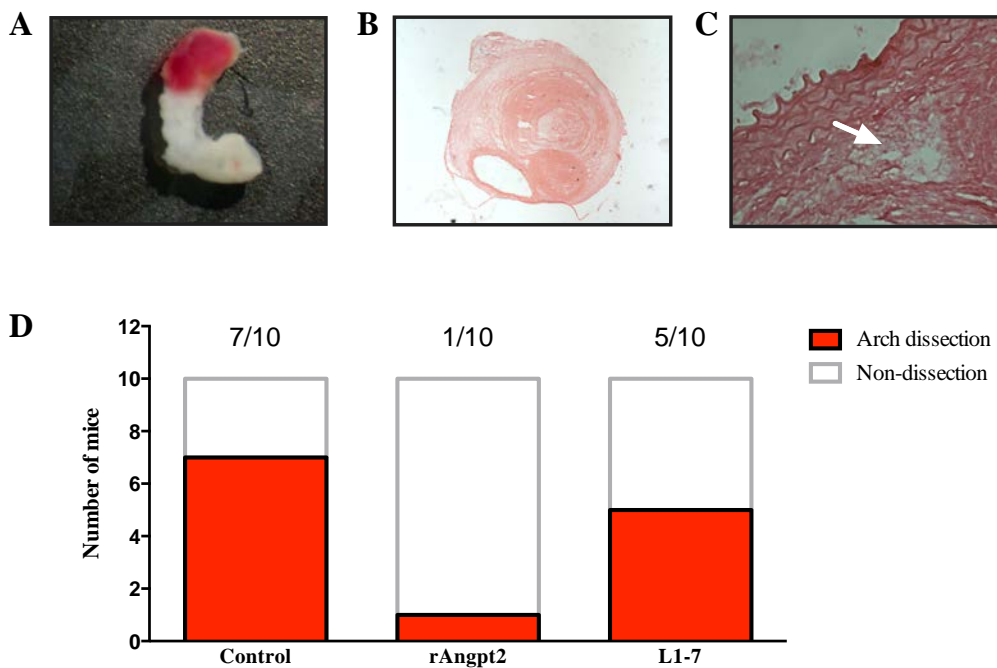
Figure 5.3 rAngpt2 administration reduced the incidence of dissection in the aortic arch.
A) an example of a digitally photographed dissected ARCH; **B**) example of a Haematoxylin & Eosin stained cross section of dissected ARCH (20X); **C**) high magnification of (B) showing blood cells infiltration (white arrow) between media and adventitia (200X); and **D**) number of mice showing dissection and non-dissection in ARCH per group (n=10 in each group). Mice that died before the endpoint with rupture in the region of ARCH were included in this statistical evaluation because they developed IMH in the ARCH. Data were analysed using Two-tailed Fisher's exact test (*versus* control).

5.3.3 rAngpt2 administration reduced suprarenal aortic diameter in AngII-infused ApoE$^{-/-}$ mice

Mice receiving rAngpt2 had significantly smaller mean SRA diameter (1.58 ± 0.11 mm, n=24) compared with the control group (2.17 ± 0.15 mm, n=23, *p*=0.002; **Figure 5.4** C). Smaller diameters of the ARCH, THX, and IRA were also observed in mice receiving rAngpt2, although there was no significant difference compared with the control group (**Figure 5.4** A, B, and D). Mice receiving L1-7 administration did not experience change in the mean SRA diameter (2.151 ± 0.181 mm, n=22, *p*<0.999) compared to control group, and there was no significant difference in ARCH, THX, and IRA region in mice receiving L1-7 compared to the mice receiving control protein (**Figure 5.4**).
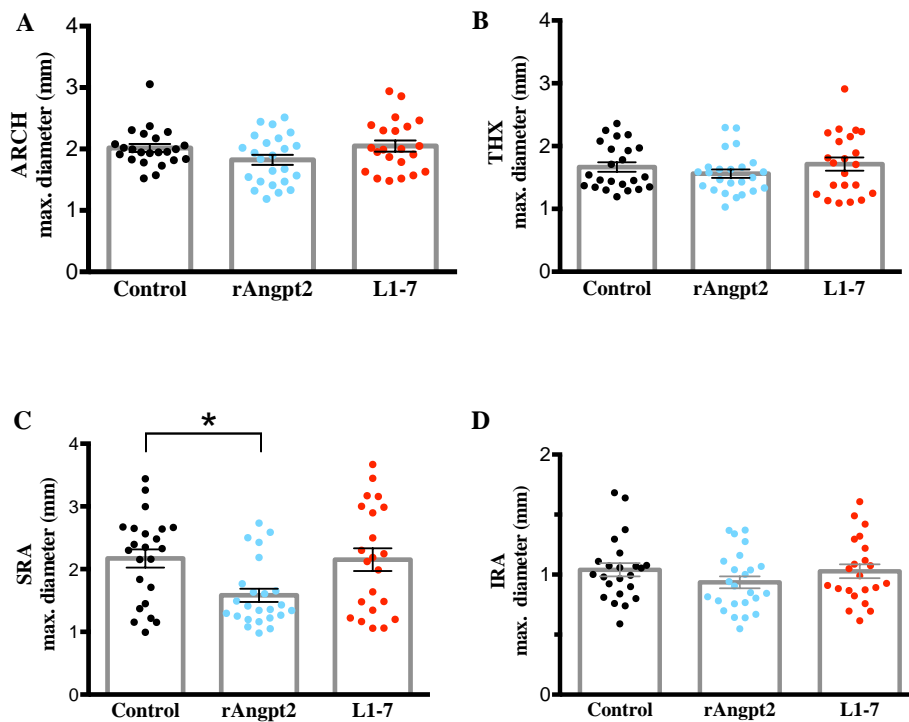
Figure 5.4 Whole aorta morphometry: maximum (max.) aortic diameters in each region of the aorta harvested on day 14.
A) ARCH: control (2.016 ± 0.065 mm), rAngpt2 (1.824 ± 0.082 mm, *p*=0.090), and L1-7 (2.048 ± 0.090 mm, *p*=0.777); **B**) THX: control (1.666 ± 0.076 mm), rAngpt2 (1.561 ± 0.067 mm, *p*=0.371), and L1-7 (1.713 ± 0.106 mm, *p*=0.695); **C**) SRA: control (2.171 ± 0.145 mm), rAngpt2 (1.582 ± 0.106 mm, *p*=0.010), and L1-7 (2.151 ± 0.181 mm, *p*>0.999); and **D**) IRA: control (1.040 ± 0.055 mm), rAngpt2 (0.935 ± 0.050 mm, *p*=0.171), and L1-7 (1.028 ± 0.056 mm, *p*=0.877). The aortic diameters from mice that died from aneurysm rupture before endpoint of the experiments were included in each group. Data were expressed as mean ± SEM (n=23 in the control group, n=24 in the rAngpt2 group and n=22 in the L1-7 group) and analysed by one-way ANOVA test followed by Fisher LSD test; **p*<0.005, *versus* control group.

5.3.4 rAngpt2 administration attenuated the severity of AngII-induced aortic aneurysm

The gross appearance of the whole harvested aorta showed that the aneurysms were varied from simple dilatation without thrombus to multiple aneurysms with pronounced thrombus. The location of the aneurysm was in the SRA region only or distributed in the whole aortic area (**Figure 5.5**).
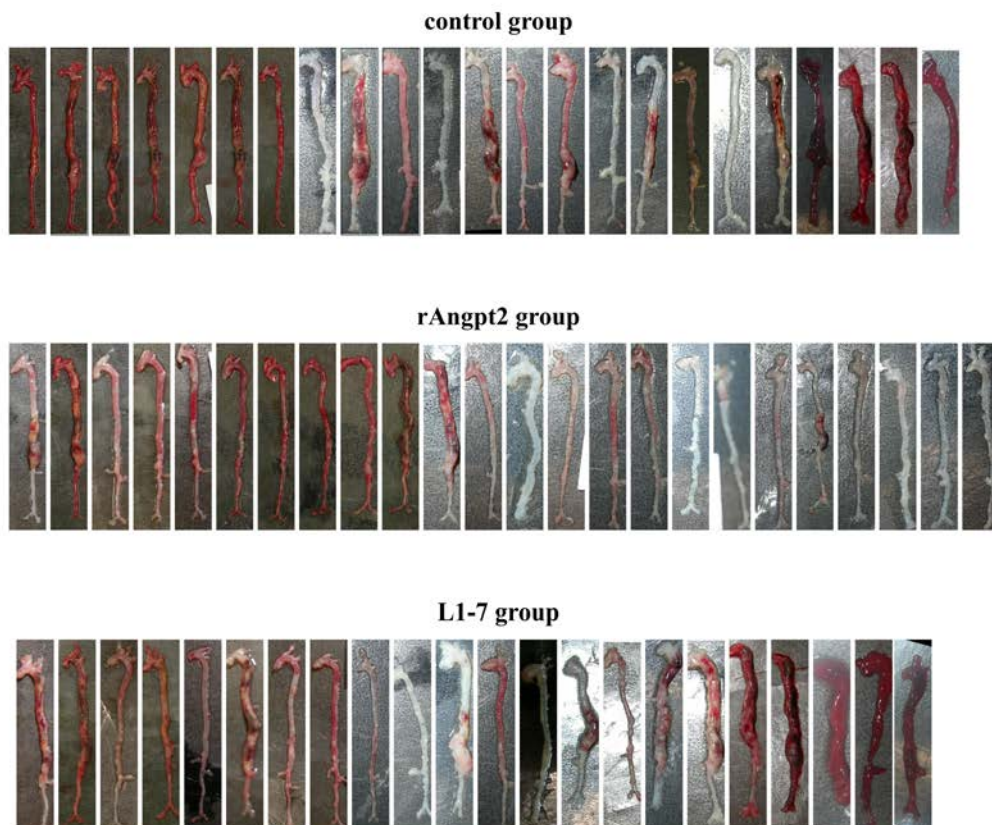
Figure 5.5 Effects of control, rAngpt2, or L1-7 administration on AngII-induced aortic dilatation in ApoE$^{-/-}$ mice.
Gross appearance of aortas harvested from different groups of mice (n=23 in the control group, n=24 in the rAngpt2 group, and n=22 in the L1-7 group).

Based on the AAA definition, there was no difference in the incidence of AAA among the three groups, with a SRA maximum aortic diameter ≥ 1.2 mm. In the control group, 20 out of 23 mice developed AAAs. In the rAngpt2 group and L1-7 group, 19 out 24 and 18 out of 23 mice, respectively, developed AAAs. Different forms of AAA were assessed according to the grading system developed by Daugherty *et al.* (Daugherty *et al.*, 2001). Under this system, Type III and Type IV AAAs were labelled a bulbous form of Type II containing multiple aneurysms

(Daugherty *et al.*, 2001). Type III and Type IV AAAs constituted 75% (15 out of 20) in the control group and 72% (13 out of 18), while only 21% (4 out of 19, *p*=0.003) AAAs were Type III and Type IV in the rAngpt2 group (**Table 5.3**).

Table 5.3 Different forms of AAA

Group	n	Type 0	Type I	Type II	Type III	Type IV
Control	23	3	5	0	5	10
rAngpt2	24	5	14	1	0	4
L1-7	22	4	5	0	1	12

5.3.5 rAngpt2 administration reduced AngII-induced atherosclerosis within the aortic arch

AngII infusion accelerates atherosclerosis development in ApoE$^{-/-}$ mice, particularly within the ARCH (Ayabe *et al.*, 2006; Daugherty *et al.*, 2000). The intimal atherosclerotic lesion area within the ARCH of mice that survived to the end of the experiments was examined. Sudan IV stained lipid-laden plaques and lesions showed a vivid red colour in contrast to the pink to white colour of the intact intima (**Figure 5.6**). Mice receiving rAngpt2 had a significantly smaller mean percentage of Sudan IV positive staining area (27.87% ± 2.63; n=24, *p*= 0.017), compared with the control group (41.15% ± 5.00; n=19). Mice receiving L1-7 had a similar mean percentage of Sudan IV positive staining area (38.05% ± 5.40, n=17, *p*=0.678), compared to the control group (**Figure 5.7**).
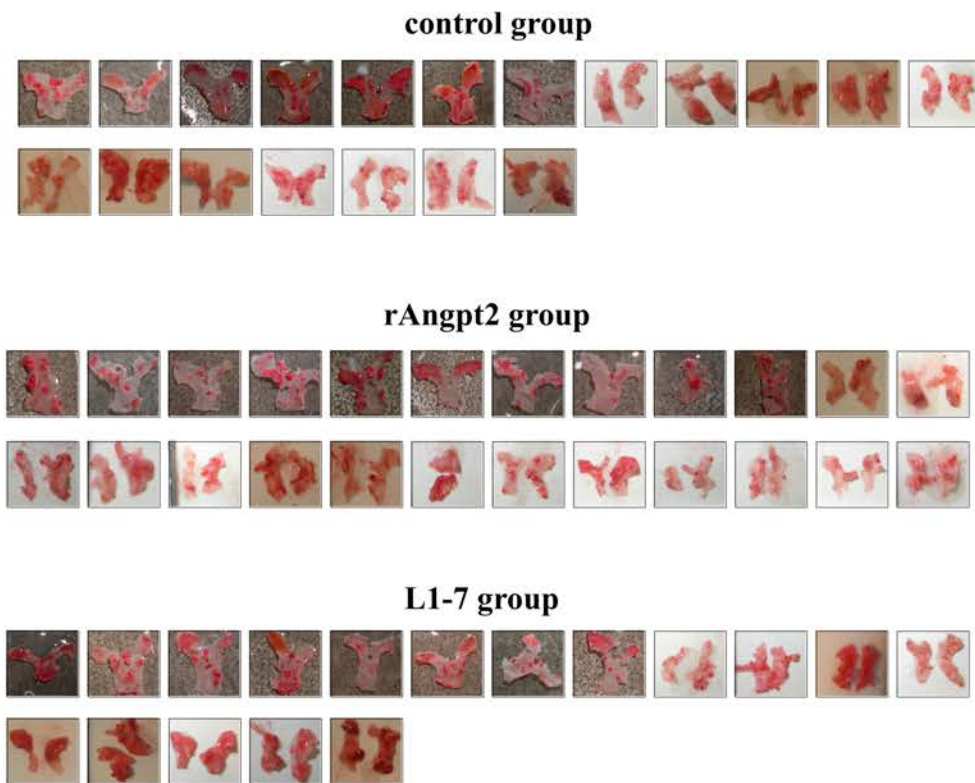
Figure 5.6 Gross appearance of Sudan IV stained aortic arch from mice receiving control, rAngpt2, or L1-7.

The atherosclerotic lesion stained with Sudan IV shows a vivid red staining while the intact intima is pink to white (n=19 in the control group, n=24 in the rAngpt2 group and n=17 in the L1-7 group).
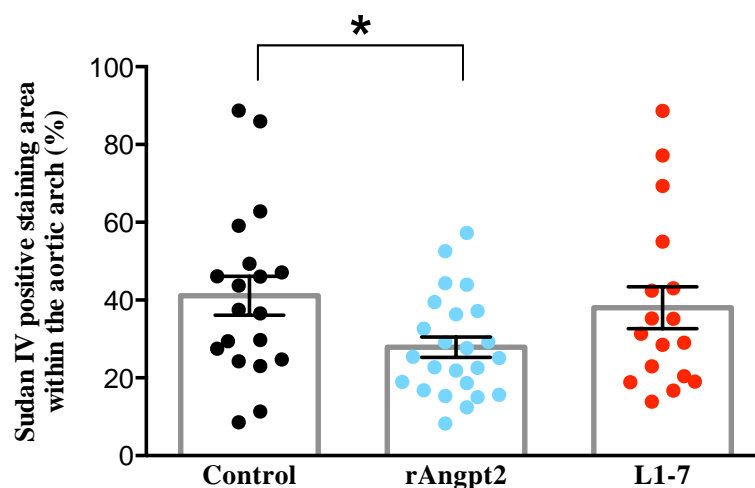
Figure 5.7 Percentage of Sudan IV positive staining atherosclerotic lesion of total area within the aortic arch.

rAngpt2 administration significantly reduced atherosclerotic lesion area compared with the control group; however, L1-7 administration did not alter AngII-induced atherosclerosis. Data were expressed as mean ± SEM (n=19 in the control group, n=24 in the rAngpt2 group and n=17 in the L1-7 group) and analysed using one-way ANOVA followed by Fisher's LSD test; *$p<0.05$ *versus* the control group.

5.3.6 rAngpt2 or L1-7 administration did not influence heart rate and AngII-induced elevation of blood pressure

In this mouse model, AngII infusion does not change the HR (Seto *et al.*, 2013). Mice receiving rAngpt2 or L1-7 had similar HR compared to the mice receiving control protein after 14 days of AngII infusion. There was no significantly different in HR between the baseline and Day14 within group (**Table 5.4**).

AngII infusion significantly increases BP in ApoE$^{-/-}$ mice (Seto *et al.*, 2013; Moran *et al.*, 2014). rAngpt2 or L1-7 administration did not affect AngII-induced BP elevation compared to the control group at Day 14. Within all groups, mice developed significantly high SBS, DBP, and MBP at Day 14 compared with their baseline (**Table 5.5**).

Table 5.4 Heart rate of mice in each group

Time points	Control (n=7)	rAngpt2 (n=10)	*p* value	L1-7 (n=8)	*p* value
Baseline	548 ± 50	496 ± 35	0.173	470 ± 45	0.173
Day 14	495 ± 46	523 ± 35	0.667	514 ± 38	0.667

HR is expressed as beats per minute; Data were expressed as Mean ± SEM and analysed by one-way ANOVA followed by Fisher's LSD test; *p* value: *versus* control.

Table 5.5 Blood pressure of mice in each group

BP (mmHg)	Time points	Control (n=7)	rAngpt2 (n=10)	*p* value	L1-7 (n=8)	*p* value
SBP	Baseline	95 ± 2	98 ± 3	0.439	102 ± 3	0.132
	Day 14	129 ± 11	123 ± 6	0.565	135 ± 8	0.661
DBP	Baseline	75 ± 2	80 ± 2	0.110	81 ± 2	0.060
	Day 14	109 ± 10	100 ± 4	0.389	112 ± 8	0.755
MBP	Baseline	81 ± 2	85 ± 2	0.190	88 ± 2	0.053
	Day 14	115 ± 10	105 ± 5	0.369	119 ± 8	0.724

Data were expressed as Mean ± SEM and analysed by one-way ANOVA followed by Fisher's LSD test; *p* value: *versus* Control

5.3.7 rAngpt2 administration reduced AngII-induced AAA and atherosclerosis was lipoprotein independent

Hyperlipidaemia is a dependent factor for AngII-induced AAA and atherosclerosis in the ApoE^{-/-} model (Daugherty *et al.*, 2000). Indeed, all mice had developed hyperlipidaemia before the experiment commenced (**Table 5.6**). The rAngpt2 administration did not alter the plasma total cholesterol concentration (3.42 µg/µl (2.87-3.98), *p*=0.627), compared to the mice receiving control protein after 14 days AngII infusion. L1-7 administration significantly increased total plasma cholesterol concentrations (5.47 µg/µl (5.21-5.69), *p*=0.022) compared to the mice receiving control protein after 14 days AngII infusion (**Table 5.6**). There was no significantly difference in the fraction of free and esterified plasma cholesterol concentration in the mice receiving rAngpt2 or L1-7 compared to the mice receiving control protein after 14 days AngII infusion.

Table 5.6 Total plasma cholesterol and its free and esterified fraction concentration

Cholesterol (µg/µl)	Time points	Control (n=7)	rAngpt2 (n=10)	*p* value	L1-7 (n=8)	*p* value
Total cholesterol	Baseline	4.40 (3.86-5.75)	4.06 (3.56-4.83)	0.660	4.92 (3.80-5.40)	>0.999
	Day 14	4.27 (3.20-4.55)	3.42 (2.87-3.98)	0.673	5.47 (5.21-5.69)	0.022
Free cholesterol	Baseline	2.16 (1.82-2.62)	2.02 (1.82-2.25)	0.540	2.19 (1.72-2.37)	>0.999
	Day 14	2.18 (1.74-2.35)	1.91 (1.71-2.11)	0.456	2.02 (1.72-2.18)	0.999
Esterified cholesterol	Baseline	2.49 (1.73-3.12)	2.23 (1.73-2.65)	0.876	2.70 (2.03-2.98)	>0.999
	Day 14	1.92 (1.37-2.66)	1.70 (0.98-2.06)	0.593	2.59 (2.37-2.80)	0.135

Data were expressed as Median (IQR) and analysed by Kruskal-Wallis test followed by Dunn's multiple comparison test; *p* value: *versus* Control.

Next, the concentration of plasma HDL and LDL/VLDL fraction was assessed. The results showed that rAngpt2, or L1-7 administration did not alter the plasma total HDL concentration, free HDL concentration and esterified HDL concentration, compared to the mice receiving control on day 14 (**Table 5.7**). There was no significant difference in the plasma total

LDL/VLDL concentration, free LDL/VLDL concentration and esterified LDL/VLDL concentration compared to the mice receiving control on day 14 (**Table 5.8**). However, mice receiving control protein had significantly lower esterified LDL/VLDL (median 0.50 µg/µl (0.32-0.83), n=7, *p*=0.040) after 14 days AngII infusion, compared with its baseline (median 1.22 µg/µl (0.69-1.56)). There was no significant difference in plasma esterified LDL/VLDL concentrations in the mice receiving rAngpt2 or L1-7 on day 14 compared with its baseline (**Table 5.8**).

Table 5.7 Total plasma HDL and its free and esterified fraction concentration

HDL (µg/µl)	Time points	Control (n=7)	rAngpt2 (n=10)	*p* value	L1-7 (n=8)	*p* value
Total HDL	Baseline	2.38 (2.07-3.12)	2.41 (1.35-3.50)	0.909	1.95 (1.32-2.66)	0.363
	Day 14	2.54 (1.67-3.01)	1.90 (1.28-2.43)	0.283	2.87 (2.27-3.16)	>0.999
Free HDL	Baseline	1.34 (0.98-1.48)	1.21 (0.63-1.46)	0.634	0.79 (0.55-1.22)	0.089
	Day 14	1.05 (0.98-1.12)	0.98 (0.76-1.14)	>0.999	1.24 (0.92-1.35)	0.609
Esterified HDL	Baseline	1.32 (1.04-1.67)	1.20 (0.71-1.96)	>0.999	1.16 (0.78-1.52)	0.984
	Day 14	1.49 (0.76-1.96)	0.77 (0.45-1.29)	0.236	1.66 (1.31-1.75)	0.777

Data were expressed as Median (IQR) and analysed by Kruskal-Wallis test followed by Dunn's multiple comparison test; *p* value: *versus* Control.

Table 5.8 Total plasma LDL/VLDL and its free and esterified fraction concentration

LDL/VLDL (µg/µl)	Time points	Control (n=7)	rAngpt2 (n=10)	*p* value	L1-7 (n=8)	*p* value
Total LDL/VLDL	Baseline	1.45 (1.08-1.66)	1.61 (1.15-2.05)	>0.999	2.60 (2.06-3.18)	0.095
	Day 14	2.08 (1.27-2.85)	1.95 (1.28-2.44)	0.764	2.80 (2.12-3.77)	0.328
Free LDL/VLDL	Baseline	0.79 (0.60-1.29)	0.94 (0.60-1.12)	>0.099	1.17 (1.06-1.42)	0.084
	Day 14	1.12 (0.75-1.17)	0.92 (0.79-1.03)	>0.999	0.85 (0.70-1.16)	0.736
Esterified LDL/VLDL	Baseline	1.22 (0.69 -1.29)	0.92 (0.67-1.25)	0.551	1.39 (1.00-1.88)	0.750
	Day 14	0.50 (0.32-0.83)*	0.58 (0.33-0.92)	>0.999	1.11 (0.73-1.42)	0.054

Data were expressed as Median (IQR) and analysed by Kruskal-Wallis test followed by Dunn's multiple comparison test; *p* value: *versus* Control; *p<0.05 *versus* baseline.

5.4 Discussion

In this chapter, the role of Angpt2 on AAA development and atherosclerosis progression was investigated using the AngII-infused ApoE$^{-/-}$ mouse model. The findings of this study were that rAngpt2 administration significantly reduced SRA maximum aortic diameter, prevented AAA from rupture, and attenuated atherosclerosis progression. These effects were independent of BP and plasma lipoprotein concentration. Inhibition of endogenous Angpt2-Tie2 interaction (via L1-7 peptide) had no effect on AngII-induced AAA development and atherosclerosis progression.

A significant finding of this study was that exogenous Angpt2 administration significantly reduced the suprarenal aortic dilatation and rupture in response to AngII infusion. In the AngII-induced experimental AAA model in ApoE$^{-/-}$ mice, approximately 70% of mice developed AAA with a 20% rupture mortality (Daugherty *et al.*, 2001). These results have been consistently observed in the control group of this study. However, exogenous Angpt2 administered mice had smaller SRA maximum aortic diameters with less severe forms of AAA, namely Type I and Type II forms, compared with control mice with majority of Type III and Type IV forms. It is noteworthy that rAngpt2 administered mice were free from aneurysm rupture. These results suggest that exogenous Angpt2 plays an important role in regulating AngII-infusion induced AAA formation and rupture. By contrast, inhibition of Angpt2-Tie2 interaction did not affect the proportion of AAA formation, mortality from rupture, and atherosclerosis progression. This suggests that Angpt2-Tie2 interaction is not required for AAA development and atherosclerosis progression in this mouse model.

Aortic dissection and rupture in the ARCH and SRA regions are significant pathological features of this model (Saraff, 2003; Tieu *et al.*, 2009; Daugherty & Cassis, 2004; Cao *et al.*, 2010). Aortic dissection is a medial destruction and accumulation of intramural hematoma that leads to rupture of the aorta (Saraff, 2003). Indeed, it has been observed that 70% mice from the control group developed aortic dissection in the region of ARCH whereas only 10% of mice

from the rAngpt2 group developed aortic dissection in the region of ARCH. This is consistent with the finding that mice were free from aneurysm rupture and suggests exogenous Angpt2 has a role in protecting aorta from AngII-induced aortic dissection.

Another significant finding of this study is that exogenous Angpt2 reduced AngII-induced atherosclerosis progression. This confirms the previously reported result that systemic administration of Angpt2 significantly reduced around 40% of the size of atherosclerosis lesions in the ApoE$^{-/-}$ mice fed with western diet (Ahmed *et al.*, 2009). Atherosclerosis is a hallmark feature of AAA (Reed *et al.*, 1992; Brady *et al.*, 2004), and shares with its common risk factors and pathological processes. Therefore, AAA intervention is commonly accompanied by a positive effect on atherosclerosis (Reed *et al.*, 1992; Golledge & Norman, 2010). Administration of rAngpt2 in the current study attenuated both AAA formation and atherosclerosis progression, suggesting that exogenous Angpt2 targets pathological processes common to both AAA development and atherosclerosis progression.

In the experiment, exogenous Angpt2 inhibited AAA and atherosclerosis development independent to elevated BP. Hypertension is considered a risk factor for human AAA; however, it is negatively associated with the growth rate of the existing aneurysm (Vardulaki *et al.*, 2000). Nevertheless, in the experiment, the role of hypertension in AAA formation is controversial in different models (Shiraya, 2006; Weiss *et al.*, 2001). AngII is a hormone peptide of the renin-angiotensin system (Suzuki *et al.*, 2003), and AngII infusion significantly increases the SBP in ApoE$^{-/-}$ mice (Jiang *et al.*, 2007; Weiss *et al.*, 2001; Seto *et al.*, 2014). However, AngII-induced AAA formation is reported to be independent to the elevated BP (Cassis *et al.*, 2009; Bruemmer *et al.*, 2003; Owens *et al.*, 2011). In this study, all the mice displayed increased BP after 14 days AngII infusion. Administration of rAngpt2 did not affect the elevated BP induced by AngII. This suggests that the action of rAngpt2 was targeted at AngII effects on the aortic wall other than hypertension.

Hyperlipidaemia is a dependent factor for AngII-induced AAA development and atherosclerosis progression in the ApoE$^{-/-}$ model, as these responses to AngII are significantly reduced in the age-matched background strain (wild-type) C57BL6 mice (Daugherty *et al.*, 2000). The fact that reduced AAA and atherosclerosis development in AngII-infused ApoE$^{-/-}$ mice receiving rAngpt2 was observed with no significant change in plasma lipoprotein concentration, supports the conclusion that exogenous Angpt2 acts on other mediators and/or pathways involved in AAA and atherosclerosis development in this model. In the mice receiving L1-7, there is significantly higher total plasma cholesterol, compared with the mice receiving control protein after 14 days AngII infusion. There is no research reporting on Angpt2-Tie2 interaction inhibitor associated with plasma cholesterol, and this topic requires a further investigation in order to clarify the mechanisms.

In summary, this study suggests that the role of Angpt2-Tie2 interaction is not indispensable in the AAA development and atherosclerosis progression induced by AngII-infusion in ApoE$^{-/-}$ mice. Furthermore, rAngpt2 administration attenuated AAA and atherosclerosis independent of elevated BP and plasma lipoprotein concentration. Emerging evidence indicates that Angpt2 dynamically regulates its receptor Tie2 and has a complex role in regulating inflammation and angiogenesis, two important pathological processes for both AAA development and atherosclerosis progression, in a context-dependent manner (Thurston & Daly, 2012; Yuan *et al.*, 2009). Investigation of the potential mechanisms by which exogenous rAngpt2 administration attenuated AAA and atherosclerosis in the current mouse model will be presented in the following chapter.

CHAPTER 6

The Role of Exogenous Angiopoietin-2 in Angiogenesis and Inflammation in the AngII-infused ApoE$^{-/-}$ Mice

6.1 Introduction

Angiogenesis and inflammation are hallmarks of atherosclerosis and AAA development (Golledge *et al.*, 2006). Angiogenesis: new capillary formation from pre-existing vessel, is implicated in CVDs (Carmeliet, 2003; Virmani *et al.*, 2005; Williams *et al.*, 1988; Chen *et al.*, 2005) and has been observed to be associated with human AAA and atherosclerosis development (Choke *et al.*, 2006; Thompson *et al.*, 1996; Paik *et al.*, 2004; Kaneko *et al.*, 2011). During pathological angiogenesis, newly formed vessels are typically immature and highly permeable, which facilitates the infiltration of inflammatory cells into affected tissue (Shimizu *et al.*, 2006; Daugherty *et al.*, 2000; Golledge *et al.*, 2006). The accumulation of inflammatory cells and the increased expression of pro-inflammatory cytokine have been observed within the atherosclerotic lesion and AAA in both human and animal models (Lowe, 2001; Berg & Scherer, 2005). Consequently, they are believed to be critically involved in atherosclerosis and AAA development (Lowe, 2001; Berg & Scherer, 2005; Libby, 2002; Shimizu *et al.*, 2006; Coussens & Werb, 2002).

Through the Tie2 receptor, Angpt2 is a complex regulator for postnatal vasculature remodelling and inflammation (Gale *et al.*, 2002; Daly *et al.*, 2006; Cao *et al.*, 2007; Imhof & Aurrand-Lions, 2006). Constitutive low phosphorylation of Tie2 is required to maintain the quiescence of the endothelium, which is critical for the maintenance of the anti-inflammatory and anti-leakage status of the vasculature (Wong *et al.*, 1997). In the setting of angiogenic sprouting, Angpt2, as an antagonist, deactivates Tie2 to destabilise ECs of an existing vessel, thereby facilitating VEGF induced angiogenesis (Maisonpierre *et al.*, 1997). However, in the absence of VEGF, the reverse effect has been demonstrated with vessel regression induced by Angpt2 that

blocks Angpt1-Tie2 axis mediated survival signalling pathways in EC (Lobov *et al.*, 2002; Maisonpierre *et al.*, 1997). In the setting of inflammation, Tie2 deactivation can sensitise ECs to inflammatory cytokines, resulting in inflammatory cell adhesion and transmigration into the aortic wall (Fiedler *et al.*, 2006; Imhof & Aurrand-Lions, 2006) and further locally activated to produce pro-inflammatory cytokines, such as MCP-1 and IL-6, regulated by NF-κB signalling pathway (Takahashi *et al.*, 2008). Nevertheless, exogenous Angpt2 has been found to reduce cell infiltration in the presence of ongoing inflammation in vivo (Roviezzo *et al.*, 2005).

Angiogenesis is a complex process that requires the balancing of pro-angiogenic and anti-angiogenic factors and the coordination of intricate signalling pathways in ECs (Carmeliet & Jain, 2000; Muñoz-Chápuli *et al.*, 2004). Angiogenic factors, such as VEGF, induce EC proliferation, migration, survival and tube-like structure formation (Hood *et al.*, 2003; Chai *et al.*, 2004). These processes are regulated by PI3K/Akt and Erk signalling pathways (Murphy *et al.*, 2006; Ilan *et al.*, 1998), and the activation of these two signalling pathways in ECs is indispensable for angiogenesis (Jiang *et al.*, 2000; Berra *et al.*, 2000). The PI3K/Akt pathway regulates eNOS activity with NO production via phosphorylation-dependent activation of eNOS, and promotes EC proliferation, survival and tube formation (Dimmeler *et al.*, 1999; Namkoong *et al.*, 2009; He *et al.*, 1999; Cooke & Losordo, 2002). EC migration is Erk-dependent (Murphy *et al.*, 2006). Inhibition of PI3K/Akt/eNOS impairs angiogenesis. Indeed, caveolin-1 is a negative regulator of eNOS activity through its scaffolding domain (Shiojima & Walsh, 2002; Sonveaux *et al.*, 2004), and down-regulation of caveolin-1 expression within the ECs is an essential step towards angiogenesis (Liu *et al.*, 1999).

It was demonstrated in the previous chapter (Chapter 5) that exogenous Angpt2 administration attenuated AngII-induced AAA and atherosclerosis development in ApoE^{-/-} mice. As Angpt2 is a complex regulator of angiogenesis and inflammation in a context-dependent manner, it was hypothesised that the effect of rAngpt2 administration in the mouse model involved limiting angiogenesis and inflammation at the aortic wall. Studies were therefore performed in aortic tissues obtained from the mouse study in Chapter 5 with the following aims:

1. To assess and compare micro-vessel density and monocyte/macrophage accumulation within the suprarenal aorta from mice receiving rAngpt2 versus control protein;

2. To evaluate Akt/eNOS and Erk signalling within the suprarenal aorta from mice receiving rAngpt2 versus control protein;

3. To assess the expression of selected pro-inflammatory cytokines within the aortic walls and plasma samples from mice receiving rAngpt2 versus control protein.

6.2   Materials and methods

6.2.1   Antibodies for Western blotting and immunofluorescence staining

Antibodies used for Western blotting and immnnofluorescence staining were listed in **Table 6.1** and **Table 6.2** respectively.

Table 6.1 Antibodies used for Western blotting

Antibody	Catalogue Number	Source
Polyclonal rabbit anti-Phospho-Tie2 (Tyr992)	Cat. # 4221, MW:160 kDa	Cell Signaling (USA)
Polyclonal rabbit anti-caveolin-1	Cat. # 3238, MW:21, 24 kDa	
Monoclonal rabbit anti-Phospho-p44/42 MAPK (Erk1/2) (Thr202/Tyr204)	Cat. # 4370, MW:42, 44 kDa	
Polyclonal rabbit anti-p44/42 MAPK (Erk1/2)	Cat. # 9102, MW:42, 44 kDa	
Monoclonal rabbit anti-eNOS (49G3)	Cat. # 9586, MW:140 kDa	
Monoclonal rabbit anti-Phospho-eNOS (Ser1177) (C9C3)	Cat. # 9102, MW:140 kDa	
Monoclonal rabbit anti-Phospho-p44/42 MAPK (Erk1/2) (Thr202/Tyr204)	Cat. # 4370, MW:42, 44 kDa	
Monoclonal rabbit anti-GAPDH (14C10)	Cat. # 2118, MW: 37 kDa	
Monoclonal mouse anti-Tie2/TEK	Cat. # 05-184, MW: 145 kDa	Millipore (USA)
Monoclonal mouse anti-Tie2/TEK	Cat. # 05-184, MW: 145 kDa	Santa Cruz (USA)
Polyclonal rabbit anti-Phospho-Akt1/2/3 (ser 473)	Cat.# sc-101629, MW:62 kDa	
Polyclonal rabbit anti-PCNA (FL-261)	Cat.# sc-7907, MW: 36 kDa	
Monoclonal rat anti-MCP-1 (ECE.2)	Cat.# sc-52701, MW: 12 kDa	
Polyclonal rabbit anti-NF- κB p65	Cat. # ab7970, MW: 69 kDa	Abcam (UK)
Polyclonal goat anti-mouse immunoglobullins/HRP	Cat.# P0447	Dako (Germany)
Polyclonal HRP-conjugated goat anti-rabbit immunoglobullins/HRP	Cat.# P0448	
Polyclonal HRP-conjugated goat anti-rat immunoglobullins/HRP	Cat.# P0450	

Table 6.2 Antibodies used for CD31 immunofluorescence staining

Antibody	Catalogue Number	Source
Primary antibody monoclonal rat anti-PECAM-1 (MEC 13.3)	CD31, Cat. # sc-18916	Santa Cruz (USA)
Primary antibody monoclonal rat anti-Monocyte + Macrophage (MOMA-2)	MOMA-2, Cat. # ab33451	Abcam (UK)
Secondary antibody Alexa Fluor 488-conjugated goat anti-rat IgG (H+L)	Cat. # A-11006	Life Technologies (USA)

6.2.2 Western blotting for assessing protein expression within suprarenal aortic tissue

The SRAs from one subset experiment, performed by the thesis author (n=10), were used to assess protein expression within the aortic tissue. Six SRAs were randomly chosen from the rAngpt2 or control group to assess protein expression by Western blotting. Tissues were homogenized by three freeze-thaw cycles. Total protein was extracted and quantified in the presence of a protease inhibitor cocktail and phosphatase inhibitor (Roche, USA) as described in Chapter 3, Section 3.9. Nuclear protein was extracted using NE-PER nuclear protein extraction kit (Piercenet, USA) as described previously (Chapter 3 Section 3.9). Western blotting procedures were described as previously (Chapter 3, Section 3.10). Briefly, a total of 30 μg of protein per sample was loaded into 4–20% Mini-PROTEAN TGX precast polyacrylamide gels (Bio-Rad, USA) and separated at 110V for 70 min. Separated proteins were transferred to a polyvinylidene fluoride membrane (Bio-Rad, USA). Non-specific antibody sites were blocked with 5% BSA for 60 min at room temperature. For protein phosphorylation evaluation, membranes were firstly probed with antibodies detecting phosphorylation forms of proteins. To evaluate phosphorylated Tie2, phosphorylated Erk1/2, phosphorylated Akt and phosphorylated eNOS, the membranes were probed with anti-Phospho-Tie2^{tyr992}, anti-Phospho-Erk1/2$^{Thr202/Tyr204}$, anti-Phospho-Akt1/2/3^{ser473} or anti-Phospho-eNOS^{ser117} antibodies at a dilution of 1:1000. This was followed by corresponding secondary HR-conjugated antibodies incubation. After the blots were developed and imaged, the membranes were immersed in 15 ml restore Western blot stripping buffer for 20 min to remove primary and secondary antibodies.

This was followed by washing with TBS buffer and blocking with 5% BSA. Membranes were then re-probed with anti-Tie2/TEK, anti-Erk1/2, anti-Akt1(7) or anti-eNOS antibody at a dilution of 1:1000 in order to evaluate total Tie2, Erk1/2, Akt and eNOS expression, respectively. To evaluate caveolin-1, GAPDH, MCP-1, p65, and PCNA, the membranes were probed with anti-caveolin-1, anti-GAPDH, anti-MCP-1, anti-p65, or anti-PCNA antibodies at a dilution 1:1000 in 2% BSA at 4°C overnight. Blots were developed with Clarity Western Enhanced Chemiluminescence Substrate (Bio-Rad, USA). Software Image Lab (v5, Bio-Rad, USA) was used for densitometry quantification as described in Chapter 3, Section 3.10.3. The phosphorylated protein signal was normalised against the signal of its total protein. A house keeping protein was used to ensure that the same amount of total protein samples were loaded and that proteins were transferred from the gel to the membrane with equal efficiency. GAPDH is a house keeping protein for total protein extraction. The signal of caveolin-1 was normalised against the signal of the loading control GAPDH. Proliferating cell nuclear antigen (PCNA) is a house keeping protein for nuclear protein. The signal of nuclear p65 was normalised against the signal of the loading control PCNA. The data were expressed as relative fold of control by normalising the interested protein's band intensity to the mean band intensity of the control mice.

6.2.3 Immunofluorescence staining and quantification of angiogenesis and monocyte/macrophage accumulation within the aortic wall

The SRAs from one subset experiment (n=10) were used to assess protein expression within the aortic tissue, and six SRA tissues were randomly chosen from rAngpt2 or control group for immunofluorescence staining. Six μm cryostat sections from the middle region of the SRA were prepared as described in Chapter 3, Section 3.11.1. immunofluorescence staining of CD31 or MOMA-2 was performed in order to evaluate angiogenesis and monocyte/macrophage accumulation respectively within the aortic wall (Chapter 3, 3.11.2). Briefly, sections were fixed in cold acetone at −20°C for 20 min and then blocked with 5% normal goat serum in PBS containing 0.5% BSA and 0.1% Triton X-100 for 60 min at room temperature. Sections were

incubated overnight at 4°C with anti-CD31 or anti-MOMA-2 antibody at a dilution of 1:100 in PBS containing 0.5% BSA. After washing, samples were incubated with Alex Fluor 488-conjugated anti-rat IgG secondary antibody at a dilution of 1:200 for 60 min at room temperature. Cell nuclei were labelled by DAPI (Sigma, USA). Slides were mounted with water based mounting medium (Proscitech, Australia), and covered with coverslips. Five images were captured from randomly chosen microscope fields of the aortic section. These were captured at x200 total magnification by a Zeiss fluorescence microscope (Zeiss, Germany) as described in Chapter 3, Section 3.11.3. The CD31 and MOMA-2 positive staining area was measured with ImageJ software (v1.4d, NIH, USA), as described in Chapter 3, Section 3.11.4. Five different areas of each section were chosen for measurement, in order to calculate the mean of the percentage of positive staining area. Data were expressed as percentage of positive staining area per analysed area. The method had a good inter-observer reproducibility, as described previously (Chapter4, Section 4.4.2).

6.2.4   Assessment of plasma inflammatory cytokine concentrations

Plasma samples, collected in one subset of the experiment at day 14 (n=10, Chapter 3, Section 3.3.2), were used for quantification of mouse pro-inflammatory concentrations, as described in Chapter 3, Section 3.8. Six samples were randomly selected from the rAngpt2 group or the control group. CBA Mouse Inflammatory kit (BD Biosciences, USA) was used to assess plasma inflammatory cytokine concentrations (IL-6, IL-10, MCP-1, IFN-γ, TNF, and IL-12p70), according to the manufacturer's instructions. In brief, 50 μl of plasma per sample or standard was mixed with 50 μl APC-conjugated anti-cytokine antibody coated beads and 50 μl PE detection reagent. The mixtures were incubated in the dark at room temperature for 2 hours. Then samples were washed with the provided washing buffer and centrifuged at 250 x g for 5 min. The beads were resuspended in 300 μl washing buffer per sample, and were ready for immediate assessment with the CyAn-ADP analyser (Chapter 3, Section 3.8.3). FCAP Array Software (v3, USA) was used for the quantitative analysis of multiple analytes (Chapter 3 Section 3.8.4). A 5-Parameter Logistic curve fit mathematical model was used to generate

standard curves. These were used to determine the concentration of the each cytokine per plasma sample.

6.2.5 Enzyme-linked Immunosorbent Assay for vascular endothelial growth factor

The SRAs from one subset experiment (n=10) were used to assess protein expression within the aortic tissue. Six suprarenal aortic tissues were randomly chosen from the rAngpt2 or the control group. The mouse VEGF Quantikine Enzyme-linked Immunosorbent Assay (ELISA) kit (R&D system, Cat. # MMV00, USA) was used according to the manufacturer's instructions, to assess VEGF protein concentrations in aortic tissue. Total protein was extracted and quantified as described previously (Chapter 3, Section 3.9.1 and 3.9.3). The provided mouse VEGF standard was reconstituted with 5 ml of calibrator diluent producing a stock solution of 2500 pg/ml. The stock solution was used to produce a 2 fold dilution series standard.

A total of 30 µg protein in 100 µl assay diluent per sample or 100 µl standards were added to each well pre-coated with capture antibody in a 96-well plate, and then were covered with an adhesive strip. Samples were incubated at room temperature for two hours, followed by five wash cycles with the wash buffer provided. Liquid was then completely removed, and 100 µl of polyclonal anti-Mouse VEGF conjugated to horseradish peroxide was added to each well. Samples were covered with an adhesive strip and incubated at room temperature for two hours. This was followed by five wash cycles with the wash buffer provided, followed by the complete removal of residual liquid. A total of 100 µl substrate solution was added to each well, and samples were incubated at room temperature protected from light for 30 min. After this, 100 µl stop solution was added to each well and mixed thoroughly. The OD value of each well was measured, using a micro plate reader (BMG Labtech, USA), at 450 nm, with 540 nm as wavelength correction. A 4-Parameter Logistic curve-fit was created according to the OD value of each standard against its concentration, using Graphpad Prism (v6, USA). The concentration of VEGF in each sample was determined according to the standard curve.

6.2.6   Statistical analysis

Data were expressed as median (IQR), and the Mann-Whitney U test was used to perform statistical analysis. This analysis compared the rAngpt2 group and control group. The Pearson correlation coefficient test was used to assess the relationship between pro-inflammatory cytokine MCP-1 concentrations within the suprarenal aortic tissue and maximum SRA aortic diameters. Data were analysed using GraphPad Prism (v6, USA). A value of $p<0.05$ was considered statistically significant.

6.3 Results

6.3.1 rAngpt2 administration induced Tie2 phosphorylation within the suprarenal aortic tissue

Exogenous Angpt2 administration has been reported to induce Tie2 phosphorylation (Daly *et al.*, 2006). Therefore, Tie2 phosphorylation (Tyr 992) were assessed within SRA tissue (**Figure 6.1** A) and it was found that mice receiving rAngpt2 had a significantly higher Tie2 Phosphorylation compared with control mice (median relative density rAngpt2: 3.26 A.U. (1.17-7.29) *versus* control: 0.70 A.U. (0.47-1.38); n=6; *p*=0.026; A.U.=arbitrary units; **Figure 6.1** B).
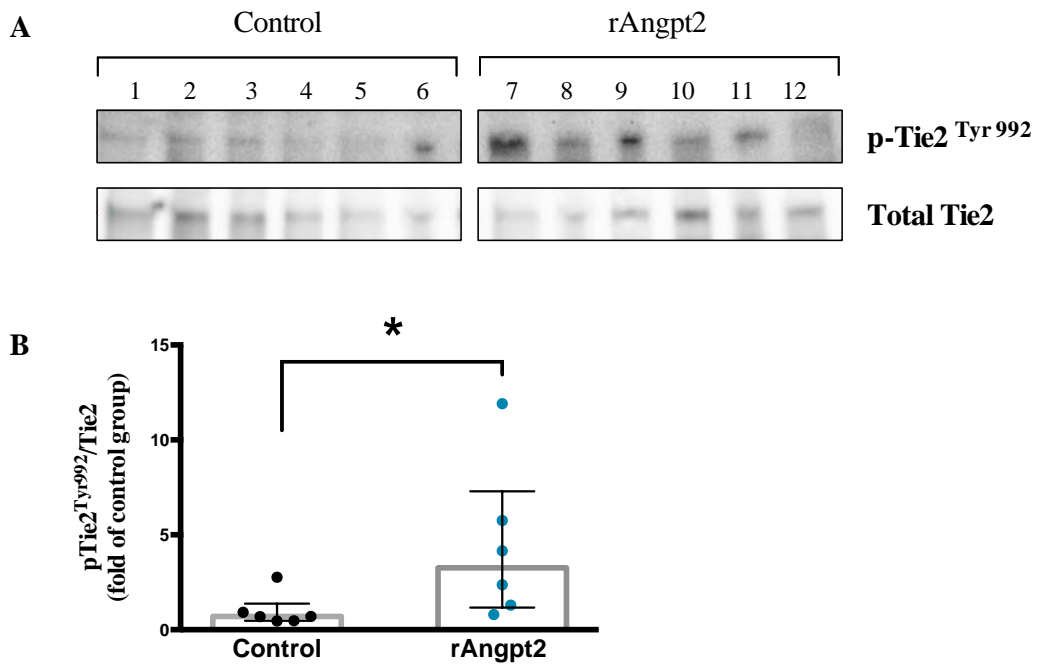
Figure 6.1 rAngpt2 administration induced significant Tie2 (Tyr992) phosphorylation within the suprarenal aortic tissue harvested at day 14.
A) Western blotting image of the phosphorylated Tie2 (Tyr992) and total Tie2; and **B**) rAngpt2 administration induced significantly Tie2(Tyr992) phosphorylation within the suprarenal aortic tissue compared with the control group. Data were expressed as median (IQR) and analysed by Mann-Whitney *U* test (n=6 per group); *$p<0.05$.

6.3.2 rAngpt2 administration reduced nuclear p65 and MCP-1 expression within the suprarenal aortic tissue

Angpt2 can sensitise ECs to inflammatory stimuli and activate NF-κB signalling pathway through Tie2 deactivation (Fiedler *et al.*, 2006; Fiedler & Augustin, 2006). NF-κB activation involves translocation cytoplasm RelA (p65) subunit to nuclear (Saito *et al.*, 2012). Infusion of AngII promotes NF-κB activation and up-regulation of MCP-1 expression, which are closely associated with aortic inflammation, aortic aneurysm progression, and rupture (Tieu *et al.*, 2009; Saito *et al.*, 2012; Pueyo *et al.*, 2000; Suzuki *et al.*, 2003). Mice receiving rAngpt2 had lower nuclear p65 expression within the SRA compared with the control group. However, the difference was not statistically significant (p=0.093; **Figure 6.2** A and C). Mice receiving rAngpt2 had significantly lower MCP-1 expression within the SRA (0.65 A.U. (0.41 − 0.87); n=6; p=0.004; **Figure 6.2** B and D) (expressed as median fold difference compared to the control group). The MCP-1 expression within the SRA was positively correlated with maximum SRA diameter (r=0.781, p=0.043; **Figure 6.2** E).
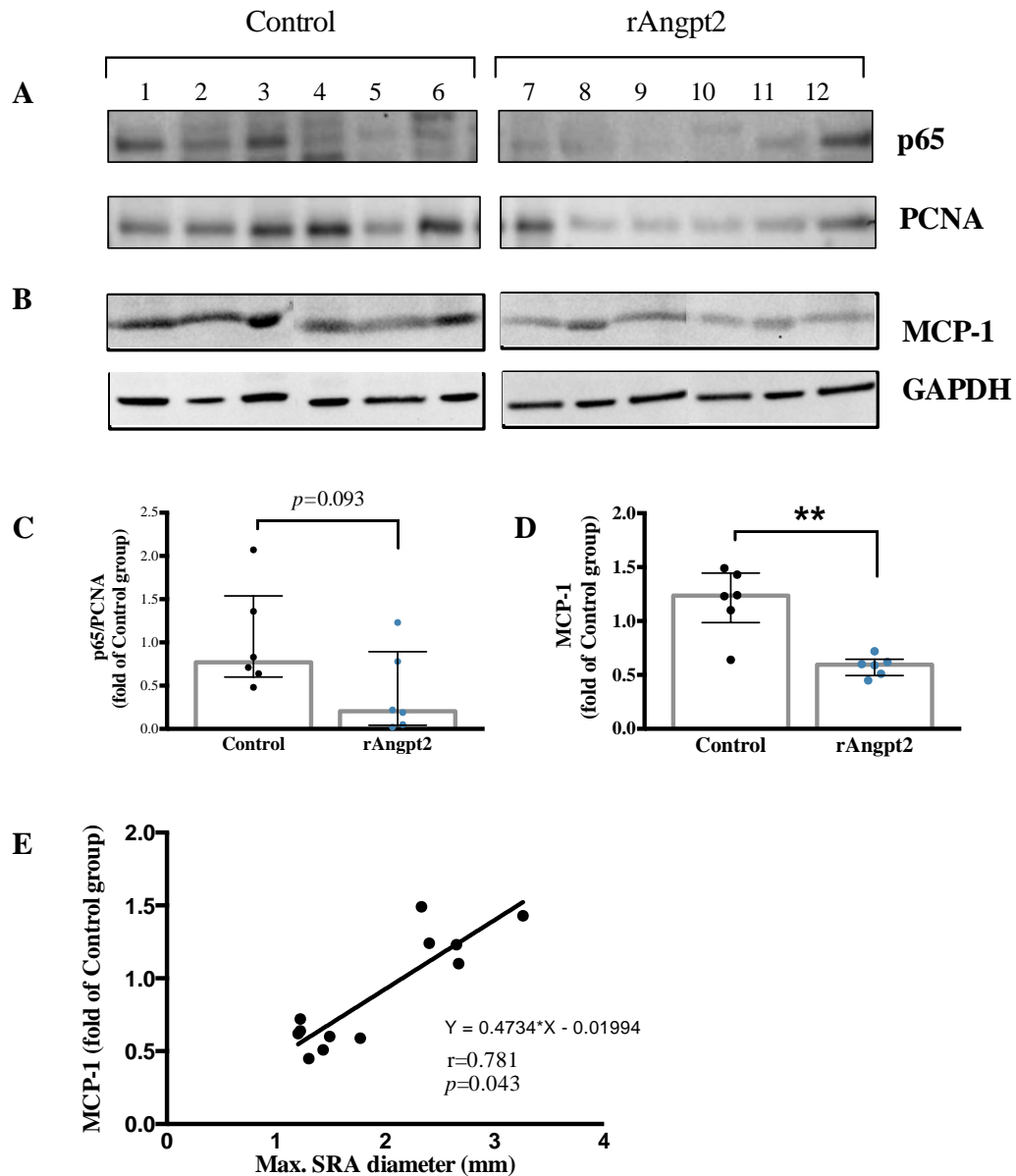
Figure 6.2 rAngpt2 administration reduced nuclear p65 expression and MCP-1 expression within the suprarenal aortic tissue harvested at day 14.
A) Western blotting image of nuclear NF-κB p65 and loading control PCNA; **B**) Western blotting image of MCP-1 and GAPDH; **C**) densitometry analysis showed that rAngpt2 administration reduced nuclear NF-κB p65 expression compared with control group; **D**) rAngpt2 administration significantly reduced MCP-1 expression compared with the control group; and **E**) the MCP-1 expression was positively correlated with maximal aortic diameters (n=6 in each group, Pearson Correlation Coefficient test; r=0.781 and *p*=0.043). Data were expressed as median (IQR) and analysed by Mann-Whitney *U* test (n=6 per group); r = correlation coefficient and ***p<0.005.

6.3.3　　rAngpt2 reduced Monocyte/Macrophage accumulation within the SRA

MCP-1 is an important chemoattractant for inflammatory monocytes recruitment and inflammatory monocyte infiltration, and accumulation within the aortic wall is one of the major pathological features of AAA (Golledge *et al.*, 2006). Immunofluorescence staining of SRA sections suggested marked monocyte-macrophage accumulation within the aortic wall, in the control group at day 14 (**Figure 6.3** A). Mice receiving rAngpt2 had significantly lower median MOMA-2 positive staining area per assessed area (rAngpt2: 0.57% (0.50-1.13) *versus* control: 4.51% (3.36-5.29); n=6; *p*=0.004; **Figure 6.3** B).
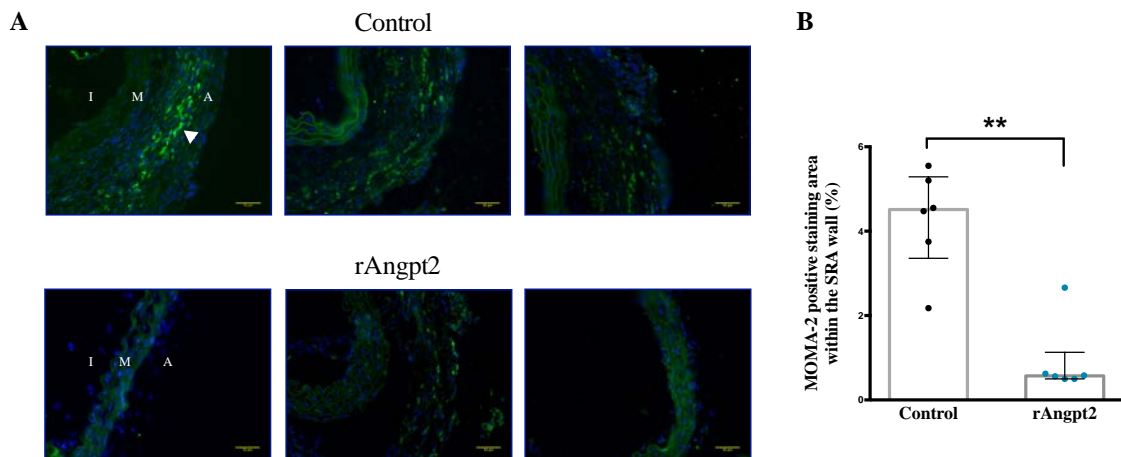
Figure 6.3 rAngpt2 administration reduced monocyte/macrophage accumulation within the suprarenal aortic tissue harvested at day 14.
A) an example of SRA trans-cross section immunofluorescence staining for MOMA-2 to detect macrophages/monocytes within the aortic wall (I=intima, M=media, A=adventitia, blue=nuclei, green=MOMA-2, Arrow indicates a typical macrophage/monocyte, 200X magnification; scale bar =50 µm); and **B**) percentage of positive MOMA-2 positive staining area in each group; Data were expressed as median (IQR) and analysed by Mann-Whitney *U* test (n=6 per group); **p<0.005.

6.3.4　　rAngpt2 administration reduced plasma MCP-1 and IL-6 concentrations

Elevated circulating inflammatory cytokines are observed in AAA patients and in the AngII-induced AAA mouse model (Juvonen *et al.*, 1997; Satoh *et al.*, 2009). Administration of rAngpt2 was associated with significantly lower median plasma concentrations of MCP-1 compared to control mice (rAngpt2: 43.63 pg/ml (29.35-58.21) *versus* control: 138.60 pg/ml (75.56-329.4); n=6; *p*= 0.011) and IL-6 (rAngpt2: 28.82 pg/ml (26.78-64.25) *versus* control: 122.10 pg/ml (78.94-152.30); n=6; *p*=0.013; **Figure 6.4**) after 14 days of AngII infusion. There was no significant difference in plasma TNF concentration between mice receiving rAngpt2 and

control mice (rAngpt2 3.68 pg/ml (3.41-6.84) *versus* control 4.49 pg/ml (3.21-8.34), n=6 in each group, *p*=0.794; **Figure 6.4**). IFN-γ and IL-12p50 were not detectable in either group.
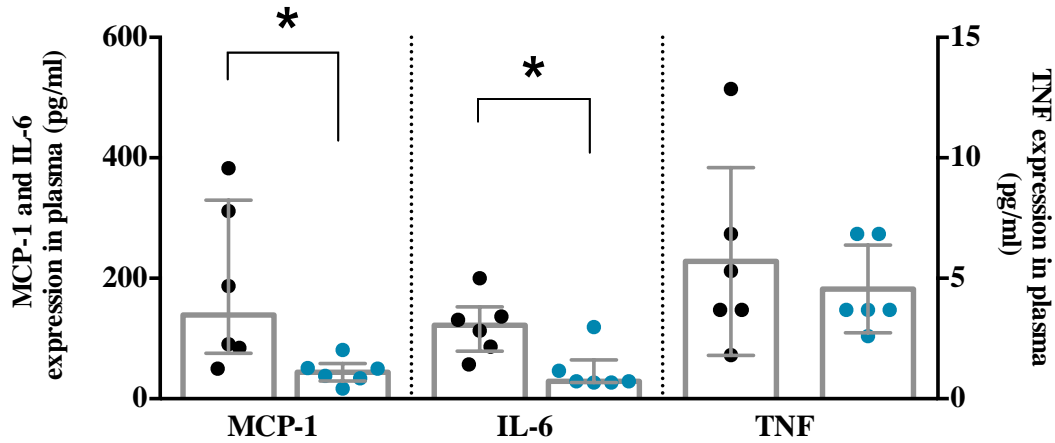
Figure 6.4 rAngpt2 administration significantly reduced plasma inflammatory cytokine MCP-1 and IL-6 concentration after 14 days of AngII infusion.
Inflammatory cytokine concentrations were determined using the CBA Mouse Inflammation Kit. Data were expressed as median (IQR) and analysed by Mann-Whitney *U* test (n=6 per group); black dots represent mice receiving control protein and blue dots represent mice receiving rAngpt2; * *P*<0.05.

6.3.5 rAngpt2 administration reduced angiogenesis marker (CD31) within aortic wall of the suprarenal aortic tissue without influencing VEGF

Endogenous Angpt2 has been reported to impair angiogenesis in different settings (Cao *et al.*, 2007; Chen *et al.*, 2011) and, in the previous chapter, it has been demonstrated that rAngpt2 administration attenuated AAA development. Therefore, angiogenesis was assessed within the SRAs harvested at day 14 by immunofluorescence staining for the EC marker CD31. The intimal and micro-vessel ECs were stained positively for CD31 as shown (**Figure 6.5** A). rAngpt2 administration was associated with significant lower median CD31 positive staining area within the SRA adventitia (rAngpt2: 0.63% (0.26 − 1.05) *versus* control: 6.30% (4.32 − 9.44); n=6; *p*=0.002; **Figure 6.5** B). The median concentration of VEGF (pg per mg aortic protein) was not significantly different between the two groups (rAngpt2: 22.50 pg/mg (9.75 − 29.50) *versus* control: 14.50 pg/mg (8.75 − 32.00); n=6; *p*=0.680; **Figure 6.5** C).
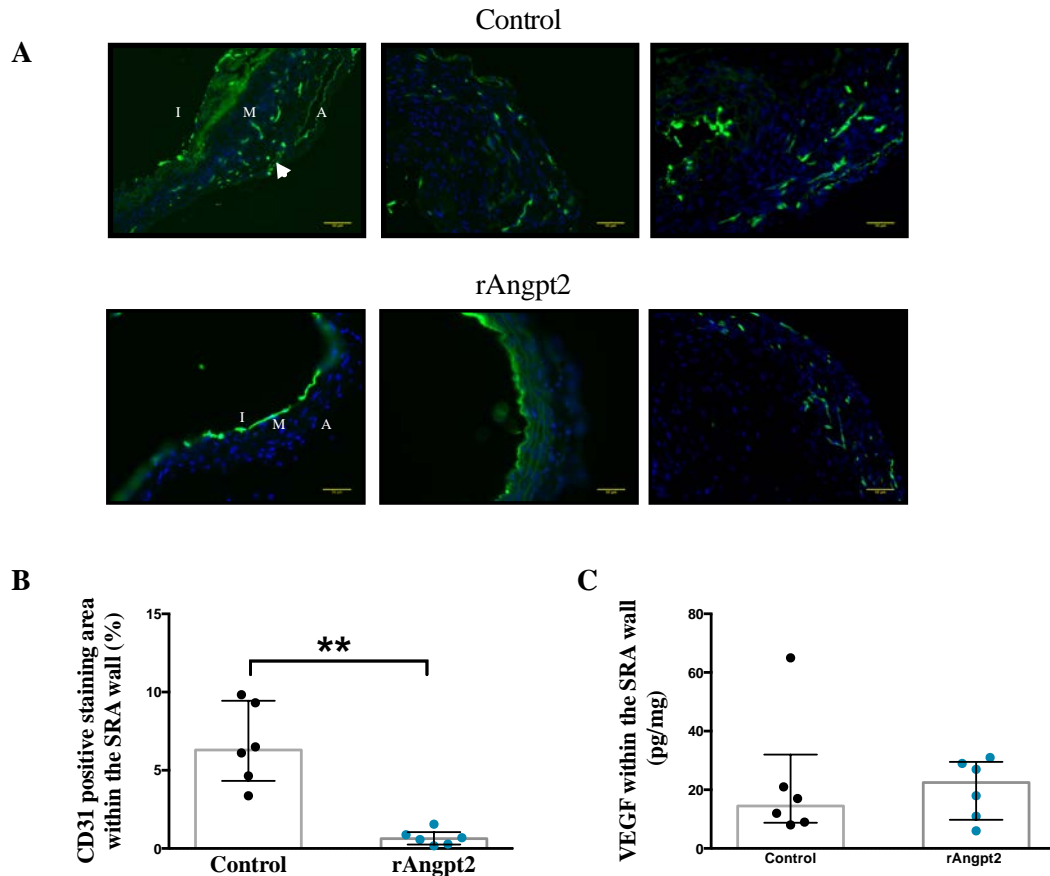
Figure 6.5 rAngpt2 administration significantly reduced the angiogenesis marker CD31 within the suprarenal aortic wall without altering VEGF expression.
A) an example of SRA transverse section showing immunofluorescence staining for CD31 to detect angiogenesis within the aortic wall (I=intima, M=media, A=adventitia, blue=nuclei, green=CD31, Arrow indicates a typical microvessel, 200X magnification; scale bar =50 µ m); **B**) percentage of positive CD31 positive staining area in each group; and **C**) concentration of VEGF per 30 µ g of protein extracted from aortic tissue assessed by ELISA. Data were expressed as median (IQR) and analysed by Mann-Whitney *U* test (n=6 per group); ******$p<0.005$.

6.3.6   rAngpt2 administration did not alter Erk and Akt-eNOS signalling within suprarenal aortic tissue.

The immunostaining of CD31 within the SRA suggests that rAngpt2 administration impaired angiogenesis within the SRA. Erk1/2, Akt, and eNOS are downstream of Tie2 signalling pathways that are regulating ECs survive, migration, and tube formation in angiogenesis (Shen *et al.*, 2014; Zhang *et al.*, 2009). Western blotting was used to assess the phosphorylation of Erk1/2 (Thr202/Tyr204), Akt (ser473), and eNOS (ser1177) within the SRA tissue (**Figure 6.6 A, B and C**)). However, there was no significant difference in the level of the phosphorylated Erk1/2, Akt, and eNOS within the SRA, harvested at Day 14, from the mice receiving rAngpt2 compared to the control mice (**Figure 6.6** D, E, and F).
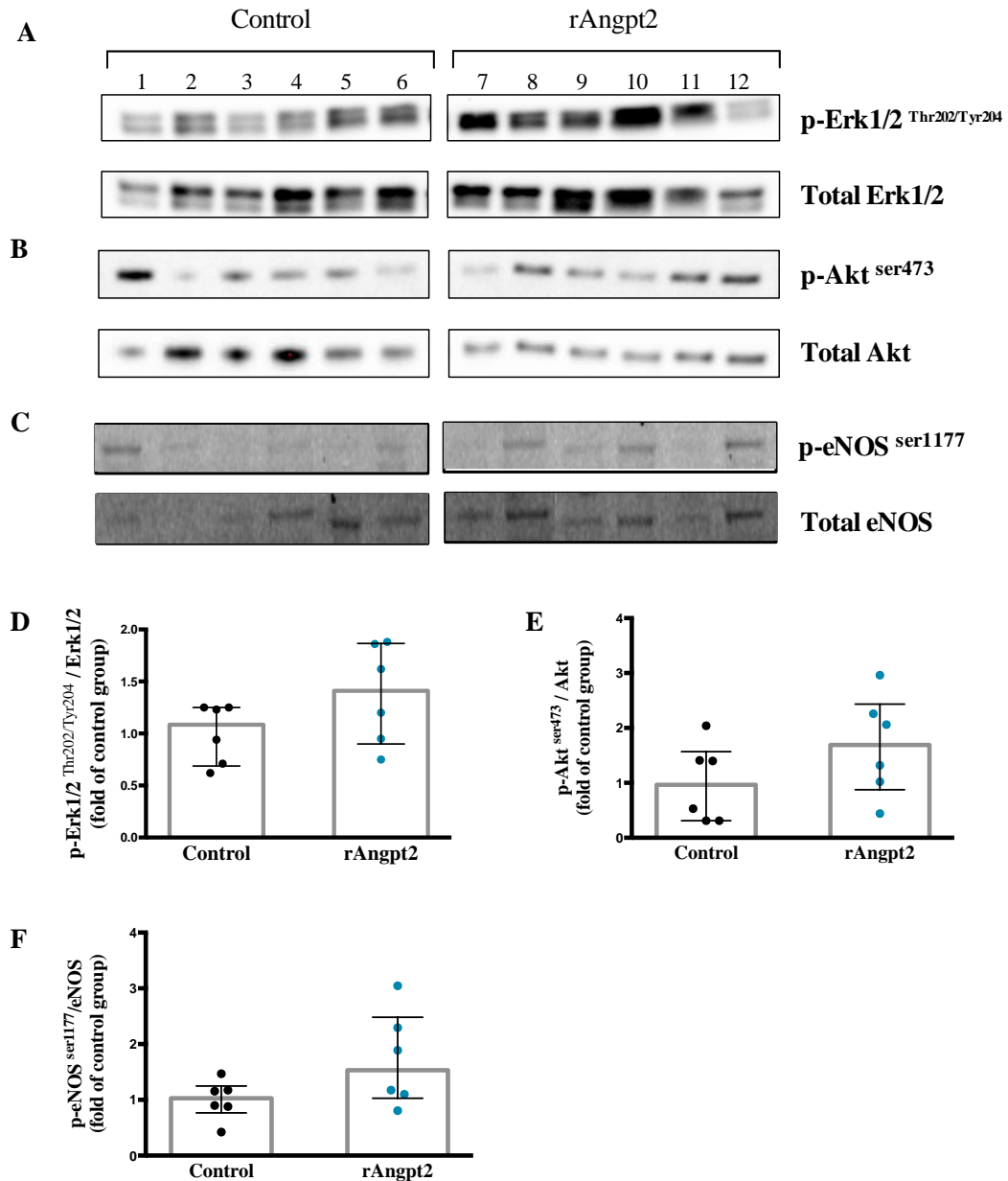
Figure 6.6 Erk1/2 and Akt-eNOS signalling pathway within the SRA tissue harvested at day 14 followed AngII infusion.

A) Western blotting image of pErk1/2 (Thr202/Tyr204) and Erk 1/2; **B**) Western blotting image of pAkt (ser473) and Akt; **C**) Western blotting image of p-eNOS (ser1177) and eNOS; **D**) there was no significant difference in Erk 1/2 phosphorylation within the SRA from the mice receiving rAngpt2 (p=0.197) compared with the mice receiving control protein; **E**) there was no significant difference in Akt phosphorylation within the SRA from the mice receiving rAngpt2 (p=0.225) compared with the mice receiving control protein; and **F**) there was no significant difference in eNOS phosphorylation within SRA from the mice receiving rAngpt2 (p=0.197) compared with the the mice receiving control protein; Data were expressed as median (IQR) and analysed by Mann-Whitney U test (n=6 per group).

6.3.7   rAngpt2 administration increased caveolin-1 expression within the SRA

Caveolin-1 expression has been demonstrated to play a critical role in regulating angiogenesis, atherosclerosis, and micro-vascular permeability (Bauer *et al.*, 2005; Liu *et al.*, 1999). The expression of caveolin-1 within the SRA was assessed by Western blotting (**Figure 6.7** A) and was significantly up-regulated in mice receiving rAngpt2 compare to control mice (median 3.00 A.U. (2.7-3.24) compared with control mice (median1.00 A.U. (0.74-1.39), *p*=0.041, **Figure 6.7** B).
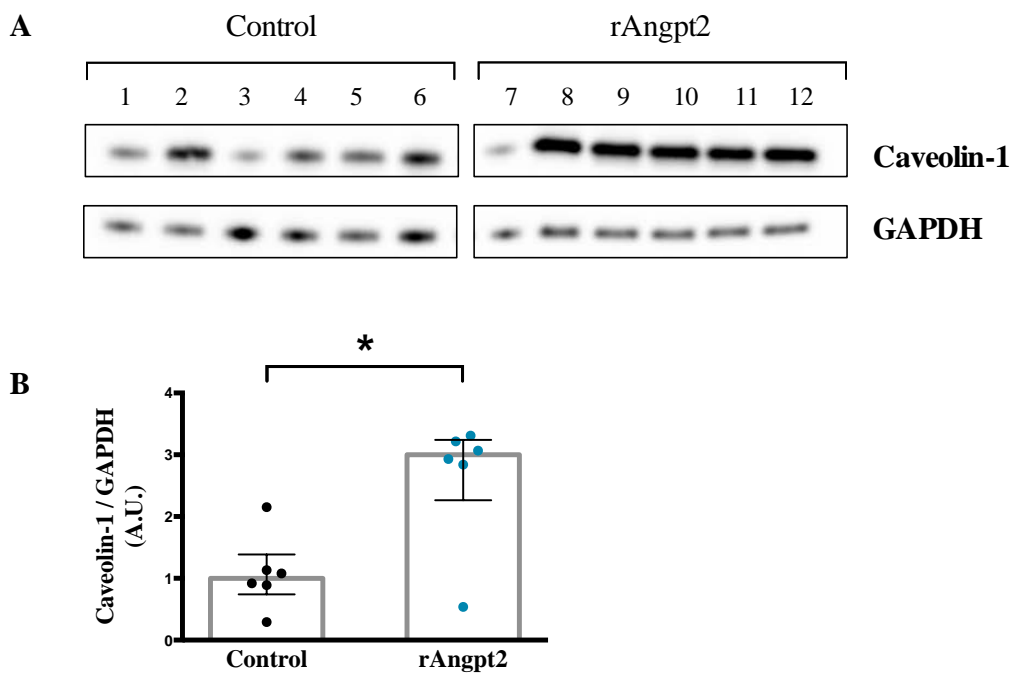
Figure 6.7 rAngpt2 administration significantly increased caveolin-1 expression within the supernal aortic tissue harvested at day 14.
A) Western blotting image of caveolin-1 and GAPDH; and **B**) rAngpt2 administration significantly induced caveolin-1 expression compared with the control group. Densitometry data were normalised to the loading control GAPDH. The data were expressed as median (IQR) and analysed by Mann-Whitney *U* test (n=6 per group); *p*<0.05.

6.4 Discussion

In this study, angiogenesis and inflammation were investigated within the aortic walls of SRAs from mice receiving rAngpt2 and control protein. It was found that rAngpt2 administration significantly induced Tie2 phosphorylation. rAngpt2 administration significantly reduced monocyte/macrophage accumulation within the suprarenal aortic wall, and pro-inflammatory cytokine expression within the aortic tissue and plasma. immunofluorescence staining of CD31, a marker of angiogenesis, showed significantly less positive staining area within the suprarenal aortic tissue in mice receiving rAngpt2. However, there was no difference in Akt/eNOS and Erk signalling pathway activation between the two groups. Caveolin-1, an important factor regulating angiogenesis and atherosclerosis development, was up-regulated within the aortic tissues from mice receiving rAngpt2. These results suggest that exogenous Angpt2 attenuated AAA and atherosclerosis, by limiting angiogenesis and inflammation.

Angpt2 regulates its receptor Tie2 activation in a context-dependent manner (Thurston & Daly, 2012). Unlike Angpt1, Angpt2 was originally identified as an antagonist of Tie2. However, Angpt2 has been observed to activate Tie2, albeit to a less extent than Angpt1 (Thurston & Daly, 2012; Yuan *et al.*, 2009). Indeed, exogenous Angpt2 has been previously reported to activate Tie2 both *in vivo* and *in vitro* (Cao *et al.*, 2007; Chen *et al.*, 2009; Chen *et al.*, 2011; Daly *et al.*, 2006; Yuan *et al.*, 2009). In this study, Tie2 activation was also observed within the aortic wall in the mice receiving rAngpt2.

Tie2 activation plays a vital role in regulating vascular inflammation (Thurston & Daly, 2012; Yuan *et al.*, 2009). Tie2 activation exerts anti-inflammatory effects by decreasing leukocytes adhesion to ECs. Therefore, Tie2 deactivation is required to sensitise the endothelium, with the inflammatory stimuli resulting in adhesion molecule expression. This increases the chance of monocyte adhesion on the endothelium, and subsequently infiltrated in the aortic wall (Fiedler *et al.*, 2006; Hughes *et al.*, 2003). The infiltrating monocytes are differentiated into macrophages producing MCP-1, which exacerbates the inflammation by recruiting more

monocytes. Consistent with Tie2 activation, a limited monocyte/macrophage accumulation and low MCP-1 expression were observed within the aortic tissue in the mice receiving rAngpt2. Together, these results suggest that exogenous Angpt2 induced Tie2 activation. Therefore, they reduced monocyte/macrophage infiltration within the aortic wall in the presence of AngII, an important regulator of the inflammatory response (Suzuki *et al.*, 2003). Exogenous Angpt2 inhibited leukocyte infiltration in the presence of inflammatory stimuli, as was also reported previously (Daly *et al.*, 2006; Roviezzo *et al.*, 2005).

The microvessel density within the SRA wall was significantly lower, without influencing VEGF expression, in the mice receiving rAngpt2. Angiogenesis is precisely coordinated by the angiogenic factors Angpt2 and VEGF. Prolonged exposure of ECs to Angpt2 induces apoptosis and vessel regression in the absence or low level of VEGF (Carmeliet, 2003; Lobov *et al.*, 2002; Maisonpierre *et al.*, 1997). Therefore, the ratio of Angpt2 to VEGF may be critical to determine whether the vessel undergoes angiogenesis or regression. Indeed, it has been reported that Angpt2 disrupted tumour vasculature without interfering with endogenous VEGF activity in animal models of cancer (Augustin *et al.*, 2009; Cao *et al.*, 2007; Chen *et al.*, 2011; Chen & Stinnett, 2008). Similarly, it was reported in this study that rAngpt2 administration reduced AngII-induced vessel formation within the aortic wall in ApoE$^{-/-}$ mice.

Akt/eNOS and Erk signalling in ECs are important in the angiogenesis process (Namkoong *et al.*, 2009). However, Tie2 phosphorylation activated downstream PI3K/Akt/eNOS, and Erk signalling is also required to maintain quiescence of the endothelium (Zhang *et al.*, 2011). Thus, the role of Akt/eNOS signalling pathways in EC function may depend on the nature of the cell-cell and cell-matrix contacts (Thurston & Daly, 2012). In this study, no difference was observed in Akt/eNOS and Erk signalling pathway activation, although there was a significantly higher density of micro-vessels within the aortic wall in the control mice. This suggests that the Tie2 phosphorylation induced Akt/eNOS and Erk activation in the rAngpt2 group diminished any difference of these two signalling pathway in the activated ECs. Indeed, the

immunofluorescence staining showed that the aortic endothelium (intima) was intact in mice receiving rAngpt2, while it was greatly disrupted in mice receiving control protein.

Another finding of this study was that caveolin-1 expression was significantly up-regulated within the aortic tissue from the mice receiving rAngpt2. Caveolin-1 is present in different cell types. The EC caveolin-1 and SMC caveolin-1 have opposing roles in atherosclerosis (Frank & Lisanti, 2004). Caveolin-1 in ECs has a pro-atherogenic role, whereas caveolin-1 in SMCs plays an anti-atherogenic role (Frank & Lisanti, 2004; Pavlides *et al.*, 2014; Elia *et al.*, 2009; Milewicz *et al.*, 2008; Guo *et al.*, 2007; Doran *et al.*, 2008). In the previous chapter, it was reported that rAngpt2 administration attenuated atherosclerosis development. Therefore, the source of up-regulated caveolin-1 expression may be from SMCs. Indeed, vascular SMC apoptosis occurs in many arterial diseases, including aneurysm formation, angioplasty restenosis, and atherosclerosis (Doran *et al.*, 2008). EC caveolin-1 is a negative regulator of Akt/eNOS signalling. However, inhibition of Akt/eNOS activation was not observed in the rAngpt2 group. This also suggested the up-regulated caveolin-1 expression is not of EC origin. However, this hypothesis and the mechanisms of up-regulation of caveolin-1 by rAngpt2 administration need to be further investigated.

Both inflammation and angiogenesis are important pathological features for human AAA and experimental AAA. The extent of angiogenesis correlates with the severity of inflammatory cell infiltration in AAA biopsies (Holmes *et al.*, 1995; Thompson *et al.*, 1996). AngII induced AAA and atherosclerosis have been associated with aortic macrophage accumulation (Daugherty *et al.*, 2000; Saraff, 2003). Such aortic inflammation may, in part, be a consequence of AngII induced angiogenesis, since newly formed pathological capillaries are normally poorly organised and highly permeable (Imhof & Aurrand-Lions, 2006). Furthermore, AngII activates macrophage inflammatory signalling pathways, such as NF-κB, to promote MCP-1 secretion (Takahashi *et al.*, 2008) and production of IL-6. Both MCP-1 and IL-6 are detected in circulation with high levels in human AAA patients, and their concentrations are associated with a high risk of aortic rupture (Dawson *et al.*, 2007; Juvonen *et al.*, 1997).

PCNA is a loading control for nuclear NF-κB subunit p65 expression within the SRA tissue in this study. However, a higher density of PCNA was observed in the control group compared with the rAngpt2 group. This is unlikely to be a loading error, as the expression pattern is group dependent. PCNA is abundantly expressed in proliferating cells, and fibroblast undergoes active proliferation within the aortic wall in the AngII-infused mice (Tieu *et al.*, 2011). This may indicate that the proliferation is higher within the aortic tissue from the mice receiving control protein compared with the mice receiving rAngpt2. Nevertheless, p65 on its own was down-regulated in the rAngpt2 group, which is consistent with the reduced expression of MCP-1, downstream protein transcribed by activated NF-κB.

In summary, this study suggests that rAngpt2 administration limited AAA and atherosclerosis associated with Tie2 activation, reduced MVD, and inflammatory cell accumulation within the aortic wall in the AngII-infusion AAA mouse model in ApoE$^{-/-}$. These results suggest that exogenous Angpt2 activates Tie2 to maintain the endothelium integrity and subsequently exert potent anti-inflammatory effect in the aorta, which attenuates both AngII-induced angiogenesis and inflammation within the aortic wall, thereby limiting the AAA development and atherosclerosis progression. The inflammatory chemokine MCP-1, via its receptor CCR2, controls inflammatory monocyte (Ly6Chi) egress from the BM into the peripheral blood. It is subsequently recruited to inflammatory sites, where they differentiate into activated macrophages (Tieu *et al.*, 2009). The author found fewer inflammatory monocytes accumulated in the aortic tissue and lower MCP-1 expression, both in the aortic tissue and plasma. In the next chapter, the distribution of inflammatory monocytes in peripheral blood, BM and spleen will be assessed.

CHAPTER 7

Effects of rAngpt2 Administration on the Proportion of Myeloid Cells, Monocytes, and Neutrophils within the Peripheral Blood, Bone Marrow, and Spleen in the AngII-infused ApoE$^{-/-}$ Mice

7.1 Introduction

Inflammation is an important feature in both human and experimental atherosclerosis and AAA (Shimizu *et al.*, 2006; Manning *et al.*, 2002). The accumulated inflammatory cells within the aortic wall produce proteolytic enzymes and inflammatory cytokines which facilitate ECM degradation, inflammatory cell activation, and angiogenesis (Longo *et al.*, 2002; Dale *et al.*, 2015; Samadzadeh *et al.*, 2014). In pathological conditions or aortic injury, the leukocyte's proportion and ability of adhesion and transmigration will increase within the peripheral blood, which results in inflammatory cell accumulation within the aortic wall for immune response (Eliason *et al.*, 2005; Rizas *et al.*, 2009). In AAA patients, circulating monocytes were found to have a high ability of transmigration compared with health controls (Samadzadeh *et al.*, 2014). In the animal studies, AngII induced atherosclerosis and AAA development was accompanied with an elevated monocyte and neutrophil proportion within the peripheral blood of ApoE$^{-/-}$ mice (Nahrendorf *et al.*, 2011; Swirski *et al.*, 2007; Tsubakimoto *et al.*, 2009). Ablation of inflammatory monocytes and depletion of neutrophils in the peripheral blood attenuated AAA formation (Owens *et al.*, 2011; Eliason *et al.*, 2005). Also, in mice with MCP-1 deficiency (Gu *et al.*, 1998) atherosclerosis was reduced due to the lack of inflammatory cell recruitment to the lesion.

MCP-1 regulates monocytes egressing from the BM and transmigrating into aortic tissue via CCR2 (Jia *et al.*, 2008). CCR2 antigen is present in the subset of monocytes expressing Ly6C, named inflammatory monocytes, whereas it is lacking in the subset of monocytes negatively

expressing Ly6C, named resident monocytes (Galkina & Ley, 2009; Freestone *et al.*, 1995). Inflammatory monocytes egress from BM to peripheral blood and enter peripheral tissue in dependence of MCP-1-CCR2 axis (Crane *et al.*, 2009; Jia *et al.*, 2008). Circulating inflammatory monocytes are diminished in CCR2 deficient mice (Jia *et al.*, 2008; Crane *et al.*, 2009). The spleen is a reservoir of inflammatory monocytes that can be rapidly deployed in response to inflammatory stimuli or injury (Swirski *et al.*, 2009). In the experimental atherosclerosis, inflammatory monocytes preferentially migrate into the aortic wall and predominantly differentiate into macrophages (Jia *et al.*, 2008; Swirski *et al.*, 2007). Both atherosclerosis and AAA development were suppressed in the CCR2-/- mice (Ishibashi *et al.*, 2004a; Daugherty *et al.*, 2010; Boring *et al.*, 1998).

AngII has been found to regulate BM progenitor cells' differentiation towards monocytes and neutrophils and mobilise splenic monocytes, thereby promoting AAA development (Manning *et al.*, 2002; Mellak *et al.*, 2015; Tsubakimoto *et al.*, 2009). In Chapter 5 and Chapter 6, it was demonstrated that rAngpt2 administration attenuated atherosclerosis and AAA development in the AngII-infused ApoE^{-/-} mice. The expression of MCP-1 was found to be significantly lower in both the suprarenal aortic tissue and plasma, which is consistent with the finding that monocyte/macrophage accumulation in the aortic tissue was significantly less in the mice receiving rAngpt2 compared with the mice receiving control protein. Taking all of these findings into consideration, together with the important roles of neutrophils and monocytes in the atherosclerosis and AAA development, it was hypothesised that rAngpt2 administration must influence the proportion of leukocytes, especially inflammatory monocytes, within the peripheral blood, BM, and spleen, thereby reducing inflammatory cell accumulation within the aortic wall. The aim of this chapter is to assess the proportions of myeloid cells, monocytes, and neutriohils within the peripheral blood, BM, and spleen in AngII-infused ApoE^{-/-} mice receiving rAngpt2 or the human Fc (control) protein in the early stage (5 days) and the late stage (14 days) of atherosclerosis and AAA development.

7.2   Materials and methods

7.2.1   Experimental design

This research was designed to study the effects of rAngpt2 administration on the alteration of the proportion of myeloid cells, monocytes, and neutrophils compared with the mice receiving control protein in AngII-infused ApoE$^{-/-}$ mice. The experimental design was previously described in Chapter 5, Section 5.2.4. Mice were infused with AngII and were administered rAngpt2 or control protein for 14 days (n=10 per group) or 5 days (n=6 per group). Mice that died before the completion of the experiment in the control group (n=3) were excluded from the analysis in the 14 day experiment.

7.2.2   Collection of peripheral blood, bone marrow cells, and splenic cells

Peripheral blood samples were collected into lithium heparin coated tubes as described previously (Chapter 3, Section 3.3.1), by tail-bleeding (baseline) before the start of the experiment, and via cardiac puncture at the end of the experiment (day 14 or 5). BMCs were collected from the left femur by inserting a 0.25 gauge needle into the left femur and injecting 500μl of DPBS containing 0.2% BSA and 1 mM EDTA (Chapter 3, Section 3.3.4). In order to collect splenic cells, spleens were homogenised in DPBS containing 0.2% BSA and 1 mM EDTA. They were then filtered through 60 micron nylon filters (Chapter 3, Section 3.3.5). BMCs and splenic cells were counted using a Scepter as described previously (Chapter 3, Section 3.6.3). Typically 35 μl of peripheral blood, 10^6 BMCs, and splenic cells were used for cell surface staining for flow cytometry.

7.2.3   Antibodies for cell surface antigen staining

The following antibodies were used for cell surface staining for flow cytometry: APC-rat anti-mouse CD11b (M1/70) (Cat# 553312), PE-rat anti-mouse Ly6G (Cat#551461), PerCP-Cy5.5 rat anti-mouse Ly6G (IA8) (Cat# 560602), FITC rat anti-mouse Ly6C (AL-21) (Cat# 553104),

PE rat anti-mouse CCR2 (clone#475301) (Cat# FAB5538P), and Fcγ III/II Receptor CD16/32 (2.4G2) (Cat# 553142). All of the antibodies were purchased from BD biosciences.

7.2.4 Cell staining for flow cytometry analysis

Single-cell suspensions of peripheral blood, BMCs, and splenic cells were prepared as described previously (Chapter 3, Section 3.6.2). The samples were stained for flow cytometry as described previously (Chapter 3, Section 3.6.4). Briefly, the samples were pre-incubated for 20 min with anti-CD16/32, in order to prevent non-specific binding. For cell phonotype analysis, a mixture of APC-CD11b (0.5 µl per 100 µl for peripheral blood and 1 µl per 100 µl for BMCs and splenic cells), PE-Ly6G (1 µl per 100 µl), and FITC-Ly6C (1 µl per 100 µl) was used to stain peripheral blood, BMCs, and splenic cells from mice with 14 days AngII infusion. A mixture of APC-CD11b (0.5 µl per µl for peripheral blood and 1 µl per 100 µl for BMCs and splenic cells), PerCP Cy5.5-Ly6G (1 µl per 100 µl), and FITC-Ly6C (1 µl per 100 µl) was used to stain peripheral blood, BMCc, and splenic cells from the mice with 5 days AngII infusion. A mixture of APC-CD11b (0.5 µl per µl), Percp Cy5.5-Ly6G (1 µl per 100 µl), FITC-Ly6C (1 µl per 100 µl), and PE-CCR2 (1 µl per 100 µl) was used to stain peripheral blood, BMCs, and splenic cells for CCR2 expressing analysis.

7.2.5 Flow cytometry data acquisition and analysis

BD FACSCalibur flow cytometer was used to assess the proportion of myeloid cells, monocytes, and neutrophils within the peripheral blood, BM, and spleen in AngII-infused mice receiving rAngpt2 or the control protein for 14 days. Due to the upgrade of the laboratory, Cyan ADP was used to assess the rest of the samples for the CCR2 expression analysis and the proportion of myeloid cells, monocytes, and neutrophils within the peripheral blood, BM, and spleen. The flow cytometry instrument and compensation settings have been previously described (Chapter 3, Section 3.7.2). Viable cells were gated based on the FSC and SSC, and 10,000 viable cells were collected per sample.

Summit software (v4.3) was used to analyse the acquired FACS data as described previously in Chapter 3, Section 3.7.3. The gating strategies for cell phenotype analysis were as follows. FSC (lin) *versus* SSC (lin) were plotted to discriminate between viable cells and dead cells or debris. These viable cells were further gated to identify different populations based on the surface marker expression. Myeloid cells were CD11b+ (CD11b log *versus* SSC lin). Neutrophils were CD11b+Ly6G+ and monocytes were CD11b+Ly6G- (CD11b log *versus* Ly6G log). Inflammatory monocytes were CD11b+Ly6C^{hi}, and resident monocytes were CD11b+Ly6C- (CD11b log *versus* Ly6C log). CCR2 expression in each population was further analysed by CD11b+ log *versus* CCR2 log. FMO controls were used to determine positive and negative boundaries, as previously described in Chapter 4, Section 4.6. Data were expressed as the proportion to total leukocytes within the peripheral blood, the proportion to total BMCs within the BM, and the proportion to total splenic cells in spleen.

7.2.6   Statistical analysis

The D'Agostino Pearson test was used to test the distribution of all data. Normally distributed continuous data were expressed as mean ± SEM. Data were compared between baseline and endpoint within the group, and the endpoints between the control and rAngpt2 group. Student *t* test was used to perform statistical analysis using GraphPad Prism (v6, USA). A value of $p<0.05$ was considered statistically significant.

7.3 Results

7.3.1 Cell type identification and gating strategy for flow cytometry analysis

Cells from peripheral blood, BM, or spleen were co-stained with APC-CD11b, FITC-Ly6C, and PE-Ly6G. Cell types were identified according to cell surface antigen expression as detailed in **Table 7.1** (Gordon, 2005), and Flow cytometry gating strategies are showed using a peripheral blood sample (**Figure 7.1**)

Table 7.1 Surface markers and cell type identification using flow cytometry

Cell surface phenotype	Cell type identified
CD11b+	Myeloid cell
CD11b+Ly6G+	Neutrophil
CD11b+Ly6G-	Monocyte
CD11b+Ly6C^{hi}	Inflammatory monocyte
CD11b+Ly6C-	Resident monocyte
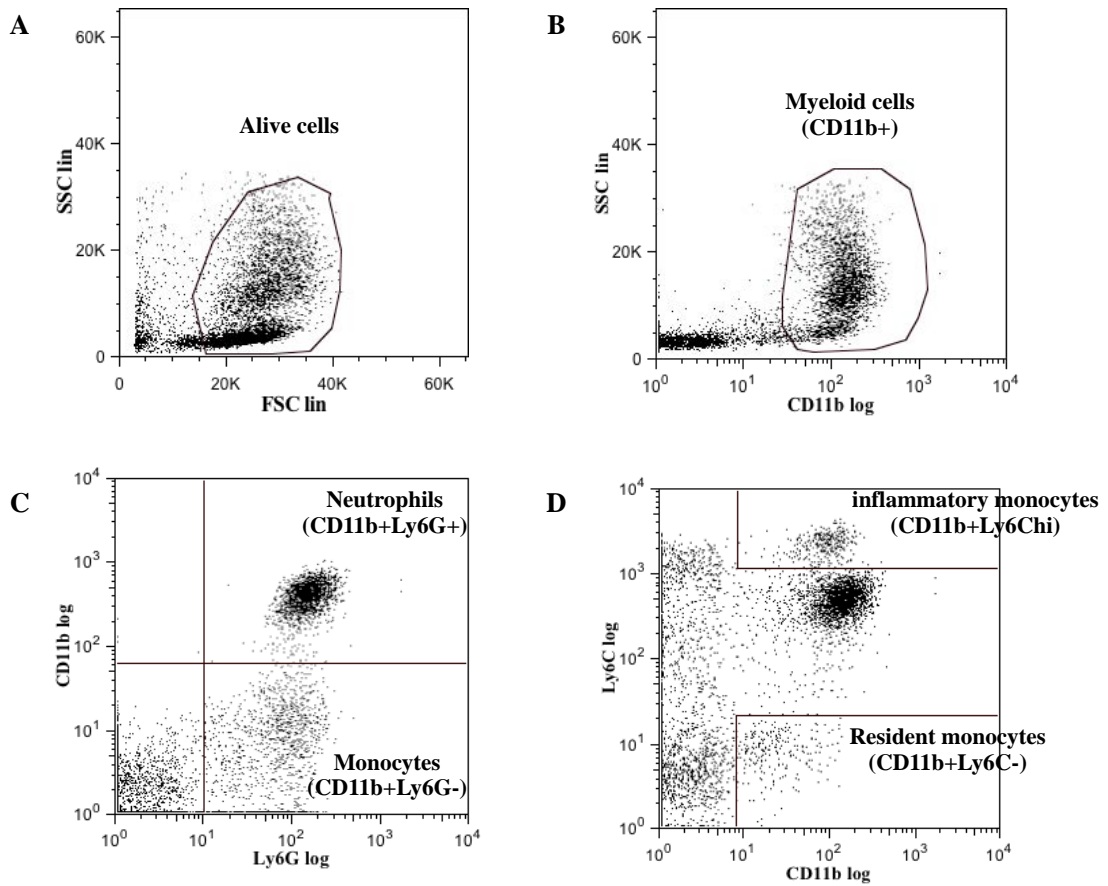
Figure 7.1 Flow cytometry analysis of the three-colour stained peripheral blood.
A) viable cells were discriminated with debris and dead cells by FSC lin *versus* SSC lin; **B**) myeloid cells
(CD11b+) were discriminated with lymphocytes (CD11b-) by CD11b log *versus* SSC lin ; **C**) neutrophils
(CD11b+Ly6G+) were discriminated with monocytes (CD11b+Ly6G-) by Ly6G log *versus* CD11b log;
and **D**) inflammatory monocytes (CD11b+Ly6C^{hi}) were discriminated with resident monocytes
(CD11b+Ly6C-) by CD11b log *versus* Ly6C log (neutrophils were CD11b+Ly6C[med]).

7.3.2   Inflammatory monocytes also express CCR2 antigen

The chemokine receptor CCR2 plays vital roles in the pathogenesis of inflammatory disorders (Kaikita *et al.*, 2004). Analysis the expression of CCR2 antigen in different populations showed that the inflammatory monocytes, not the resident monocytes, express CCR2 antigen within the peripheral blood, BM, and spleen (**Figure 7.2**). Therefore, inflammatory monocytes are defined as CD11b+Ly6C^{hi}CCR2+, and resident monocytes as CD11b+Ly6C-CCR2-. In this thesis, inflammatory monocytes are referred as CD11b+Ly6C^{hi} and resident monocytes as CD11b+Ly6C-.
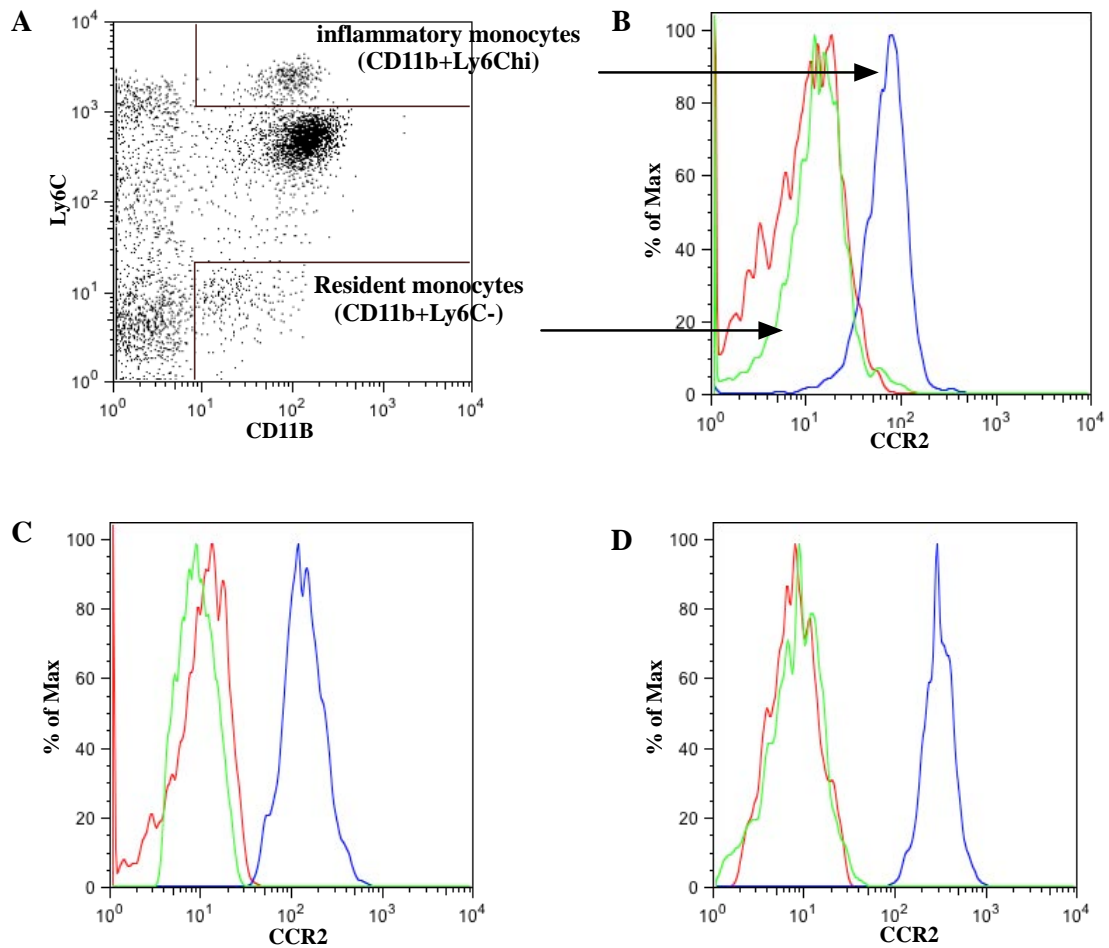
Figure 7.2 Expression of CCR2 antigen in monocyte subsets.
A) inflammatory monocytes (CD11b+Ly6C^{hi}) and resident monocytes (CD11b+Ly6C-) were gated by CD11b log *versus* Ly6C log; Histogram overlay of these two monocytes subset and FMO control staining from **B**) peripheral blood, **C**) BM, and **D**) spleen. The blue line represents inflammatory monocytes, the green line represents resident monocytes, and the red line represents FMO control staining.

7.3.3 Effects of rAngpt2 administration on the proportion of myeloid cells, neutrophils, and monocytes within the peripheral blood after 14 days AngII infusion

The proportion of myeloid cells, neutrophils, and monocytes to total leukocytes within the peripheral blood was assessed in the AngII-infused ApoE$^{-/-}$ mice receiving either rAngpt2 (n=10) or control protein (n=7) for 14 days (**Figure 7.3**). The proportion of CD11b+ myeloid cells was significantly increased in both the rAngpt2 group (62.09% ± 4.17, $p<0.0001$) and the control group (66.89% ± 4.71, $p<0.0001$), compared with the baseline (**Figure 7.4** A). A further analysis of myeloid cell subpopulations consistently found that the proportion of CD11b+Ly6G+ neutrophils and CD11b+Ly6G- monocytes was 3 times and 2 times higher respectively, compared with the baseline in both groups (**Figure 7.4** B and C). However, rAngpt2 administration did not alter the significantly elevated proportions of myeloid cells, neutrophils, and monocytes proportions induced by AngII infusion at day 14.
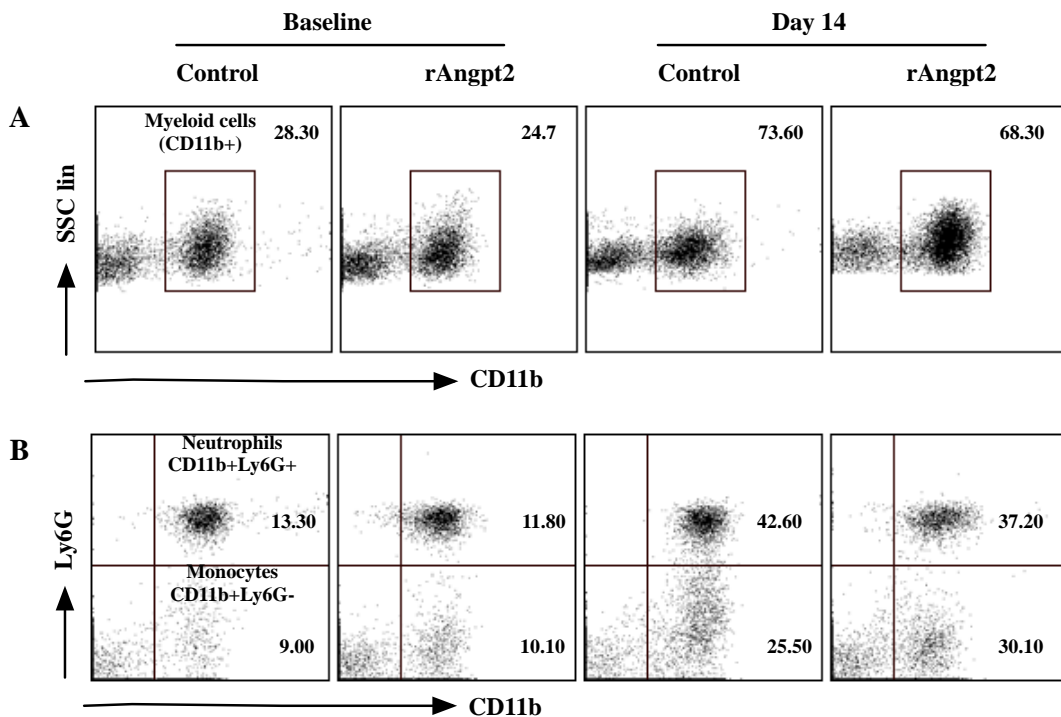
Figure 7.3 Flow cytometry analysis the proportion of myeloid cells, neutrophils, and monocytes to total leukocytes within the peripheral blood from AngII infused ApoE$^{-/-}$ mice receiving either rAngpt2 or control protein for 14 days.
A) an example of dot plot showing Myeloid cells (CD11b+), and **B**) neutrophils (CD11b+Ly6G+) and monocytes (CD11b+Ly6G-) from the mice receiving either rAngpt2 or control protein at baseline and day 14 (the number is the proportion to total leukocytes).
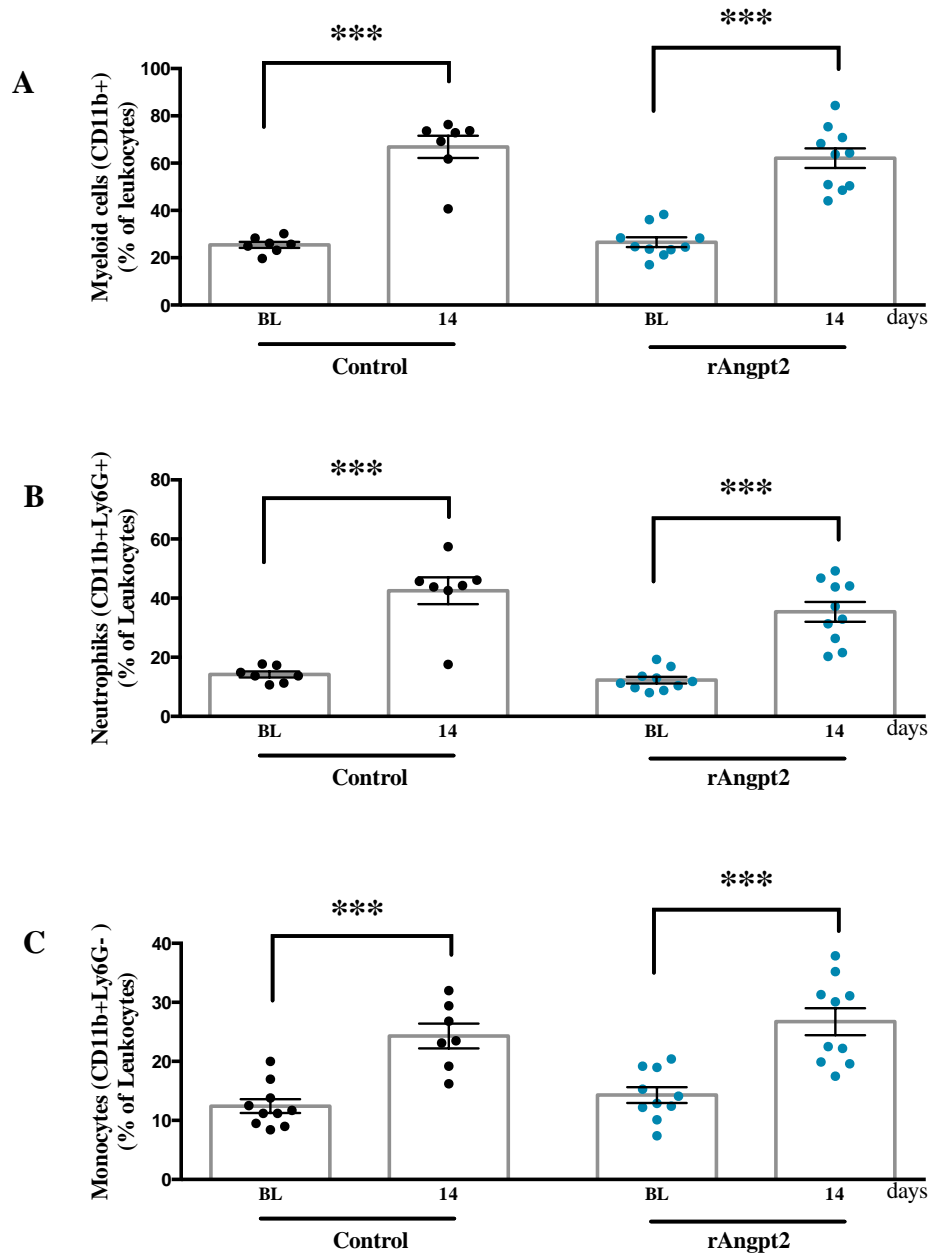
Figure 7.4 rAngpt2 administration did not alter the significantly elevated proportion of myeloid cells, neutrophils, and monocytes to total leukocytes within the peripheral blood induced by AngII infusion for 14 days.

A) the proportion of myeloid cells to total leukocytes; **B**) the proportion of neutrophils to total leukocytes; and **C**) the proportion of monocytes to total leukocytes; Data were expressed as mean ± SEM and analysed with student *t* test. ***$p< 0.0001$ *versus* baseline (BL); n=7 in control group and n=10 in rAngpt2 group; each dot represents data from an individual mouse.

7.3.4 Effects of rAngpt2 administration on the proportion of monocyte subsets within the peripheral blood after 14 days AngII infusion

There are two different monocyte subsets with differential surface expression of Ly6C: inflammatory monocytes (CD11b+Ly6C^{hi}) and resident monocytes (CD11b+Ly6C-) (**Figure 7.5** A). AngII infusion induced a significant increase of the proportion of inflammatory monocytes to total leukocytes in both the rAngpt2 group (Day 14 9.94% ± 1.26 *versus* Baseline 4.97% ± 0.37, $p<0.0001$) and the control group (Day 14 14.49% ± 1.45 *versus* Baseline 4.36% ± 0.45, $p=0.0004$, **Figure 7.5** B) at day 14, compared with their baseline. However, the mice receiving rAngpt2 had a significantly lower proportion of inflammatory monocytes ($p=0.003$) compared with the mice receiving control protein at day 14 (**Figure 7.5** B). The proportion of resident monocytes to total leukocytes was not significantly different before and after AngII infusion in both groups (**Figure 7.5** C). These results suggest that the increase of CD11b+Ly6C^{hi} inflammatory monocytes proportion was responsible for the elevated monocyte proportion induced by AngII infusion. Also, they suggest that rAngpt2 administration plays a role in regulating the proportion of inflammatory monocytes within the peripheral blood.
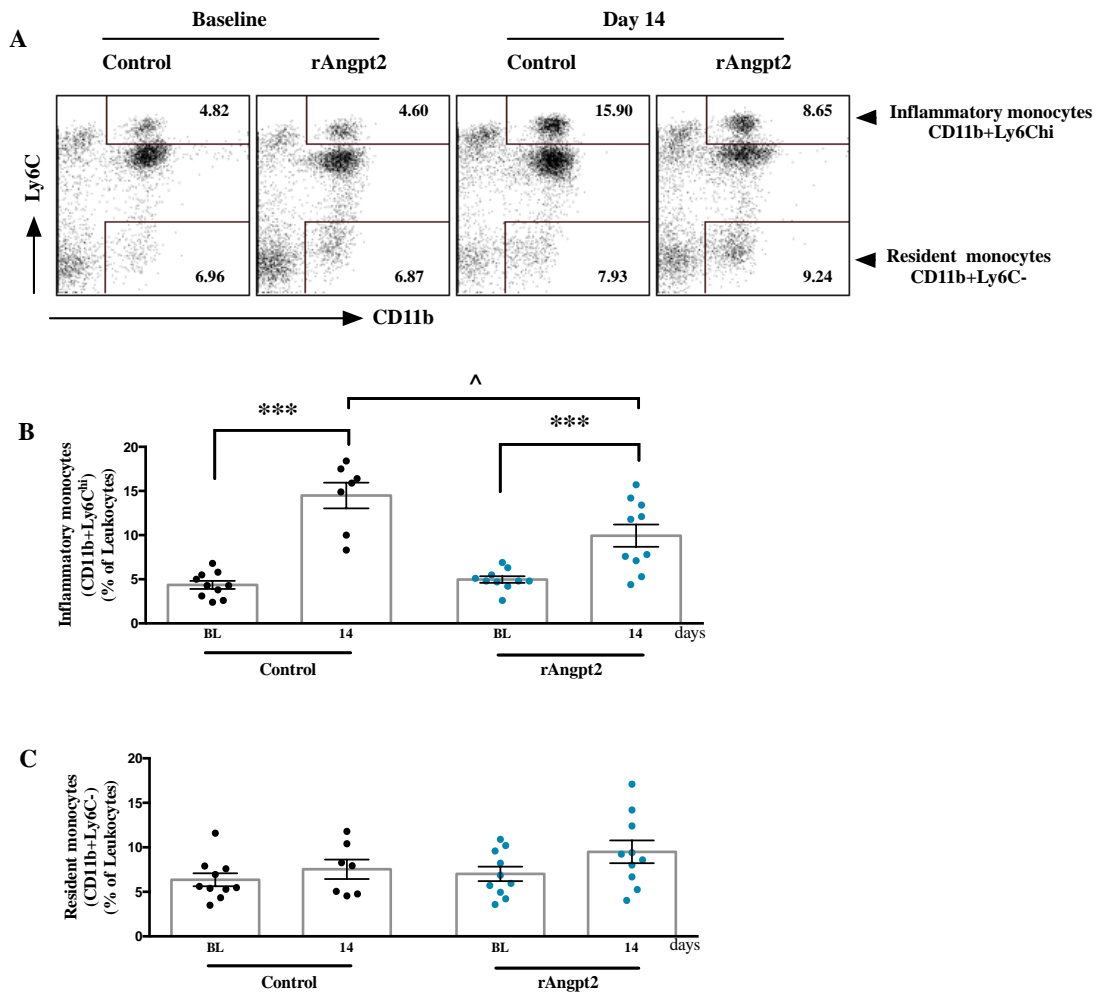
Figure 7.5 Mice receiving rAngpt2 had a significantly lower proportion of inflammatory monocytes to total leukocytes compared with the mice receiving control protein within the peripheral blood after AngII infusion for 14 days.

A) an example of dot plot showing inflammatory monocytes (CD11b+Ly6C^{hi}) and resident monocytes (CD11b+Ly6C-) from the mice receiving control protein or rAngpt2 at baseline and day 14 (number is the proportion to total leukocytes); **B**) the proportion of inflammatory monocytes to total leukocytes; and **C**) the proportion of resident monocytes to total leukocytes. Data were expressed as mean ± SEM and analysed with Student *t* test. ***$p < 0.0005$ *versus* BL and ^ $p < 0.005$ control *versus* rAngpt2; n=7 in control group and n=10 in rAngpt2 group; each dot represents data from an individual mouse.

142

7.3.5 **Effects of rAngpt2 administration on the proportion of myeloid cells, neutrophils, and monocytes within the bone marrow after 14 days AngII infusion**

CD11b+Ly6C^{hi} inflammatory monocytes differentiate within the BM and egress to peripheral blood, and enter injured or infected sites, depending on the chemokine MCP-1-CCR2 axis (Shi, 2011). The proportion of myeloid cells, neutrophils, and monocytes to total BMCs within the BM from mice that survived to the end of the experiment at day 14 were assessed (n=7 and n=10 in the control and rAngpt2 group respectively, **Figure 7.6** A). rAngpt2 administration did not change the proportions of myeloid cells (p=0.651, **Figure 7.6** B), neutrophils (p=0.617 **Figure 7.6** C), or monocytes (p=0.643, **Figure 7.6** D), compared with the mice receiving control protein. However, a further analysis of the monocyte subsets revealed that there was a significantly higher proportion of CD11b+Ly6C^{hi} inflammatory monocytes within the BM from the mice receiving rAngpt2 (8.85% ± 0.54, p=0.019), compared with the mice receiving control protein (7.09% ± 0.36, n=7, **Figure 7.6** E). There was no statistically significant difference in the proportions of CD11b+Ly6C- resident monocytes within the BM between the two groups (p=0.852, **Figure 7.6** F).
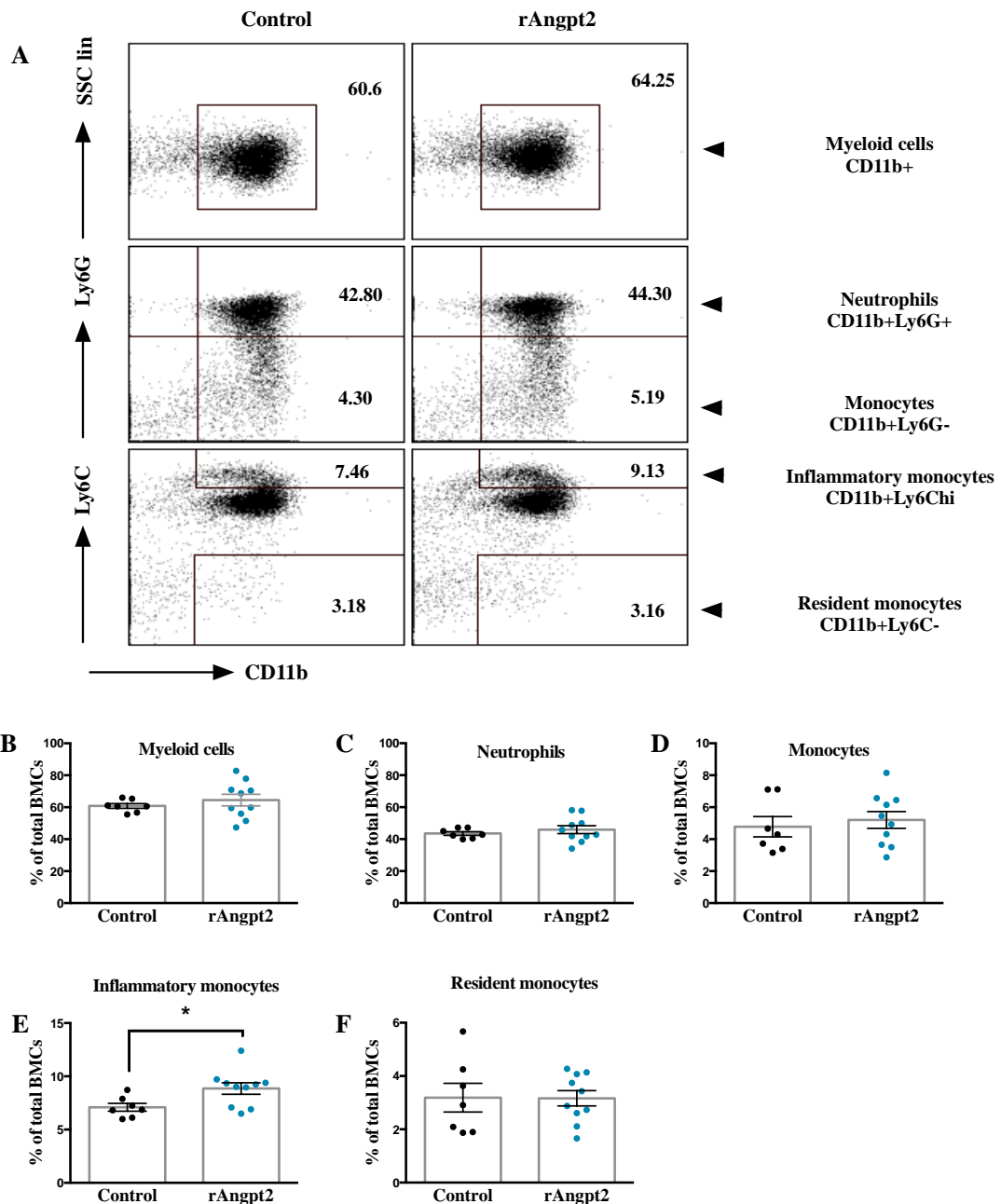
Figure 7.6 Mice receiving rAngpt2 had significantly higher proportion of inflammatory monocytes to total BMCs compared with the mice receiving control protein.
A) an example of dot plot showing myeloid cells, neutrophils, monocytes, inflammatory monocytes and resident monocytes within the BM (number is the proportion to total BMCs); and the proportion of **B**) myeloid cells; **C**) neutrophils ; **D**) monocytes; **E**) inflammatory monocytes; and **F**) resident monocytes to total BMCs. Data were expressed as mean ± SEM and analysed with Student *t* test; *$p< 0.05$; n=7 in control group and n=10 in rAngpt2 group; each dot represents data in an individual mouse.

7.3.6   Effects of rAngpt2 administration on proportion of myeloid cells, neutrophils, and monocytes within the spleen after 14 days AngII infusion

The spleen is CD11b+Ly6C^{hi} inflammatory cell reservoir, where they are rapidly mobilised to the peripheral blood in response to stimulation or injury (Swirski *et al.*, 2009). The proportion of myeloid cells, neutrophils, and monocytes to total splenic cells from mice that survived to the end of the experiment at day 14 were assessed (n=7 and n=10 in the control and rAngpt2 group respectively, **Figure 7.7** A). rAngpt2 administration did not change the proportion of myeloid cells (p=0.281, **Figure 7.7** B), neutrophils (p=0.403, **Figure 7.7** C), or monocytes (p=0.711, **Figure 7.7** D), compared with the mice receiving control protein. A further analysis of the monocyte subsets showed that there was no statistically significantly difference in the proportion of CD11b+Ly6C^{hi} inflammatory monocytes (p=0.516, **Figure 7.7** E) and CD11b+ Ly6C- resident monocytes (p=0.582, **Figure 7.7** F), compared with the mice receiving control protein.
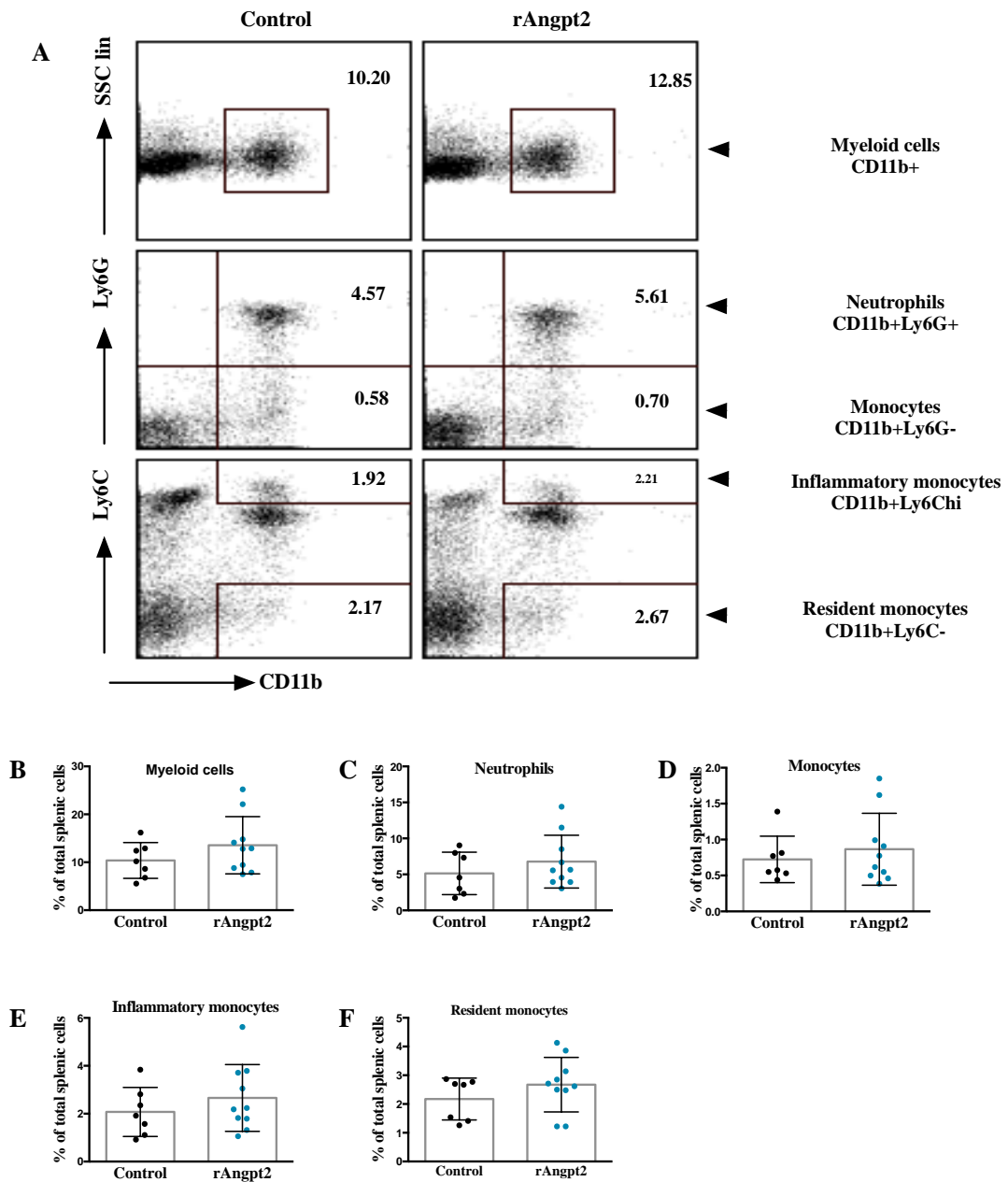
Figure 7.7 Mice receiving rAngpt2 did not alter the proportion of myeloid cells, neutrophils and monocytes to total splenic cells in spleen compared with the mice receiving control protein.
A) an example of dot plot showing myeloid cells, neutrophils, monocytes, inflammatory monocytes and resident monocytes in spleen (number is the proportion to total splenic cells); and the proportion of **B**) myeloid cells; **C**) neutrophils ; **D**) monocytes; **E**) inflammatory monocytes; and **F**) resident monocytes to total splenic cells. Data were expressed as mean ± SEM and analysed with Student t test. *$p < 0.05$; n=7 in control group and n=10 in rAngpt2 group; each dot represents data in an individual mouse

7.3.7   Effects of rAngpt2 administration on the proportions of myeloid cells, neutrophils, and monocytes within the peripheral blood, BM, and spleen after AngII infusion for 5 days

It has been reported that the transient increase of CD11b+Ly6C^{hi} inflammatory monocytes peaked at 3 to 7 days within the peripheral blood after AngII infusion in the experimental AAA models (Mellak *et al.*, 2015; Ishibashi *et al.*, 2004b). Therefore, the effects of rAngpt2 administration on the proportion of myeloid cells, neutrophils, and monocytes within the peripheral blood, BM, and spleen was assessed at an early time point, day 5, a critical time point when AAA started rupture, as was shown in Chapter 5. The results showed that rAngpt2 administration did not change the proportion of these cells within the peripheral blood and BM, although there was a trend of towards a lower proportion of CD11b+Ly6C^{hi} inflammatory monocytes compared with the mice receiving control protein (**Figure 7.8** A, B, C, and D). Interestingly, the mice receiving rAngpt2 have a significantly higher proportion of myeloid cells (*p*=0.005) in the spleen, compared with the mice receiving control protein. A further analysis revealed that a higher proportion of neutrophils (*p*=0.028), not monocytes, was responsible for the elevated proportion of myeloid cells within the spleen (**Figure 7.8** E). Further analysis of the monocyte subsets showed that there was a statistically significant higher proportion of CD11b+Ly6C^{hi} inflammatory monocytes in the spleen from the mice receiving rAngpt2 (3.41% ± 0.54, *p*=0.042), compared with the mice receiving control protein (2.27% ± 0.36, **Figure 7.8** E). There was no statistical significant in the proportion of resident monocytes (*p*=0.168, **Figure 7.8** F).
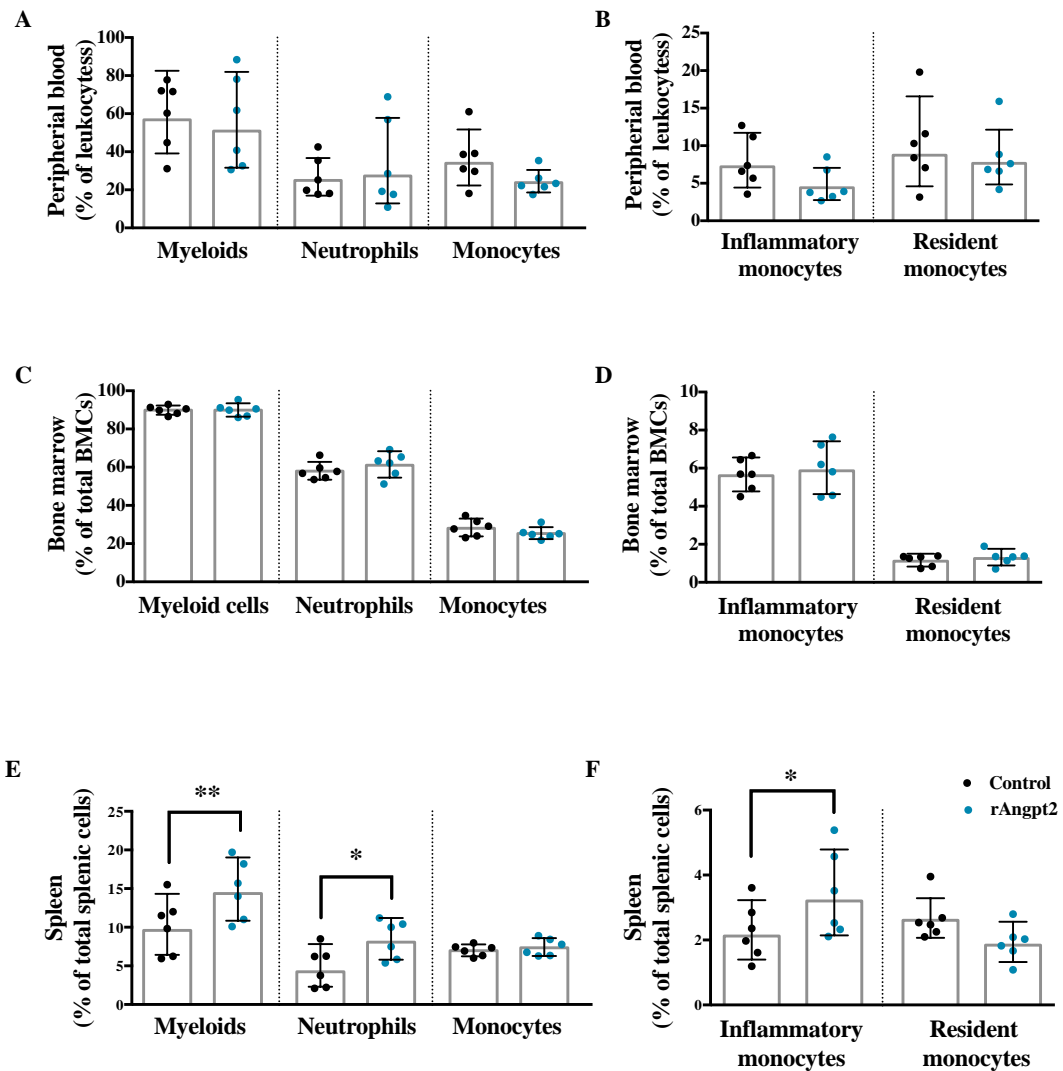
Figure 7.8 Effects of rAngpt2 administration on the proportion of myeloid cells, neutrophils, and monocytes within the peripheral blood, BM, and spleen after AngII infusion for 5 days.
A) the proportion of myeloid, neutrophils and monocytes and **B**) the proportion of inflammatory and resident monocytes to total leukocytes within the peripheral blood; **C**) the proportion of myeloid, neutrophils, and monocytes and **D**) the proportion of inflammatory and resident monocytes to total BMCs within the BM; **E**) the proportion of myeloid, neutrophils, and monocytes and **F**) the proportion of inflammatory and resident monocytes to total splenic cells in the spleen. Data expressed as mean ± SEM and analysed with Student t test (n=6 per group); *$p<0.05$ *versus* control and **$p<0.005$ *versus* control; each dot represents data in an individual mouse.

7.4 Discussion

In this study, the effects of rAngpt2 administration on the proportion of myeloid cells, neutrophils, and monocytes within the peripheral blood, BM, and spleen were investigated in the AngII-infused ApoE$^{-/-}$ mice for 5 and 14 days. In the 14 day AngII infusion, the significant finding was that, after 14 days AngII infusion, the mice receiving rAngpt2 had a significantly lower and conversely higher proportion of CD11b+Ly6C^{hi} inflammatory monocytes within the peripheral blood and the BM respectively, compared with the mice receiving control protein. In the 5 day AngII infusion, the mice receiving rAngpt2 had a significantly higher proportion of neutrophils and CD11b+Ly6C^{hi} inflammatory monocytes in their spleens, compared with the mice receiving control protein.

The CCR2-MCP-1 axis has an important role in AAA and atherosclerosis development in rodent models (Jia *et al.*, 2008; Weber *et al.*, 2008; Serbina & Pamer, 2006; Moehle *et al.*, 2011). The MCP-1-CCR2 axis controls the release of inflammatory monocytes from the BM to peripheral blood and their entry into the aortic tissue, where they then differentiate into activated macrophages (Tieu *et al.*, 2009). In the mice receiving rAngpt2, the reduction of plasma MCP-1 resulted in the retention of inflammatory monocytes within the BM. The number of infiltrated cells within the aortic wall also determines the proportion of inflammatory monocytes within the peripheral blood. However, it is unlikely that the difference in the proportion of inflammatory monocytes within the peripheral blood was caused by the different infiltrations. It has been previously demonstrated that both MCP-1 expression and monocyte/macrophage accumulation within the aortic tissue were reduced in the mice receiving rAngpt2, which suggests a low rate of infiltration in the mice receiving rAngpt2. Together, these results suggest that rAngpt2 administration may inhibit the inflammation within the aortic wall, which resulted in plasma MCP-1 reduction. This inhibition thus limits the inflammatory monocytes entering peripheral blood from BM to transmigrate to aortic wall resulting in exaggerated inflammatory response.

The spleen is a reservoir of inflammatory monocytes that can be rapidly mobilised to peripheral blood in response to injury and inflammation (Swirski *et al.*, 2009), and a place where neutrophils are cleared to maintain homeostatic levels of neutrophils in peripheral blood (Furze & Rankin, 2008). AngII expelled inflammatory monocytes from the spleen into peripheral blood, which would transiently increase numbers of inflammatory monocytes available for early infiltration. This peaked at 3 days in the AngII-infused mouse models (Mellak *et al.*, 2015). In this study, the mice receiving rAngpt2 had a higher proportion of inflammatory monocytes and a higher proportion of neutrophils in the spleen at the early stage of AngII infusion. These results suggest that rAngpt2 may protect the aorta from AAA development and rupture by inhibiting the mobilisation of inflammatory monocytes in the spleen. Also, the results suggest that rAngpt2 promotes neutrophils back to spleen for clearance at the early stage. Consequently, inflammatory monocytes and neutrophils were reduced for infiltration in the peripheral blood, thereby attenuating the atherosclerosis and AAA formation. However, the mechanisms underlying this need further investigation.

The fact that infiltrated cells within the aorta were not assessed is a limitation of this study. The rates of infiltration will also influence the proportion of neutrophils and monocytes within the peripheral blood. In the 5 day AngII infusion, there was a higher proportion of inflammatory monocytes and neutrophils in the spleen; however, there was no difference in the proportion of these cells within the peripheral blood and BM. This could be caused by the different rate of infiltration. In Chapter 6, it was found that rAngpt2 induced Tie2 phosphorylation, indicating the anti-inflammatory effects of the endothelium, and thereby reducing the inflammatory cells' infiltration induced by AngII infusion. Therefore, the insignificant difference of neutrophils and inflammatory monocytes within the peripheral blood and BM may suggest a reduced rate of infiltration in the mice receiving rAngpt2, which is consistent with the findings documented in Chapter 5 that rAngpt2 administration inhibits AAA development and rupture in the early and late stage of AngII infusion. However, this needs to be confirmed by future investigations.

In Summary, rAngpt2 administration induced the retention of inflammatory monocytes in the spleen, and promoted neutrophils back to spleen for clearance at the early stage of AngII infusion. Also, rAngpt2 administration limited the entry of inflammatory monocytes into peripheral blood from BM to transmigrate to aortic wall in a MCP-1 CCR2 axis dependence at the later stage of AngII infusion. These results are consistent with previous findings that rAngpt2 administration prevented AAA from rupture as early as 5 days and reduced plasma MCP-1 expression and inflammatory cell accumulation within the aortic wall after 14 days AngII infusion.

CHAPTER 8

General Discussion

AAA is an abnormal dilatation of the aorta and affects around 2-5% of men older than 65. Most AAAs are asymptotic until rupture, a severe consequence of AAA with high mortality; therefore the main goal of AAA management is to prevent a fatal rupture. Surgical repair is the only treatment for ruptured AAAs, and an elective surgical repair is suggested for patients with an aortic diameter larger than 50 mm, in whom the risk of rupture is high. However, this selection standard for surgical repair is debatable, as ruptures of small AAAs are not rare and large AAAs may not necessarily rupture during the life of the patient. Therefore, it is pivotal to develop new clinical treatments targeting the mechanisms of AAA expansion and rupture, and to find reliable biomarkers associated with AAA rupture (Fillinger *et al.*, 2003). The mechanisms and biomarkers related to AAA progression and rupture have been intensively studied in human end-stage AAAs and experimental rodent models in the past two decades; however, efficient clinical interventions to limit AAA progression and rupture are still lacking. Recently, Golledge and colleagues reported that serum Angpt2 is elevated in men with AAA, and is associated with an increased risk of cardiovascular mortality in older men (Golledge *et al.*, 2012). This finding points to Angpt2 as a potential target and/or biomarker for AAA progression. Angpt2 is a member of the Angpt family involved in regulating angiogenesis and inflammation, two important pathological features of both human and experimental AAAs. This thesis focused on the role of Angpt2 in AAA development, using an AngII-infused AAA mouse model in ApoE$^{-/-}$ mice.

Angpts regulate vascular homeostasis, angiogenesis, and inflammation via activation and deactivation of its receptor, Tie2 (Augustin *et al.*, 2009; Peters *et al.*, 2004). Tie2 is activated to maintain the anti-inflammation, anti-permeability, and quiescent state of the vasculature (Fiedler & Augustin, 2006), whereas Tie2 is deactivated in the process of angiogenesis and

inflammation (Fiedler *et al.*, 2006; Murakami, 2012; Scharpfenecker *et al.*, 2005). Angpt2 plays a complex role, dynamically regulating Tie2 in a context-dependent manner (Thurston & Daly, 2012; Yuan *et al.*, 2009). Angpt2 is mainly expressed by ECs and stored in intracellular granules, where it may be rapidly released in an autocrine manner to deactivate Tie2 in response to inflammatory and angiogenic stimuli (Thurston & Daly, 2012; Maisonpierre *et al.*, 1997). In contrast, exogenously administered Angpt2 has been demonstrated to activate Tie2 both *in vivo* and *in vitro* (Cao *et al.*, 2007; Chen *et al.*, 2009; Chen *et al.*, 2011; Daly *et al.*, 2006; Yuan *et al.*, 2009; Kim *et al.*, 2000; Teichert-Kuliszewska *et al.*, 2001). Moreover, it has been reported that exogenous Angpt2 inhibits leukocyte infiltration in the presence of inflammatory stimuli (Daly *et al.*, 2006; Roviezzo *et al.*, 2005), has a role as an autocrine protective factor for stressed ECs *in vitro,* and induces Tie2 phosphorylation *in vivo* (Daly *et al.*, 2006). In clinical studies, patients with coronary artery disease have lower plasma Angpt2 compared to healthy individuals (Jaumdally *et al.*, 2011; David *et al.*, 2009). In addition, serum angpt2 is elevated in patients with Diabetes mellitus (Lip *et al.*, 2004), a patient cohort in which the prevalence of AAA and aortic expansion rate is low (Shantikumar *et al.*, 2010; Le *et al.*, 2007; Golledge *et al.*, 2008; Brady *et al.*, 2004), indicating that increased Angpt2 may be protective in response to tissue injury.

It was demonstrated in the current study that inhibition of Angpt2-Tie2 interaction did not alter AAA formation or atherosclerosis progression induced by AngII infusion in ApoE$^{-/-}$ mouse model. This suggests that endogenous Angpt2-induced Tie2 deactivation is not essential in this mouse model. Tie2 activation is maintained by Angpt1, secreted by pericytes and SMCs. AngII has been reported to have effects on pericytes and SMCs, thereby affecting Angpt1 expression and Tie2 activation (Felcht *et al.*, 2012). Moreover, Angpt2, a ligand for Tie2 receptor, can alternatively bind integrins and Tie1 for signal transduction in regulating angiogenesis (Carlson *et al.*, 2001; Yancopoulos *et al.*, 2000). Indeed, Angpt2-Tie2 targeted anti-angiogenesis has been shown to reduce tumour neo-vessel formation by only 40% (Huang *et al.*, 2011; Mazzieri *et al.*, 2011). Integrin binding of Angpt2 has been observed in invading and migrating tip ECs,

inflammation stimulated ECs, and Tie2-deficient tumour cells (Koh *et al.*, 2010; Felcht *et al.*, 2012; Imanishi *et al.*, 2007; Hu *et al.*, 2006). Thus, an action of endogenous Angpt2, independent of Angpt2-Tie2 interaction, influencing AAA and atherosclerosis progression cannot be ruled out in the AngII-infusion AAA mouse model in ApoE$^{-/-}$. Further investigation to identify the role of endogenous Angpt2 and integrin interaction, for example, in the AAA and atherosclerosis is required.

Historically, atherosclerosis has been considered a hallmark feature of AAA (Reed *et al.*, 1992; Brady *et al.*, 2004) as it presents consistently in biopsies of advanced-stage AAA (Golledge *et al.*, 2006; Reed *et al.*, 1992; Golledge & Norman, 2010). AAA and atherosclerosis share common risk factors and pathological processes; therefore, AAA intervention is usually accompanied by a positive change in atherosclerosis (Reed *et al.*, 1992; Golledge & Norman, 2010). In this research, systemic rAngpt2 administration reduced atherosclerosis in the ARCH region. This is consistent with previous reports that up-regulation of Angpt2 by systemic administration of an adenovirus vector inhibited atherosclerosis progression by 40% (Ahmed *et al.*, 2009). Angpt2 may regulate atherosclerosis progression in a timely manner, as it has been reported that Angpt2 is relatively absent from the early atherosclerotic lesion, whereas it is abundantly expressed in patients with advanced atherosclerotic lesions (Calvi, 2004). Therefore, increased Angpt2 expression at the early stage of atherosclerosis may hamper atherosclerosis progression. However, this needs to be further investigated and confirmed. Hyperlipidemia is a dependent factor, whereas hypertension is an independent factor for AAA and atherosclerosis development in the AngII-infusion mouse model (Daugherty *et al.*, 2000; Cassis *et al.*, 2009). In this study, systemic rAngpt2 administration did not alter hyperlipidaemia, lipid profiles, or BP, which suggested that the action of rAngpt2 targeted AngII created effects at the aortic wall other than hypertension and plasma lipids.

The significant finding of this study is that systemic rAngpt2 administration attenuated AAA and atherosclerosis, and limited aneurysm related aortic rupture. Lack of intramural haemorrhage within the ARCH suggested that systemic rAngpt2 administration played an

important role in maintaining the integrity of the aorta, thereby protecting the aorta from AngII-induced medial destruction and, ultimately, from rupture. Activated immune/inflammatory cells are a primary source of the proteases which are responsible for aortic matrix degradation (Shimizu *et al.*, 2006), and the up-regulation of proteolytic activity within the aorta is believed to be critical in the degeneration of medial architecture associated with advanced-stage human AAA (Koole *et al.*, 2012). Dysfunctional ECs up-regulate adhesion molecule expression and increase their permeability via NF-κB signalling pathway activation, thereby promoting inflammatory cell adhesion and extravasation within the aortic wall (Imhof & Aurrand-Lions, 2006). Tie2 activation is essential in maintaining the functions of ECs lining the intima. Exogenous Angpt2 has been reported to active Tie2 both *in vitro* and *in vivo* (Cao *et al.*, 2007; Chen *et al.*, 2009; Daly *et al.*, 2006; Kim *et al.*, 2000; Teichert-Kuliszewska *et al.*, 2001). Tie2 activation interacting with the ABIN-2 inhibits NF-κB activation and induces anti-inflammatory and anti-apoptotic effects in ECs (Tadros *et al.*, 2003; Hughes *et al.*, 2003). In the current study, the significant increase in Tie2 phosphorylation observed within the aortic wall of the mice receiving rAngpt2 was associated with markedly reduced aortic accumulation of monocytes/macrophages.

Proinflammatory cytokine MCP-1 is a chemoattractant for inflammatory cells and plays an important role in AAA and atherosclerosis development in rodent models (Jia *et al.*, 2008; Saraff, 2003). MCP-1 knockout mice have been found to resist elastase perfusion induced AAA (Moehle *et al.*, 2011). Consistent with reduced monocyte/macrophage accumulation within the aortic wall, MCP-1 expressions within both the aortic tissue and plasma were significantly less in the mice receiving rAngpt2 compared with the mice receiving control protein. These results further confirmed the limited inflammation in mice receiving rAngpt2.

Inflammatory monocytes, expressing the CCR2 antigen, preferentially migrate into the aortic wall and predominantly differentiate into macrophages (Jia *et al.*, 2008; Swirski *et al.*, 2007). Both atherosclerosis and AAA development were suppressed in the CCR2-/- mice (Ishibashi *et al.*, 2004a; Daugherty *et al.*, 2010; Boring *et al.*, 1998). Inflammatory monocytes, originating in

the BM, egress to peripheral blood and are recruited to inflammatory sites in a dependent MCP-1-CCR2 axis (Jia *et al.*, 2008; Tieu *et al.*, 2009). It was demonstrated in the current study that lower and higher proportion of inflammatory cells within the peripheral blood and BM, respectively, were present in mice receiving rAngpt2 compared to the control. This could be the consequence of the reduced plasma concentration of MCP-1. It is unlikely that the higher proportion of inflammatory monocytes within the BM is due to an increase in the differentiation rate of progenitor cells as there is no difference observed in the BM at the early stage. Thus it is suggested that rAngpt2 administration abrogated an AngII-induced up-regulation of plasma and aortic tissue MCP-1, thereby limiting the egress of BM inflammatory monocytes into the circulation and the aortic wall. Alternatively, the spleen is a reservoir of mature inflammatory monocytes that can be rapidly deployed in response to injury and inflammation (Swirski *et al.*, 2009). It has been shown that in response to AngII-infusion, inflammatory monocytes are transiently expelled from spleen, increasing the circulating numbers of these cells (Mellak *et al.*, 2015). The administration of rAngpt2 to AngII-infused ApoE$^{-/-}$ mice in the present study resulted in the retention of inflammatory monocytes within the BM accounting for the reduced overall number of these cells within the circulation.

There is evidence that AAA and atherosclerosis are associated with excessive angiogenesis in both human and animal models (Choke *et al.*, 2006; Choke *et al.*, 2010; Kaneko *et al.*, 2011; Suzuki *et al.*, 2003; Thompson *et al.*, 1996). Indeed, anti-angiogenic interventions have been shown to attenuate experimental AAA (Kaneko *et al.*, 2011; Miwa *et al.*, 2005). The extent of angiogenesis correlates with the severity of inflammatory cell infiltration in AAA biopsies and AngII-induced AAA and atherosclerosis (Holmes *et al.*, 1995; Thompson *et al.*, 1996; Daugherty *et al.*, 2000; Saraff, 2003). This may, in part, be a consequence of angiogenesis, since newly formed pathological capillaries are normally poorly organised with highly permeability (Imhof & Aurrand-Lions, 2006). Thrombus is another pathological feature that is believed to be partly the consequence of increased permeability of adventitial micro-vessels (Kaneko *et al.*, 2011; Nienaber & Sievers, 2002). Intramural thrombus is present in AngII-

induced AAAs (Barisione *et al.*, 2006; Saraff, 2003; Schriefl *et al.*, 2012) and has been implicated in promoting aortic wall inflammation and rupture (Cao *et al.*, 2010; Saraff, 2003). Angpt2-mediated deactivation of Tie2, resulting in the activation of ECs, is required to initiate angiogenesis (Munoz-Chapuli*et al.*, 2004). This effect is transient and survival angiogenic factors, such as VEGF, are then required to support ECs' survival and proliferation. Prolonged exposure of ECs to Angpt2 induces apoptosis and vessel regression in the absence of VEGF (Carmeliet, 2003; Lobov *et al.*, 2002; Maisonpierre *et al.*, 1997). It has been reported that up-regulation of Angpt2 in animal models of cancer disrupted tumour vasculature (Augustin *et al.*, 2009; Cao *et al.*, 2007; Chen *et al.*, 2011; Chen & Stinnett, 2008). In the current study, expression of the EC marker CD31 within the aortic media and adventitia was significantly lower in mice receiving rAngpt2 compared to mice receiving control protein. This indicated that angiogenesis within the aortic wall in response to AngII infusion was limited with the administration of rAngpt2. Tie2 phosphorylation activates downstream Akt/eNOS and Erk signalling (Zhang *et al.*, 2011). In examining the Akt/eNOS and Erk signalling pathways involved in angiogenesis (Namkoong *et al.*, 2009), no effect of rAngpt2 on Akt/eNOS and Erk signalling was observed; however a significantly higher density of micro-vessels within the aortic wall of control mice was observed. This discrepancy may be the result of the known pleiotropic effects of Akt/eNOS and Erk signalling on cell-cell and cell-matrix interactions (Thurston & Daly, 2012). In the current study, mice receiving rAngpt2 had reduced aortic inflammatory cell accumulation, decreased aortic CD31 expression, and limited aortic intramural hematoma formation. Together, these results support an action of rAngpt2 to inhibit experimental AAA and atherosclerosis associated with the limiting of new vessel formation within the aortic wall.

The proposed mechanism/s by which Angpt2 acted to limit AAA and atherosclerosis in the AngII-infusion ApoE$^{-/-}$ mouse model is summarised in **Figure 8.1**. In the promotion of AAA and atherosclerosis, activation of intimal EC in response to the infusion of AngII facilitates leukocyte attraction, adhesion, and extravasation at the vessel wall. Infiltrated cells release

cytokines, chemokines, and proteolytic enzymes that promote inflammatory remodelling of the aortic wall. Pro-angiogenic factors stimulate the formation of neo-vessels that are immature and highly permeable, conveying more inflammatory cells to the local environment. In the attenuation of AAA and atherosclerosis, endothelial Tie2 activation (phosphorylation) in response to Angpt2 administration acts to maintain the integrity and anti-inflammatory state of the intima, and thus limits aortic wall infiltration by inflammatory cells in response to AngII. Regression of neo-vessels sensitive to pro-longed exposure to Angpt2 reduces the conveyance of inflammatory cells to the aortic wall.
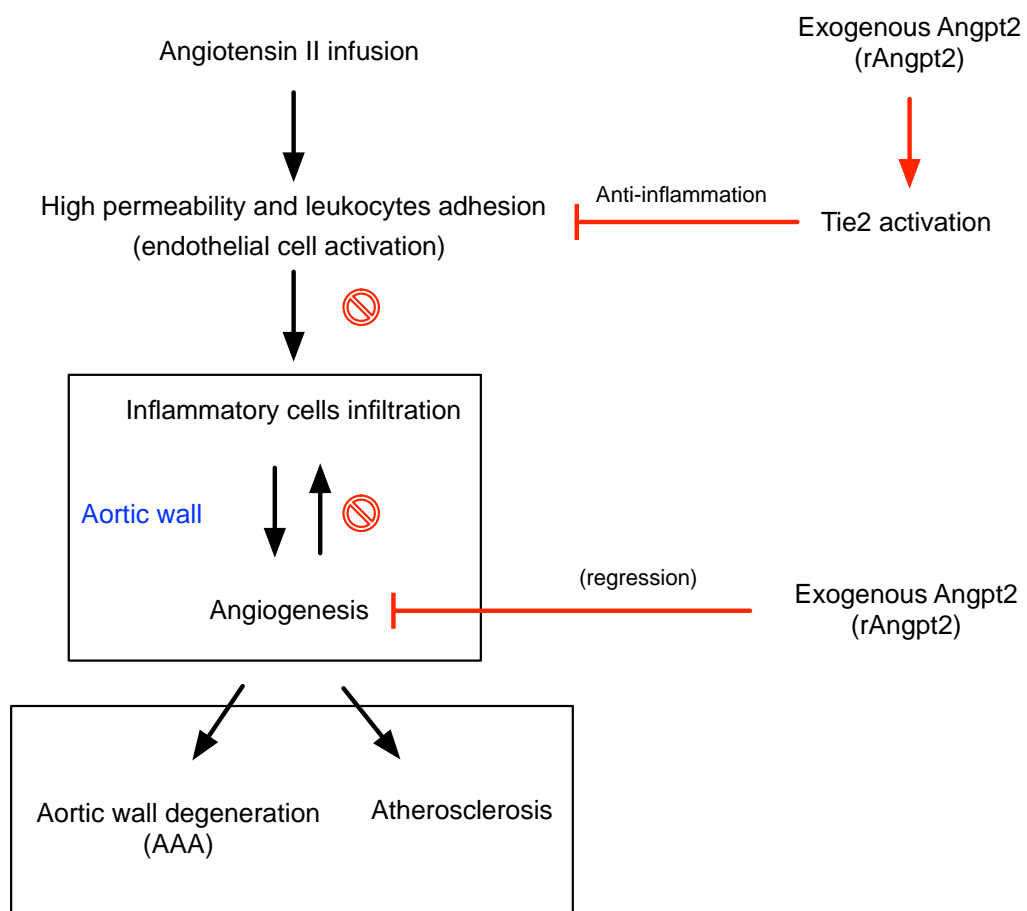
Figure 8.1 Proposed mechanisms for systemic exogenous Angpt2 administration on the attenuation of AAA development and atherosclerosis progression in the AngII-infusion mouse model.
Black arrow represents the roles of AngII in AAA development and atherosclerosis progression. The red arrow and stop sign represents the roles of exogenous Angpt2 and its consequence.

This study has a number of limitations. First, rAngpt2 administration was associated with reduction in both AAA and atherosclerosis. Thus it is possible that the reduction in

atherosclerosis may have caused a secondary reduction in AAA. The role of atherosclerosis in AAA is controversial, however it is not likely that atherosclerosis is the primary cause of AAA in the model used in the current study (Golledge & Norman, 2010; Deng et al., 2003). Second, since Angpt2 has many actions, the precise mechanism by which rAngpt2 limits AAA and atherosclerosis in our study remains unclear. Angpt2 is needed for functional lymphatics as mice deficient in Angpt2 show defective lymphatic patterning (Gale et al., 2002). Human AAA samples suggest that lymphatic vessel may be involved in AAA (Scott et al., 2013). The effect of Angpt2 on lymphatics was not investigated. Third, inflammatory cell infiltration predisposes a local environment to be pro-angiogenic, while angiogenesis conveys inflammatory cells into the local tissue. Whether exogenous Angpt2 administration acted to reduce inflammation within the aortic wall and thus angiogenesis, or, limited angiogenesis within the aortic wall initially, thereby reducing inflammatory cell infiltration was not clarified and requires further investigation.

The goal of AAA management is to prevent it from progression and rupture. This study has provided promising results of systemic endogenous Angpt2 administration in preventing AAAs formation and rupture in the AngII-infusion mouse model. These results suggest the potential beneficial effects of rAngpt2 administration in patients with cardiovascular disease and provide a possible strategy for AAA treatment. However, further pre-clinical investigation is needed to assess the value of Angpt2 in the management of AAA and whether administrating rAngpt2 in patients with AAA would be safe:

1. **The effect of rAngpt2 on the progression and rupture of established AAA:** Administration rAngpt2 in the current study commenced prior to initiating the infusion of AngII and induction of AAA in the mouse model. Clinically, patients present with already developing or established AAAs. Determining the efficacy of rAngpt2 to limit progression and rupture of established experimental AAA would be of value.

2. **Further investigation into the role of Angpt2 in the sequence of angiogenesis and inflammation of AAA development:** Mice receiving rAngpt2 still developed AAAs

although less severe. This suggests that rAngpt2 administration did not completely inhibit the initiation of inflammation and angiogenesis induced by AngII infusion but attenuated the progress. Inflammation predisposes local environment to angiogenesis and angiogenesis facilitates inflammatory cell infiltration through the new-formed leaky micro-vessels. In this thesis, the effect of rAngpt2 administration was assessed on the samples from later-stage experimental AAA. Therefore, it is difficult to obtain information on which is the primary outcome of the rAngpt2 administration: inflammation or angiogenesis. Assessing aortic tissue from early time points may resolve this.

3. **The optimal protective level of Angpt2:** In this thesis, rAngpt2 was administrated in a single dosage. The minimal dosage of Angpt2 for protecting AAA from progression and rupture needs to be determined to ensure minimal clinical side effects. This dosage would be also useful for patients whose endogenous Angpt2 elevates but does not reach a level to generate protective effects.

REFERENCES

Ahmed, A., Fujisawa, T., Niu, X. L., Ahmad, S., Al-Ani, B., Chudasama, K.*, et al.* (2009). Angiopoietin-2 confers Atheroprotection in ApoE$^{-/-}$ mice by inhibiting LDL oxidation via nitric oxide. *Circ Res, 104*(12), 1333-1336.

Albini, A., Tosetti, F., Benelli, R., & Noonan, D. M. (2005). Tumor inflammatory angiogenesis and its chemoprevention. *Cancer Res, 65*(23), 10637-10641.

Alcorn, H. G., Wolfson, S. K., Jr., Sutton-Tyrrell, K., Kuller, L. H., & O'Leary, D. (1996). Risk factors for abdominal aortic aneurysms in older adults enrolled in The Cardiovascular Health Study. *Arterioscler Thromb Vasc Biol, 16*(8), 963-970.

Altman, D. G., & Bland, J. M. (1983). Measurement in medicine: the analysis of method comparison studies. *The statistician*, 307-317.

Altman, D. G., & De Stavola, B. L. (1994). Practical problems in fitting a proportional hazards model to data with udated measurements of the covariates. *Statistics in Medicine, 13*(4), 301-341.

Amento, E. P., Ehsani, N., Palmer, H., & Libby, P. (1991). Cytokines and growth factors positively and negatively regulate interstitial collagen gene expression in human vascular smooth muscle cells. *Arterioscler Thromb, 11*(5), 1223-1230.

Ando, K., Kaneko, N., Doi, T., Aoshima, M., & Takahashi, K. (2014). Prevalence and risk factors of aortic aneurysm in patients with chronic obstructive pulmonary disease. *J Thorac Dis, 6*(10), 1388-1395.

Andrews, E. J., White, W. J., & Bullock, L. P. (1975). Spontaneous aortic aneurysms in blotchy mice. *Am J Pathol, 78*(2), 199-210.

Anidjar, S., Dobrin, P. B., Eichorst, M., Graham, G. P., & Chejfec, G. (1992). Correlation of inflammatory infiltrate with the enlargement of experimental aortic aneurysms. *J Vasc Surg, 16*(2), 139-147.

Anidjar, S., Salzmann, J. L., Gentric, D., Lagneau, P., Camilleri, J. P., & Michel, J. B. (1990). Elastase-induced experimental aneurysms in rats. *Circulation, 82*(3), 973-981.

Antoniou, G. A., Georgiadis, G. S., Antoniou, S. A., Granderath, F. A., Giannoukas, A. D., & Lazarides, M. K. (2011). Abdominal aortic aneurysm and abdominal wall hernia as manifestations of a connective tissue disorder. *J Vasc Surg, 54*(4), 1175-1181.

Armstrong, A. W., Voyles, S. V., Armstrong, E. J., Fuller, E. N., & Rutledge, J. C. (2011). Angiogenesis and oxidative stress: common mechanisms linking psoriasis with atherosclerosis. *J Dermatol Sci, 63*(1), 1-9.

Arora, P. D., & McCulloch, C. A. (1994). Dependence of collagen remodelling on alpha-smooth muscle actin expression by fibroblasts. *J Cell Physiol, 159*(1), 161-175.

Ashton, H. A., Buxton, M. J., Day, N. E., Kim, L. G., Marteau, T. M., Scott, R. A.*, et al.* (2002). The Multicentre Aneurysm Screening Study (MASS) into the effect of abdominal aortic aneurysm screening on mortality in men: a randomised controlled trial. *Lancet, 360*(9345), 1531-1539.

Augustin, H. G., Koh, G. Y., Thurston, G., & Alitalo, K. (2009). Control of vascular morphogenesis and homeostasis through the angiopoietin-Tie system. *Nat Rev Mol Cell Biol, 10*(3), 165-177.

Ayabe, N., Babaev, V. R., Tang, Y., Tanizawa, T., Fogo, A. B., Linton, M. F.*, et al.* (2006). Transiently heightened angiotensin II has distinct effects on atherosclerosis and aneurysm formation in hyperlipidemic mice. *Atherosclerosis, 184*(2), 312-321.

Babamusta, F., Rateri, D. L., Moorleghen, J. J., Howatt, D. A., Li, X. A., & Daugherty, A. (2006). Angiotensin II infusion induces site-specific intra-laminar hemorrhage in macrophage colony-stimulating factor-deficient mice. *Atherosclerosis, 186*(2), 282-290.

Barger, A. C., & Beeuwkes, R., 3rd. (1990). Rupture of coronary vasa vasorum as a trigger of acute myocardial infarction. *Am J Cardiol, 66*(16), 41G-43G.

Barisione, C., Charnigo, R., Howatt, D. A., Moorleghen, J. J., Rateri, D. L., & Daugherty, A. (2006). Rapid dilation of the abdominal aorta during infusion of angiotensin II detected by noninvasive high-frequency ultrasonography. *J Vasc Surg, 44*(2), 372-376.

Bartlett, J. W., & Frost, C. (2008). Reliability, repeatability and reproducibility: analysis of measurement errors in continuous variables. *Ultrasound Obstet Gynecol, 31*(4), 466-475.

Bauer, P. M., Yu, J., Chen, Y., Hickey, R., Bernatchez, P. N., Looft-Wilson, R.*, et al.* (2005). Endothelial-specific expression of caveolin-1 impairs microvascular permeability and angiogenesis. *Proc Natl Acad Sci U S A, 102*(1), 204-209.

Baxter, B. T., Davis, V. A., Minion, D. J., Wang, Y. P., Lynch, T. G., & McManus, B. M. (1994). Abdominal aortic aneurysms are associated with altered matrix proteins of the nonaneurysmal aortic segments. *J Vasc Surg, 19*(5), 797-802; discussion 803.

Baxter, B. T., & Pipinos, I. (2006). Commentary. Neutrophil depletion inhibits experimental abdominal aortic aneurysm formation. *Perspect Vasc Surg Endovasc Ther, 18*(3), 273-274.

Baxter, B. T., Terrin, M. C., & Dalman, R. L. (2008). Medical management of small abdominal aortic aneurysms. *Circulation, 117*(14), 1883-1889.

Berg, A. H., & Scherer, P. E. (2005). Adipose tissue, inflammation, and cardiovascular disease. *Circ Res, 96*(9), 939-949.

Bergoeing, M. P., Arif, B., Hackmann, A. E., Ennis, T. L., Thompson, R. W., & Curci, J. A. (2007). Cigarette smoking increases aortic dilatation without affecting matrix metalloproteinase-9 and -12 expression in a modified mouse model of aneurysm formation. *J Vasc Surg, 45*(6), 1217-1227.

Berra, E., Milanini, J., Richard, D. E., Le Gall, M., Vinals, F., Gothie, E.*, et al.* (2000). Signaling angiogenesis via p42/p44 MAP kinase and hypoxia. *Biochem Pharmacol, 60*(8), 1171-1178.

Blankensteijn, J. D., de Jong, S. E., Prinssen, M., van der Ham, A. C., Buth, J., van Sterkenburg, S. M.*, et al.* (2005). Two-year outcomes after conventional or endovascular repair of abdominal aortic aneurysms. *N Engl J Med, 352*(23), 2398-2405.

Blomkalns, A. L., Gavrila, D., Thomas, M., Neltner, B. S., Blanco, V. M., Benjamin, S. B.*, et al.* (2013). CD14 directs adventitial macrophage precursor recruitment: role in early abdominal aortic aneurysm formation. *J Am Heart Assoc, 2*(2), e000065.

Boring, L., Gosling, J., Cleary, M., & Charo, I. F. (1998). Decreased lesion formation in CCR2-/- mice reveals a role for chemokines in the initiation of atherosclerosis. *Nature, 394*(6696), 894-897.

Boytard, L., Spear, R., Chinetti-Gbaguidi, G., Acosta-Martin, A. E., Vanhoutte, J., Lamblin, N.*, et al.* (2013). Role of proinflammatory CD68(+) mannose receptor(-) macrophages in peroxiredoxin-1 expression and in abdominal aortic aneurysms in humans. *Arterioscler Thromb Vasc Biol, 33*(2), 431-438.

Brady, A. R., Thompson, S. G., Fowkes, F. G., Greenhalgh, R. M., Powell, J. T., & Participants, U. K. S. A. T. (2004). Abdominal aortic aneurysm expansion: risk factors and time intervals for surveillance. *Circulation, 110*(1), 16-21.

Brophy, C. M., Marks, W. H., Reilly, J. M., & Tilson, M. D. (1991). Decreased tissue inhibitor of metalloproteinases (TIMP) in abdominal aortic aneurysm tissue: a preliminary report. *J Surg Res, 50*(6), 653-657.

Brown, M., & Wittwer, C. (2000). Flow cytometry: principles and clinical applications in hematology. *Clin Chem, 46*(8 Pt 2), 1221-1229.

Brown, P. M., Zelt, D. T., & Sobolev, B. (2003). The risk of rupture in untreated aneurysms: the impact of size, gender, and expansion rate. *J Vasc Surg, 37*(2), 280-284.

Bruemmer, D., Collins, A. R., Noh, G., Wang, W., Territo, M., Arias-Magallona, S.*, et al.* (2003). Angiotensin II-accelerated atherosclerosis and aneurysm formation is attenuated in osteopontin-deficient mice. *J Clin Invest, 112*(9), 1318-1331.

Bruemmer, D., Daugherty, A., Lu, H., & Rateri, D. L. (2011). Relevance of angiotensin II-induced aortic pathologies in mice to human aortic aneurysms. *Ann N Y Acad Sci, 1245*(1), 7-10.

Cai, H., & Harrison, D. G. (2000). Endothelial dysfunction in cardiovascular diseases: the role of oxidant stress. *Circ Res, 87*(10), 840-844.

Calvi, C., Dentelli, P., Pagano, M., Rosso, A., Pegoraro, M., Giunti, S.*, et al.* (2004). Angiopoietin 2 induces cell cycle arrest in endothelial cells: a possible mechanism involved in advanced plaque neovascularization. *Arterioscler Thromb Vasc Biol, 24*(3), 511-518.

Cao, R. Y., Amand, T., Ford, M. D., Piomelli, U., & Funk, C. D. (2010). The Murine Angiotensin II-Induced Abdominal Aortic Aneurysm Model: Rupture Risk and Inflammatory Progression Patterns. *Front Pharmacol, 1*, 9.

Cao, Y., Sonveaux, P., Liu, S., Zhao, Y., Mi, J., Clary, B. M.*, et al.* (2007). Systemic overexpression of angiopoietin-2 promotes tumor microvessel regression and inhibits angiogenesis and tumor growth. *Cancer Res, 67*(8), 3835-3844.

Carlson, T. R., Feng, Y., Maisonpierre, P. C., Mrksich, M., & Morla, A. O. (2001). Direct cell adhesion to the angiopoietins mediated by integrins. *J Biol Chem, 276*(28), 26516-26525.

Carmeliet, P. (2003). Angiogenesis in health and disease. *Nat Med, 9*(6), 653-660.

Carmeliet, P., & Jain, R. K. (2000). Angiogenesis in cancer and other diseases. *Nature, 407*(6801), 249-257.

Cascone, I., Audero, E., Giraudo, E., Napione, L., Maniero, F., Philips, M. R*., et al.* (2003). Tie-2-dependent activation of RhoA and Rac1 participates in endothelial cell motility triggered by angiopoietin-1. *Blood, 102*(7), 2482-2490.

Cassis, L. A., Gupte, M., Thayer, S., Zhang, X., Charnigo, R., Howatt, D. A*., et al.* (2009). ANG II infusion promotes abdominal aortic aneurysms independent of increased blood pressure in hypercholesterolemic mice. *Am J Physiol Heart Circ Physiol, 296*(5), H1660-1665.

Celletti, F. L., Waugh, J. M., Amabile, P. G., Brendolan, A., Hilfiker, P. R., & Dake, M. D. (2001). Vascular endothelial growth factor enhances atherosclerotic plaque progression. *Nat Med, 7*(4), 425-429.

Chai, J., Jones, M. K., & Tarnawski, A. S. (2004). Serum response factor is a critical requirement for VEGF signaling in endothelial cells and VEGF-induced angiogenesis. *FASEB J, 18*(11), 1264-1266.

Chavakis, E., & Dimmeler, S. (2002). Regulation of endothelial cell survival and apoptosis during angiogenesis. *Arterioscler Thromb Vasc Biol, 22*(6), 887-893.

Chen, F., Eriksson, P., Kimura, T., Herzfeld, I., & Valen, G. (2005). Apoptosis and angiogenesis are induced in the unstable coronary atherosclerotic plaque. *Coron Artery Dis, 16*(3), 191-197.

Chen, H. H., Shi, Z. J., Wang, S. Q., & Wu, Q. L. (2009). The effects of angiopoietin-2 on the growth of tongue carcinoma. *Br J Oral Maxillofac Surg, 47*(1), 14-19.

Chen, J. X., & Stinnett, A. (2008). Disruption of Ang-1/Tie-2 signaling contributes to the impaired myocardial vascular maturation and angiogenesis in type II diabetic mice. *Arterioscler Thromb Vasc Biol, 28*(9), 1606-1613.

Chen, J. X., Zeng, H., Reese, J., Aschner, J. L., & Meyrick, B. (2012). Overexpression of angiopoietin-2 impairs myocardial angiogenesis and exacerbates cardiac fibrosis in the diabetic db/db mouse model. *Am J Physiol Heart Circ Physiol, 302*(4), H1003-1012.

Chen, L. C., & Nadziejko, C. (2005). Effects of subchronic exposures to concentrated ambient particles (CAPs) in mice. V. CAPs exacerbate aortic plaque development in hyperlipidemic mice. *Inhal Toxicol, 17*(4-5), 217-224.

Chen, L. C., Quan, C., Hwang, J. S., Jin, X., Li, Q., Zhong, M*., et al.* (2010). Atherosclerosis lesion progression during inhalation exposure to environmental tobacco smoke: a comparison to concentrated ambient air fine particles exposure. *Inhal Toxicol, 22*(6), 449-459.

Chen, X., Fu, W., Tung, C. E., & Ward, N. L. (2009). Angiopoietin-1 induces neurite outgrowth of PC12 cells in a Tie2-independent, beta1-integrin-dependent manner. *Neurosci Res, 64*(4), 348-354.

Chiou, A. C., Chiu, B., & Pearce, W. H. (2001). Murine aortic aneurysm produced by periarterial application of calcium chloride. *J Surg Res, 99*(2), 371-376.

Chlench, S., Mecha Disassa, N., Hohberg, M., Hoffmann, C., Pohlkamp, T., Beyer, G.*, et al.* (2007). Regulation of Foxo-1 and the angiopoietin-2/Tie2 system by shear stress. *FEBS Lett, 581*(4), 673-680.

Cho, B. S., Woodrum, D. T., Roelofs, K. J., Stanley, J. C., Henke, P. K., & Upchurch, G. R., Jr. (2009). Differential regulation of aortic growth in male and female rodents is associated with AAA development. *J Surg Res, 155*(2), 330-338.

Choke, E., Cockerill, G., Wilson, W. R., Sayed, S., Dawson, J., Loftus, I.*, et al.* (2005). A review of biological factors implicated in abdominal aortic aneurysm rupture. *Eur J Vasc Endovasc Surg, 30*(3), 227-244.

Choke, E., Cockerill, G. W., Dawson, J., Howe, F., Wilson, W. R., Loftus, I. M.*, et al.* (2010). Vascular endothelial growth factor enhances angiotensin II-induced aneurysm formation in apolipoprotein E-deficient mice. *J Vasc Surg, 52*(1), 159-166 e151.

Choke, E., Cockerill, G. W., Dawson, J., Wilson, R. W., Jones, A., Loftus, I. M.*, et al.* (2006). Increased angiogenesis at the site of abdominal aortic aneurysm rupture. *Ann N Y Acad Sci, 1085*(1), 315-319.

Choke, E., Thompson, M. M., Dawson, J., Wilson, W. R., Sayed, S., Loftus, I. M.*, et al.* (2006). Abdominal aortic aneurysm rupture is associated with increased medial neovascularization and overexpression of proangiogenic cytokines. *Arterioscler Thromb Vasc Biol, 26*(9), 2077-2082.

Chow, M. J., Mondonedo, J. R., Johnson, V. M., & Zhang, Y. (2013). Progressive structural and biomechanical changes in elastin degraded aorta. *Biomech Model Mechanobiol, 12*(2), 361-372.

Clifton, M. A. (1977). Familial abdominal aortic aneurysms. *Br J Surg, 64*(11), 765-766.

Coen, M., Gabbiani, G., & Bochaton-Piallat, M. L. (2011). Myofibroblast-mediated adventitial remodeling: an underestimated player in arterial pathology. *Arterioscler Thromb Vasc Biol, 31*(11), 2391-2396.

Coffelt, S. B., Chen, Y. Y., Muthana, M., Welford, A. F., Tal, A. O., Scholz, A.*, et al.* (2011). Angiopoietin 2 stimulates TIE2-expressing monocytes to suppress T cell activation and to promote regulatory T cell expansion. *J Immunol, 186*(7), 4183-4190.

Coffelt, S. B., Tal, A. O., Scholz, A., De Palma, M., Patel, S., Urbich, C.*, et al.* (2010). Angiopoietin-2 regulates gene expression in TIE2-expressing monocytes and augments their inherent proangiogenic functions. *Cancer Res, 70*(13), 5270-5280.

Cohen, B., Barkan, D., Levy, Y., Goldberg, I., Fridman, E., Kopolovic, J.*, et al.* (2001). Leptin induces angiopoietin-2 expression in adipose tissues. *J Biol Chem, 276*(11), 7697-7700.

Cooke, J. P., & Losordo, D. W. (2002). Nitric oxide and angiogenesis. *Circulation, 105*(18), 2133-2135.

Coussens, L. M., & Werb, Z. (2002). Inflammation and cancer. *Nature, 420*(6917), 860-867.

Crane, M. J., Hokeness-Antonelli, K. L., & Salazar-Mather, T. P. (2009). Regulation of inflammatory monocyte/macrophage recruitment from the bone marrow during murine

cytomegalovirus infection: role for type I interferons in localized induction of CCR2 ligands. *J Immunol, 183*(4), 2810-2817.

Crowley, S. D., Gurley, S. B., Herrera, M. J., Ruiz, P., Griffiths, R., Kumar, A. P*., et al.* (2006). Angiotensin II causes hypertension and cardiac hypertrophy through its receptors in the kidney. *Proc Natl Acad Sci U S A, 103*(47), 17985-17990.

Dai, G., Kaazempur-Mofrad, M. R., Natarajan, S., Zhang, Y., Vaughn, S., Blackman, B. R*., et al.* (2004). Distinct endothelial phenotypes evoked by arterial waveforms derived from atherosclerosis-susceptible and -resistant regions of human vasculature. *Proc Natl Acad Sci U S A, 101*(41), 14871-14876.

Dale, M. A., Ruhlman, M. K., & Baxter, B. T. (2015). Inflammatory Cell Phenotypes in AAAs: Their Role and Potential as Targets for Therapy. *Arterioscler Thromb Vasc Biol, 2015 Jun 4. pii: ATVBAHA.115.305269. [Epub ahead of print]*.

Daly, C., Eichten, A., Castanaro, C., Pasnikowski, E., Adler, A., Lalani, A. S*., et al.* (2013). Angiopoietin-2 functions as a Tie2 agonist in tumor models, where it limits the effects of VEGF inhibition. *Cancer Res, 73*(1), 108-118.

Daly, C., Pasnikowski, E., Burova, E., Wong, V., Aldrich, T. H., Griffiths, J*., et al.* (2006). Angiopoietin-2 functions as an autocrine protective factor in stressed endothelial cells. *Proc Natl Acad Sci U S A, 103*(42), 15491-15496.

Das, A., Fanslow, W., Cerretti, D., Warren, E., Talarico, N., & McGuire, P. (2003). Angiopoietin/Tek interactions regulate mmp-9 expression and retinal neovascularization. *Lab Invest, 83*(11), 1637-1645.

Daugherty, A., & Cassis, L. (2004). Angiotensin II-mediated development of vascular diseases. *Trends Cardiovasc Med, 14*(3), 117-120.

Daugherty, A., & Cassis, L. A. (2004). Mouse models of abdominal aortic aneurysms. *Arterioscler Thromb Vasc Biol, 24*(3), 429-434.

Daugherty, A., Manning, M. W., & Cassis, L. A. (2000). Angiotensin II promotes atherosclerotic lesions and aneurysms in apolipoprotein E-deficient mice. *J Clin Invest, 105*(11), 1605-1612.

Daugherty, A., Manning, M. W., & Cassis, L. A. (2001). Antagonism of AT2 receptors augments angiotensin II-induced abdominal aortic aneurysms and atherosclerosis. *Br J Pharmacol, 134*(4), 865-870.

Daugherty, A., Rateri, D. L., Charo, I. F., Owens, A. P., Howatt, D. A., & Cassis, L. A. (2010). Angiotensin II infusion promotes ascending aortic aneurysms: attenuation by CCR2 deficiency in ApoE$^{-/-}$ mice. *Clin Sci (Lond), 118*(11), 681-689.

David, S., Kumpers, P., Lukasz, A., Kielstein, J. T., Haller, H., & Fliser, D. (2009). Circulating angiopoietin-2 in essential hypertension: relation to atherosclerosis, vascular inflammation, and treatment with olmesartan/pravastatin. *J Hypertens, 27*(8), 1641-1647.

Davies, M. J. (1998). Aortic aneurysm formation: lessons from human studies and experimental models. *Circulation, 98*(3), 193-195.

Davis, S., Aldrich, T. H., Jones, P. F., Acheson, A., Compton, D. L., Jain, V*., et al.* (1996). Isolation of angiopoietin-1, a ligand for the TIE2 receptor, by secretion-trap expression cloning. *Cell, 87*(7), 1161-1169.

Davis, S., Papadopoulos, N., Aldrich, T. H., Maisonpierre, P. C., Huang, T., Kovac, L*., et al.* (2003). Angiopoietins have distinct modular domains essential for receptor binding, dimerization and superclustering. *Nat Struct Biol, 10*(1), 38-44.

Dawson, J., Cockerill, G. W., Choke, E., Belli, A. M., Loftus, I., & Thompson, M. M. (2007). Aortic aneurysms secrete interleukin-6 into the circulation. *J Vasc Surg, 45*(2), 350-356.

De Palma, M., & Naldini, L. (2011). Angiopoietin-2 TIEs up macrophages in tumor angiogenesis. *Clin Cancer Res, 17*(16), 5226-5232.

De Spiegelaere, W., Cornillie, P., Van den Broeck, W., Plendl, J., & Bahramsoltani, M. (2011). Angiopoietins differentially influence in vitro angiogenesis by endothelial cells of different origin. *Clin Hemorheol Microcirc, 48*(1), 15-27.

Deng, G. G., Martin-McNulty, B., Sukovich, D. A., Freay, A., Halks-Miller, M., Thinnes, T*., et al.* (2003). Urokinase-type plasminogen activator plays a critical role in angiotensin II-induced abdominal aortic aneurysm. *Circ Res, 92*(5), 510-517.

Dimmeler, S., Fleming, I., Fisslthaler, B., Hermann, C., Busse, R., & Zeiher, A. M. (1999). Activation of nitric oxide synthase in endothelial cells by Akt-dependent phosphorylation. *Nature, 399*(6736), 601-605.

Dobrin, P. B. (1989). Pathophysiology and pathogenesis of aortic aneurysms. Current concepts. *Surg Clin North Am, 69*(4), 687-703.

Dobrin, P. B., & Mrkvicka, R. (1994). Failure of elastin or collagen as possible critical connective tissue alterations underlying aneurysmal dilatation. *Cardiovasc Surg, 2*(4), 484-488.

Dong, Z. M., Chapman, S. M., Brown, A. A., Frenette, P. S., Hynes, R. O., & Wagner, D. D. (1998). The combined role of P- and E-selectins in atherosclerosis. *J Clin Invest, 102*(1), 145-152.

Doran, A. C., Meller, N., & McNamara, C. A. (2008). Role of smooth muscle cells in the initiation and early progression of atherosclerosis. *Arterioscler Thromb Vasc Biol, 28*(5), 812-819.

Drake, C. J. (2003). Embryonic and adult vasculogenesis. *Birth Defects Res C Embryo Today, 69*(1), 73-82.

Duftner, C., Seiler, R., Dejaco, C., Fraedrich, G., & Schirmer, M. (2006). Increasing evidence for immune-mediated processes and new therapeutic approaches in abdominal aortic aneurysms--a review. *Ann N Y Acad Sci, 1085*(1), 331-338.

Dumont, D. J., Gradwohl, G., Fong, G. H., Puri, M. C., Gertsenstein, M., Auerbach, A*., et al.* (1994). Dominant-negative and targeted null mutations in the endothelial receptor tyrosine kinase, tek, reveal a critical role in vasculogenesis of the embryo. *Genes Dev, 8*(16), 1897-1909.

Dutertre, C. A., Clement, M., Morvan, M., Schakel, K., Castier, Y., Alsac, J. M*., et al.* (2014). Deciphering the stromal and hematopoietic cell network of the adventitia from non-aneurysmal and aneurysmal human aorta. *PLoS One, 9*(2), e89983.

Eagleton, M. J. (2012). Inflammation in abdominal aortic aneurysms: cellular infiltrate and cytokine profiles. *Vascular, 20*(5), 278-283.

Elia, L., Quintavalle, M., Zhang, J., Contu, R., Cossu, L., Latronico, M. V*., et al.* (2009). The knockout of miR-143 and -145 alters smooth muscle cell maintenance and vascular homeostasis in mice: correlates with human disease. *Cell Death Differ, 16*(12), 1590-1598.

Eliason, J. L., Hannawa, K. K., Ailawadi, G., Sinha, I., Ford, J. W., Deogracias, M. P*., et al.* (2005). Neutrophil depletion inhibits experimental abdominal aortic aneurysm formation. *Circulation, 112*(2), 232-240.

Felcht, M., Luck, R., Schering, A., Seidel, P., Srivastava, K., Hu, J*., et al.* (2012). Angiopoietin-2 differentially regulates angiogenesis through TIE2 and integrin signaling. *J Clin Invest, 122*(6), 1991-2005.

Feng, M., Whitesall, S., Zhang, Y., Beibel, M., D'Alecy, L., & DiPetrillo, K. (2008). Validation of volume-pressure recording tail-cuff blood pressure measurements. *Am J Hypertens, 21*(12), 1288-1291.

Fiedler, U., & Augustin, H. G. (2006). Angiopoietins: a link between angiogenesis and inflammation. *Trends Immunol, 27*(12), 552-558.

Fiedler, U., Krissl, T., Koidl, S., Weiss, C., Koblizek, T., Deutsch, U*., et al.* (2003). Angiopoietin-1 and angiopoietin-2 share the same binding domains in the Tie-2 receptor involving the first Ig-like loop and the epidermal growth factor-like repeats. *J Biol Chem, 278*(3), 1721-1727.

Fiedler, U., Reiss, Y., Scharpfenecker, M., Grunow, V., Koidl, S., Thurston, G*., et al.* (2006). Angiopoietin-2 sensitizes endothelial cells to TNF-alpha and has a crucial role in the induction of inflammation. *Nat Med, 12*(2), 235-239.

Fiedler, U., Scharpfenecker, M., Koidl, S., Hegen, A., Grunow, V., Schmidt, J. M*., et al.* (2004). The Tie-2 ligand angiopoietin-2 is stored in and rapidly released upon stimulation from endothelial cell Weibel-Palade bodies. *Blood, 103*(11), 4150-4156.

Fillinger, M. F., Marra, S. P., Raghavan, M. L., & Kennedy, F. E. (2003). Prediction of rupture risk in abdominal aortic aneurysm during observation: wall stress versus diameter. *J Vasc Surg, 37*(4), 724-732.

Forester, N. D., Cruickshank, S. M., Scott, D. J., & Carding, S. R. (2005). Functional characterization of T cells in abdominal aortic aneurysms. *Immunology, 115*(2), 262-270.

Forsdahl, S. H., Singh, K., Solberg, S., & Jacobsen, B. K. (2009). Risk factors for abdominal aortic aneurysms: a 7-year prospective study: the Tromso Study, 1994-2001. *Circulation, 119*(16), 2202-2208.

Frank, P. G., & Lisanti, M. P. (2004). Caveolin-1 and caveolae in atherosclerosis: differential roles in fatty streak formation and neointimal hyperplasia. *Curr Opin Lipidol, 15*(5), 523-529.

Freestone, T., Turner, R. J., Coady, A., Higman, D. J., Greenhalgh, R. M., & Powell, J. T. (1995). Inflammation and matrix metalloproteinases in the enlarging abdominal aortic aneurysm. *Arterioscler Thromb Vasc Biol, 15*(8), 1145-1151.

Fujiyama, S., Matsubara, H., Nozawa, Y., Maruyama, K., Mori, Y., Tsutsumi, Y., *et al.* (2001). Angiotensin AT(1) and AT(2) receptors differentially regulate angiopoietin-2 and vascular endothelial growth factor expression and angiogenesis by modulating heparin binding-epidermal growth factor (EGF)-mediated EGF receptor transactivation. *Circ Res, 88*(1), 22-29.

Fukuhara, S., Sako, K., Noda, K., Zhang, J., Minami, M., & Mochizuki, N. (2010). Angiopoietin-1/Tie2 receptor signaling in vascular quiescence and angiogenesis. *Histol Histopathol, 25*(3), 387-396.

Furze, R. C., & Rankin, S. M. (2008). The role of the bone marrow in neutrophil clearance under homeostatic conditions in the mouse. *FASEB J, 22*(9), 3111-3119.

Gadowski, G. R., Ricci, M. A., Hendley, E. D., & Pilcher, D. B. (1993). Hypertension accelerates the growth of experimental aortic aneurysms. *J Surg Res, 54*(5), 431-436.

Gale, N. W., Thurston, G., Hackett, S. F., Renard, R., Wang, Q., McClain, J., *et al.* (2002). Angiopoietin-2 is required for postnatal angiogenesis and lymphatic patterning, and only the latter role is rescued by Angiopoietin-1. *Dev Cell, 3*(3), 411-423.

Galkina, E., & Ley, K. (2009). Immune and inflammatory mechanisms of atherosclerosis (*). *Annu Rev Immunol, 27*, 165-197.

Galle, C., Schandene, L., Stordeur, P., Peignois, Y., Ferreira, J., Wautrecht, J. C., *et al.* (2005). Predominance of type 1 CD4+ T cells in human abdominal aortic aneurysm. *Clin Exp Immunol, 142*(3), 519-527.

Gamble, J. R., Drew, J., Trezise, L., Underwood, A., Parsons, M., Kasminkas, L., *et al.* (2000). Angiopoietin-1 is an antipermeability and anti-inflammatory agent in vitro and targets cell junctions. *Circ Res, 87*(7), 603-607.

Gassmann, M., Grenacher, B., Rohde, B., & Vogel, J. (2009). Quantifying Western blots: pitfalls of densitometry. *ELECTROPHORESIS, 30*(11), 1845-1855.

Gavard, J., & Gutkind, J. S. (2006). VEGF controls endothelial-cell permeability by promoting the beta-arrestin-dependent endocytosis of VE-cadherin. *Nat Cell Biol, 8*(11), 1223-1234.

Gavard, J., Patel, V., & Gutkind, J. S. (2008). Angiopoietin-1 prevents VEGF-induced endothelial permeability by sequestering Src through mDia. *Dev Cell, 14*(1), 25-36.

Gavrila, D., Li, W. G., McCormick, M. L., Thomas, M., Daugherty, A., Cassis, L. A., *et al.* (2005). Vitamin E inhibits abdominal aortic aneurysm formation in angiotensin II-infused apolipoprotein E-deficient mice. *Arterioscler Thromb Vasc Biol, 25*(8), 1671-1677.

Genre, F., Lopez-Mejias, R., Miranda-Filloy, J. A., Ubilla, B., Carnero-Lopez, B., Gomez-Acebo, I., *et al.* (2014). Correlation between two biomarkers of atherosclerosis, osteopontin and angiopoietin-2, in non-diabetic ankylosing spondylitis patients undergoing TNF-alpha antagonist therapy. *Clin Exp Rheumatol, 32*(2), 231-236.

Gerald, D., Chintharlapalli, S., Augustin, H. G., & Benjamin, L. E. (2013). Angiopoietin-2: an attractive target for improved antiangiogenic tumor therapy. *Cancer Res, 73*(6), 1649-1657.

Gertz, S. D., Kurgan, A., & Eisenberg, D. (1988). Aneurysm of the rabbit common carotid artery induced by periarterial application of calcium chloride in vivo. *J Clin Invest, 81*(3), 649-656.

Giannotti, G., & Landmesser, U. (2007). Endothelial dysfunction as an early sign of atherosclerosis. *Herz, 32*(7), 568-572.

Glass, C. K., & Witztum, J. L. (2001). Atherosclerosis. the road ahead. *Cell, 104*(4), 503-516.

Golledge, J., Clancy, P., Yeap, B. B., Hankey, G. J., & Norman, P. E. (2013). Increased serum angiopoietin-2 is associated with abdominal aortic aneurysm prevalence and cardiovascular mortality in older men. *Int J Cardiol, 167*(4), 1159-1163.

Golledge, J., Cullen, B., Rush, C., Moran, C. S., Secomb, E., Wood, F., *et al.* (2010). Peroxisome proliferator-activated receptor ligands reduce aortic dilatation in a mouse model of aortic aneurysm. *Atherosclerosis, 210*(1), 51-56.

Golledge, J., Karan, M., Moran, C. S., Muller, J., Clancy, P., Dear, A. E., *et al.* (2008). Reduced expansion rate of abdominal aortic aneurysms in patients with diabetes may be related to aberrant monocyte-matrix interactions. *Eur Heart J, 29*(5), 665-672.

Golledge, J., Muller, J., Daugherty, A., & Norman, P. (2006). Abdominal aortic aneurysm: pathogenesis and implications for management. *Arterioscler Thromb Vasc Biol, 26*(12), 2605-2613.

Golledge, J., & Norman, P. E. (2010). Atherosclerosis and abdominal aortic aneurysm: cause, response, or common risk factors? *Arterioscler Thromb Vasc Biol, 30*(6), 1075-1077.

Golledge, J., & Norman, P. E. (2011). Current status of medical management for abdominal aortic aneurysm. *Atherosclerosis, 217*(1), 57-63.

Gordon, S., & Taylor, P. R. (2005). Monocyte and macrophage heterogeneity. *Nat Rev Immunol, 5*(12), 953-964.

Gossl, M., Versari, D., Mannheim, D., Ritman, E. L., Lerman, L. O., & Lerman, A. (2007). Increased spatial vasa vasorum density in the proximal LAD in hypercholesterolemia--implications for vulnerable plaque-development. *Atherosclerosis, 192*(2), 246-252.

Greenhalgh, R. M., & Powell, J. T. (2008). Endovascular repair of abdominal aortic aneurysm. *N Engl J Med, 358*(5), 494-501.

Gu, L., Okada, Y., Clinton, S. K., Gerard, C., Sukhova, G. K., Libby, P., *et al.* (1998). Absence of monocyte chemoattractant protein-1 reduces atherosclerosis in low density lipoprotein receptor-deficient mice. *Mol Cell, 2*(2), 275-281.

Guo, D. C., Pannu, H., Tran-Fadulu, V., Papke, C. L., Yu, R. K., Avidan, N., *et al.* (2007). Mutations in smooth muscle alpha-actin (ACTA2) lead to thoracic aortic aneurysms and dissections. *Nat Genet, 39*(12), 1488-1493.

Gupta, S., Pablo, A. M., Jiang, X., Wang, N., Tall, A. R., & Schindler, C. (1997). IFN-gamma potentiates atherosclerosis in ApoE knock-out mice. *J Clin Invest, 99*(11), 2752-2761.

Halpern, V. J., Nackman, G. B., Gandhi, R. H., Irizarry, E., Scholes, J. V., Ramey, W. G., *et al.* (1994). The elastase infusion model of experimental aortic aneurysms: synchrony of induction of endogenous proteinases with matrix destruction and inflammatory cell response. *J Vasc Surg, 20*(1), 51-60.

Hance, K. A., Tataria, M., Ziporin, S. J., Lee, J. K., & Thompson, R. W. (2002). Monocyte chemotactic activity in human abdominal aortic aneurysms: role of elastin degradation peptides and the 67-kD cell surface elastin receptor. *J Vasc Surg, 35*(2), 254-261.

Hansen, T. M., Singh, H., Tahir, T. A., & Brindle, N. P. (2010). Effects of angiopoietins-1 and -2 on the receptor tyrosine kinase Tie2 are differentially regulated at the endothelial cell surface. *Cell Signal, 22*(3), 527-532.

Hasan, D., Chalouhi, N., Jabbour, P., & Hashimoto, T. (2012). Macrophage imbalance (M1 vs. M2) and upregulation of mast cells in wall of ruptured human cerebral aneurysms: preliminary results. *J Neuroinflammation, 9*, 222.

Hattori, K., Dias, S., Heissig, B., Hackett, N. R., Lyden, D., Tateno, M., *et al.* (2001). Vascular endothelial growth factor and angiopoietin-1 stimulate postnatal hematopoiesis by recruitment of vasculogenic and hematopoietic stem cells. *J Exp Med, 193*(9), 1005-1014.

He, H., Venema, V. J., Gu, X., Venema, R. C., Marrero, M. B., & Caldwell, R. B. (1999). Vascular endothelial growth factor signals endothelial cell production of nitric oxide and prostacyclin through flk-1/KDR activation of c-Src. *J Biol Chem, 274*(35), 25130-25135.

Helgadottir, A., Thorleifsson, G., Magnusson, K. P., Gretarsdottir, S., Steinthorsdottir, V., Manolescu, A., *et al.* (2008). The same sequence variant on 9p21 associates with myocardial infarction, abdominal aortic aneurysm and intracranial aneurysm. *Nat Genet, 40*(2), 217-224.

Hellenthal, F. A., Buurman, W. A., Wodzig, W. K., & Schurink, G. W. (2009a). Biomarkers of AAA progression. Part 1: extracellular matrix degeneration. *Nat Rev Cardiol, 6*(7), 464-474.

Hellenthal, F. A., Buurman, W. A., Wodzig, W. K., & Schurink, G. W. (2009b). Biomarkers of abdominal aortic aneurysm progression. Part 2: inflammation. *Nat Rev Cardiol, 6*(8), 543-552.

Henderson, E. L., Geng, Y. J., Sukhova, G. K., Whittemore, A. D., Knox, J., & Libby, P. (1999). Death of smooth muscle cells and expression of mediators of apoptosis by T lymphocytes in human abdominal aortic aneurysms. *Circulation, 99*(1), 96-104.

Hennessy, A., Barry, M. C., McGee, H., O'Boyle, C., Hayes, D. B., & Grace, P. A. (1998). Quality of life following repair of ruptured and elective abdominal aortic aneurysms. *Eur J Surg, 164*(9), 673-677.

Herrmann, J., Lerman, L. O., Rodriguez-Porcel, M., Holmes, D. R., Jr., Richardson, D. M., Ritman, E. L., *et al.* (2001). Coronary vasa vasorum neovascularization precedes epicardial endothelial dysfunction in experimental hypercholesterolemia. *Cardiovasc Res, 51*(4), 762-766.

Holash, J., Wiegand, S. J., & Yancopoulos, G. D. (1999). New model of tumor angiogenesis: dynamic balance between vessel regression and growth mediated by angiopoietins and VEGF. *Oncogene, 18*(38), 5356-5362.

Holmes, D. R., Liao, S., Parks, W. C., & Thompson, R. W. (1995). Medial neovascularization in abdominal aortic aneurysms: a histopathologic marker of aneurysmal degeneration with pathophysiologic implications. *J Vasc Surg, 21*(5), 761-771; discussion 771-762.

Hood, J. D., Frausto, R., Kiosses, W. B., Schwartz, M. A., & Cheresh, D. A. (2003). Differential alphav integrin-mediated Ras-ERK signaling during two pathways of angiogenesis. *J Cell Biol, 162*(5), 933-943.

Hu, B., Guo, P., Fang, Q., Tao, H. Q., Wang, D., Nagane, M.*, et al.* (2003). Angiopoietin-2 induces human glioma invasion through the activation of matrix metalloprotease-2. *Proc Natl Acad Sci U S A, 100*(15), 8904-8909.

Hu, B., Jarzynka, M. J., Guo, P., Imanishi, Y., Schlaepfer, D. D., & Cheng, S. Y. (2006). Angiopoietin 2 induces glioma cell invasion by stimulating matrix metalloprotease 2 expression through the alphavbeta1 integrin and focal adhesion kinase signaling pathway. *Cancer Res, 66*(2), 775-783.

Huang, H., Lai, J. Y., Do, J., Liu, D., Li, L., Del Rosario, J.*, et al.* (2011). Specifically targeting angiopoietin-2 inhibits angiogenesis, Tie2-expressing monocyte infiltration, and tumor growth. *Clin Cancer Res, 17*(5), 1001-1011.

Huang, L., Turck, C. W., Rao, P., & Peters, K. G. (1995). GRB2 and SH-PTP2: potentially important endothelial signaling molecules downstream of the TEK/TIE2 receptor tyrosine kinase. *Oncogene, 11*(10), 2097-2103.

Hughes, D. P., Marron, M. B., & Brindle, N. P. (2003). The antiinflammatory endothelial tyrosine kinase Tie2 interacts with a novel nuclear factor-kappaB inhibitor ABIN-2. *Circ Res, 92*(6), 630-636.

Ichihara, E., Kiura, K., & Tanimoto, M. (2011). Targeting angiogenesis in cancer therapy. *Acta Med Okayama, 65*(6), 353-362.

Ilan, N., Mahooti, S., & Madri, J. A. (1998). Distinct signal transduction pathways are utilized during the tube formation and survival phases of in vitro angiogenesis. *J Cell Sci, 111 (Pt 24)*(Pt 24), 3621-3631.

Imanishi, Y., Hu, B., Jarzynka, M. J., Guo, P., Elishaev, E., Bar-Joseph, I.*, et al.* (2007). Angiopoietin-2 stimulates breast cancer metastasis through the alpha(5)beta(1) integrin-mediated pathway. *Cancer Res, 67*(9), 4254-4263.

Imhof, B. A., & Aurrand-Lions, M. (2006). Angiogenesis and inflammation face off. *Nat Med, 12*(2), 171-172.

Isenburg, J. C., Simionescu, D. T., Starcher, B. C., & Vyavahare, N. R. (2007). Elastin stabilization for treatment of abdominal aortic aneurysms. *Circulation, 115*(13), 1729-1737.

Ishibashi, M., Egashira, K., Zhao, Q., Hiasa, K., Ohtani, K., Ihara, Y.*, et al.* (2004). Bone marrow-derived monocyte chemoattractant protein-1 receptor CCR2 is critical in angiotensin II-induced acceleration of atherosclerosis and aneurysm formation in hypercholesterolemic mice. *Arterioscler Thromb Vasc Biol, 24*(11), e174-178.

Ishibashi, M., Hiasa, K., Zhao, Q., Inoue, S., Ohtani, K., Kitamoto, S.*, et al.* (2004). Critical role of monocyte chemoattractant protein-1 receptor CCR2 on monocytes in hypertension-induced vascular inflammation and remodeling. *Circ Res, 94*(9), 1203-1210.

Ishibashi, S., Goldstein, J. L., Brown, M. S., Herz, J., & Burns, D. K. (1994). Massive xanthomatosis and atherosclerosis in cholesterol-fed low density lipoprotein receptor-negative mice. *J Clin Invest, 93*(5), 1885-1893.

Isner, J. M., Kearney, M., Bortman, S., & Passeri, J. (1995). Apoptosis in human atherosclerosis and restenosis. *Circulation, 91*(11), 2703-2711.

Jackson, C. (2002). Matrix metalloproteinases and angiogenesis. *Curr Opin Nephrol Hypertens, 11*(3), 295-299.

Jaffer, F. A., O'Donnell, C. J., Larson, M. G., Chan, S. K., Kissinger, K. V., Kupka, M. J.*, et al.* (2002). Age and sex distribution of subclinical aortic atherosclerosis: a magnetic resonance imaging examination of the Framingham Heart Study. *Arterioscler Thromb Vasc Biol, 22*(5), 849-854.

Jain, R. K., & Munn, L. L. (2000). Leaky vessels? Call Ang1! *Nat Med, 6*(2), 131-132.

Jaumdally, R. J., Lip, G. Y., Varma, C., & Blann, A. D. (2011). Impact of high-dose atorvastatin on endothelial, platelet, and angiogenic indices: effect of ethnicity, cardiovascular disease, and diabetes. *Angiology, 62*(7), 571-578.

Jaumdally, R. J., Varma, C., Blann, A. D., Macfadyen, R. J., & Lip, G. Y. (2007). Indices of angiogenesis, platelet activation, and endothelial damage/dysfunction in relation to ethnicity and coronary artery disease: differences in central versus peripheral levels. *Ann Med, 39*(8), 628-633.

Jeltsch, M., Leppanen, V. M., Saharinen, P., & Alitalo, K. (2013). Receptor tyrosine kinase-mediated angiogenesis. *Cold Spring Harb Perspect Biol, 5*(9).

Jeon, B. H., Khanday, F., Deshpande, S., Haile, A., Ozaki, M., & Irani, K. (2003). Tie-ing the antiinflammatory effect of angiopoietin-1 to inhibition of NF-kappaB. *Circ Res, 92*(6), 586-588.

Jeziorska, M., & Woolley, D. E. (1999). Local neovascularization and cellular composition within vulnerable regions of atherosclerotic plaques of human carotid arteries. *J Pathol, 188*(2), 189-196.

Jia, T., Serbina, N. V., Brandl, K., Zhong, M. X., Leiner, I. M., Charo, I. F.*, et al.* (2008). Additive roles for MCP-1 and MCP-3 in CCR2-mediated recruitment of inflammatory monocytes during Listeria monocytogenes infection. *J Immunol, 180*(10), 6846-6853.

Jiang, B. H., Zheng, J. Z., Aoki, M., & Vogt, P. K. (2000). Phosphatidylinositol 3-kinase signaling mediates angiogenesis and expression of vascular endothelial growth factor in endothelial cells. *Proc Natl Acad Sci U S A, 97*(4), 1749-1753.

Jiang, F., Jones, G. T., & Dusting, G. J. (2007). Failure of antioxidants to protect against angiotensin II-induced aortic rupture in aged apolipoprotein(E)-deficient mice. *Br J Pharmacol, 152*(6), 880-890.

Johnston, W. F., Salmon, M., Pope, N. H., Meher, A., Su, G., Stone, M. L.*, et al.* (2014). Inhibition of interleukin-1beta decreases aneurysm formation and progression in a novel model of thoracic aortic aneurysms. *Circulation, 130*(11 Suppl 1), S51-59.

Jones, A., Deb, R., Torsney, E., Howe, F., Dunkley, M., Gnaneswaran, Y.*, et al.* (2009). Rosiglitazone reduces the development and rupture of experimental aortic aneurysms. *Circulation, 119*(24), 3125-3132.

Jones, N., Chen, S. H., Sturk, C., Master, Z., Tran, J., Kerbel, R. S.*, et al.* (2003). A unique autophosphorylation site on Tie2/Tek mediates Dok-R phosphotyrosine binding domain binding and function. *Mol Cell Biol, 23*(8), 2658-2668.

Jones, N., Master, Z., Jones, J., Bouchard, D., Gunji, Y., Sasaki, H.*, et al.* (1999). Identification of Tek/Tie2 binding partners. Binding to a multifunctional docking site mediates cell survival and migration. *J Biol Chem, 274*(43), 30896-30905.

Joussen, A. M., Poulaki, V., Tsujikawa, A., Qin, W., Qaum, T., Xu, Q.*, et al.* (2002). Suppression of diabetic retinopathy with angiopoietin-1. *Am J Pathol, 160*(5), 1683-1693.

Juvonen, J., Surcel, H. M., Satta, J., Teppo, A. M., Bloigu, A., Syrjala, H.*, et al.* (1997). Elevated circulating levels of inflammatory cytokines in patients with abdominal aortic aneurysm. *Arterioscler Thromb Vasc Biol, 17*(11), 2843-2847.

Kaikita, K., Hayasaki, T., Okuma, T., Kuziel, W. A., Ogawa, H., & Takeya, M. (2004). Targeted deletion of CC chemokine receptor 2 attenuates left ventricular remodeling after experimental myocardial infarction. *Am J Pathol, 165*(2), 439-447.

Kaneko, H., Anzai, T., Takahashi, T., Kohno, T., Shimoda, M., Sasaki, A.*, et al.* (2011). Role of vascular endothelial growth factor-A in development of abdominal aortic aneurysm. *Cardiovasc Res, 91*(2), 358-367.

Karlan, B. Y., Oza, A. M., Richardson, G. E., Provencher, D. M., Hansen, V. L., Buck, M.*, et al.* (2012). Randomized, double-blind, placebo-controlled phase II study of AMG 386 combined with weekly paclitaxel in patients with recurrent ovarian cancer. *J Clin Oncol, 30*(4), 362-371.

Kassab, G. S. (2006). Biomechanics of the cardiovascular system: the aorta as an illustratory example. *J R Soc Interface, 3*(11), 719-740.

Kim, I., Kim, H. G., So, J. N., Kim, J. H., Kwak, H. J., & Koh, G. Y. (2000). Angiopoietin-1 regulates endothelial cell survival through the phosphatidylinositol 3'-Kinase/Akt signal transduction pathway. *Circ Res, 86*(1), 24-29.

Kim, I., Kim, J. H., Moon, S. O., Kwak, H. J., Kim, N. G., & Koh, G. Y. (2000). Angiopoietin-2 at high concentration can enhance endothelial cell survival through the phosphatidylinositol 3'-kinase/Akt signal transduction pathway. *Oncogene, 19*(39), 4549-4552.

Kim, I., Moon, S. O., Kim, S. H., Kim, H. J., Koh, Y. S., & Koh, G. Y. (2001). Vascular endothelial growth factor expression of intercellular adhesion molecule 1 (ICAM-1), vascular cell adhesion molecule 1 (VCAM-1), and E-selectin through nuclear factor-kappa B activation in endothelial cells. *J Biol Chem, 276*(10), 7614-7620.

Kim, I., Moon, S. O., Park, S. K., Chae, S. W., & Koh, G. Y. (2001). Angiopoietin-1 reduces VEGF-stimulated leukocyte adhesion to endothelial cells by reducing ICAM-1, VCAM-1, and E-selectin expression. *Circ Res, 89*(6), 477-479.

Kinlay, S., & Ganz, P. (1997). Role of endothelial dysfunction in coronary artery disease and implications for therapy. *Am J Cardiol, 80*(9A), 11I-16I.

Kitamoto, S., Sukhova, G. K., Sun, J., Yang, M., Libby, P., Love, V.*, et al.* (2007). Cathepsin L deficiency reduces diet-induced atherosclerosis in low-density lipoprotein receptor-knockout mice. *Circulation, 115*(15), 2065-2075.

Klink, A., Hyafil, F., Rudd, J., Faries, P., Fuster, V., Mallat, Z.*, et al.* (2011). Diagnostic and therapeutic strategies for small abdominal aortic aneurysms. *Nat Rev Cardiol, 8*(6), 338-347.

Knowles, J. W., Reddick, R. L., Jennette, J. C., Shesely, E. G., Smithies, O., & Maeda, N. (2000). Enhanced atherosclerosis and kidney dysfunction in eNOS(-/-)Apoe(-/-) mice are ameliorated by enalapril treatment. *J Clin Invest, 105*(4), 451-458.

Knox, J. B., Sukhova, G. K., Whittemore, A. D., & Libby, P. (1997). Evidence for altered balance between matrix metalloproteinases and their inhibitors in human aortic diseases. *Circulation, 95*(1), 205-212.

Koch, A. E., Haines, G. K., Rizzo, R. J., Radosevich, J. A., Pope, R. M., Robinson, P. G., *et al.* (1990). Human abdominal aortic aneurysms. Immunophenotypic analysis suggesting an immune-mediated response. *Am J Pathol, 137*(5), 1199-1213.

Kockx, M. M., Cromheeke, K. M., Knaapen, M. W., Bosmans, J. M., De Meyer, G. R., Herman, A. G., *et al.* (2003). Phagocytosis and macrophage activation associated with hemorrhagic microvessels in human atherosclerosis. *Arterioscler Thromb Vasc Biol, 23*(3), 440-446.

Koh, G. Y. (2013). Orchestral actions of angiopoietin-1 in vascular regeneration. *Trends Mol Med, 19*(1), 31-39.

Koh, G. Y., Kim, I., Kwak, H. J., Yun, M. J., & Leem, J. C. (2002). Biomedical significance of endothelial cell specific growth factor, angiopoietin. *Exp Mol Med, 34*(1), 1-11.

Koh, Y. J., Kim, H. Z., Hwang, S. I., Lee, J. E., Oh, N., Jung, K., *et al.* (2010). Double antiangiogenic protein, DAAP, targeting VEGF-A and angiopoietins in tumor angiogenesis, metastasis, and vascular leakage. *Cancer Cell, 18*(2), 171-184.

Kolodgie, F. D., Gold, H. K., Burke, A. P., Fowler, D. R., Kruth, H. S., Weber, D. K., *et al.* (2003). Intraplaque hemorrhage and progression of coronary atheroma. *N Engl J Med, 349*(24), 2316-2325.

Kontos, C. D., Stauffer, T. P., Yang, W. P., York, J. D., Huang, L., Blanar, M. A., *et al.* (1998). Tyrosine 1101 of Tie2 is the major site of association of p85 and is required for activation of phosphatidylinositol 3-kinase and Akt. *Mol Cell Biol, 18*(7), 4131-4140.

Koole, D., Hurks, R., Schoneveld, A., Vink, A., Golledge, J., Moran, C. S., *et al.* (2012). Osteoprotegerin is associated with aneurysm diameter and proteolysis in abdominal aortic aneurysm disease. *Arterioscler Thromb Vasc Biol, 32*(6), 1497-1504.

Korpelainen, E. I., Karkkainen, M., Gunji, Y., Vikkula, M., & Alitalo, K. (1999). Endothelial receptor tyrosine kinases activate the STAT signaling pathway: mutant Tie-2 causing venous malformations signals a distinct STAT activation response. *Oncogene, 18*(1), 1-8.

Krettek, A., Sukhova, G. K., Schonbeck, U., & Libby, P. (2004). Enhanced expression of CD44 variants in human atheroma and abdominal aortic aneurysm: possible role for a feedback loop in endothelial cells. *Am J Pathol, 165*(5), 1571-1581.

Krikos, A., Laherty, C. D., & Dixit, V. M. (1992). Transcriptional activation of the tumor necrosis factor alpha-inducible zinc finger protein, A20, is mediated by kappa B elements. *J Biol Chem, 267*(25), 17971-17976.

Kuivaniemi, H., Platsoucas, C. D., & Tilson, M. D., 3rd. (2008). Aortic aneurysms: an immune disease with a strong genetic component. *Circulation, 117*(2), 242-252.

Lacraz, S., Nicod, L. P., Chicheportiche, R., Welgus, H. G., & Dayer, J. M. (1995). IL-10 inhibits metalloproteinase and stimulates TIMP-1 production in human mononuclear phagocytes. *J Clin Invest, 96*(5), 2304-2310.

LaMorte, W. W., Scott, T. E., & Menzoian, J. O. (1995). Racial differences in the incidence of femoral bypass and abdominal aortic aneurysmectomy in Massachusetts: relationship to cardiovascular risk factors. *J Vasc Surg, 21*(3), 422-431.

Landis, J. R., & Koch, G. G. (1977). The measurement of observer agreement for categorical data. *Biometrics, 33*(1), 159-174.

Le Dall, J., Ho-Tin-Noe, B., Louedec, L., Meilhac, O., Roncal, C., Carmeliet, P.*, et al.* (2010). Immaturity of microvessels in haemorrhagic plaques is associated with proteolytic degradation of angiogenic factors. *Cardiovasc Res, 85*(1), 184-193.

Le, M. T., Jamrozik, K., Davis, T. M., & Norman, P. E. (2007). Negative association between infra-renal aortic diameter and glycaemia: the Health in Men Study. *Eur J Vasc Endovasc Surg, 33*(5), 599-604.

Lederle, F. A. (2011). The rise and fall of abdominal aortic aneurysm. *Circulation, 124*(10), 1097-1099.

Lederle, F. A., Johnson, G. R., Wilson, S. E., Chute, E. P., Hye, R. J., Makaroun, M. S.*, et al.* (2000). The aneurysm detection and management study screening program: validation cohort and final results. Aneurysm Detection and Management Veterans Affairs Cooperative Study Investigators. *Arch Intern Med, 160*(10), 1425-1430.

Lee, J., Park, D. Y., Park do, Y., Park, I., Chang, W., Nakaoka, Y.*, et al.* (2014). Angiopoietin-1 suppresses choroidal neovascularization and vascular leakage. *Invest Ophthalmol Vis Sci, 55*(4), 2191-2199.

Leow, C. C., Coffman, K., Inigo, I., Breen, S., Czapiga, M., Soukharev, S.*, et al.* (2012). MEDI3617, a human anti-angiopoietin 2 monoclonal antibody, inhibits angiogenesis and tumor growth in human tumor xenograft models. *Int J Oncol, 40*(5), 1321-1330.

Lepidi, S., Kenagy, R. D., Raines, E. W., Chiu, E. S., Chait, A., Ross, R.*, et al.* (2001). MMP9 production by human monocyte-derived macrophages is decreased on polymerized type I collagen. *J Vasc Surg, 34*(6), 1111-1118.

Li, X., Hahn, C. N., Parsons, M., Drew, J., Vadas, M. A., & Gamble, J. R. (2004). Role of protein kinase Czeta in thrombin-induced endothelial permeability changes: inhibition by angiopoietin-1. *Blood, 104*(6), 1716-1724.

Libby, P. (2002). Inflammation in atherosclerosis. *Nature, 420*(6917), 868-874.

Libby, P. (2009). Molecular and cellular mechanisms of the thrombotic complications of atherosclerosis. *J Lipid Res, 50 Suppl*, S352-357.

Libby, P., & Lee, R. T. (2000). Matrix matters. *Circulation, 102*(16), 1874-1876.

Libby, P., Ridker, P. M., & Hansson, G. K. (2011). Progress and challenges in translating the biology of atherosclerosis. *Nature, 473*(7347), 317-325.

Lim, H. S., Lip, G. Y., & Blann, A. D. (2005). Angiopoietin-1 and angiopoietin-2 in diabetes mellitus: relationship to VEGF, glycaemic control, endothelial damage/dysfunction and atherosclerosis. *Atherosclerosis, 180*(1), 113-118.

Limet, R., Sakalihassan, N., & Albert, A. (1991). Determination of the expansion rate and incidence of rupture of abdominal aortic aneurysms. *J Vasc Surg, 14*(4), 540-548.

Lindblad, B., Borner, G., & Gottsater, A. (2005). Factors associated with development of large abdominal aortic aneurysm in middle-aged men. *Eur J Vasc Endovasc Surg, 30*(4), 346-352.

Lindholt, J. S., Ashton, H. A., Heickendorff, L., & Scott, R. A. (2001). Serum elastin peptides in the preoperative evaluation of abdominal aortic aneurysms. *Eur J Vasc Endovasc Surg, 22*(6), 546-550.

Lindholt, J. S., Erlandsen, E. J., & Henneberg, E. W. (2001). Cystatin C deficiency is associated with the progression of small abdominal aortic aneurysms. *Br J Surg, 88*(11), 1472-1475.

Lindholt, J. S., & Shi, G. P. (2006). Chronic inflammation, immune response, and infection in abdominal aortic aneurysms. *Eur J Vasc Endovasc Surg, 31*(5), 453-463.

Lip, P. L., Chatterjee, S., Caine, G. J., Hope-Ross, M., Gibson, J., Blann, A. D.*, et al.* (2004). Plasma vascular endothelial growth factor, angiopoietin-2, and soluble angiopoietin receptor tie-2 in diabetic retinopathy: effects of laser photocoagulation and angiotensin receptor blockade. *Br J Ophthalmol, 88*(12), 1543-1546.

Liu, J., Razani, B., Tang, S., Terman, B. I., Ware, J. A., & Lisanti, M. P. (1999). Angiogenesis activators and inhibitors differentially regulate caveolin-1 expression and caveolae formation in vascular endothelial cells. Angiogenesis inhibitors block vascular endothelial growth factor-induced down-regulation of caveolin-1. *J Biol Chem, 274*(22), 15781-15785.

Lobov, I. B., Brooks, P. C., & Lang, R. A. (2002). Angiopoietin-2 displays VEGF-dependent modulation of capillary structure and endothelial cell survival in vivo. *Proc Natl Acad Sci U S A, 99*(17), 11205-11210.

Longo, G. M., Xiong, W., Greiner, T. C., Zhao, Y., Fiotti, N., & Baxter, B. T. (2002). Matrix metalloproteinases 2 and 9 work in concert to produce aortic aneurysms. *J Clin Invest, 110*(5), 625-632.

Lopez-Mejias, R., Corrales, A., Genre, F., Hernandez, J. L., Ochoa, R., Blanco, R.*, et al.* (2013). Angiopoietin-2 serum levels correlate with severity, early onset and cardiovascular disease in patients with rheumatoid arthritis. *Clin Exp Rheumatol, 31*(5), 761-766.

Lorbeer, R., Baumeister, S. E., Dorr, M., Felix, S. B., Nauck, M., Grotevendt, A.*, et al.* (2015). Angiopoietin-2, its soluble receptor Tie-2 and subclinical cardiovascular disease in a population-based sample. *Heart, 101*(3), 178-184.

Lowe, G. D. (2001). The relationship between infection, inflammation, and cardiovascular disease: an overview. *Ann Periodontol, 6*(1), 1-8.

MacTaggart, J. N., Xiong, W., Knispel, R., & Baxter, B. T. (2007). Deletion of CCR2 but not CCR5 or CXCR3 inhibits aortic aneurysm formation. *Surgery, 142*(2), 284-288.

Maisonpierre, P. C., Suri, C., Jones, P. F., Bartunkova, S., Wiegand, S. J., Radziejewski, C.*, et al.* (1997). Angiopoietin-2, a natural antagonist for Tie2 that disrupts in vivo angiogenesis. *Science, 277*(5322), 55-60.

Majesky, M. W., Dong, X. R., Hoglund, V., Mahoney, W. M., Jr., & Daum, G. (2011). The adventitia: a dynamic interface containing resident progenitor cells. *Arterioscler Thromb Vasc Biol, 31*(7), 1530-1539.

Mandriota, S. J., & Pepper, M. S. (1998). Regulation of angiopoietin-2 mRNA levels in bovine microvascular endothelial cells by cytokines and hypoxia. *Circ Res, 83*(8), 852-859.

Mandriota, S. J., Pyke, C., Di Sanza, C., Quinodoz, P., Pittet, B., & Pepper, M. S. (2000). Hypoxia-inducible angiopoietin-2 expression is mimicked by iodonium compounds and occurs in the rat brain and skin in response to systemic hypoxia and tissue ischemia. *Am J Pathol, 156*(6), 2077-2089.

Mangan, S. H., Van Campenhout, A., Rush, C., & Golledge, J. (2007). Osteoprotegerin upregulates endothelial cell adhesion molecule response to tumor necrosis factor-alpha associated with induction of angiopoietin-2. *Cardiovasc Res, 76*(3), 494-505.

Manning, M. W., Cassi, L. A., Huang, J., Szilvassy, S. J., & Daugherty, A. (2002). Abdominal aortic aneurysms: fresh insights from a novel animal model of the disease. *Vasc Med, 7*(1), 45-54.

Manning, M. W., Cassis, L. A., & Daugherty, A. (2003). Differential effects of doxycycline, a broad-spectrum matrix metalloproteinase inhibitor, on angiotensin II-induced atherosclerosis and abdominal aortic aneurysms. *Arterioscler Thromb Vasc Biol, 23*(3), 483-488.

Martin, V., Liu, D., Fueyo, J., & Gomez-Manzano, C. (2008). Tie2: a journey from normal angiogenesis to cancer and beyond. *Histol Histopathol, 23*(6), 773-780.

Mayranpaa, M. I., Trosien, J. A., Fontaine, V., Folkesson, M., Kazi, M., Eriksson, P.*, et al.* (2009). Mast cells associate with neovessels in the media and adventitia of abdominal aortic aneurysms. *J Vasc Surg, 50*(2), 388-395; discussion 395-386.

Mazzieri, R., Pucci, F., Moi, D., Zonari, E., Ranghetti, A., Berti, A.*, et al.* (2011). Targeting the ANG2/TIE2 axis inhibits tumor growth and metastasis by impairing angiogenesis and disabling rebounds of proangiogenic myeloid cells. *Cancer Cell, 19*(4), 512-526.

McEniery, C. M., Wilkinson, I. B., & Avolio, A. P. (2007). Age, hypertension and arterial function. *Clin Exp Pharmacol Physiol, 34*(7), 665-671.

Meir, K. S., & Leitersdorf, E. (2004). Atherosclerosis in the apolipoprotein-E-deficient mouse: a decade of progress. *Arterioscler Thromb Vasc Biol, 24*(6), 1006-1014.

Mellak, S., Ait-Oufella, H., Esposito, B., Loyer, X., Poirier, M., Tedder, T. F.*, et al.* (2015). Angiotensin II mobilizes spleen monocytes to promote the development of abdominal aortic aneurysm in ApoE^{-/-} mice. *Arterioscler Thromb Vasc Biol, 35*(2), 378-388.

Merali, F. S., & Anand, S. S. (2002). Immediate repair compared with surveillance of small abdominal aortic aneurysms. *Vasc Med, 7*(3), 249-250.

Michel, J. B., Martin-Ventura, J. L., Egido, J., Sakalihasan, N., Treska, V., Lindholt, J.*, et al.* (2011). Novel aspects of the pathogenesis of aneurysms of the abdominal aorta in humans. *Cardiovasc Res, 90*(1), 18-27.

Michel, J. B., Thaunat, O., Houard, X., Meilhac, O., Caligiuri, G., & Nicoletti, A. (2007). Topological determinants and consequences of adventitial responses to arterial wall injury. *Arterioscler Thromb Vasc Biol, 27*(6), 1259-1268.

Milewicz, D. M., Guo, D. C., Tran-Fadulu, V., Lafont, A. L., Papke, C. L., Inamoto, S.*, et al.* (2008). Genetic basis of thoracic aortic aneurysms and dissections: focus on smooth muscle cell contractile dysfunction. *Annu Rev Genomics Hum Genet, 9*, 283-302.

Miwa, K., Nakashima, H., Aoki, M., Miyake, T., Kawasaki, T., Iwai, M.*, et al.* (2005). Inhibition of ets, an essential transcription factor for angiogenesis, to prevent the development of abdominal aortic aneurysm in a rat model. *Gene Ther, 12*(14), 1109-1118.

Moehle, C. W., Bhamidipati, C. M., Alexander, M. R., Mehta, G. S., Irvine, J. N., Salmon, M.*, et al.* (2011). Bone marrow-derived MCP1 required for experimental aortic aneurysm formation and smooth muscle phenotypic modulation. *J Thorac Cardiovasc Surg, 142*(6), 1567-1574.

Moran, C. S., Jose, R. J., Biros, E., & Golledge, J. (2014). Osteoprotegerin deficiency limits angiotensin II-induced aortic dilatation and rupture in the apolipoprotein E-knockout mouse. *Arterioscler Thromb Vasc Biol, 34*(12), 2609-2616.

Moran, C. S., Jose, R. J., Moxon, J. V., Roomberg, A., Norman, P. E., Rush, C.*, et al.* (2013). Everolimus limits aortic aneurysm in the apolipoprotein E-deficient mouse by downregulating C-C chemokine receptor 2 positive monocytes. *Arterioscler Thromb Vasc Biol, 33*(4), 814-821.

Morrissey, C., Dowell, A., Koreckij, T. D., Nguyen, H., Lakely, B., Fanslow, W. C.*, et al.* (2010). Inhibition of angiopoietin-2 in LuCaP 23.1 prostate cancer tumors decreases tumor growth and viability. *Prostate, 70*(16), 1799-1808.

Moss, A. (2013). The angiopoietin:Tie 2 interaction: a potential target for future therapies in human vascular disease. *Cytokine Growth Factor Rev, 24*(6), 579-592.

Moulton, K. S., Heller, E., Konerding, M. A., Flynn, E., Palinski, W., & Folkman, J. (1999). Angiogenesis inhibitors endostatin or TNP-470 reduce intimal neovascularization and plaque growth in apolipoprotein E-deficient mice. *Circulation, 99*(13), 1726-1732.

Moulton, K. S., Vakili, K., Zurakowski, D., Soliman, M., Butterfield, C., Sylvin, E.*, et al.* (2003). Inhibition of plaque neovascularization reduces macrophage accumulation and progression of advanced atherosclerosis. *Proc Natl Acad Sci U S A, 100*(8), 4736-4741.

Munoz-Chapuli, R., Quesada, A. R., & Angel Medina, M. (2004). Angiogenesis and signal transduction in endothelial cells. *Cell Mol Life Sci, 61*(17), 2224-2243.

Murakami, M. (2012). Signaling required for blood vessel maintenance: molecular basis and pathological manifestations. *Int J Vasc Med, 2012*, 293641.

Murphy, D. A., Makonnen, S., Lassoued, W., Feldman, M. D., Carter, C., & Lee, W. M. (2006). Inhibition of tumor endothelial ERK activation, angiogenesis, and tumor growth by sorafenib (BAY43-9006). *Am J Pathol, 169*(5), 1875-1885.

Murphy, E. A., Danna-Lopes, D., Sarfati, I., Rao, S. K., & Cohen, J. R. (1998). Nicotine-stimulated elastase activity release by neutrophils in patients with abdominal aortic aneurysms. *Ann Vasc Surg, 12*(1), 41-45.

Nahrendorf, M., Keliher, E., Marinelli, B., Leuschner, F., Robbins, C. S., Gerszten, R. E.*, et al.* (2011). Detection of macrophages in aortic aneurysms by nanoparticle positron emission tomography-computed tomography. *Arterioscler Thromb Vasc Biol, 31*(4), 750-757.

Nakashima, Y., Plump, A. S., Raines, E. W., Breslow, J. L., & Ross, R. (1994). ApoE-deficient mice develop lesions of all phases of atherosclerosis throughout the arterial tree. *Arterioscler Thromb, 14*(1), 133-140.

Nakashima, Y., Raines, E. W., Plump, A. S., Breslow, J. L., & Ross, R. (1998). Upregulation of VCAM-1 and ICAM-1 at atherosclerosis-prone sites on the endothelium in the ApoE-deficient mouse. *Arterioscler Thromb Vasc Biol, 18*(5), 842-851.

Namkoong, S., Kim, C. K., Cho, Y. L., Kim, J. H., Lee, H., Ha, K. S*., et al.* (2009). Forskolin increases angiogenesis through the coordinated cross-talk of PKA-dependent VEGF expression and Epac-mediated PI3K/Akt/eNOS signaling. *Cell Signal, 21*(6), 906-915.

Nangaku, M., Izuhara, Y., Takizawa, S., Yamashita, T., Fujii-Kuriyama, Y., Ohneda, O*., et al.* (2007). A novel class of prolyl hydroxylase inhibitors induces angiogenesis and exerts organ protection against ischemia. *Arterioscler Thromb Vasc Biol, 27*(12), 2548-2554.

Newman, K. M., Jean-Claude, J., Li, H., Scholes, J. V., Ogata, Y., Nagase, H*., et al.* (1994). Cellular localization of matrix metalloproteinases in the abdominal aortic aneurysm wall. *J Vasc Surg, 20*(5), 814-820.

Nicholls, E. A., Norman, P. E., Lawrence-Brown, M. M., Goodman, M. A., & Pedersen, B. (1992). Screening for abdominal aortic aneurysms in Western Australia. *Aust N Z J Surg, 62*(11), 858-861.

Nienaber, C. A., & Sievers, H. H. (2002). Intramural hematoma in acute aortic syndrome: more than one variant of dissection? *Circulation, 106*(3), 284-285.

Nordon, I. M., Hinchliffe, R. J., Loftus, I. M., & Thompson, M. M. (2011). Pathophysiology and epidemiology of abdominal aortic aneurysms. *Nat Rev Cardiol, 8*(2), 92-102.

Nordskog, B. K., Fields, W. R., & Hellmann, G. M. (2005). Kinetic analysis of cytokine response to cigarette smoke condensate by human endothelial and monocytic cells. *Toxicology, 212*(2-3), 87-97.

Nykanen, A. I., Krebs, R., Saaristo, A., Turunen, P., Alitalo, K., Yla-Herttuala, S*., et al.* (2003). Angiopoietin-1 protects against the development of cardiac allograft arteriosclerosis. *Circulation, 107*(9), 1308-1314.

Nykanen, A. I., Pajusola, K., Krebs, R., Keranen, M. A., Raisky, O., Koskinen, P. K*., et al.* (2006). Common protective and diverse smooth muscle cell effects of AAV-mediated angiopoietin-1 and -2 expression in rat cardiac allograft vasculopathy. *Circ Res, 98*(11), 1373-1380.

Oh, H., Takagi, H., Suzuma, K., Otani, A., Matsumura, M., & Honda, Y. (1999). Hypoxia and vascular endothelial growth factor selectively up-regulate angiopoietin-2 in bovine microvascular endothelial cells. *J Biol Chem, 274*(22), 15732-15739.

Olin, K. L., Potter-Perigo, S., Barrett, P. H., Wight, T. N., & Chait, A. (1999). Lipoprotein lipase enhances the binding of native and oxidized low density lipoproteins to versican and biglycan synthesized by cultured arterial smooth muscle cells. *J Biol Chem, 274*(49), 34629-34636.

Oliner, J., Min, H., Leal, J., Yu, D., Rao, S., You, E*., et al.* (2004). Suppression of angiogenesis and tumor growth by selective inhibition of angiopoietin-2. *Cancer Cell, 6*(5), 507-516.

Oshima, Y., Deering, T., Oshima, S., Nambu, H., Reddy, P. S., Kaleko, M.*, et al.* (2004). Angiopoietin-2 enhances retinal vessel sensitivity to vascular endothelial growth factor. *J Cell Physiol, 199*(3), 412-417.

Otani, A., Takagi, H., Oh, H., Koyama, S., & Honda, Y. (2001). Angiotensin II induces expression of the Tie2 receptor ligand, angiopoietin-2, in bovine retinal endothelial cells. *Diabetes, 50*(4), 867-875.

Owens, A. P., 3rd, Rateri, D. L., Howatt, D. A., Moore, K. J., Tobias, P. S., Curtiss, L. K.*, et al.* (2011). MyD88 deficiency attenuates angiotensin II-induced abdominal aortic aneurysm formation independent of signaling through Toll-like receptors 2 and 4. *Arterioscler Thromb Vasc Biol, 31*(12), 2813-2819.

Paik, D. C., Fu, C., Bhattacharya, J., & Tilson, M. D. (2004). Ongoing angiogenesis in blood vessels of the abdominal aortic aneurysm. *Exp Mol Med, 36*(6), 524-533.

participants, E. t. (2005). Endovascular aneurysm repair and outcome in patients unfit for open repair of abdominal aortic aneurysm (EVAR trial 2): randomised controlled trial. *The Lancet, 365*(9478), 2187-2192.

Participants, T. U. S. A. T. (1998). Mortality results for randomised controlled trial of early elective surgery or ultrasonographic surveillance for small abdominal aortic aneurysms. The UK Small Aneurysm Trial Participants. *Lancet, 352*(9141), 1649-1655.

Pavlides, S., Gutierrez-Pajares, J. L., Iturrieta, J., Lisanti, M. P., & Frank, P. G. (2014). Endothelial caveolin-1 plays a major role in the development of atherosclerosis. *Cell Tissue Res, 356*(1), 147-157.

Pepper, M. S. (2001). Extracellular proteolysis and angiogenesis. *Thromb Haemost, 86*(1), 346-355.

Peters, K. G., Kontos, C. D., Lin, P. C., Wong, A. L., Rao, P., Huang, L.*, et al.* (2004). Functional significance of Tie2 signaling in the adult vasculature. *Recent Prog Horm Res, 59*, 51-71.

Post, S., Peeters, W., Busser, E., Lamers, D., Sluijter, J. P., Goumans, M. J.*, et al.* (2008). Balance between angiopoietin-1 and angiopoietin-2 is in favor of angiopoietin-2 in atherosclerotic plaques with high microvessel density. *J Vasc Res, 45*(3), 244-250.

Prall, A. K., Longo, G. M., Mayhan, W. G., Waltke, E. A., Fleckten, B., Thompson, R. W.*, et al.* (2002). Doxycycline in patients with abdominal aortic aneurysms and in mice: comparison of serum levels and effect on aneurysm growth in mice. *J Vasc Surg, 35*(5), 923-929.

Pueyo, M. E., Gonzalez, W., Nicoletti, A., Savoie, F., Arnal, J. F., & Michel, J. B. (2000). Angiotensin II stimulates endothelial vascular cell adhesion molecule-1 via nuclear factor-kappaB activation induced by intracellular oxidative stress. *Arterioscler Thromb Vasc Biol, 20*(3), 645-651.

Pulinx, B., Hellenthal, F. A., Hamulyak, K., van Dieijen-Visser, M. P., Schurink, G. W., & Wodzig, W. K. (2011). Differential protein expression in serum of abdominal aortic aneurysm patients - a proteomic approach. *Eur J Vasc Endovasc Surg, 42*(5), 563-570.

Pyo, R., Lee, J. K., Shipley, J. M., Curci, J. A., Mao, D., Ziporin, S. J.*, et al.* (2000). Targeted gene disruption of matrix metalloproteinase-9 (gelatinase B) suppresses development of experimental abdominal aortic aneurysms. *J Clin Invest, 105*(11), 1641-1649.

Quill, D. S., Colgan, M. P., & Sumner, D. S. (1989). Ultrasonic screening for the detection of abdominal aortic aneurysms. *Surg Clin North Am, 69*(4), 713-720.

Raines, E. W., & Ferri, N. (2005). Thematic review series: The immune system and atherogenesis. Cytokines affecting endothelial and smooth muscle cells in vascular disease. *J Lipid Res, 46*(6), 1081-1092.

Rajantie, I., Ekman, N., Iljin, K., Arighi, E., Gunji, Y., Kaukonen, J.*, et al.* (2001). Bmx tyrosine kinase has a redundant function downstream of angiopoietin and vascular endothelial growth factor receptors in arterial endothelium. *Mol Cell Biol, 21*(14), 4647-4655.

Ramos-Mozo, P., Madrigal-Matute, J., Martinez-Pinna, R., Blanco-Colio, L. M., Lopez, J. A., Camafeita, E.*, et al.* (2011). Proteomic analysis of polymorphonuclear neutrophils identifies catalase as a novel biomarker of abdominal aortic aneurysm: potential implication of oxidative stress in abdominal aortic aneurysm progression. *Arterioscler Thromb Vasc Biol, 31*(12), 3011-3019.

Ramshaw, A. L., Roskell, D. E., & Parums, D. V. (1994). Cytokine gene expression in aortic adventitial inflammation associated with advanced atherosclerosis (chronic periaortitis). *J Clin Pathol, 47*(8), 721-727.

Rateri, D. L., Howatt, D. A., Moorleghen, J. J., Charnigo, R., Cassis, L. A., & Daugherty, A. (2011). Prolonged infusion of angiotensin II in apoE(-/-) mice promotes macrophage recruitment with continued expansion of abdominal aortic aneurysm. *Am J Pathol, 179*(3), 1542-1548.

Recinos, A., 3rd, LeJeune, W. S., Sun, H., Lee, C. Y., Tieu, B. C., Lu, M.*, et al.* (2007). Angiotensin II induces IL-6 expression and the Jak-STAT3 pathway in aortic adventitia of LDL receptor-deficient mice. *Atherosclerosis, 194*(1), 125-133.

Reed, D., Reed, C., Stemmermann, G., & Hayashi, T. (1992). Are aortic aneurysms caused by atherosclerosis? *Circulation, 85*(1), 205-211.

Ribatti, D., Levi-Schaffer, F., & Kovanen, P. T. (2008). Inflammatory angiogenesis in atherogenesis--a double-edged sword. *Ann Med, 40*(8), 606-621.

Rizas, K. D., Ippagunta, N., & Tilson, M. D., 3rd. (2009). Immune cells and molecular mediators in the pathogenesis of the abdominal aortic aneurysm. *Cardiol Rev, 17*(5), 201-210.

Roviezzo, F., Tsigkos, S., Kotanidou, A., Bucci, M., Brancaleone, V., Cirino, G.*, et al.* (2005). Angiopoietin-2 causes inflammation in vivo by promoting vascular leakage. *J Pharmacol Exp Ther, 314*(2), 738-744.

Rowe, V. L., Stevens, S. L., Reddick, T. T., Freeman, M. B., Donnell, R., Carroll, R. C.*, et al.* (2000). Vascular smooth muscle cell apoptosis in aneurysmal, occlusive, and normal human aortas. *J Vasc Surg, 31*(3), 567-576.

Saharinen, P., Eklund, L., Miettinen, J., Wirkkala, R., Anisimov, A., Winderlich, M.*, et al.* (2008). Angiopoietins assemble distinct Tie2 signalling complexes in endothelial cell-cell and cell-matrix contacts. *Nat Cell Biol, 10*(5), 527-537.

Saito, T., Hasegawa, Y., Ishigaki, Y., Yamada, T., Gao, J., Imai, J.*, et al.* (2013). Importance of endothelial NF-kappaB signalling in vascular remodelling and aortic aneurysm formation. *Cardiovasc Res, 97*(1), 106-114.

Sakalihasan, N., Delvenne, P., Nusgens, B. V., Limet, R., & Lapiere, C. M. (1996). Activated forms of MMP2 and MMP9 in abdominal aortic aneurysms. *J Vasc Surg, 24*(1), 127-133.

Sakalihasan, N., Limet, R., & Defawe, O. D. (2005). Abdominal aortic aneurysm. *Lancet, 365*(9470), 1577-1589.

Sakata, N., Nabeshima, K., Iwasaki, H., Tashiro, T., Uesugi, N., Nakashima, O., *et al.* (2007). Possible involvement of myofibroblast in the development of inflammatory aortic aneurysm. *Pathol Res Pract, 203*(1), 21-29.

Salem, M. K., Rayt, H. S., Hussey, G., Rafelt, S., Nelson, C. P., Sayers, R. D., *et al.* (2009). Should Asian men be included in abdominal aortic aneurysm screening programmes? *Eur J Vasc Endovasc Surg, 38*(6), 748-749.

Samadzadeh, K. M., Chun, K. C., Nguyen, A. T., Baker, P. M., Bains, S., & Lee, E. S. (2014). Monocyte activity is linked with abdominal aortic aneurysm diameter. *J Surg Res, 190*(1), 328-334.

Sandford, R. M., Bown, M. J., London, N. J., & Sayers, R. D. (2007). The genetic basis of abdominal aortic aneurysms: a review. *Eur J Vasc Endovasc Surg, 33*(4), 381-390.

Saraff, K., Babamusta, F., Cassis, L. A., & Daugherty, A. (2003). Aortic dissection precedes formation of aneurysms and atherosclerosis in angiotensin II-infused, apolipoprotein E-deficient mice. *Arterioscler Thromb Vasc Biol, 23*(9), 1621-1626.

Sato, A., Iwama, A., Takakura, N., Nishio, H., Yancopoulos, G. D., & Suda, T. (1998). Characterization of TEK receptor tyrosine kinase and its ligands, Angiopoietins, in human hematopoietic progenitor cells. *Int Immunol, 10*(8), 1217-1227.

Sato, T. N., Tozawa, Y., Deutsch, U., Wolburg-Buchholz, K., Fujiwara, Y., Gendron-Maguire, M., *et al.* (1995). Distinct roles of the receptor tyrosine kinases Tie-1 and Tie-2 in blood vessel formation. *Nature, 376*(6535), 70-74.

Satoh, K., Nigro, P., Matoba, T., O'Dell, M. R., Cui, Z., Shi, X., *et al.* (2009). Cyclophilin A enhances vascular oxidative stress and the development of angiotensin II-induced aortic aneurysms. *Nat Med, 15*(6), 649-656.

Scharpfenecker, M., Fiedler, U., Reiss, Y., & Augustin, H. G. (2005). The Tie-2 ligand angiopoietin-2 destabilizes quiescent endothelium through an internal autocrine loop mechanism. *J Cell Sci, 118*(Pt 4), 771-780.

Scholz, A., Lang, V., Henschler, R., Czabanka, M., Vajkoczy, P., Chavakis, E., *et al.* (2011). Angiopoietin-2 promotes myeloid cell infiltration in a beta(2)-integrin-dependent manner. *Blood, 118*(18), 5050-5059.

Schonbeck, U., Sukhova, G. K., Gerdes, N., & Libby, P. (2002). T(H)2 predominant immune responses prevail in human abdominal aortic aneurysm. *Am J Pathol, 161*(2), 499-506.

Schriefl, A. J., Collins, M. J., Pierce, D. M., Holzapfel, G. A., Niklason, L. E., & Humphrey, J. D. (2012). Remodeling of intramural thrombus and collagen in an Ang-II infusion ApoE^{-/-} model of dissecting aortic aneurysms. *Thromb Res, 130*(3), e139-146.

Scott, D. J., Allen, C. J., Honstvet, C. A., Hanby, A. M., Hammond, C., Johnson, A. B., *et al.* (2013). Lymphangiogenesis in abdominal aortic aneurysm. *Br J Surg, 100*(7), 895-903.

Seegar, T. C., Eller, B., Tzvetkova-Robev, D., Kolev, M. V., Henderson, S. C., Nikolov, D. B., *et al.* (2010). Tie1-Tie2 interactions mediate functional differences between angiopoietin ligands. *Mol Cell, 37*(5), 643-655.

Serbina, N. V., & Pamer, E. G. (2006). Monocyte emigration from bone marrow during bacterial infection requires signals mediated by chemokine receptor CCR2. *Nat Immunol, 7*(3), 311-317.

Seto, S. W., Krishna, S. M., Moran, C. S., Liu, D., & Golledge, J. (2014). Aliskiren limits abdominal aortic aneurysm, ventricular hypertrophy and atherosclerosis in an apolipoprotein-E-deficient mouse model. *Clin Sci (Lond), 127*(2), 123-134.

Seto, S. W., Krishna, S. M., Yu, H., Liu, D., Khosla, S., & Golledge, J. (2013). Impaired acetylcholine-induced endothelium-dependent aortic relaxation by caveolin-1 in angiotensin II-infused apolipoprotein-E (ApoE-/-) knockout mice. *PLoS One, 8*(3), e58481.

Shantikumar, S., Ajjan, R., Porter, K. E., & Scott, D. J. (2010). Diabetes and the abdominal aortic aneurysm. *Eur J Vasc Endovasc Surg, 39*(2), 200-207.

Shen, J., Frye, M., Lee, B. L., Reinardy, J. L., McClung, J. M., Ding, K., *et al.* (2014). Targeting VE-PTP activates TIE2 and stabilizes the ocular vasculature. *J Clin Invest, 124*(10), 4564-4576.

Shi, C., & Pamer, E. G. (2011). Monocyte recruitment during infection and inflammation. *Nat Rev Immunol, 11*(11), 762-774.

Shimizu, K., Mitchell, R. N., & Libby, P. (2006). Inflammation and cellular immune responses in abdominal aortic aneurysms. *Arterioscler Thromb Vasc Biol, 26*(5), 987-994.

Shiojima, I., & Walsh, K. (2002). Role of Akt signaling in vascular homeostasis and angiogenesis. *Circ Res, 90*(12), 1243-1250.

Shiraya, S., Miwa, K., Aoki, M., Miyake, T., Oishi, M., Kataoka, K., *et al.* (2006). Hypertension accelerated experimental abdominal aortic aneurysm through upregulation of nuclear factor kappaB and Ets. *Hypertension, 48*(4), 628-636.

Smith, J. D., Trogan, E., Ginsberg, M., Grigaux, C., Tian, J., & Miyata, M. (1995). Decreased atherosclerosis in mice deficient in both macrophage colony-stimulating factor (op) and apolipoprotein E. *Proc Natl Acad Sci U S A, 92*(18), 8264-8268.

Sonveaux, P., Martinive, P., DeWever, J., Batova, Z., Daneau, G., Pelat, M., *et al.* (2004). Caveolin-1 expression is critical for vascular endothelial growth factor-induced ischemic hindlimb collateralization and nitric oxide-mediated angiogenesis. *Circ Res, 95*(2), 154-161.

Spin, J. M., Hsu, M., Azuma, J., Tedesco, M. M., Deng, A., Dyer, J. S., *et al.* (2011). Transcriptional profiling and network analysis of the murine angiotensin II-induced abdominal aortic aneurysm. *Physiol Genomics, 43*(17), 993-1003.

Stary, H. C., Chandler, A. B., Dinsmore, R. E., Fuster, V., Glagov, S., Insull, W., Jr., *et al.* (1995). A definition of advanced types of atherosclerotic lesions and a histological classification of atherosclerosis. A report from the Committee on Vascular Lesions of the Council on Arteriosclerosis, American Heart Association. *Circulation, 92*(5), 1355-1374.

Stratmann, A., Risau, W., & Plate, K. H. (1998). Cell type-specific expression of angiopoietin-1 and angiopoietin-2 suggests a role in glioblastoma angiogenesis. *Am J Pathol, 153*(5), 1459-1466.

Sun, J., Sukhova, G. K., Yang, M., Wolters, P. J., MacFarlane, L. A., Libby, P.*, et al.* (2007). Mast cells modulate the pathogenesis of elastase-induced abdominal aortic aneurysms in mice. *J Clin Invest, 117*(11), 3359-3368.

Suri, C., Jones, P. F., Patan, S., Bartunkova, S., Maisonpierre, P. C., Davis, S.*, et al.* (1996). Requisite role of angiopoietin-1, a ligand for the TIE2 receptor, during embryonic angiogenesis. *Cell, 87*(7), 1171-1180.

Suzuki, Y., Ruiz-Ortega, M., Lorenzo, O., Ruperez, M., Esteban, V., & Egido, J. (2003). Inflammation and angiotensin II. *Int J Biochem Cell Biol, 35*(6), 881-900.

Swedenborg, J., & Eriksson, P. (2006). The intraluminal thrombus as a source of proteolytic activity. *Ann N Y Acad Sci, 1085*, 133-138.

Swedenborg, J., Mayranpaa, M. I., & Kovanen, P. T. (2011). Mast cells: important players in the orchestrated pathogenesis of abdominal aortic aneurysms. *Arterioscler Thromb Vasc Biol, 31*(4), 734-740.

Swirski, F. K., Libby, P., Aikawa, E., Alcaide, P., Luscinskas, F. W., Weissleder, R.*, et al.* (2007). Ly-6Chi monocytes dominate hypercholesterolemia-associated monocytosis and give rise to macrophages in atheromata. *J Clin Invest, 117*(1), 195-205.

Swirski, F. K., Nahrendorf, M., Etzrodt, M., Wildgruber, M., Cortez-Retamozo, V., Panizzi, P.*, et al.* (2009). Identification of splenic reservoir monocytes and their deployment to inflammatory sites. *Science, 325*(5940), 612-616.

Tadros, A., Hughes, D. P., Dunmore, B. J., & Brindle, N. P. (2003). ABIN-2 protects endothelial cells from death and has a role in the antiapoptotic effect of angiopoietin-1. *Blood, 102*(13), 4407-4409.

Takahashi, M., Suzuki, E., Takeda, R., Oba, S., Nishimatsu, H., Kimura, K.*, et al.* (2008). Angiotensin II and tumor necrosis factor-alpha synergistically promote monocyte chemoattractant protein-1 expression: roles of NF-kappaB, p38, and reactive oxygen species. *Am J Physiol Heart Circ Physiol, 294*(6), H2879-2888.

Tangirala, R. K., Rubin, E. M., & Palinski, W. (1995). Quantitation of atherosclerosis in murine models: correlation between lesions in the aortic origin and in the entire aorta, and differences in the extent of lesions between sexes in LDL receptor-deficient and apolipoprotein E-deficient mice. *J Lipid Res, 36*(11), 2320-2328.

Teichert-Kuliszewska, K., Maisonpierre, P. C., Jones, N., Campbell, A. I., Master, Z., Bendeck, M. P.*, et al.* (2001). Biological action of angiopoietin-2 in a fibrin matrix model of angiogenesis is associated with activation of Tie2. *Cardiovasc Res, 49*(3), 659-670.

Telford, W. G., Babin, S. A., Khorev, S. V., & Rowe, S. H. (2009). Green fiber lasers: an alternative to traditional DPSS green lasers for flow cytometry. *Cytometry A, 75*(12), 1031-1039.

Tham, D. M., Martin-McNulty, B., Wang, Y. X., Wilson, D. W., Vergona, R., Sullivan, M. E.*, et al.* (2002). Angiotensin II is associated with activation of NF-kappaB-mediated genes and downregulation of PPARs. *Physiol Genomics, 11*(1), 21-30.

Thatcher, S. E., Zhang, X., Howatt, D. A., Yiannikouris, F., Gurley, S. B., Ennis, T., *et al.* (2014). Angiotensin-converting enzyme 2 decreases formation and severity of angiotensin II-induced abdominal aortic aneurysms. *Arterioscler Thromb Vasc Biol, 34*(12), 2617-2623.

Thomas, M., & Augustin, H. G. (2009). The role of the Angiopoietins in vascular morphogenesis. *Angiogenesis, 12*(2), 125-137.

Thompson, M. M., Jones, L., Nasim, A., Sayers, R. D., & Bell, P. R. (1996). Angiogenesis in abdominal aortic aneurysms. *Eur J Vasc Endovasc Surg, 11*(4), 464-469.

Thompson, R. W., Curci, J. A., Ennis, T. L., Mao, D., Pagano, M. B., & Pham, C. T. (2006). Pathophysiology of abdominal aortic aneurysms: insights from the elastase-induced model in mice with different genetic backgrounds. *Ann N Y Acad Sci, 1085*, 59-73.

Thompson, R. W., Geraghty, P. J., & Lee, J. K. (2002). Abdominal aortic aneurysms: basic mechanisms and clinical implications. *Curr Probl Surg, 39*(2), 110-230.

Thurston, G., & Daly, C. (2012). The complex role of angiopoietin-2 in the angiopoietin-tie signaling pathway. *Cold Spring Harb Perspect Med, 2*(9), a006550.

Thurston, G., Rudge, J. S., Ioffe, E., Zhou, H., Ross, L., Croll, S. D., *et al.* (2000). Angiopoietin-1 protects the adult vasculature against plasma leakage. *Nat Med, 6*(4), 460-463.

Thurston, G., Suri, C., Smith, K., McClain, J., Sato, T. N., Yancopoulos, G. D., *et al.* (1999). Leakage-resistant blood vessels in mice transgenically overexpressing angiopoietin-1. *Science, 286*(5449), 2511-2514.

Tieu, B. C., Ju, X., Lee, C., Sun, H., Lejeune, W., Recinos, A., 3rd, *et al.* (2011). Aortic adventitial fibroblasts participate in angiotensin-induced vascular wall inflammation and remodeling. *J Vasc Res, 48*(3), 261-272.

Tieu, B. C., Lee, C., Sun, H., Lejeune, W., Recinos, A., 3rd, Ju, X., *et al.* (2009). An adventitial IL-6/MCP1 amplification loop accelerates macrophage-mediated vascular inflammation leading to aortic dissection in mice. *J Clin Invest, 119*(12), 3637-3651.

Tousoulis, D., Charakida, M., & Stefanadis, C. (2006). Endothelial function and inflammation in coronary artery disease. *Heart, 92*(4), 441-444.

Towbin, H., Staehelin, T., & Gordon, J. (1979). Electrophoretic transfer of proteins from polyacrylamide gels to nitrocellulose sheets: procedure and some applications. *Proc Natl Acad Sci U S A, 76*(9), 4350-4354.

Treska, V., Topolcan, O., & Pecen, L. (2000). Cytokines as plasma markers of abdominal aortic aneurysm. *Clin Chem Lab Med, 38*(11), 1161-1164.

Tressel, S. L., Kim, H., Ni, C. W., Chang, K., Velasquez-Castano, J. C., Taylor, W. R., *et al.* (2008). Angiopoietin-2 stimulates blood flow recovery after femoral artery occlusion by inducing inflammation and arteriogenesis. *Arterioscler Thromb Vasc Biol, 28*(11), 1989-1995.

Trollope, A., Moxon, J. V., Moran, C. S., & Golledge, J. (2011). Animal models of abdominal aortic aneurysm and their role in furthering management of human disease. *Cardiovasc Pathol, 20*(2), 114-123.

Tsubakimoto, Y., Yamada, H., Yokoi, H., Kishida, S., Takata, H., Kawahito, H., *et al.* (2009). Bone marrow angiotensin AT1 receptor regulates differentiation of monocyte lineage progenitors from hematopoietic stem cells. *Arterioscler Thromb Vasc Biol, 29*(10), 1529-1536.

Tsui, J. C. (2010). Experimental models of abdominal aortic aneurysms. *Open Cardiovasc Med J, 4*, 221-230.

Tsuruda, T., Kato, J., Hatakeyama, K., Kojima, K., Yano, M., Yano, Y., *et al.* (2008). Adventitial mast cells contribute to pathogenesis in the progression of abdominal aortic aneurysm. *Circ Res, 102*(11), 1368-1377.

Uchida, H. A., Kristo, F., Rateri, D. L., Lu, H., Charnigo, R., Cassis, L. A., *et al.* (2010). Total lymphocyte deficiency attenuates AngII-induced atherosclerosis in males but not abdominal aortic aneurysms in apoE deficient mice. *Atherosclerosis, 211*(2), 399-403.

Valenzuela, D. M., Griffiths, J. A., Rojas, J., Aldrich, T. H., Jones, P. F., Zhou, H., *et al.* (1999). Angiopoietins 3 and 4: diverging gene counterparts in mice and humans. *Proc Natl Acad Sci U S A, 96*(5), 1904-1909.

Vardulaki, K. A., Walker, N. M., Day, N. E., Duffy, S. W., Ashton, H. A., & Scott, R. A. (2000). Quantifying the risks of hypertension, age, sex and smoking in patients with abdominal aortic aneurysm. *Br J Surg, 87*(2), 195-200.

Veikkola, T., & Alitalo, K. (2002). Dual role of Ang2 in postnatal angiogenesis and lymphangiogenesis. *Dev Cell, 3*(3), 302-304.

Vijaynagar, B., Bown, M. J., Sayers, R. D., & Choke, E. (2013). Potential role for anti-angiogenic therapy in abdominal aortic aneurysms. *Eur J Clin Invest, 43*(7), 758-765.

Virmani, R., Kolodgie, F. D., Burke, A. P., Finn, A. V., Gold, H. K., Tulenko, T. N., *et al.* (2005). Atherosclerotic plaque progression and vulnerability to rupture: angiogenesis as a source of intraplaque hemorrhage. *Arterioscler Thromb Vasc Biol, 25*(10), 2054-2061.

Von Allmen, R. S., & Powell, J. T. (2012). The management of ruptured abdominal aortic aneurysms: screening for abdominal aortic aneurysm and incidence of rupture. *J Cardiovasc Surg (Torino), 53*(1), 69-76.

Vorp, D. A., & Vande Geest, J. P. (2005). Biomechanical determinants of abdominal aortic aneurysm rupture. *Arterioscler Thromb Vasc Biol, 25*(8), 1558-1566.

Wahlgren, C. M., Larsson, E., Magnusson, P. K., Hultgren, R., & Swedenborg, J. (2010). Genetic and environmental contributions to abdominal aortic aneurysm development in a twin population. *J Vasc Surg, 51*(1), 3-7; discussion 7.

Wang, Y., Krishna, S., & Golledge, J. (2013). The calcium chloride-induced rodent model of abdominal aortic aneurysm. *Atherosclerosis, 226*(1), 29-39.

Wassef, M., Baxter, B. T., Chisholm, R. L., Dalman, R. L., Fillinger, M. F., Heinecke, J., *et al.* (2001). Pathogenesis of abdominal aortic aneurysms: a multidisciplinary research program supported by the National Heart, Lung, and Blood Institute. *J Vasc Surg, 34*(4), 730-738.

Weber, C., Zernecke, A., & Libby, P. (2008). The multifaceted contributions of leukocyte subsets to atherosclerosis: lessons from mouse models. *Nat Rev Immunol, 8*(10), 802-815.

Weiss, D., Kools, J. J., & Taylor, W. R. (2001). Angiotensin II-induced hypertension accelerates the development of atherosclerosis in apoE-deficient mice. *Circulation, 103*(3), 448-454.

Whitman, S. C., Ravisankar, P., & Daugherty, A. (2002). IFN-gamma deficiency exerts gender-specific effects on atherogenesis in apolipoprotein E-/- mice. *J Interferon Cytokine Res, 22*(6), 661-670.

Williams, J. K., Armstrong, M. L., & Heistad, D. D. (1988). Vasa vasorum in atherosclerotic coronary arteries: responses to vasoactive stimuli and regression of atherosclerosis. *Circ Res, 62*(3), 515-523.

Wilmink, A. B., Vardulaki, K. A., Hubbard, C. S., Day, N. E., Ashton, H. A., Scott, A. P.*, et al.* (2002). Are antihypertensive drugs associated with abdominal aortic aneurysms? *J Vasc Surg, 36*(4), 751-757.

Wolinsky, H., & Glagov, S. (1964). Structural Basis for the Static Mechanical Properties of the Aortic Media. *Circ Res, 14*, 400-413.

Wong, A. L., Haroon, Z. A., Werner, S., Dewhirst, M. W., Greenberg, C. S., & Peters, K. G. (1997). Tie2 expression and phosphorylation in angiogenic and quiescent adult tissues. *Circ Res, 81*(4), 567-574.

Xiong, W., Knispel, R., MacTaggart, J., Greiner, T. C., Weiss, S. J., & Baxter, B. T. (2009). Membrane-type 1 matrix metalloproteinase regulates macrophage-dependent elastolytic activity and aneurysm formation in vivo. *J Biol Chem, 284*(3), 1765-1771.

Xiong, W., MacTaggart, J., Knispel, R., Worth, J., Persidsky, Y., & Baxter, B. T. (2009). Blocking TNF-alpha attenuates aneurysm formation in a murine model. *J Immunol, 183*(4), 2741-2746.

Xiong, W., Zhao, Y., Prall, A., Greiner, T. C., & Baxter, B. T. (2004). Key roles of CD4+ T cells and IFN-gamma in the development of abdominal aortic aneurysms in a murine model. *J Immunol, 172*(4), 2607-2612.

Yan, Z. X., Jiang, Z. H., & Liu, N. F. (2012). Angiopoietin-2 promotes inflammatory lymphangiogenesis and its effect can be blocked by the specific inhibitor L1-10. *Am J Physiol Heart Circ Physiol, 302*(1), H215-223.

Yancopoulos, G. D., Davis, S., Gale, N. W., Rudge, J. S., Wiegand, S. J., & Holash, J. (2000). Vascular-specific growth factors and blood vessel formation. *Nature, 407*(6801), 242-248.

Yin, M., Zhang, J., Wang, Y., Wang, S., Bockler, D., Duan, Z.*, et al.* (2010). Deficient CD4+CD25+ T regulatory cell function in patients with abdominal aortic aneurysms. *Arterioscler Thromb Vasc Biol, 30*(9), 1825-1831.

Yokoyama, K., Erickson, H. P., Ikeda, Y., & Takada, Y. (2000). Identification of amino acid sequences in fibrinogen gamma -chain and tenascin C C-terminal domains critical for binding to integrin alpha vbeta 3. *J Biol Chem, 275*(22), 16891-16898.

Yoshimura, K., Aoki, H., Ikeda, Y., Fujii, K., Akiyama, N., Furutani, A.*, et al.* (2005). Regression of abdominal aortic aneurysm by inhibition of c-Jun N-terminal kinase. *Nat Med, 11*(12), 1330-1338.

Yuan, H. T., Khankin, E. V., Karumanchi, S. A., & Parikh, S. M. (2009). Angiopoietin 2 is a partial agonist/antagonist of Tie2 signaling in the endothelium. *Mol Cell Biol, 29*(8), 2011-2022.

Zhang, J., Fukuhara, S., Sako, K., Takenouchi, T., Kitani, H., Kume, T., *et al.* (2011). Angiopoietin-1/Tie2 signal augments basal Notch signal controlling vascular quiescence by inducing delta-like 4 expression through AKT-mediated activation of beta-catenin. *J Biol Chem, 286*(10), 8055-8066.

Zhang, S. H., Reddick, R. L., Piedrahita, J. A., & Maeda, N. (1992). Spontaneous hypercholesterolemia and arterial lesions in mice lacking apolipoprotein E. *Science, 258*(5081), 468-471.

Zhang, Y., Naggar, J. C., Welzig, C. M., Beasley, D., Moulton, K. S., Park, H. J., *et al.* (2009). Simvastatin inhibits angiotensin II-induced abdominal aortic aneurysm formation in apolipoprotein E-knockout mice: possible role of ERK. *Arterioscler Thromb Vasc Biol, 29*(11), 1764-1771.

Zhang, Z. G., Zhang, L., Croll, S. D., & Chopp, M. (2002). Angiopoietin-1 reduces cerebral blood vessel leakage and ischemic lesion volume after focal cerebral embolic ischemia in mice. *Neuroscience, 113*(3), 683-687.

Zhang, Z. X., Zhou, J., Zhang, Y., Zhu, D. M., Li, D. C., & Zhao, H. (2013). Knockdown of angiopoietin-2 suppresses metastasis in human pancreatic carcinoma by reduced matrix metalloproteinase-2. *Mol Biotechnol, 53*(3), 336-344.

Zhou, Y., Wu, W., Lindholt, J. S., Sukhova, G. K., Libby, P., Yu, X., *et al.* (2015). Regulatory T cells in human and angiotensin II-induced mouse abdominal aortic aneurysms. *Cardiovasc Res, 107*(1), 98-107.

Ziegler, S. F., Bird, T. A., Schneringer, J. A., Schooley, K. A., & Baum, P. R. (1993). Molecular cloning and characterization of a novel receptor protein tyrosine kinase from human placenta. *Oncogene, 8*(3), 663-670.
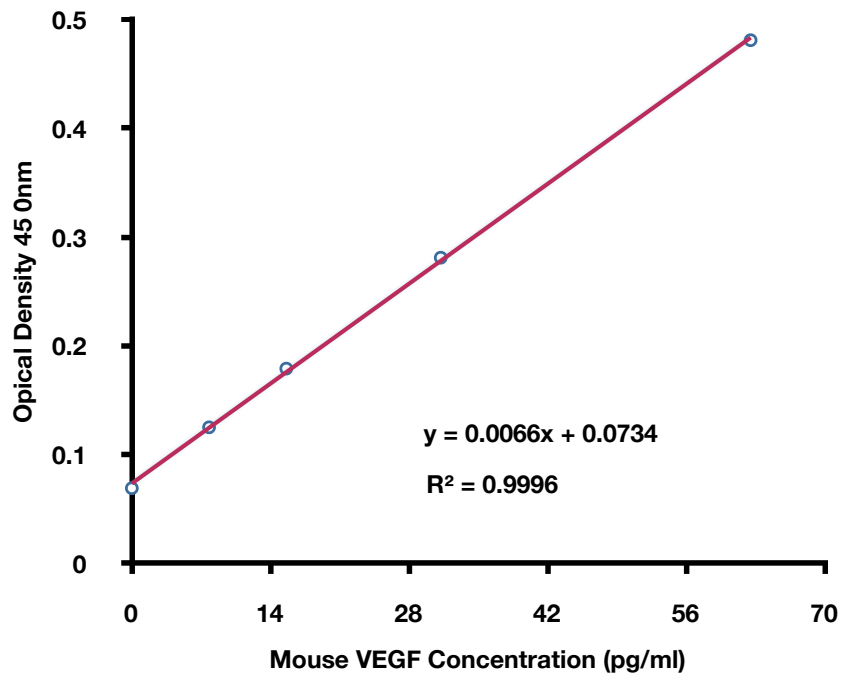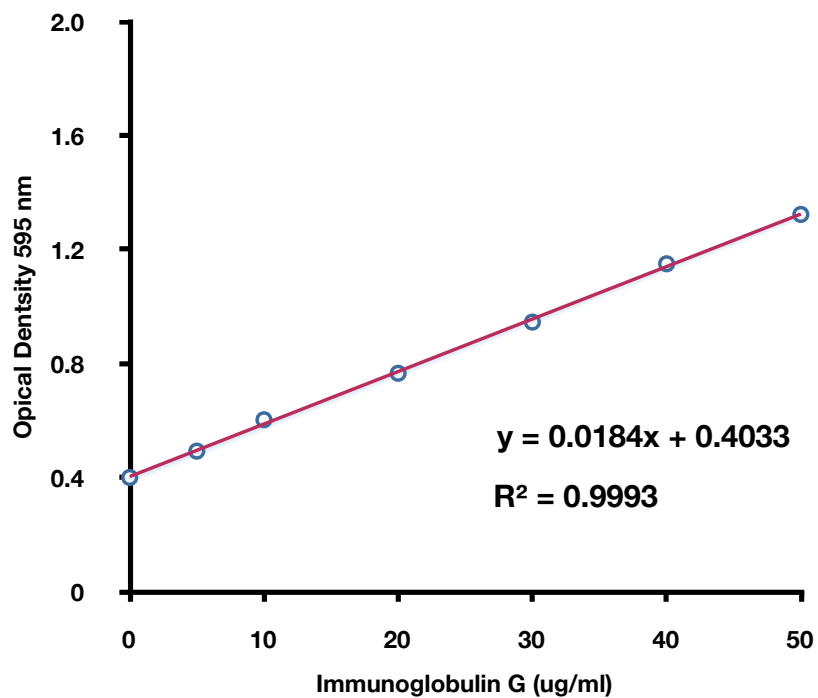
APPENDICES

Appendix 1 Ethics Approval

This administrative form
has been removed
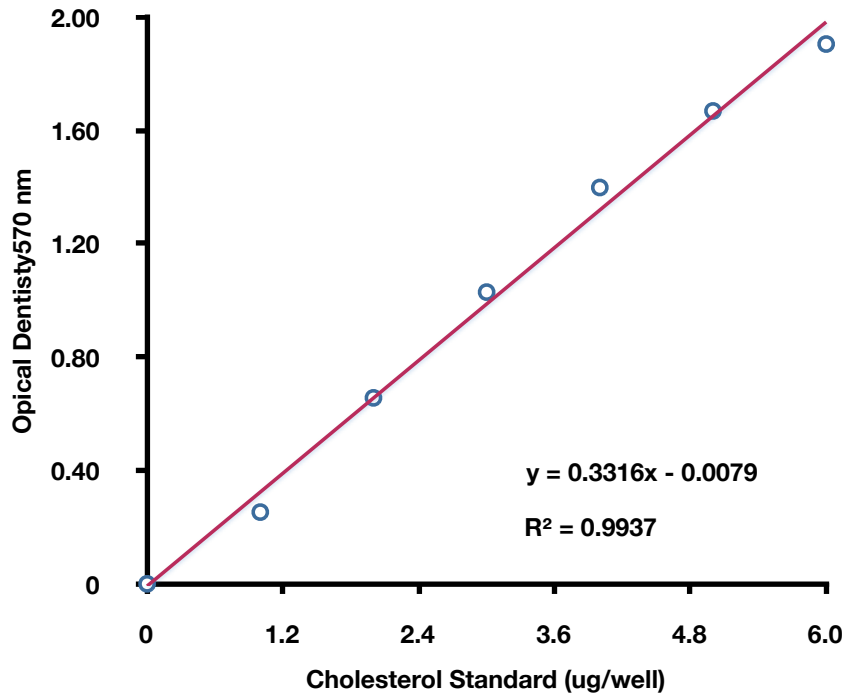
Appendix 2 Standard Curves

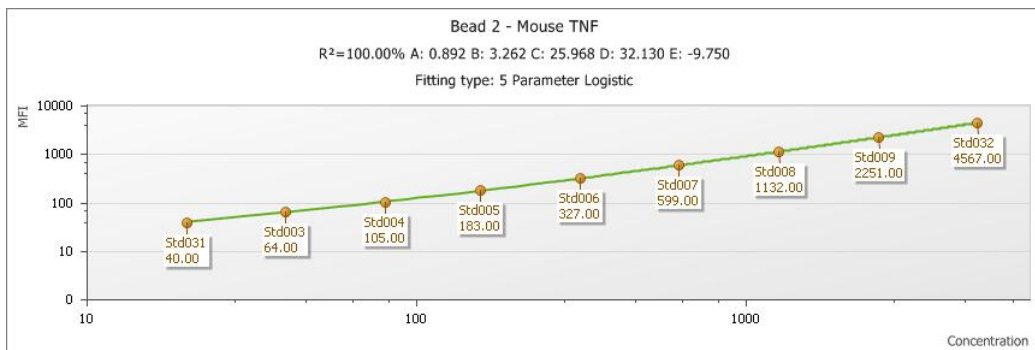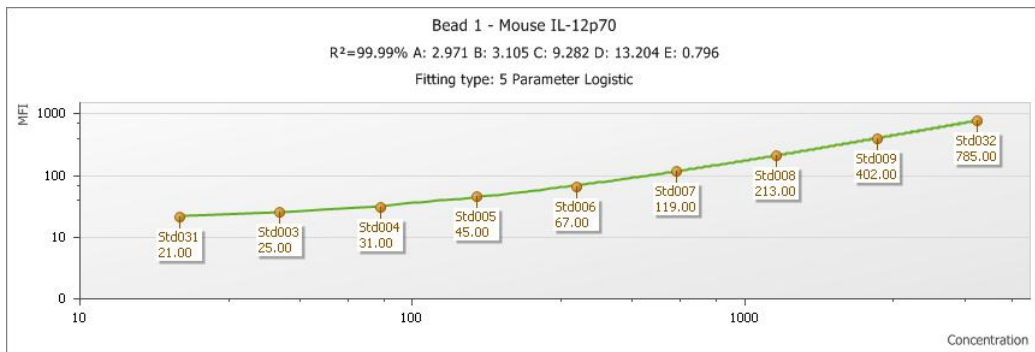**Mouse Vascular Endothelial Growth Factor (VEGF) Quantikine ELISA Immunoassay (R&D systems) standard curve**

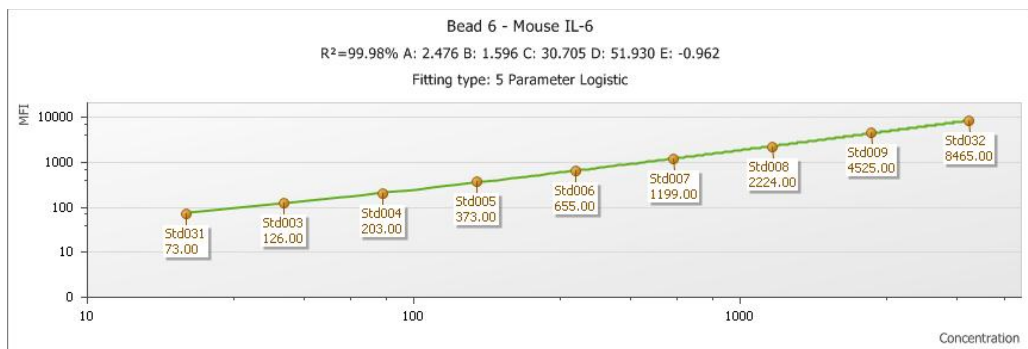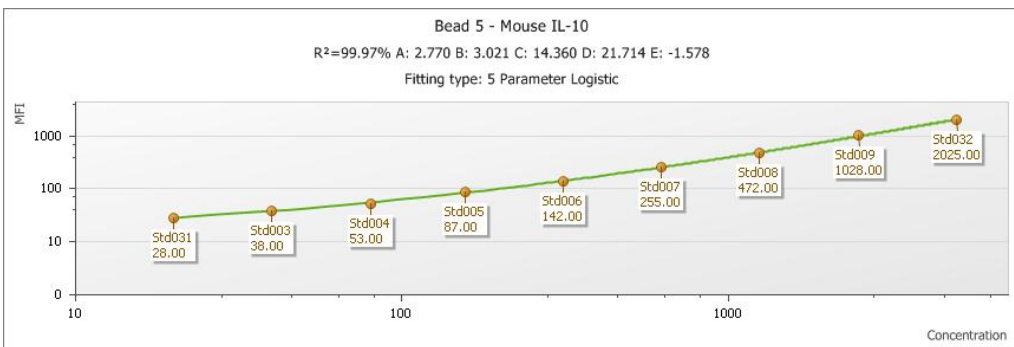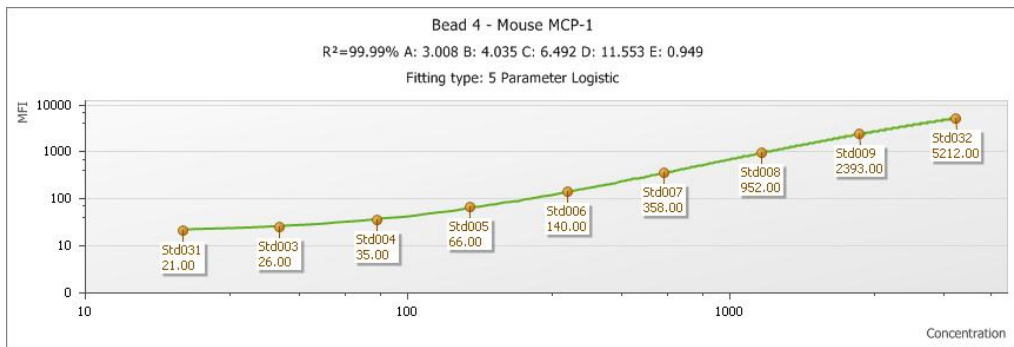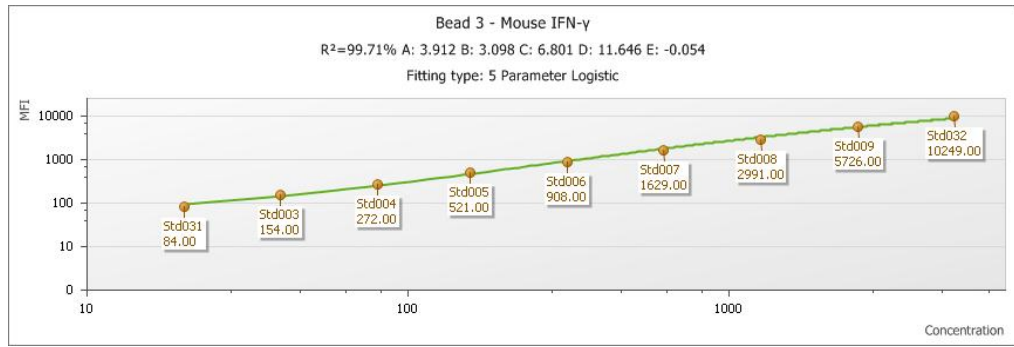**Bradford Protein Assay (Bio-Rad) standard curve**

HDL and LDL/VLDL Cholesterol Assay Kit (Abcam) standard curve

Cytometric Bead Array Mouse Inflammation Kit (BD) standard curve

Cytometric Bead Array Mouse Inflammation Kit (BD) standard curve (continue)

Bead 3 - Mouse IFN-γ
R²=99.71% A: 3.912 B: 3.098 C: 6.801 D: 11.646 E: -0.054
Fitting type: 5 Parameter Logistic

Std031 84.00 · Std003 154.00 · Std004 272.00 · Std005 521.00 · Std006 908.00 · Std007 1629.00 · Std008 2991.00 · Std009 5726.00 · Std032 10249.00

Bead 4 - Mouse MCP-1
R²=99.99% A: 3.008 B: 4.035 C: 6.492 D: 11.553 E: 0.949
Fitting type: 5 Parameter Logistic

Std031 21.00 · Std003 26.00 · Std004 35.00 · Std005 66.00 · Std006 140.00 · Std007 358.00 · Std008 952.00 · Std009 2393.00 · Std032 5212.00

Bead 5 - Mouse IL-10
R²=99.97% A: 2.770 B: 3.021 C: 14.360 D: 21.714 E: -1.578
Fitting type: 5 Parameter Logistic

Std031 28.00 · Std003 38.00 · Std004 53.00 · Std005 87.00 · Std006 142.00 · Std007 255.00 · Std008 472.00 · Std009 1028.00 · Std032 2025.00

Bead 6 - Mouse IL-6
R²=99.98% A: 2.476 B: 1.596 C: 30.705 D: 51.930 E: -0.962
Fitting type: 5 Parameter Logistic

Std031 73.00 · Std003 126.00 · Std004 203.00 · Std005 373.00 · Std006 655.00 · Std007 1199.00 · Std008 2224.00 · Std009 4525.00 · Std032 8465.00

Appendix 3 Reagents and Solutions

Sudan IV Staining Buffer

1% Sudan IV (g) in acetone and 70% ethanol (v, 1:1)

Western blotting

Tissue Protein Extraction Buffer (Modified Ripa Buffer)

50mM Tris-HCl pH7.4

150 nM NaCl

2 mM EDTA

1% TritonX-100

0.1% SDS

0.1% sodium deoxycholate

in diH$_2$O

SDS Gel-Loading Buffer

2% SDS

2 mM beta-mercapto-ethanol

4% Glycerol

50 mM Tris-HCl, pH 6.8

0.01% Bromophenolblue

100mM dithiothreitol

in diH$_2$O

TBST buffer (pH7.6)

50 mM Tris-HCL

150 mM NACL

0.05% Tween-20 (v/v)

Gel Running Buffer (pH 8.3)

25 mM Tris

192mM glycine

0.1% SDS

in diH$_2$O

Transfer Buffer (Bjurrum Schater-Nielsen, pH 9.2)

48 mM Tris

39 mM Glycine

10% Methanol

0.0375% SDS

in diH$_2$O

Immunofluorescence Staining

Immunofluorescence Staining Buffer

0.5% BSA

0.1% Triton X-100

in PBS

Flow Cytometry

FACS Staining Buffer

1% BSA

0.1% sodium azide

in DPBS